

Spike-specific T cell immunity following  
vaccination against the human coronaviruses  
SARS-CoV-2 and MERS-CoV

**Cumulative Dissertation**

to obtain the doctoral degree of the natural sciences

Dr. rer. nat.

submitted to the University Hamburg

Faculty of Mathematics, Informatics and Natural Sciences

Department of Biology

by

**Leonie Mayer**

Hamburg, 2024

This work was performed between October 2020 and December 2023 at the Institute for Infection Research and Vaccine Development (IIRVD) of the University Medical Center Hamburg-Eppendorf (UKE, Hamburg, Germany) in association with the Department for Clinical Immunology of Infectious Diseases at the Bernhard Nocht Institute for Tropical Medicine (BNITM, Hamburg, Germany) under the supervision of Prof. Dr. med. Marylyn M. Addo.

Date of thesis defense:  
April 9th, 2024

Evaluated by:  
Prof. Dr. med. Marylyn M. Addo  
Prof. Dr. med. Jonas Schmidt-Chanasit

Persistent Identifier:  
[urn:nbn:de:gbv:18-ediss-117098](https://nbn-resolving.org/urn:nbn:de:gbv:18-ediss-117098)

## List of Publications

- I. **Leonie Mayer\***, Leonie M. Weskamm\*, Anahita Fathi, Maya Kono, Jasmin Heidepriem, Verena Krähling, Sibylle C. Mellinghoff, My Linh Ly, Monika Friedrich, Svenja Hardtke, Saskia Borregaard, Thomas Hesterkamp, Felix F. Loeffler, the MVA-SARS-2 Study Group, Asisa Volz, Gerd Sutter, Stephan Becker, Christine Dahlke, Marylyn M. Addo. MVA-based vaccine candidates encoding the native or prefusion-stabilized SARS-CoV-2 spike protein reveal differential immunogenicity in humans. *npj Vaccines* [accepted manuscript, 12 December 2023].
- II. Caroline E. Harrer\*, **Leonie Mayer\***, Anahita Fathi, Susan Lassen, My L. Ly, Madeleine E. Zinser, MVA-MERS-S Study Group, Timo Wolf, Stephan Becker, Gerd Sutter, Christine Dahlke, Marylyn M. Addo. Identification of a spike-specific CD8<sup>+</sup> T cell epitope following vaccination against the Middle East respiratory syndrome coronavirus in humans. *The Journal of Infectious Diseases*, [advance online publication, 9 January 2024]. doi: [10.1093/infdis/jiad612](https://doi.org/10.1093/infdis/jiad612)
- III. Sibylle C. Mellinghoff\*, **Leonie Mayer\***, Sandra Robrecht, Leonie M. Weskamm, Christine Dahlke, Henning Gruell, Maike Schlotz, Kanika Vanshylla, Hans A. Schloser, Martin Thelen, Anna-Maria Fink, Kirsten Fischer, Florian Klein, Marylyn M. Addo, Barbara Eichhorst, Michael Hallek, Petra Langerbeins. SARS-CoV-2-specific cellular response following third COVID-19 vaccination in patients with chronic lymphocytic leukemia. *Haematologica* **107**, 2480–2484 (2022). doi: [10.3324/haematol.2022.280982](https://doi.org/10.3324/haematol.2022.280982)
- IV. Sibylle C. Mellinghoff, Sandra Robrecht, **Leonie Mayer**, Leonie M. Weskamm, Christine Dahlke, Henning Gruell, Kanika Vanshylla, Hans A. Schlösser, Martin Thelen, Anna-Maria Fink, Kirsten Fischer, Florian Klein, Marylyn M. Addo, Barbara Eichhorst, Michael Hallek, Petra Langerbeins. SARS-CoV-2 specific cellular response following COVID-19 vaccination in patients with chronic lymphocytic leukemia. *Leukemia* **36**, 562–565 (2022). doi: [10.1038/s41375-021-01500-1](https://doi.org/10.1038/s41375-021-01500-1)
- V. Darius F. Ruether, Golda M. Schaub, Paul M. Duengelhof, Friedrich Haag, Thomas T. Brehm, Anahita Fathi, Malte Wehmeyer, Jacqueline Jahnke-Triankowski, **Leonie Mayer**, Armin Hoffmann, Lutz Fischer, Marylyn M. Addo, Marc Lütgehetmann, Ansgar W. Lohse, Julian Schulze Zur Wiesch, Martina Sterneck. SARS-CoV-2-specific Humoral and T cell Immune Response After Second Vaccination in Liver Cirrhosis and Transplant Patients. *Clinical Gastroenterology and Hepatology* **20**, 162-172 (2022). doi: [10.1016/j.cgh.2021.09.003](https://doi.org/10.1016/j.cgh.2021.09.003)
- VI. Christian Meyer Zu Natrup, Alina Tscherne, Christine Dahlke, Malgorzata Ciurkiewicz, Dai-Lun Shin, Anahita Fathi, Cornelius Rohde, Georgia Kalodimou, Sandro Halwe, Leonard Limpinsel, Jan H. Schwarz, Martha Klug, Meral Esen, Nicole Schneiderhan-Marra, Alex Dulovic, Alexandra Kupke, Katrin Brosinski, Sabrina Clever, Lisa-Marie Schünemann, Georg Beythien, Federico Armando, **Leonie Mayer**, Marie L. Weskamm, Sylvia Jany, Astrid Freudenstein, Tamara Tüchel, Wolfgang Baumgärtner, Peter Kremsner, Rolf Fendel, Marylyn M. Addo, Stephan Becker, Gerd Sutter, Asisa Volz. Stabilized recombinant SARS-CoV-2 spike antigen enhances vaccine immunogenicity and protective capacity. *The Journal of Clinical Investigation* **132(24)**, e159895 (2022). doi: [10.1172/JCI159895](https://doi.org/10.1172/JCI159895)

\*These authors contributed equally.

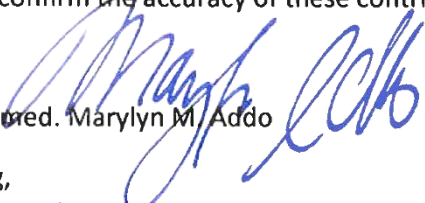
## Author Contributions

- I. This manuscript was jointly prepared by Leonie Mayer, responsible for the investigation of T cell responses, and Leonie M. Weskamm, responsible for the investigation of the antibody and B cell responses. Leonie Mayer planned, established and conducted the IFN- $\gamma$  ELISpot, whole-blood IGRA, and intracellular cytokine staining assays and analyzed, interpreted and visualized the data presented in Figures 5-6. She created Figures 1-4 together with Leonie M. Weskamm and Jasmin. Heidepriem. Leonie Mayer wrote the first version of the manuscript text contributed to the revision process. As a corresponding author, she was responsible for the publication process, including communication with the editors and co-authors. She also contributed to the isolation and preservation of serum, plasma and PBMCs from the human blood samples of the phase 1 clinical trials. She was also involved in the coordination, sample collection, and sample processing of the control cohorts analyzed in this manuscript.
- II. This manuscript was jointly prepared by Caroline E. Harrer and Leonie Mayer. Leonie Mayer established the intracellular cytokine staining protocol for the spectral flow cytometer, planned and conducted the experiments, analyzed, interpreted and visualized the data shown in Figure 2. She coordinated the HLA-typing. She contributed to the writing of the first version of the manuscript text, and conducted the editing and the revision process together with Caroline E. Harrer.
- III. Leonie Mayer planned, established and conducted the IFN- $\gamma$  ELISpot assay and analyzed and interpreted the data presented in Figure 2. She conceptualized the project together with Sibylle C. Mellinghoff and contributed to the writing of the first version of the manuscript text and editing of the manuscript. She was also involved in the coordination and laboratory work to establish the healthy control cohort, including isolation and preservation of PBMCs, plasma, and serum from human blood samples.
- IV. Leonie Mayer planned, established and conducted the IFN- $\gamma$  ELISpot assay and analyzed and interpreted the data presented in Figure 1 c and d. She contributed to the writing, revision, and editing of the manuscript. She also contributed to the coordination, sample collection, and sample processing of the control cohorts.
- V. Leonie Mayer showed the first co-author, Golda Schaub, how to perform the whole-blood IGRA assay and contributed to the collection and interpretation of the data shown in Figure 2 c and f.
- VI. Leonie Mayer contributed to the processing of the human serum samples that were used to analyze antibody responses following MVA-SARS-2-S vaccination, shown in Figure 1. She also contributed to the coordination, protocol optimization and processing of human blood samples of the MVA-S and MVA-ST phase 1 clinical trials.

I hereby confirm the accuracy of these contributions.

Prof. Dr. med. Marilyn M. Addo

Hamburg,



19.12.2023

## Abstract

Emerging infectious diseases (EIDs) are an increasing threat to the human population. In the past two decades, three coronaviruses (CoVs) have spilled over to humans and caused outbreaks of the following respiratory diseases: The severe acute respiratory syndrome (SARS), the Middle East respiratory syndrome (MERS), and the coronavirus disease 2019 (COVID-19), caused by infection with SARS-CoV, MERS-CoV, and SARS-CoV-2, respectively. Vaccination is an important cornerstone in pandemic preparedness against pathogens, in particular concerning the WHO-prioritized CoVs. Vaccine development can be accelerated by the employment of adaptable vaccine platforms, such as mRNA technology and viral vectors, as exemplified by the COVID-19 pandemic. Within a year of the emergence of SARS-CoV-2, one ChAdOx1 viral vector-based and two mRNA-based COVID-19 vaccines were licensed. While vaccine-induced antibodies can provide protection against infection, T cell responses are important for the clearance of virus-infected cells and provide long-term protection against disease.

The aim of this thesis was a comprehensive, longitudinal analysis of the T cell response following vaccination against SARS-CoV-2 and MERS-CoV in humans. Vaccine candidates based on the recombinant Modified Vaccinia virus Ankara (rMVA) viral vector were developed against MERS (MVA-MERS-S) and COVID-19 (MVA-SARS-2-S and MVA-SARS-2-ST) and investigated in phase 1 clinical trials at the University Medical Center Hamburg-Eppendorf between 2017 and 2023. Frequent blood sampling in these phase 1 clinical trials provided the unique opportunity to study T cell immunity in detail. Blood samples were collected from trial participants before and longitudinally after vaccination, and compared to blood samples from healthy and immunocompromised individuals, who were vaccinated with licensed vaccines. The magnitude, function, and antigen-specificity of T cell responses were investigated in various assays.

The comparative study of the COVID-19 vaccines revealed a higher T cell immunogenicity of MVA-SARS-2-ST encoding a prefusion-stabilized SARS-CoV-2 spike protein, compared to MVA-SARS-2-S encoding the native spike protein. While both vaccine candidates were less immunogenic in SARS-CoV-2 naïve individuals compared to the licensed vaccine regimens, in heterologous vaccination they showed promising results: MVA-SARS-2-S could prime a polyfunctional CD8<sup>+</sup> response when given before mRNA-based immunization. MVA-SARS-2-ST as a third vaccination following mRNA-based immunization could boost the T cell response in individuals with low residual immunity. In contrast to healthy individuals who generated a robust T cell response following prime-boost immunization with licensed COVID-19 vaccines, immunocompromised patients with chronic lymphocytic leukemia, liver cirrhosis or liver transplant had a reduced response. Notably, a third booster dose and heterologous regimens combining mRNA- and viral vector-based vaccines enhanced the T cell response in these patients considerably. The analysis of the MVA-MERS-S vaccine candidate revealed that using a lower vaccine dose and a prolonged time interval between prime and boost immunization enhanced the T cell immunogenicity. Furthermore, CD8<sup>+</sup> T cells against a newly identified immunodominant epitope were shown to have a long-lived, polyfunctional phenotype.

In summary, these findings underline that vaccine characteristics, vaccination regimen, as well as host factors, can shape the vaccine-induced T cell response. These findings provide important insights for the development of more effective immunization strategies which aim to build up a long-lived T cell memory for protection against disease. This is of particular relevance for immunocompromised patients.

## Zusammenfassung

Neu auftretende Infektionskrankheiten stellen eine zunehmende Bedrohung für die Bevölkerung dar. In den vergangenen zwei Jahrzehnten sind drei Coronaviren (CoV) auf den Menschen übergelassen und haben Ausbrüche der folgenden Atemwegserkrankungen verursacht: Das *severe acute respiratory syndrome* (SARS), das *Middle East respiratory syndrome* (MERS), und das *coronavirus disease 2019* (COVID-19), die durch die Ansteckung mit SARS-CoV, MERS-CoV bzw. SARS-CoV-2 verursacht werden. Impfungen sind ein wichtiger Grundpfeiler der Pandemievorsorge, insbesondere in Bezug auf die von der WHO als prioritär eingestufteten Coronaviren. Die Impfstoffentwicklung kann durch anpassungsfähige Impfstoffplattformen wie die mRNA-Technologie und virale Vektoren beschleunigt werden, wie das Beispiel der COVID-19-Pandemie zeigte. Innerhalb eines Jahres wurden ein ChAdOx1-Vektor-basierter und zwei mRNA-basierte COVID-19-Impfstoffe zugelassen. Während impfstoffinduzierte Antikörper einen Schutz vor einer Infektion bieten können, ist die T-Zell-Antwort entscheidend für die Beseitigung von virusinfizierten Zellen und den langfristigen Schutz vor einer Erkrankung.

Ziel dieser Arbeit war eine umfassende, longitudinale Analyse der T-Zell-Antwort nach Impfung gegen SARS-CoV-2 und MERS-CoV. Impfstoffkandidaten, die auf rekombinanten Modifizierten Vacciniaviren Ankara (rMVA) basieren, wurden gegen MERS (MVA-MERS-S) und COVID-19 (MVA-SARS-2-S und MVA-SARS-2-ST) entwickelt und zwischen 2017 und 2023 in klinischen Phase-1-Studien am Universitätsklinikum Hamburg-Eppendorf untersucht. Regelmäßige Blutentnahmen in diesen klinischen Phase-1-Studien boten die besondere Möglichkeit, die T-Zell-Immunität im Detail zu untersuchen. Es wurden Blutproben von Studienteilnehmern vor und longitudinal nach Impfung genommen und mit Blutproben von gesunden und immungeschwächten Personen verglichen, die mit zugelassenen Impfstoffen geimpft wurden. Die Stärke, die Funktion und die Antigenspezifität der T-Zell-Antwort wurden in verschiedenen Assays untersucht.

Die vergleichende COVID-19 Studie ergab eine höhere T-Zell-Immunogenität des Impfstoffkandidaten MVA-SARS-2-ST, der ein präfusionsstabilisiertes SARS-CoV-2-Spike-Protein kodiert, im Vergleich zu MVA-SARS-2-S, der das native Spike-Protein kodiert. Während beide Impfstoffkandidaten bei SARS-CoV-2-naïven Individuen im Vergleich zu den zugelassenen Impfstoffen weniger immunogen waren, erwiesen sie sich bei der heterologen Impfung als vielversprechend: MVA-SARS-2-S konnte eine polyfunktionelle CD8<sup>+</sup>-Antwort auslösen, wenn es vor der mRNA-basierten Immunisierung verabreicht wurde. MVA-SARS-2-ST als Auffrischungsimpfung nach einer mRNA-basierten Immunisierung konnte die T-Zell-Antwort bei Personen mit geringer Restimmunität verstärken. Im Gegensatz zu gesunden Personen, die nach der Grundimmunisierung mit zugelassenen COVID-19-Impfstoffen eine robuste T-Zell-Antwort entwickelten, zeigten immungeschwächte Patienten mit chronischer lymphatischer Leukämie, Leberzirrhose oder Lebertransplantation eine geringere Antwort. Insbesondere eine dritte Auffrischungsimpfung und ein heterologes Impfschema aus mRNA- und vektorbasierten Impfstoffen, verstärkten die T-Zell-Antwort bei diesen Patienten deutlich. Die Untersuchung des MVA-MERS-S-Impfstoffkandidaten ergab, dass eine niedrigere Impfstoffdosis und ein längeres Zeitintervall zwischen den ersten beiden Impfungen die T-Zell-Immunogenität verbesserte. Darüber hinaus wurde gezeigt, dass CD8<sup>+</sup> T-Zellen gegen ein neu identifiziertes immundominantes Epitop einen langlebigen, polyfunktionalen Phänotyp aufweisen.

Zusammenfassend verdeutlichen diese Ergebnisse, dass Impfstoffcharakteristika, Impfschema sowie individuelle Faktoren die durch den Impfstoff ausgelöste T-Zell-Antwort beeinflussen können. Diese Ergebnisse liefern wichtige Erkenntnisse für die Entwicklung von effektiveren Immunisierungsstrategien, die den Aufbau eines langlebigen T-Zell-Gedächtnisses als Schutz vor Krankheit zum Ziel haben. Dies ist besonders für immungeschwächte Patienten von Bedeutung.

## Table of Contents

1.	INTRODUCTION .....	1
1.1.	Emerging infectious diseases (EID).....	1
1.1.1.	Coronaviruses .....	2
1.1.2.	Emerging human coronaviruses .....	3
1.2.	Vaccine development against EIDs.....	4
1.2.1.	Vaccine platforms.....	5
1.2.2.	Characteristics of mRNA and viral vector platforms .....	6
1.3.	Vaccine-induced immunity.....	7
1.3.1.	From innate to adaptive immune responses .....	7
1.3.2.	T cell development .....	8
1.3.3.	Dynamics of the T cell response .....	9
1.3.4.	T cells in vaccine-induced protection .....	13
2.	AIM OF THE STUDY.....	15
3.	STUDY DESIGN .....	15
3.1.	Vaccines.....	15
3.1.1.	Experimental rMVA viral vector vaccines.....	15
3.1.2.	Licensed vaccines based on the ChAdOx1 viral vector and mRNA .....	16
3.2.	Study cohorts.....	17
3.2.1.	COVID-19 vaccination cohorts.....	17
3.2.2.	MERS vaccination cohorts .....	18
3.3.	Experimental methods .....	19
4.	PUBLISHED RESULTS.....	20
5.	UNPUBLISHED RESULTS.....	21
5.1.	SARS-CoV-2 vaccination and infection .....	21
5.1.1.	SARS-CoV-2-spike-specific T cell response after vaccination or infection .....	21
5.1.2.	Longitudinal analysis of epitope-specific CD8+ T cells .....	24
5.2.	Vaccination against MERS-CoV.....	27
5.2.1.	Longitudinal analysis of T cell responses following MVA-MERS-S vaccination .....	27
5.2.2.	Correlation of T cell and humoral responses following MVA-MERS-S vaccination.....	29
5.2.3.	Function and memory phenotype of spike-specific T cell responses.....	29
5.2.4.	Epitope-specific CD8+ T cell responses .....	32
6.	DISCUSSION .....	34
6.1.	T cell immunogenicity of rMVA-based vaccine candidates.....	34
6.1.1.	The MVA-MERS-S vaccine candidate.....	34
6.1.2.	The MVA-S and MVA-ST vaccine candidates.....	36

6.2.	Vaccine characteristics shaping T cell immunogenicity .....	37
6.2.1.	Spike antigen design.....	37
6.2.2.	Vaccine dose.....	38
6.2.3.	Vaccine platform .....	40
6.3.	Vaccination regimen shaping T cell immunogenicity.....	41
6.3.1.	Heterologous prime-boost .....	41
6.3.2.	Prime-boost time interval .....	42
6.3.3.	Re-boosting.....	43
6.4.	Host factors affecting T cell immunogenicity .....	44
6.4.1.	T cells response in patients with underlying disease .....	44
6.4.2.	Demographic factors affecting vaccine response .....	46
6.4.3.	T cells and HLA-polymorphism .....	46
6.5.	From vaccine immunology to T cell correlates of protection .....	47
6.5.1.	Protective T cell responses.....	47
6.5.2.	Role of T cells in protection against COVID-19 and MERS.....	48
6.5.3.	Importance of T cells in protection against viral variants .....	48
6.5.4.	Cross-reactive T cell responses to other virus strains .....	49
6.6.	Future Outlook .....	50
6.6.1.	Systems vaccinology .....	50
6.6.2.	Rational vaccine design .....	50
6.6.3.	Future of the rMVA vaccine platform .....	51
7.	REFERENCES .....	52
8.	ACKNOWLEDGEMENTS .....	73
9.	EIDESSTATTLICHE VERSICHERUNG – DECLARATION ON OATH.....	74
10.	PUBLICATIONS.....	75
I.	MVA-based vaccine candidates encoding the native or prefusion-stabilized SARS-CoV-2 spike protein reveal differential immunogenicity in humans .....	75
II.	Identification of a spike-specific CD8 <sup>+</sup> T cell epitope following vaccination against the Middle East respiratory syndrome coronavirus in humans.....	100
III.	SARS-CoV-2-specific cellular response following third COVID-19 vaccination in patients with chronic lymphocytic leukemia.....	119
IV.	SARS-CoV-2 specific cellular response following COVID-19 vaccination in patients with chronic lymphocytic leukemia.....	125
V.	SARS-CoV-2-specific Humoral and T cell Immune Response After Second Vaccination in Liver Cirrhosis and Transplant Patients.....	133
VI.	Stabilized recombinant SARS-CoV-2 spike antigen enhances vaccine immunogenicity and protective capacity .....	154



## 1. INTRODUCTION

### 1.1. Emerging infectious diseases (EID)

Emerging infectious diseases (EIDs) pose a serious threat to human health worldwide. An EID is defined as an infectious disease that appears in the human population for the first time or that has existed but is rapidly spreading to a new population or geographic region<sup>1</sup>. Most EIDs are of zoonotic origin and are transmitted to humans in a direct spillover event from an animal source or via an intermediate host. Viruses are often the cause of EIDs, as they can acquire the ability to infect humans and be transmitted between humans through viral evolution and recombination events<sup>1</sup>. Since 2002, at least 30 newly emerging pathogens have been identified in humans (Figure 1, blue<sup>2</sup>). The incidence of EIDs has increased in recent years. This increase is primarily the consequence of human action<sup>3</sup>: (1) Global warming alters habitats and increases the geographical range of vectors. Recent cases of locally transmitted chikungunya virus (CHIKV) and dengue virus (DENV) in Europe are examples of vector-borne diseases that are not confined to tropical areas anymore<sup>4-6</sup>. (2) Population growth and closer contact with the habitat of wild animals and between humans increase the risk of spillover, as highlighted by the Ebola outbreaks<sup>7</sup>. (3) Increased mobility and international travel have facilitated the rapid global spread of respiratory EIDs, as became apparent with the 2009 H1N1 influenza<sup>8</sup> and the recent COVID-19 pandemic.

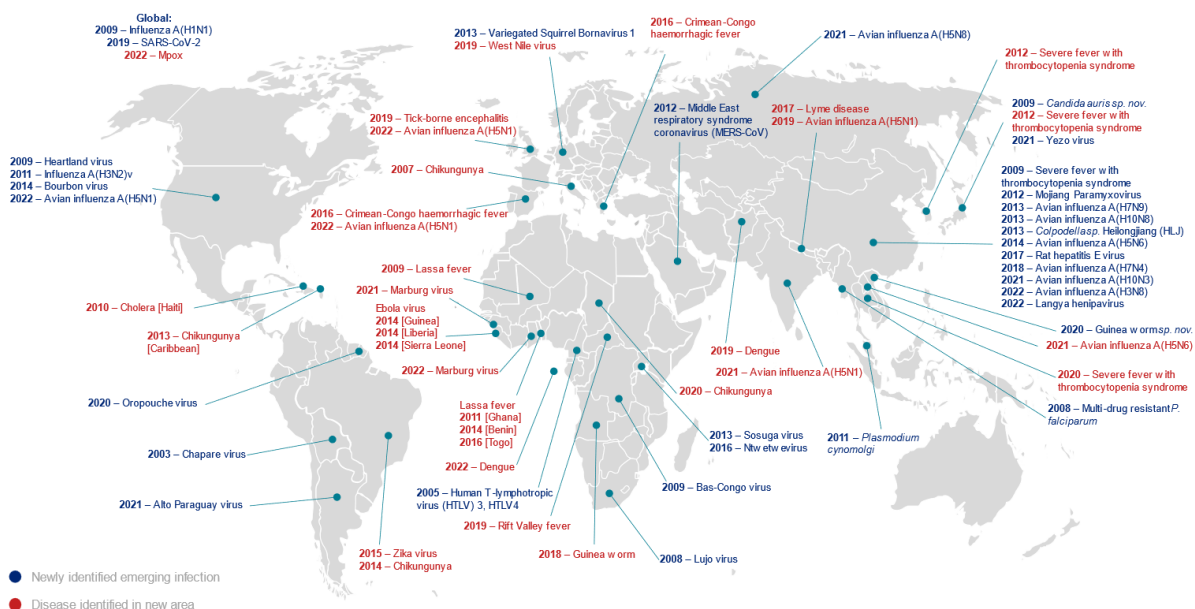


**Figure 1: World map of emerging infectious diseases (EIDs) since 2003.** Newly identified EIDs (blue) and diseases previously described but identified in a new geographical area (red). Figure from UK Health Security Services<sup>2</sup>.

Pathogens that are newly emerging are a particular threat to the human population due to the lack of natural immunity<sup>9</sup>. To anticipate and mitigate the detrimental outcomes of EIDs, the World Health Organization (WHO) has created a roadmap for research and development<sup>10</sup>. The aim is to accelerate the development of diagnostic tests, medicines, and vaccines against priority EIDs that pose the greatest public health risk owing to their epidemic potential and lack of countermeasures<sup>10,11</sup>. This list of EIDs currently includes: Crimean-Congo hemorrhagic fever, Ebola and Marburg virus diseases, Lassa fever, Nipah and henipaviral diseases, Rift Valley fever, Zika fever, diseases caused by so far unknown EIDs (“disease X”) and respiratory disease caused by three coronaviruses (CoVs): Middle East respiratory syndrome (MERS)-CoV, severe acute respiratory syndrome (SARS)-CoV, and SARS-CoV-2.

### 1.1.1. Coronaviruses

Coronaviruses (CoVs) of the subfamily *Coronavirinae*, in the family *Coronaviridae* and order *Nidovirales*, are highly diverse, enveloped, single-stranded, positive-sense, RNA viruses<sup>12</sup>. The CoV genome of 26 to 32 kb is unusually large for an RNA virus. It consists of two open reading frames (ORF 1a and 1b) encoding nonstructural proteins required for replication<sup>13</sup>. The remaining ORFs encode four structural proteins, namely the spike, envelope, membrane, and nucleocapsid proteins, as well as accessory proteins involved in innate immune evasion (Figure 2)<sup>13</sup>. The spike molecules form the characteristic surface structure resembling a corona. They are responsible for viral entry into host cells. The spike consists of two subunits: the receptor-binding S1 subunit and the membrane-fusion S2 subunit<sup>14</sup>. The spike is expressed on the viral membrane as a pre-fusion trimeric structure, where the S2 subunits form the stalk and the S1 subunits form the head (Figure 2)<sup>15</sup>. Upon receptor binding, the spike must be cleaved by host proteases at the S1/S2 and S2' cleavage sites to facilitate membrane fusion, which renders the spike in a post-fusion conformation<sup>16,17</sup>. Owing to its surface exposure and critical function in viral entry, it is an important target of the host immune response<sup>14</sup>.

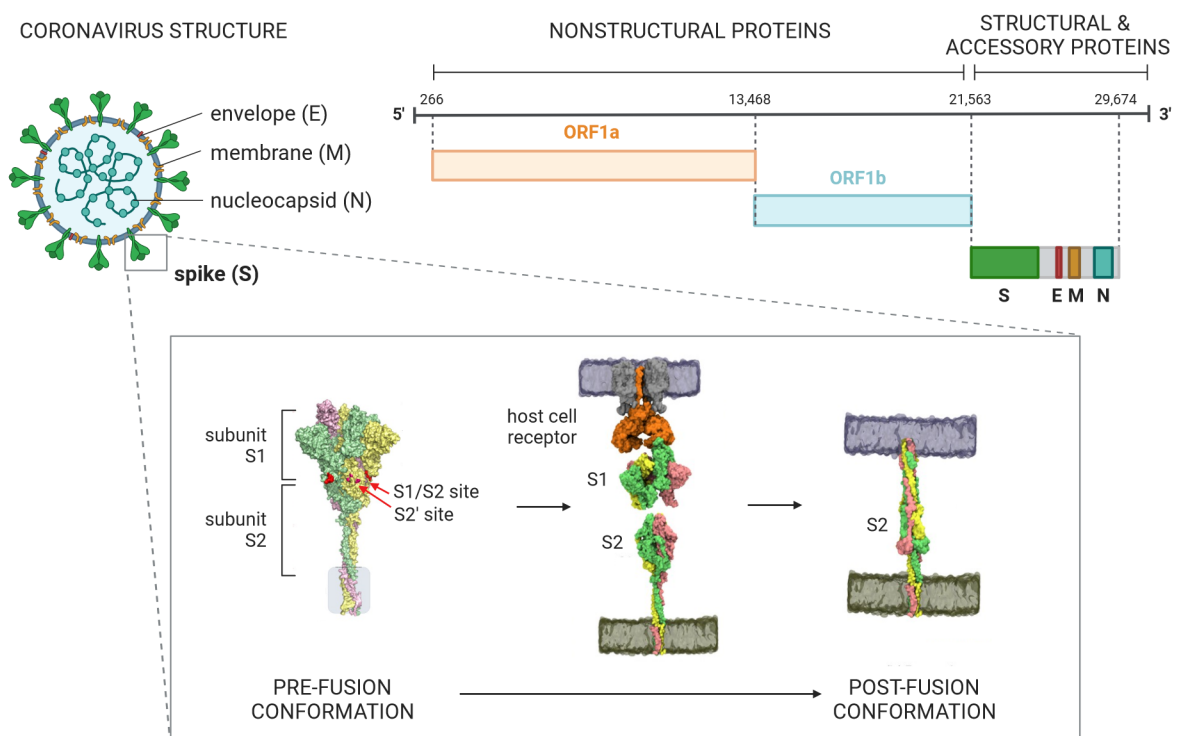


**Figure 2: Structure, genome organization, and spike conformations of CoVs.** The coronavirus genome (top right) consists of ORF1a and ORF1b encoding for nonstructural proteins. The remaining ORFs encode for accessory proteins and the structural proteins: spike (S), envelope (E), membrane (M), nucleocapsid (N), shown on the left. The spike, in its membrane-bound, pre-fusion conformation, consists of the receptor-binding S1 subunit and the S2 subunit mediating membrane fusion (bottom). Upon binding to the host cell receptor, the spike is cleaved by proteases at the S1/S2 and S2' sites. The S1 subunit dissociates and the S2 subunit adopts a post-fusion conformation. This figure was created by Leonie Mayer using Biorender, adapted from Raghuvamsi et al.<sup>16</sup>

CoVs are divided into four genera: *Alphacoronavirus*, *Betacoronavirus*, *Gammacoronavirus*, and *Deltacoronavirus*. Gammacoronaviruses and deltacoronaviruses mostly infect avian species, and some can also infect mammals<sup>18</sup>. Alphacoronaviruses and betacoronaviruses infect only mammals. They cause respiratory disease in humans and cause gastroenteritis in animals, including livestock<sup>19,20</sup>. The expression and distribution of host receptors determines viral tropism, host range and also, in part, explains the differential pathogenicity of CoVs<sup>13,21,22</sup>.

To date, four endemic human CoVs (HCoVs) have been described: HCoV-OC43<sup>23</sup>, -229E<sup>24</sup>, -NL63<sup>25</sup>, and -HKU1<sup>26</sup> (Figure 3, orange). They are transmitted via aerosols and mostly cause mild respiratory disease in immunocompetent hosts<sup>27</sup>. However, in the past two decades, three epidemic betacoronaviruses causing more severe disease in humans have emerged<sup>21,28</sup>: SARS-CoV, MERS-CoV, and SARS-CoV-2 (Figure 3, red).

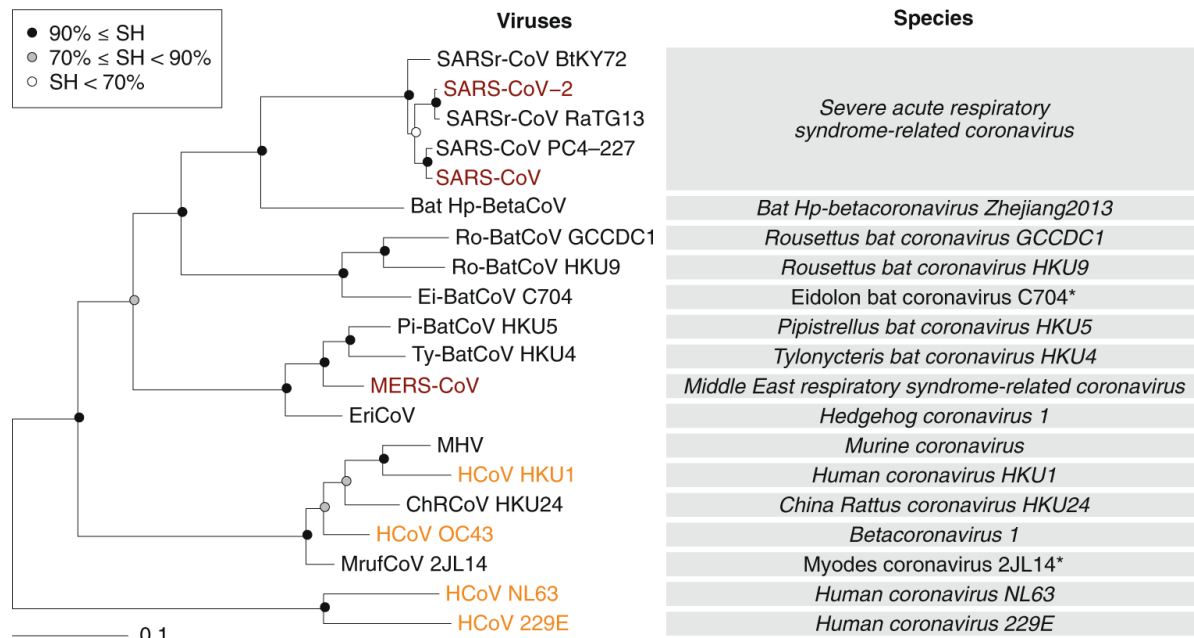


**Figure 3: Phylogenetic tree of representative alpha- and betacoronaviruses.** Shown are five single viruses of the *Severe acute respiratory syndrome-related coronavirus* species and further 13 representative betacoronaviruses, as well as the two human alphacoronaviruses (HCoV-NL63, HCoV-229E). Endemic HCoVs are highlighted in yellow and epidemic HCoVs in red. Asterisks denote species names with pending approval from the International Committee on Taxonomy of Viruses (ICTV). Percentage of sequence homology is shown in white, grey, and black circles. This figure was created by the Coronaviridae Study Group of the ICTV using IQ-TREE maximum likelihood<sup>27</sup>.

### 1.1.2. Emerging human coronaviruses

SARS-CoV was first isolated in 2002 from a patient in Guangdong Province, China<sup>29,30</sup>. It caused a total of 8096 reported SARS cases with 774 deaths (case fatality rate (CFR) ~ 10%)<sup>31</sup>. SARS-CoV uses angiotensin-converting enzyme 2 (ACE2) as a receptor infecting mainly type II pneumocytes and ciliated bronchial epithelial cells leading to a disease that manifests mostly in the lower respiratory tract<sup>32</sup>. SARS-CoV is thought to have been first transmitted to humans from infected palm civets and was then spread between humans via aerosol transmission<sup>22</sup>. Since viral shedding occurred only after symptom onset when patients were already seeking medical attention, most transmissions occurred in hospitals<sup>33</sup>. Through the isolation of patients and other non-pharmaceutical measures, the epidemic was contained within one year and no cases have been reported since 2004<sup>33</sup>.

MERS-CoV was first isolated from a patient in Saudi Arabia in 2012<sup>34</sup>. Between 2012 and 2023, 2605 MERS cases and 936 deaths (CFR ~ 36%) were reported<sup>35</sup>. MERS-CoV uses dipeptidyl peptidase 4 (DPP4) as a receptor, infecting type II pneumocytes and unciliated bronchial epithelial cells of the lower respiratory tract<sup>36</sup>. MERS-CoV is the most lethal and least transmissible of the three epidemic HCoVs<sup>37</sup>. Nonetheless, MERS-CoV-specific T cell responses have been measured in people in the absence of disease or antibody titers, highlighting that the number of MERS-CoV infections is likely underestimated<sup>38-40</sup>. MERS-CoV is endemic to dromedary camels, which transmit the virus to humans via close contact<sup>41,42</sup>. Most MERS cases have thus been geographically restricted to the Arabian Peninsula and mainly affect camel workers, but exported cases have also caused nosocomial outbreaks

in other countries<sup>35,43</sup>. In fact, approximately half of the reported cases in larger outbreaks resulted from human-to-human transmission<sup>44</sup>. In contrast to SARS-CoV, MERS-CoV still infects humans sporadically, as infected dromedary camels continuously shed the virus from nasal secretions without having clinical symptoms<sup>37</sup>.

SARS-CoV-2, the causative agent of Coronavirus Disease-2019 (COVID-19)<sup>28</sup>, was first reported in December 2019 in Wuhan, China<sup>45</sup>. SARS-CoV-2 shares 80% sequence homology with SARS-CoV and 50% sequence homology with MERS-CoV<sup>46</sup>. The sequence of the SARS-CoV-2 spike is 76% and 35% similar to the SARS-CoV and MERS-CoV spikes, respectively<sup>47</sup>. SARS-CoV-2 uses the same receptor as SARS-CoV, namely ACE2, for viral entry<sup>48</sup>. It mostly causes upper respiratory infections; however, severe pneumonia as a consequence of lower respiratory tract infection and immunopathology can occur. The mechanisms of pathology have been reviewed in detail elsewhere<sup>49</sup>. SARS-CoV-2 is more transmissible than SARS-CoV and MERS-CoV<sup>50</sup>. In particular, viral shedding from asymptomatic carriers or before symptom onset made it difficult to contain the initial outbreak<sup>51</sup>. The virus spread rapidly across the globe, and in early 2020, the WHO declared a public health emergency of international concern (PHEIC). The COVID-19 pandemic has had tremendous effects, not only on health but also socially and economically. Three years later, the PHEIC was declared over<sup>52</sup>, and the virus was projected to transition into endemicity<sup>53,54</sup>. During the pandemic, SARS-CoV-2 has undergone viral evolution, with the emergence of several variants characterized by higher transmissibility and immune escape mutations in the spike protein. The evolutionary trajectory and epidemiology of the different variants have been reviewed elsewhere<sup>55</sup>.

SARS-CoV, MERS-CoV, and SARS-CoV-2 all have their evolutionary roots in animal CoVs<sup>22,56</sup>. Several phylogenetically related CoVs have been isolated from bats and have been shown to coexist within the same bat population<sup>57-59</sup>. It is likely that their progenitor virus was produced by recombination in bats and acquired further mutations in the intermediate host before spillover to humans<sup>22</sup>. While the epidemiological link between bat CoVs and SARS-CoV-2 has not yet been found, SARS-CoV-2 has 96% genome sequence identity with the bat coronavirus RaTG13<sup>60</sup>. Bats are well-known natural reservoirs of emerging viruses. Pathogens that cause disease in humans and originate from bats include the Hendra virus, Nipah virus<sup>61</sup>, Ebola virus<sup>62</sup>, and Marburg virus<sup>63</sup>. Studies using next generation sequencing have shown that bats also carry a large variety of CoVs<sup>64,65</sup> with promiscuity for receptor usage<sup>60,66,67</sup>. Overall, with the potential for adaptive mutation and recombination between these bat CoVs in combination with human behavior (e.g., closer proximity to natural habitats), the emergence of novel CoVs in the human population is expected in the future. This threat to global health underscores the need for improved surveillance and pandemic preparedness against emerging CoVs, including the need for vaccine development.

## **1.2. Vaccine development against EIDs**

Vaccination is one of the most effective public health measures, having dramatically improved health outcomes and prolonged life expectancy worldwide<sup>68</sup>. In particular, prophylactic vaccination against infectious diseases such as diphtheria, polio, measles, pertussis, and meningitis has substantially reduced childhood mortality<sup>69</sup>. According to the WHO, 2 to 3 million lives are saved annually due to existing vaccination programs<sup>70</sup>. If the goals of the Immunization Agenda 2030 are met, an estimated 51.5 million deaths will be averted between 2021 and 2030<sup>71,72</sup>. New vaccines that received licensure in 2023 were the first vaccines against respiratory syncytial virus (RSV) and CHIKV<sup>73,74</sup>. Promising vaccine candidates on the horizon include those against human cytomegalovirus (HCMV)<sup>75</sup>, while vaccine development against diseases such as HIV infection, malaria, and tuberculosis remains a challenge<sup>76</sup>.

Vaccines are a cornerstone of pandemic preparedness. The sooner a vaccine can be employed, the faster the EID outbreak can be controlled<sup>77</sup>. However, time is a major challenge as the traditional vaccine development cycle takes several years. To overcome this, early-stage clinical development must be completed before the emergence of the pathogen such that efficacy testing of the vaccine can be initiated when there is an outbreak.

Prophylactic vaccines exploit the ability of the immune system to remember encountered pathogens and respond more efficiently to them upon subsequent re-exposure<sup>78</sup>. To do so, they contain the pathogen or an antigenic part, which can induce a strong immune response without causing disease. Historically, vaccines against infectious diseases caused by viruses have been developed empirically, mostly using whole viruses that are either live attenuated or inactivated (whole virus vaccines; Figure 4, left). Recombinant technologies have spurred the development of subunit vaccines containing antigenic proteins of viruses that are produced in cell culture<sup>79</sup> (subunit vaccines; Figure 4, right). Some subunit vaccines consist of proteins that can self-assemble into virus-like particles that mimic the viral surface structure<sup>80</sup>.

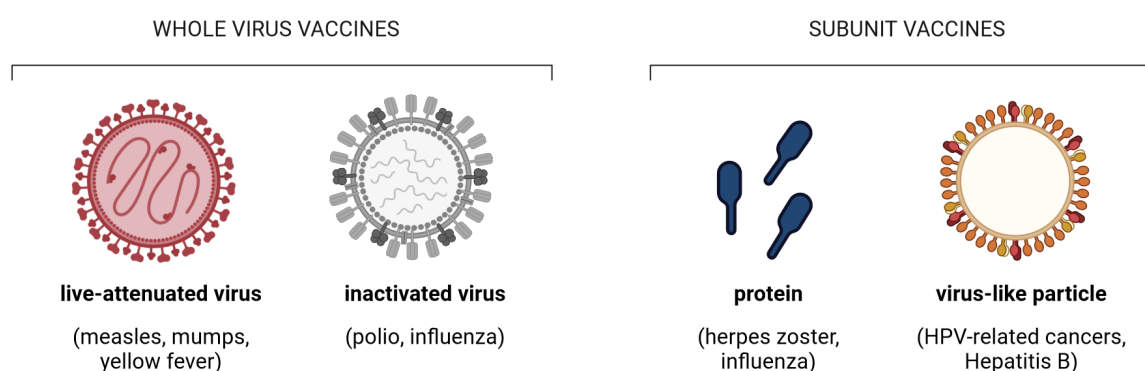


**Figure 4: Whole virus and subunit vaccines.** Examples of licensed live-attenuated vaccines include those against measles, mumps and yellow fever. Inactivated vaccines include the inactivated poliovirus vaccine and several vaccines against influenza. Protein vaccines have been developed, e.g. against herpes zoster and influenza. The two licensed virus-like particle vaccines are against human papillomavirus (HPV)-related cancers and Hepatitis B. This figure was created by Leonie Mayer using BioRender.

### 1.2.1. Vaccine platforms

The development of next-generation vaccine is based on so-called “vaccine platforms”, which use nucleic acids to deliver the vaccine antigen within a delivery system<sup>81</sup>. This can be in the form of a transgene inserted into a viral vector (viral vector vaccines; Figure 5, left), messenger RNA (mRNA) encapsulated into a lipid nanoparticle (LNP), or DNA as a plasmid (nucleic acid vaccines; Figure 5, right).

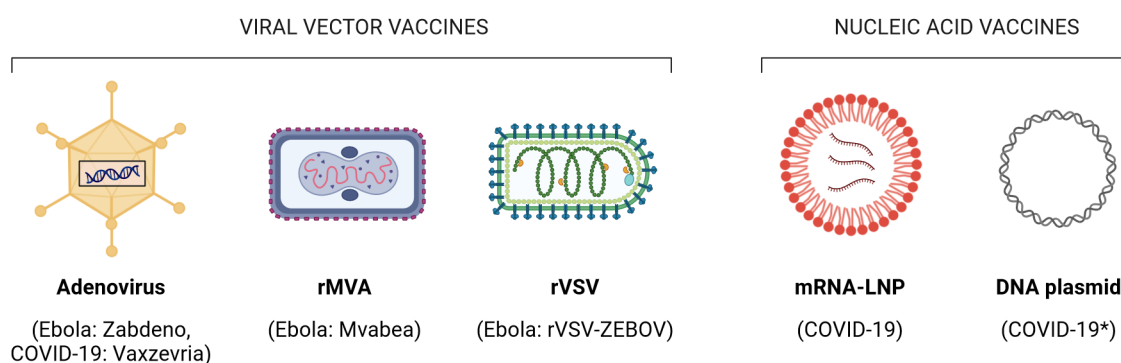


**Figure 5: Vaccine platforms used in licensed human vaccines.** Licensed viral vectors include different adenoviruses (against Ebola and COVID-19), as well as recombinant modified vaccinia virus Ankara (rMVA) and recombinant vesicular stomatitis virus (rVSV) (both against Ebola virus disease). Nucleic acid vaccines consist either of mRNA molecules encapsulated by lipid nanoparticles (LNPs) or DNA plasmids. mRNA have been licensed against COVID-19. \*DNA vaccines have not been licensed yet. This figure was created by Leonie Mayer using BioRender.

These vaccine platforms have the advantage that they can be readily adapted to deliver a novel antigen in the case of a newly emerging pathogen. While the design of traditional vaccines can take several years, antigens in the form of nucleic acids can be designed within days and evaluated more easily owing to previous (pre-)clinical experience with the vaccine platform<sup>82</sup>. This became evident during the COVID-19 pandemic, when several effective vaccines were developed and licensed within a year. The first licensed COVID-19 vaccines in the EU were viral vectors and mRNA-based vaccines<sup>83</sup>.

Several viruses have been engineered to serve as vaccine vectors against infectious diseases<sup>75</sup>. The choice of virus is mainly based on the available human safety data of the virus, ease of manufacturing, ability to efficiently express a foreign antigen, tropism for various cell types, and lack of pre-existing immunity<sup>84</sup>. To date, four viral vectors have been licensed in infectious disease vaccines for human use in the EU and/or USA: Adenovirus type 26 vector against Ebola (Ad26.ZEBOV)<sup>85</sup> and COVID-19 (Ad26.COVS.S)<sup>86</sup>, the engineered chimpanzee adenoviral vector ChAdOx1 against COVID-19 (ChAdOx1 nCoV-19)<sup>87</sup>, the recombinant vesicular stomatitis virus against Ebola (rVSV-ZEBOV)<sup>88</sup>, and the recombinant Modified Vaccinia virus Ankara (rMVA) poxviral vector against Ebola (MVA-BN-Filo)<sup>85</sup>. Several other viral vectors are in (pre-)clinical development, such as integrase-defective lentiviral vectors, adeno-associated viruses, and the recombinant measles virus<sup>75</sup>.

The mRNA vaccine platform has been in development for a long time<sup>89</sup>, but it was not until the COVID-19 pandemic that the first two mRNA-based vaccines were licensed for use in humans<sup>90,91</sup>. The mRNA vaccines contain synthetic mRNA molecules that encode the vaccine antigen<sup>92</sup>. These mRNA molecules are produced from a DNA template during an *in vitro* transcription process. The mRNA is nucleoside-modified to dampen excessive innate immune sensing and is optimized with noncoding sequences to enhance *in vivo* translation<sup>93</sup>. The mRNA molecules are formulated inside lipid nanoparticles to enable cell entry *in vivo*<sup>94</sup>. Several other mRNA-based vaccine candidates are in development, the most advanced candidates against RSV (NCT05127434) and HCMV (NCT05085366)<sup>95</sup>.

### 1.2.2. Characteristics of mRNA and viral vector platforms

Viral vectors and mRNA technology have several technological advantages, making them ideal platforms for rapid vaccine development against emerging infections<sup>77</sup>: (1) Optimization of the development cycle and safety testing of the platform can partially be done independent of the pathogen of concern. (2) The production process can be standardized and does not require biosafety level manufacturing plants, in contrast to the production of inactivated or live-attenuated viral vaccines. (3) Platforms are rapidly adaptable to recombinantly express antigens from newly emerging pathogens. (4) They do not require additional adjuvants because both mRNA and viral vectors have intrinsic adjuvant properties. (5) They can be easily administered, for example, by intramuscular or subcutaneous injection, in contrast to DNA vaccines that require electroporation devices<sup>77</sup>.

Additionally, viral vectors and mRNA vaccines mirror some immunological advantages of live-attenuated vaccines. Live-attenuated vaccines against smallpox, yellow fever, and measles are considered some of the most effective vaccines. This may, in part, be explained by the fact that they closely resemble natural infection<sup>96</sup>. Following vaccination, they effectively stimulate the innate immune system, which engages both the humoral and cellular arms of the adaptive immune response. It has been shown that live vaccines elicit potent CD8+ T cell responses, which are important effectors to confer protection against intracellular pathogens. Subunit vaccines, in contrast, have the limitation that they mostly elicit an antibody response but little immune memory without the addition of adjuvants<sup>96</sup>. Viral vectors and mRNA vaccines partially overcome these limitations. One of the main immunological rationales for developing viral vector vaccines is that they can deliver antigens in a way that can induce CD8+ T cell responses<sup>97</sup>. The following chapter describes how T cell immunity develops upon exposure to vaccination and protects against infections.

### 1.3. Vaccine-induced immunity

#### 1.3.1. From innate to adaptive immune responses

Vaccination is based on the ability of the immune system to remember an encountered pathogen by mounting a long-term immune response against its antigens<sup>78</sup>. The immune response consists of two branches: the innate and adaptive immune responses. The innate response is non-specific and involves the action of phagocytic cells (neutrophils, macrophages, and natural killer cells), secretion of inflammation mediators (e.g. cytokines), and antigen presentation (discussed later)<sup>98</sup>. In turn, the adaptive response is highly specific, adaptable, and has the ability to “remember” antigens. It consists of the action of lymphocytes, particularly memory B and T cells, and antibody-secreting plasma cells<sup>99</sup>. The innate and adaptive responses are connected as shown in Figure 6 and described below:

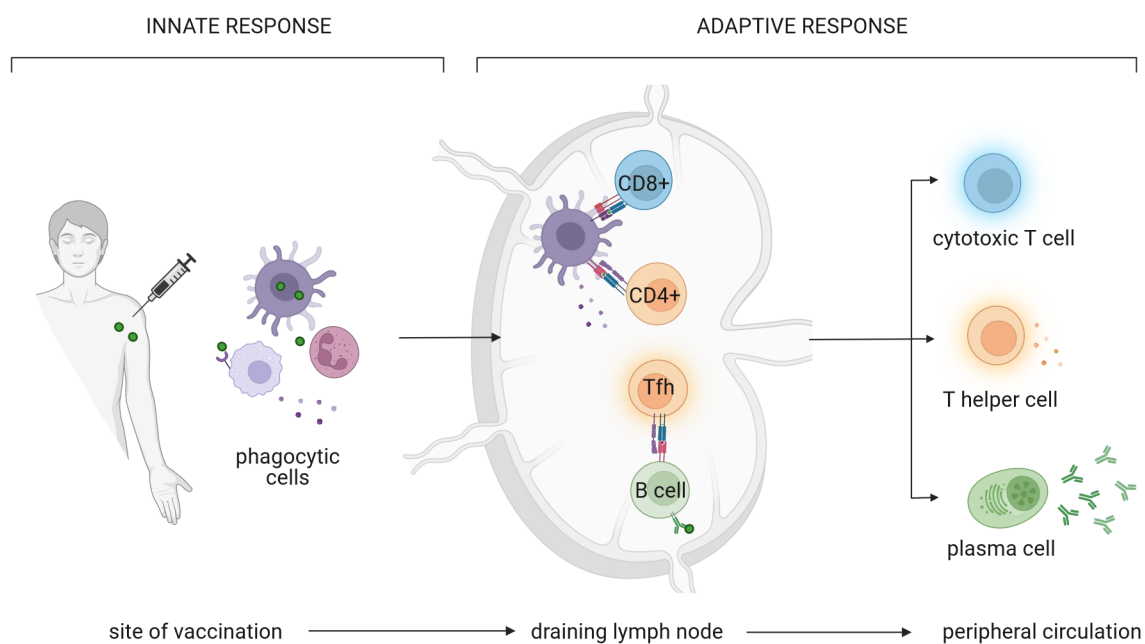


**Figure 6: Innate and adaptive immune response following vaccination.** Phagocytic cells at the site of vaccination engulf the antigen and circulate to the draining lymph node where they present it in the form of peptides to CD4+ and CD8+ T cells of the adaptive immune system. T follicular helper cells aid in the induction of a B cell response. Activated T cells and antibody-secreting plasma cells leave the lymph node and circulate through the periphery. This figure was created by Leonie Mayer using BioRender.

In brief, the induction of an antigen-specific immune response following vaccination unfolds as follows: Innate cells are activated by danger signals, triggering cytokine secretion and local inflammation at the site of vaccination<sup>78</sup> (Figure 6, left). Danger signals can be pathogen-associated patterns (PRRs) on live-attenuated or inactivated vaccines<sup>100,101</sup> or other inflammatory signals induced by vaccine adjuvants in subunit vaccines<sup>102</sup>. The most commonly used vaccine adjuvant is alum, which activates several innate pathways, including the inflammasome<sup>103,104</sup>. Other adjuvant systems, such as combinations of oil-in-water emulsions and alum or synthetic ligands of innate receptors, have been developed and licensed for several vaccines<sup>105–108</sup>. The mRNA vaccines have intrinsic adjuvant properties because nucleic acids are sensed by several PRRs<sup>94,109</sup>. Viral vector vaccines, such as attenuated or inactivated viral vaccines, also activate several pathways of the innate response through PRR sensing<sup>110,111</sup>. Overall, the type of adjuvant affects innate activation, which in turn shapes the adaptive response<sup>96,112</sup>. Thus, adjuvant properties are an important consideration in vaccine design<sup>113</sup>. The vaccine antigens are then taken up by innate cells and delivered to the draining lymph node, the site of induction of the adaptive response (Figure 6, center).

Antigens are presented on major histocompatibility complex (MHC) molecules in the form of short peptides to naïve T cells that differentiate into CD8+ cytotoxic T cells, CD4+ T helper cells and T follicular helper cells (discussed in detail later)<sup>114</sup>. B cells recognize antigens through their B cell receptor, and with the stimulatory help of T follicular helper cells, they differentiate into antibody-secreting plasma cells<sup>115</sup>. The generation of a highly specific and effective B cell response includes several complex maturation steps, which are not the focus of this thesis but are reviewed in detail elsewhere<sup>78,116</sup>. The adaptive immune response increases in magnitude, specificity, and effector function with successive exposure. This ability is exploited by prophylactic vaccination, building a strong memory response that can be activated more quickly in the case of an infection<sup>78</sup>.

T cells are an important arm of the vaccine-induced immune response and are the focus of this thesis. They play a dual role in the vaccine-induced immune response. They provide stimulatory help to the B cell response and exert effector functions to eliminate infected cells<sup>78</sup>. Following development, antigen-exposed T cells can exert effector functions and form immune memory. The general mechanisms of this process are described below.

### 1.3.2. T cell development

T lymphocytes originate from hematopoietic stem cells that reside in the bone marrow, where they differentiate into lymphoid progenitor cells and migrate to the thymus. The thymus is the primary site of T cell development, also known as thymopoiesis, with various cell types coordinating this process<sup>117</sup>. Early immature T cells called thymocytes undergo a series of maturation and selection steps, resulting in a pool of naïve T cells as outlined in Figure 7.

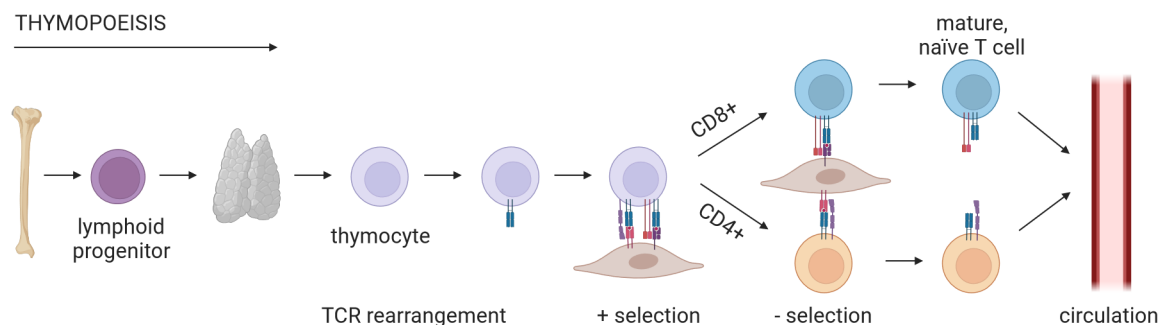


**Figure 7: Thymopoiesis.** Lymphoid progenitors from the bone marrow mature in the thymus by generation of TCRs, positive selection, lineage commitment and negative selection. Mature, naïve CD4+ and CD8+ T cells leave the thymus and circulate through the periphery. This figure was created by Leonie Mayer using BioRender.

During this process, thymocytes commit to the CD4+ or CD8+ lineages. The genetic mechanisms by which this lineage is determined are not fully understood and have been reviewed elsewhere<sup>118,119</sup>. Furthermore, T cell receptors (TCRs) are generated. TCRs are distinct surface molecules of T cells that can recognize antigens in the form of peptides. They consist of an alpha and beta chain, which form a constant region proximal to the cell membrane and a hypervariable region for antigen recognition<sup>120</sup>. TCRs are produced early in T cell development by somatic V(D)J recombination, the process of rearrangement of TCR gene loci. This results in a large pool of thymocytes that express unique clonal TCRs. Next, rounds of positive and negative selection take place to select thymocytes expressing TCRs that are functional, but also to eliminate those that are self-reactive. During positive selection, cortical epithelial cells provide survival signals only to thymocytes that express TCRs, which can bind self-MHC molecules with a high affinity. Subsequently, antigen-presenting cells negatively select self-reactive thymocytes by providing apoptotic signals to cells that can bind MHC molecules loaded with self-peptides with too high affinity<sup>114</sup>. The result is a pool of mature naïve T cells, each expressing unique TCRs that leave the thymus and circulate through the lymphatic system and peripheral blood scouting for foreign antigens.



The collection of all the unique TCRs expressed by one human is referred to as the TCR repertoire. Because TCRs are produced by stochastic gene arrangements, each human has a unique TCR repertoire, much like a fingerprint. A human TCR repertoire consists of approximately  $2 \times 10^7$  unique TCRs that can recognize an enormous number of antigens<sup>121</sup>. To add complexity, recent studies have shown that a single TCR can recognize multiple antigens and that a single antigen can be recognized by multiple TCRs. Although thymic output declines with age, humans maintain a large naïve T cell pool throughout life by homeostatic proliferation, which allows them to respond to novel antigens even at an old age. The mechanism by which a T cell response is elicited upon encounter of a foreign antigen is described in detail below.

### 1.3.3. Dynamics of the T cell response

The developmental path of a naïve T cell that recognizes a foreign antigen towards T cell memory and reactivation can be divided into different stages (Figure 8): (1) Upon antigen encounter, naïve T cells are activated and expand clonally. (2) Activated T cells differentiate into effector cells and migrate to the site of infection or vaccination. (3) Following antigen clearance, the T cell response contracts, stabilizes, and a small pool of antigen-specific memory T cells are maintained. (4) Memory T cells are re-activated upon re-exposure with the antigen and react with a more efficient secondary recall response<sup>99</sup>. In the following sections these four stages of the T cell development path are described in detail:

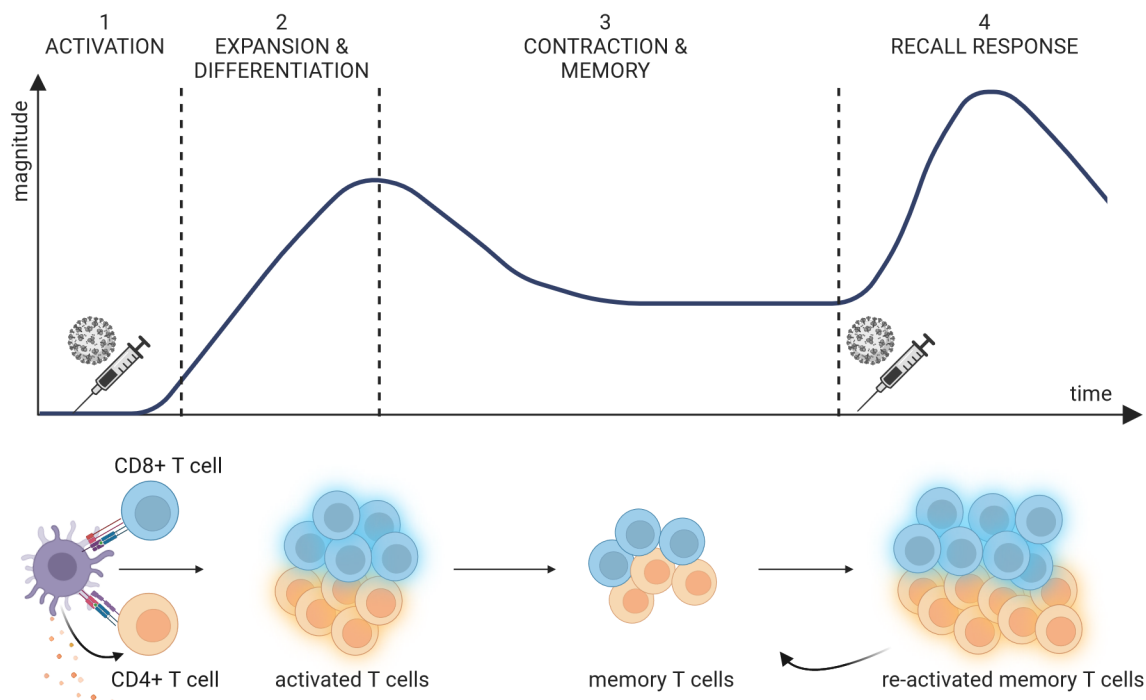


**Figure 8: Dynamics of the T cell response following vaccination and/or infection.** (1) T cells are activated upon antigen presentation, (2) clonally expand and differentiate into effector T cells. (3) Once antigen is cleared, the T cell response contracts and a pool of long-lived memory cells remains, which is activated more quickly in a (4) recall response upon secondary antigen exposure. This figure was created by Leonie Mayer using BioRender.

#### 1) Activation

Priming of the T cell response occurs in draining lymph nodes. Antigen-presenting cells (APCs) take up foreign antigens at the site of infection or vaccination and digest the antigen into short peptides. They then circulate to the draining lymph node, where they present these peptides loaded onto MHC molecules to T cells<sup>122</sup>. CD4+ T cells can only recognize peptides presented by MHC class II molecules. CD8+ T cells are restricted to recognizing peptides presented by MCH class I molecules<sup>123</sup>. The MHC

locus is the most polymorphic region in the human genome<sup>120</sup>. MHC alleles differ structurally in their peptide-binding groove, indicating that the allelic variation modulates the repertoire of peptides that can be presented by different individuals<sup>124</sup>.

Endogenous antigens are presented via the MHC class I pathway (Figure 9, left). They are derived from a pathogen or a vaccine that enters the cell, are digested by cytosolic proteases, and are loaded onto MHC class I molecules<sup>123</sup>. All nucleated cell types in the body express MHC class I molecules, and can thus present antigens to CD8+ T cells. MHC class I molecules have a closed binding groove that limits the size of the peptides they can bind to 8-10 amino acids<sup>124</sup>. Exogenous antigens are presented via the MHC class II pathway (Figure 9, right). They are endocytosed by APCs, digested in lysosomes and loaded onto MHC class II molecules<sup>123</sup>. Typically, only macrophages, dendritic cells, and B cells (also known as professional APCs) express MHC class II molecules and can present antigens to CD4+ T cells. MHC class II molecules have an open binding groove that can accommodate peptides that are 13-25 amino acids long<sup>124</sup>. Interestingly, dendritic cells can also load peptides derived from exogenous antigens onto MHC class I molecules in a process called cross-presentation<sup>125,126</sup>. This is important for mounting a CD8+ T cell response against pathogens that do not directly infect APCs and against exogenous antigens that are delivered by subunit vaccines.

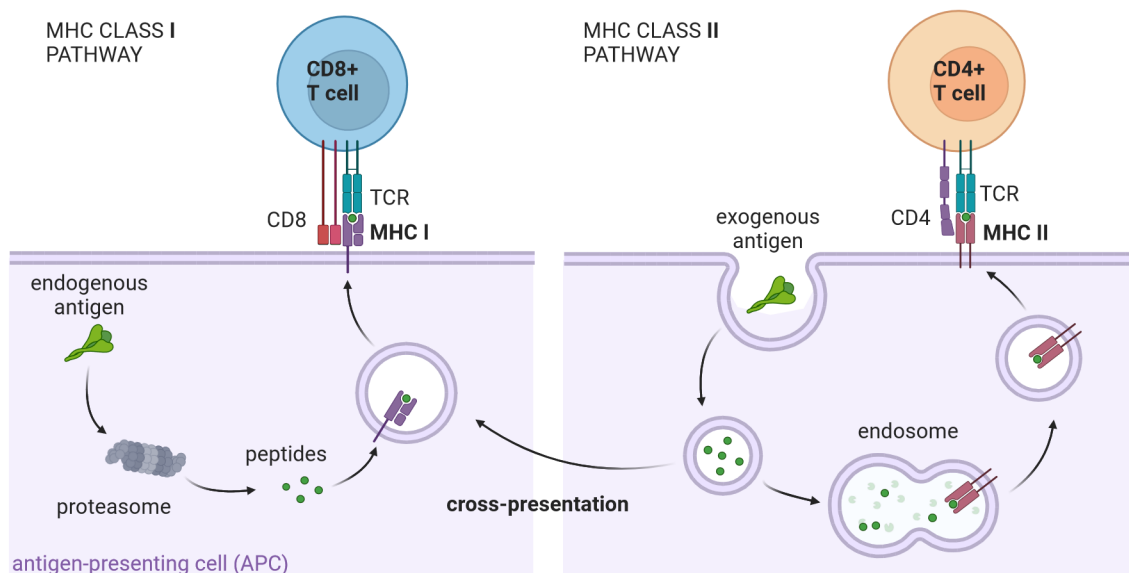


**Figure 9: Induction of a T cell response via antigen presentation.** MHC class I pathway: Endogenous antigen is digested into peptides in the host protease, loaded onto MHC class I molecules, and presented to CD8+ T cells. MHC class II pathway: Exogenous antigen is ingested via phagocytosis, digested in the endosome, loaded onto MHC class II molecules and presented to CD4+ T cells. Exogenous antigens can also escape the MHC class II pathway and be loaded onto MHC class I molecules in a process called cross-presentation. This figure was created by Leonie Mayer using a BioRender template from Akiko Iwasaki.

Once a T cell recognizes the peptide-MHC complex through its TCR, an immunological synapse is formed between the T cell and APC, and a signaling cascade through the T cell co-receptor, namely cluster of differentiation 3 (CD3), is initiated<sup>114</sup>. This alone does not suffice, but in total, three signals are required for complete T cell activation: 1) recognition of the peptide-HLA complex, 2) engagement of co-stimulatory molecules and their ligands (such as CD28–CD80, CD40–CD154, 4-1BB–4-1BBL, OX40–OX40L and CD27–CD70, and 3) cytokines that drive differentiation (such as type 1 interferons)<sup>127</sup>.

## 2) Expansion and differentiation

Activated T cells clonally expand and differentiate into effector cells with different functions. Studies analyzing smallpox vaccination have shown that clonal expansion usually occurs two to four weeks

after vaccination. Factors that determine burst size, that is, the number of T cell clones generated during expansion, are not well understood<sup>128</sup>. The direction of T cell differentiation is directly modulated by the innate response and thus indirectly linked to the nature of the pathogen or vaccine. Interactions between pathogens and pattern recognition receptors on innate cells result in differential cytokine production. This cytokine milieu drives the polarization of T cells through the regulation of transcription factors. Recent analyses have shown that the TCR sequence of a cell can influence its transcriptional fate<sup>129</sup>. This process ensures that the induced T cell response possesses appropriate effector mechanisms for eliminating pathogens<sup>130</sup>.

Effector T cells are a heterogeneous group of cells that can be classified into several subsets based on cytokine expression regulated by distinct transcription factors. The six major CD4+ T cell subsets are Th1, Th2, Th17, Th9, T follicular helper (Tfh) and induced regulatory T cells (iTregs)<sup>99</sup>. The different functions of these subsets are briefly summarized in Figure 10. The transcriptional, epigenetic, and metabolic mechanisms that orchestrate this differentiation have been reviewed in detail elsewhere<sup>130</sup>.

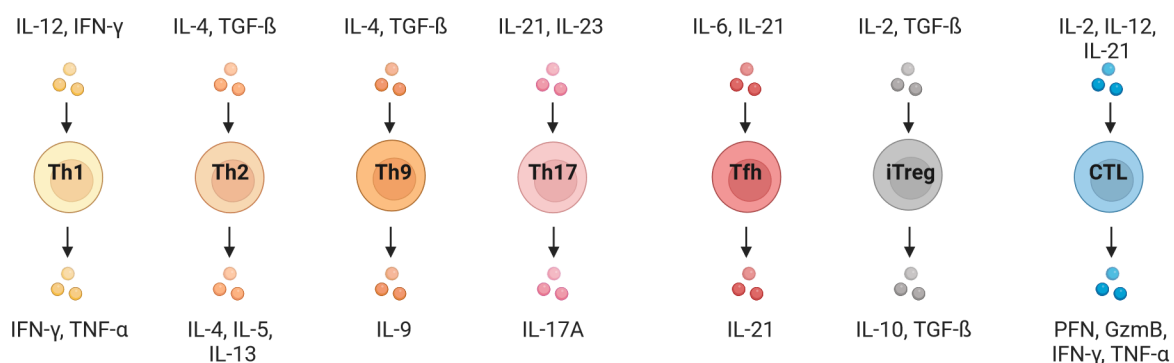


**Figure 10: T cell subsets.** Naïve T cells differentiate in the presence of antigens and cytokines into T helper (Th) 1, Th2, Th9, T follicular helper (Tfh), induced T regulatory cells (iTreg) or cytotoxic T cells (CTL), each with different functions. IL = interleukin, IFN = interferon, TNF = tumor necrosis factor, TGF = transforming growth factor, PFN = perforin, GzmB = granzyme B. This figure was created by Leonie Mayer using BioRender.

The differentiation of naïve T cells into Th1 cells is driven by the interferon gamma (IFN- $\gamma$ ) and interleukin (IL)-12 cytokine milieu. Th1 cells secrete pro-inflammatory cytokines, such as IFN- $\gamma$  and tumor necrosis factor alpha (TNF- $\alpha$ ), which activate phagocytosis and antigen presentation by macrophages, which are important for the clearance of viruses and intracellular bacteria<sup>131</sup>. Th2 cells are induced by IL-4 and transforming growth factor beta (TGF- $\beta$ ) secretion of dendritic cells. Th2 cells produce IL-4, IL-5, and IL-13 which activate eosinophils, mast cells, and basophils, and drive the production of immunoglobulin E (IgE) by B cells, which is necessary for an anti-parasitic immune response. They also facilitate tissue repair and contribute to asthma and allergy<sup>132</sup>. Th9 cells are a newly identified subset that has been described to play a role in allergy, cancer, and autoimmunity. Th9 cells are induced by IL-4 and TGF- $\beta$  and secrete high levels of IL-9. CD4+ T cells differentiate into Th17 cells in the presence of IL-21 and IL-23. They secrete IL-17, which activates the migration of neutrophils to the site of extracellular bacterial or fungal infections. Th17 cells also contribute to the mucosal defense against respiratory pathogens<sup>131</sup>. Tfh cells differentiate in the presence of IL-6 and IL-21 and home to SLOs to support the induction of a B cell response. iTregs respond to proinflammatory signals and regulate overexuberant immune responses by secreting suppressive cytokines IL-10 or TGF- $\beta$ . This “self-check” of the immune response is critical to limit exaggerated inflammatory processes and avoid autoimmunity<sup>131</sup>. CD8+ T cells differentiate into cytotoxic T lymphocytes (CTLs). Like Th1 cells, they secrete the pro-inflammatory cytokines IFN- $\gamma$  and TNF- $\alpha$ . CTLs are essential in the fight against intracellular pathogens. Through Fas/Fas ligand interaction, they can directly induce cell death of infected cells. Furthermore, they generate secretory vesicles containing perforin molecules, which create pores and granzyme proteases that induce apoptosis in the infected cells<sup>133</sup>.

### 3) T cell contraction and memory

As the antigen is cleared, the T cell response contracts and develops into memory. Studies in mice have shown that approximately one-tenth of the T cell effector pool turns into long-lived memory cells<sup>127</sup>. However, the amount of memory cells depends on the burst size of the effector pool and cytokine milieu during the contraction phase<sup>127</sup>. Classically, memory T cells are classified by using a linear differentiation model based on the expression of CCR7 and CD45RA (Figure 11)<sup>134</sup>.

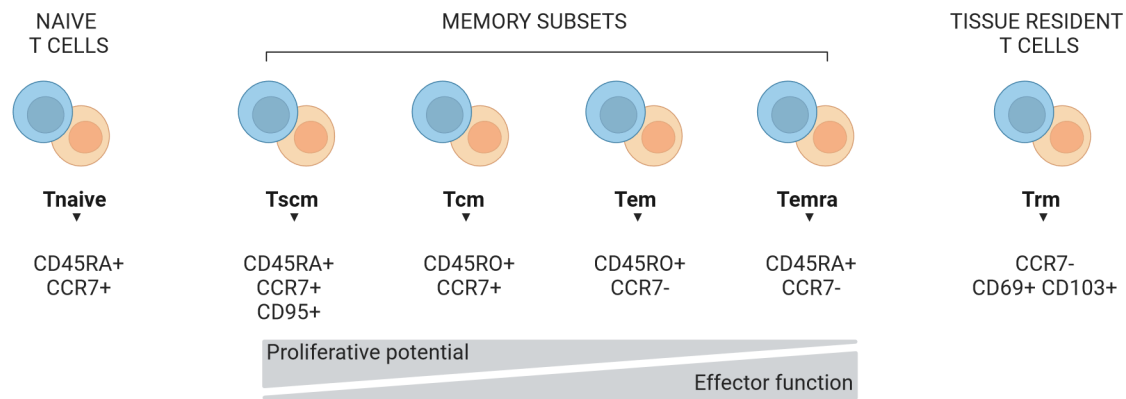


**Figure 11: Memory T cells.** T cell subsets can be distinguished based on the expression of CD45RA/RO and CCR7 surface markers into T cells of naïve ( $T_{naive}$ ), stem-cell memory ( $T_{scm}$ ), central memory ( $T_{cm}$ ), effector memory ( $T_{em}$ ), terminally differentiated ( $T_{emra}$ ) phenotype and based on CD69 and CD103 expression into those of tissue resident ( $T_{rm}$ ) phenotype. This figure was created by Leonie Mayer using BioRender.

Naïve T cells ( $T_{naive}$ ) express the secondary lymphoid organ (SLO)-homing receptor CCR7 and the A isoform of the signaling molecule CD45 (CD45RA). Central memory T cells ( $T_{cm}$ ) express the O isoform of CD45 (CD45RO) as well as the receptors for IL-7 and IL-15 signaling which facilitate survival and homeostatic proliferation. They recirculate to SLOs and have high proliferative potential upon antigen re-encounter. Effector memory T cells ( $T_{em}$ ) also express CD45RO; however, in contrast to  $T_{cm}$ , CCR7 expression is downregulated. They exhibit limited proliferative potential but have a more immediate effector function: they mediate cytotoxicity through various mechanisms, such as secretion of cytokines, chemokines, granzymes, and perforins.  $T_{em}$  that re-express CD45RA ( $T_{emra}$ ) have been considered terminally differentiated effector cells. However, recent findings have challenged this view, showing that  $T_{emra}$  can retain the capacity to self-renew and persist<sup>134</sup>.

Several other memory subsets have recently been defined. This includes  $T_{cm}$  that re-express CD45RA, termed T memory stem cells ( $T_{scm}$ )<sup>135</sup>.  $T_{scm}$  can be distinguished from  $T_{naive}$  by the expression of CD95. They have a superior re-expansion capacity, are maintained long-term, and are thought to be important mediators of long-term immunity after vaccination. Precursors of exhausted T cells ( $T_{pex}$ ) are  $T_{scm}$  identified in persistent and chronic infections as a subset of continuously proliferating T cells that generate exhaustive effector T cells<sup>136</sup>. Tissue-resident memory T cells ( $T_{rm}$ ) were termed following the discovery that the majority of effector memory-like cells reside in non-lymphoid tissues and only a small fraction circulates within the peripheral blood<sup>137–139</sup>. However, studies on their phenotype and function are limited because of the difficulty in accessing the human tissue<sup>137</sup>. Single-cell analyses in recent years have revealed that the memory T cell pool, in reality, does not consist of discrete subsets but rather forms a continuous landscape<sup>140</sup>. In particular,  $T_{ems}$  are highly heterogeneous in their function, phenotype, and localization.

### 4) Recall response

Memory T cells remain quiescent until they are re-exposed to the same antigen. This can be through an infection following vaccination or a second (booster) vaccine dose. A secondary response undergoes

the same three stages of activation, expansion-differentiation, and contraction-memory, but with the difference that expansion is more rapid and effective<sup>78</sup>. Memory T cells that have already acquired effector functions during primary exposure expand rapidly and are ready to act. In addition, the contraction phase is less pronounced, resulting in a larger memory pool after the secondary exposure. This advantage is the basis for prime-boost vaccination and additional booster doses, which enhance the memory response to increase protection<sup>141</sup>.

#### 1.3.4. T cells in vaccine-induced protection

Vaccine efficacy (VE) is a measure of how well a vaccine protects. VE is defined as the percentage reduction of disease cases in the vaccinated group compared to the reduction of disease cases in the unvaccinated (placebo) group<sup>142</sup>. VE can generally only be determined at the last stage of the vaccine development process, in large phase 3, placebo-controlled, clinical efficacy trials. Vaccine effectiveness refers to how well a vaccine protects in a real-world setting when it is administered to the general population<sup>142</sup>. Several highly efficacious vaccines have been licensed and have also proven to be highly effective, but the exact immunological mechanisms by which they provide protection are not fully understood. For most pathogens, it is difficult to define one immunological readout that is responsible for protection, since several functions of the immune system act synergistically<sup>78</sup>. It is easier to search for a biomarker that can be used to predict protection. A so-called “correlate of protection” is an immune marker that correlates with, but is not necessarily responsible for VE<sup>143</sup>. In animal challenge studies, neutralizing antibodies have been shown to correlate with protection against disease caused by arboviruses, including yellow fever<sup>144</sup>, Japanese encephalitis<sup>145</sup>, and tick-borne encephalitis<sup>146</sup>. Recently, it was shown that SARS-CoV-2 neutralizing antibody and spike-specific binding IgG titers both correlate with VE against symptomatic COVID-19<sup>147,148</sup>.

Which type of correlate of protection is relevant depends on how protection is defined. It can be defined as protection against different clinical states, such as VE against infection, symptomatic disease, hospitalization, or death. In theory, high titers of neutralizing antibodies at the site of infection are necessary to protect from infection, referred to as sterilizing immunity<sup>149</sup>. Therefore, antibody titers can be a useful correlate of protection against infection. However, achieving sterilizing immunity through vaccination and maintaining it over time is difficult, specifically for respiratory pathogens. Firstly, most intramuscularly or subcutaneously administered vaccines elicit immune effectors that are systemic and not present at the site of infection, e.g. mucosal antibodies. Secondly, neutralizing antibodies wane over time, and then long-term protection is mediated by the re-activation of memory cells which takes some time<sup>78</sup>. Protection against disease, in turn, is often a more achievable and also more clinically relevant goal of vaccination. To reach this goal the induction of a T cell response is necessary, as T cells can eliminate infected cells before the pathogen starts to replicate. A classic example for the meaning of different correlates of protection in the context of different clinically relevant states is smallpox, an eradicated infectious disease caused by the *Variola virus*. Antibodies are a correlate of protection from infection<sup>150,151</sup>. However, in the case that an infection occurs, CD8+ T cells correlate with protection from smallpox disease<sup>152</sup>.

Correlates of protection are also not universally applicable to all populations and pathogens. For example, serum antibody titers are predictive of vaccine-induced protection against influenza in young adults<sup>153</sup>. In the elderly, however, cytotoxic T cells correlate better with protection from disease than antibody titers<sup>154</sup>. Individuals with higher frequencies of vaccine-induced T cells are also less likely to have reactivation of latent infections, such as HCMV<sup>155</sup> and varicella-zoster virus<sup>156</sup>. T cells are especially important for protection against variable pathogens that can escape the neutralizing antibody response, such as emerging HCoV variants. Since the T cell response is directed against a very large pool of peptides and does not rely on the structural conformation of surface antigens of a pathogen, it is less prone to immune escape by changing pathogens<sup>130</sup>.

To date, there are more limited data on vaccine-induced T cell responses, as T cells, in contrast to antibodies, are often not measured in large clinical trials. Measuring T cell responses usually requires the collection of peripheral blood samples and isolation and cryopreservation of cells, which is operationally difficult. Furthermore, T cell assays are time-consuming and lack optimal standardization. Thus, it has traditionally been difficult to define cellular correlates of protection. Nevertheless, in early-stage clinical trials (phase 1), study participants are monitored very closely at multiple time points after vaccination. While safety is the primary objective of phase 1 trials, immunogenicity, i.e. the ability of the vaccine to induce an immune response, is often the secondary objective. Blood samples can be collected longitudinally, which provides the opportunity to assess vaccine-induced T cell responses in more detail over time.

Overall, the human T cell immune response is complex and is influenced by many factors. It is shaped, for example, by the signals of the innate response, the type of antigen, site of exposure and it adapts with multiple exposures<sup>96</sup>. Both the quality and quantity of memory T cells are thought to be important parameters of long-term vaccine-induced protection. A better understanding of the exact functions and magnitude of T cell memory would allow for a more “rational” vaccine design, exploiting these immunological mechanisms<sup>96,157</sup>. This includes improving the vaccination schedule, for example by optimizing the time interval between vaccinations or by optimizing the dose levels, combining different vaccine platforms (heterologous prime-boost), giving additional booster vaccinations, or exploring different routes of administration. Improved vaccine formulations could enhance the breadth of the innate response affecting the polarization of the T cell response towards the different Th types<sup>122</sup>. In addition, optimized vaccine antigen design could direct the antigen-specificity of the T cell response.

## 2. AIM OF THE STUDY

The aim of this study was a comprehensive longitudinal analysis of T cell responses following vaccination against SARS-CoV-2 and MERS-CoV. For this purpose, peripheral blood samples were collected and analyzed from participants of several first-in-human phase 1 clinical trials testing rMVA-based vaccine candidates and observational cohorts of healthy and immunosuppressed individuals vaccinated with licensed vaccines. We hypothesized that vaccine platform, immunization schedule and vaccine dose influence the function, antigen-specificity and magnitude of the T cell response.

## 3. STUDY DESIGN

### 3.1. Vaccines

In this thesis project, T cell responses were investigated before and vaccination of individuals with different vaccine candidates and licensed vaccines. These vaccines are briefly discussed below.

#### 3.1.1. Experimental rMVA viral vector vaccines

Modified Vaccinia virus Ankara (MVA) is a highly attenuated orthopoxvirus. It originates from a vaccinia virus strain that was transferred in the 1950s from Ankara, Turkey, to Munich, Germany, to develop vaccines against smallpox<sup>158</sup>. Through serial passaging in chicken embryo fibroblasts (CEF), the virus lost substantial parts of its genome including several virulence factors<sup>159</sup>. It efficiently infects but does not replicate in human cells. MVA was shown to be safe and effective in protecting humans against smallpox and was thus licensed and used in Germany's smallpox eradication campaign in the 1970s<sup>160</sup>. It was later also approved for the closely related monkeypox virus and has been widely used since the monkeypox outbreak in 2020<sup>161</sup>. Due to its excellent safety profile and large insert capacity, recombinant MVA (rMVA) was developed as a viral vector vaccine platform by the insertion of foreign genes encoding antigens of different pathogens<sup>162</sup>. In 2020, the first rMVA-based vaccine (MVA-BN-Filo) was licensed in combination with an adenoviral vector (Ad26.ZEBOV), against Ebola virus disease<sup>163</sup>. Sutter and colleagues constructed several rMVA-based vaccine candidates against other infectious diseases, including MERS and COVID-19 (Figure 12).

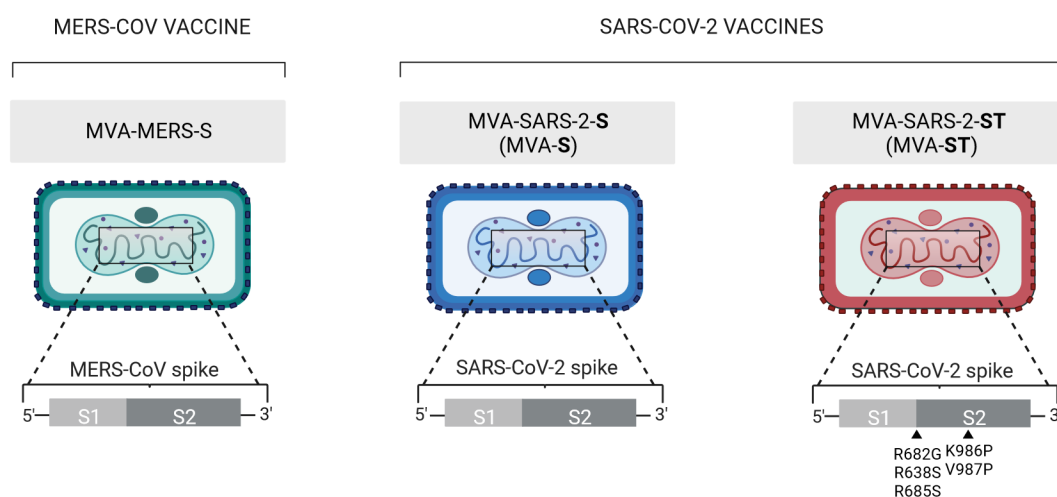


**Figure 12: rMVA-based vaccine candidates.** The rMVA platform encoding the native (MVA-S) and a prefusion-stabilized (MVA-ST) SARS-CoV-2 spike or the native MERS-CoV spike (MVA-MERS-S). This figure was created by Leonie Mayer using BioRender.

MVA-MERS-S is an rMVA-based vaccine candidate, encoding the native full-length MERS-CoV spike (Figure 12, left). In preclinical studies, it induced virus-neutralizing antibody titers<sup>164</sup> and was shown to be safe and protective in mice<sup>165</sup>. The candidate vaccine was also tested in dromedary camels where immunized animals had reduced viral replication upon MERS-CoV challenge<sup>166</sup>. Safety and

immunogenicity of MVA-MERS-S was demonstrated in a dose-ascending phase 1a clinical trial that was conducted between 2017 and 2019 at the University Medical Center Hamburg-Eppendorf (UKE)<sup>167</sup>.

MVA-SARS-2-S (Figure 12, center, MVA-S) and MVA-SARS-2-ST (Figure 12, right, MVA-ST) are rMVA-based vaccine candidates encoding the native, or an optimized, prefusion-stabilized version of the full-length SARS-CoV-2 spike, respectively. Two proline amino acid substitutions in the S2 subunit and additional mutations in the S1/S2 cleavage site were introduced into the spike sequence encoded by MVA-ST. These modifications render the spike in a prefusion-stabilized conformation that is not cleaved into S1 and S2 subunits. Both vaccine candidates showed protective efficacy in mice and hamsters<sup>168,169</sup>. MVA-S and MVA-ST proceeded to two subsequent phase 1 clinical trials in October 2020 and July 2021 at the UKE, respectively.

### 3.1.2. Licensed vaccines based on the ChAdOx1 viral vector and mRNA

In response to the COVID-19 pandemic, several vaccines encoding the SARS-CoV-2 spike were licensed and delivered. These included the BNT162b2 and mRNA-1273 vaccines based on the mRNA platform and the ChAdOx1 nCoV-19 viral vector-based vaccine as shown in Figure 13.

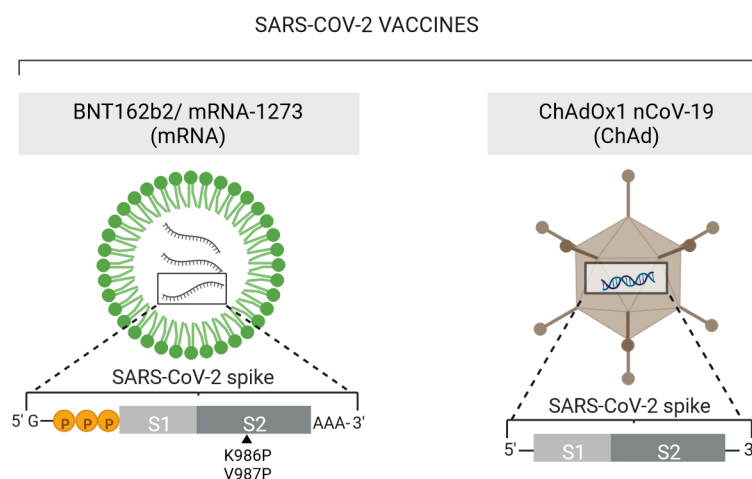


**Figure 13: Licensed SARS-CoV-2 vaccines.** BNT162b2 and mRNA-1273 vaccines (mRNA) encode the prefusion-stabilized SARS-CoV-2 spike protein. ChAdOx1 nCoV-19 vaccine (ChAd) encodes the native, full-length SARS-CoV-2 spike protein. This figure was created by Leonie Mayer using BioRender.

BNT162b2 (Comirnaty<sup>®</sup>) and mRNA-1273 (Spikevax<sup>®</sup>), here referred to collectively as “mRNA”, are licensed mRNA vaccines encoding the prefusion-stabilized SARS-CoV-2 spike, but with a native S1/S2 cleavage site<sup>82,170</sup> (Figure 13, left). Both vaccines were shown to protect nonhuman primates from lower respiratory tract infection upon SARS-CoV-2 challenge<sup>170,171</sup>. A two-dose regimen (21 days apart) of BNT162b2 (30 µg per dose) or mRNA-1273 (100 µg per dose) conferred 95%<sup>90</sup> and 94.1%<sup>91</sup> protection against symptomatic COVID-19 in humans, respectively.

ChAdOx1 is a replication-deficient viral vector derived from the chimpanzee adenovirus strain Y25<sup>172</sup>. It was attenuated through genetic engineering by deleting the E1 region, which is essential for viral replication. To optimize insertion capacity and viral production, additional regions of the genome were edited. ChAdOx1 nCoV-19 (Vaxzevria<sup>®</sup>), here referred to as “ChAd”, is a licensed viral vector vaccine based on the ChAdOx1 platform expressing a codon-optimized sequence of the native, full-length SARS-CoV-2 spike (Figure 13, right). It was shown to protect nonhuman primates from pneumonia with reduced viral load upon SARS-CoV-2 challenge<sup>173</sup>. In a combined analysis of four randomized trials, a two-dose ChAd vaccination regimen was shown to have an efficacy of 66.7% against symptomatic COVID-19<sup>174</sup>. Vaccine efficacy was enhanced when the second dose was given after > 12 weeks (81.3%)



compared to < 6 weeks (55.1%)<sup>174</sup>. The standard dose is  $5 \times 10^{10}$  viral particles. In comparison to the licensed mRNA vaccines, there was no significant difference in efficacy against severe disease<sup>175</sup>.

### 3.2. Study cohorts

This thesis is based on different human vaccine cohorts. This includes two phase 1 clinical trials testing MVA-based COVID-19 vaccine candidates in comparison to licensed vaccines (chapter 3.2.1, Figure 14). The MERS part includes participants of the two phase 1 clinical trials testing the MVA-MERS-S vaccine candidate (chapter 3.2.2, Figure 15). The here described phase 1 clinical trials are investigator-initiated studies sponsored by and performed at the UKE between 2020 and 2023 under the principal investigator Prof. Marylyn M. Addo.

#### 3.2.1. COVID-19 vaccination cohorts

The MVA-SARS-2-S phase 1a clinical trial (NCT04569383) consisted of a prime-boost regimen of MVA-SARS-S given four weeks apart. Study participants were divided into two dose cohorts: low dose ( $1 \times 10^7$  plaque-forming units (PFU);  $n = 15$ ) and high dose ( $1 \times 10^8$  PFU;  $n = 15$ ). A study amendment was added later on, where 12 participants received two additional doses of the licensed BNT162b2 vaccine, the first dose eight months following MVA-S vaccination and the second dose three weeks later (Figure 14, blue).

The MVA-SARS-2-ST phase 1b clinical trial (NCT04895449) comprises two parts. In part A, MVA-SARS-2-ST was given in a prime-boost regimen, four weeks apart, to SARS-CoV-naïve individuals. Study participants were divided into two dose groups: low dose ( $1 \times 10^7$  PFU;  $n = 8$ ) and middle dose ( $5 \times 10^7$  PFU;  $n = 7$ ) (Figure 14, red). In part B, MVA-SARS-2-ST was tested as a third booster vaccination. It was given as a single dose to individuals who had received two doses of BNT162b2, at least six months before. Study participants were divided into three dose groups: low dose ( $1 \times 10^7$  PFU;  $n = 12$ ) middle dose ( $5 \times 10^7$  PFU;  $n = 10$ ), and high dose ( $1 \times 10^8$  PFU;  $n = 8$ ) (Figure 14, purple).

#### SARS-COV-2 VACCINATION COHORTS

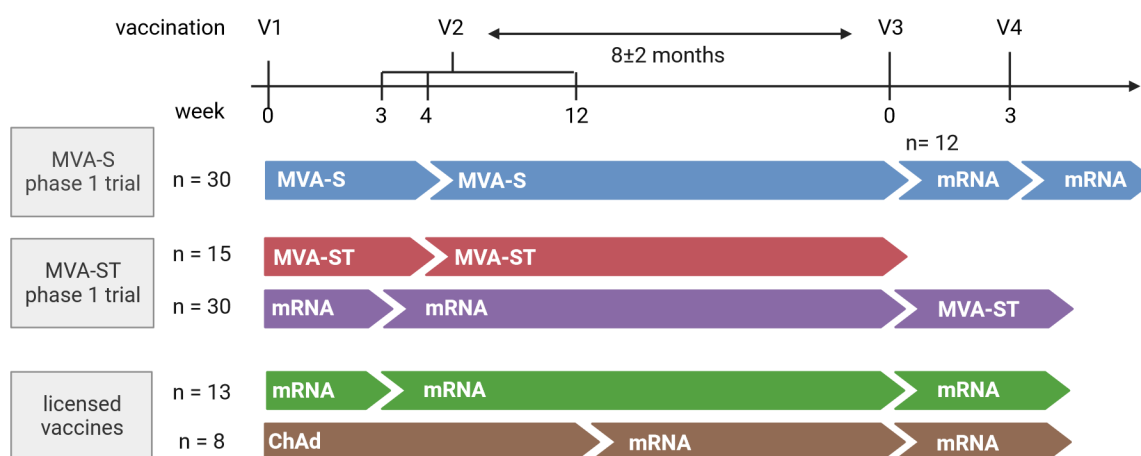


**Figure 14: COVID-19 vaccination cohorts.** Phase 1 clinical trials consist of the MVA-S cohort (2x MVA-S; blue,  $n = 30$ ) with a study amendment (2x mRNA, blue,  $n = 12$ ), the MVA-ST cohort (2x MVA-ST; red,  $n = 15$ ) and the mRNA/MVA-ST cohort (2xmRNA + MVA-ST; purple,  $n = 30$ ). Control cohorts with licensed vaccines consist of the mRNA cohort (3x mRNA; green,  $n = 13$ ) and the ChAd/mRNA cohort (ChAd + 2x mRNA; brown,  $n = 8$ ). Vaccinations are labeled as V1, V2, V3, V4. This figure was created by Leonie Mayer using BioRender.

The observational cohorts are made up of individuals who received licensed COVID-19 vaccines according to the recommended vaccination regimens in Germany. The mRNA cohort received two doses of an mRNA vaccine (BNT162b2 or mRNA-1273), three weeks apart, and an additional booster

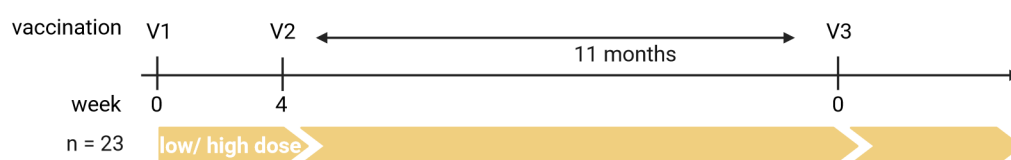
dose at least six months later ( $n = 13$ ) (Figure 14, green). The ChAd/mRNA cohort received one dose of the ChAd vaccine followed by one dose of mRNA 12 weeks later and a booster vaccination with mRNA at least six months later ( $n = 8$ ) (Figure 14, brown).

In addition to the side-by-side comparison of rMVA-based and licensed COVID-19 vaccines in healthy individuals, the T cell immune response following COVID-19 vaccination was also analyzed in two cohorts of immunosuppressed patients. The first cohort consisted of patients with chronic lymphocytic leukemia ( $n = 21$ ). T cell responses were measured after the second and third COVID-19 vaccination. The second cohort consisted of cirrhotic ( $n = 26$ ) and liver transplant recipients ( $n = 82$ ). In both cohorts, T cell responses were compared to healthy controls. Details of the study design and patient characteristics can be found in publications III, IV, and V<sup>176–178</sup>.

### 3.2.2. MERS vaccination cohorts

The MVA-MERS-S phase 1a clinical trial (NCT03615911) was conducted between 2017 and 2019, testing the safety and immunogenicity of a prime-boost vaccination of two different doses of MVA-MERS-S (low dose:  $1 \times 10^7$  PFU, high dose:  $1 \times 10^8$  PFU;  $n = 23$ ) (Figure 15, top).

#### MVA-MERS-S PHASE 1a TRIAL



#### MVA-MERS-S PHASE 1b TRIAL - UKE STUDY SITE

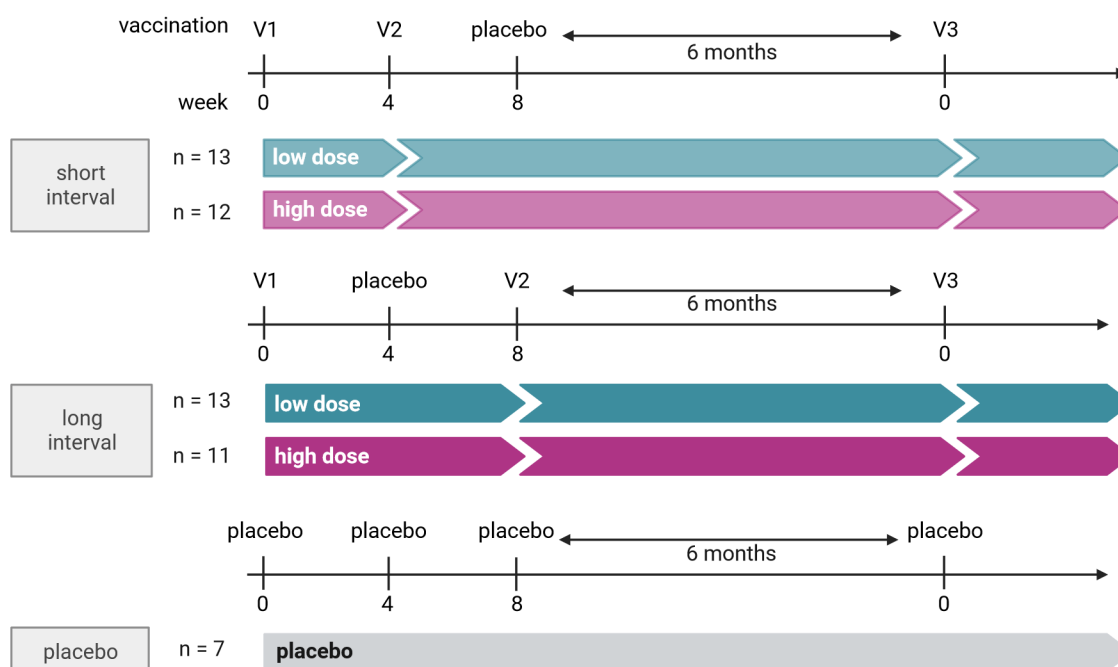


**Figure 15: MERS vaccination cohorts.** The MVA-MERS-S phase 1b clinical trial consists of 5 cohorts: Low dose ( $n = 13$ ) and high dose ( $n = 12$ ) with a short vaccination interval (4 weeks between V1 and V2), and low dose ( $n = 13$ ) and high dose ( $n = 11$ ) with a long vaccination interval (8 weeks between V1 and V2). A placebo cohort ( $n = 7$ ), given 4 placebo vaccinations was included. This figure was created by Leonie Mayer using BioRender.

After prime-boost vaccination, 75% and 100% of the low dose ( $1 \times 10^7$  PFU) and the high dose ( $1 \times 10^8$  PFU) cohorts seroconverted, respectively<sup>167</sup>. In a follow-up proof-of-concept study, ten participants received a late third MVA-MERS-S immunization 11 months following prime-boost<sup>179,180</sup>. The T cell immunogenicity has been published by Koch et al. In short, MERS-CoV-spike-specific T cell responses were detected in 87% of participants in total<sup>167</sup>. As part of this thesis, the epitope-specific CD8+ T cell response of two participants of this trial was characterized in detail as described in publication II<sup>181</sup>.

The MVA-MERS-S phase 1b clinical trial (NCT04119440) is a two-center, randomized, double-blind, placebo-controlled trial. It consists of five study arms (Figure 15, bottom). Participants were randomized to receive three vaccinations of the low dose (green) or high dose (purple) of MVA-MERS-S. In addition, two different time intervals between the first and second vaccinations were investigated. Participants received either the second vaccination at week four and a placebo at week eight (short interval), or a placebo at week four and the second vaccination at week eight (long interval). The third vaccination was given six months later. A placebo arm was also included, in which participants received four placebo doses (grey). The cohort analyzed in this study encompasses all participants recruited at the UKE who received all three MVA-MERS-S vaccinations (referred to as the modified intention-to-treat cohort).

### 3.3. Experimental methods

Peripheral blood samples were collected by venipuncture before vaccination and longitudinally after vaccination at specific time points. Peripheral blood mononuclear cells (PBMCs) were isolated from ethylenediaminetetraacetic acid (EDTA) blood using Ficoll-Histopaque (Sigma) or SepMate™ (Stemcell), cryopreserved, and later thawed for the T cell assays described in this study. Additionally, lithium-heparin blood was collected for assessing T cell responses in a whole-blood interferon-gamma release assay (IGRA). Assays are based on PBMCs analyzed directly *ex vivo* or after re-stimulation with overlapping peptide (OLP) pools (JPT Peptide Technologies) *in vitro*. The expression of surface markers and production of cytokines were measured by flow cytometry (using the BD Fortessa or Cytex Aurora), enzyme-linked immunospot assay (ELISpot), and enzyme-linked immunosorbent assay (ELISA). Methods and materials are described in detail in the respective publications and unpublished results chapters. Data were analyzed and visualized using FlowJo (v10.9.0), GraphPad Prism (v10.0.0), Microsoft Excel, and R (v4.2.0).

#### 4. PUBLISHED RESULTS

The published results of this cumulative doctoral thesis consist of three first-author publications (publication I, II, and III) and three co-author publications (publication IV, V, and VI). The publications are listed on page ii and the manuscript files are attached in chapter 10. The main findings of these publications in the context of this thesis are briefly summarized below:

The phase 1 clinical trial of the MVA-S vaccine candidate against COVID-19 started in October 2020. An interim analysis at the beginning of 2021 revealed, that antibody responses and seroconversion rates were lower than expected. These results are published in ***“Stabilized recombinant SARS-CoV-2 spike antigen enhances vaccine immunogenicity and protective capacity”***, publication VI. The manuscript also provides detailed immunogenicity and efficacy analyses in preclinical models comparing MVA-S with the optimized MVA-ST candidate. These analyses showed, that MVA-ST elicits higher neutralizing and S1-specific binding antibody responses in animals.

Subsequently, a phase 1 clinical trial testing the optimized MVA-ST candidate started in June 2021. Alongside these clinical studies and throughout the pandemic, we collected samples from convalescent individuals and those vaccinated with licensed vaccines as control cohorts. We then performed a comparative immunogenicity analysis of the MVA-S, MVA-ST, and control cohorts. The results are published in the manuscript ***“MVA-based vaccine candidates encoding the native or prefusion-stabilized SARS-CoV-2 spike protein reveal differential immunogenicity in humans”***, publication I. In brief, we show the differential antibody, B cell, and T cell immunogenicity of the different vaccine regimens. A distinct bias towards the S1 and S2 subunits was observed after MVA-ST and MVA-S vaccination, respectively. Even though MVA-S was not immunogenic enough by itself to proceed to further clinical evaluation, our analyses showed, that it has the potential to enhance the frequency and polyfunctionality of T cell responses when given prior to a prime-boost regimen with the licensed mRNA vaccine. MVA-ST, in turn, could boost the T cell response when given as a third booster dose following a prime-boost vaccination regimen with the licensed mRNA vaccine.

Given the fact that not healthy, but immunocompromised individuals are most vulnerable to COVID-19, we also set out to investigate vaccine responses in different immunocompromised patient cohorts in collaboration with Dr. Sibylle C. Mellinghoff and Golda Schaub. We could show that the T cell response was sub-optimal after the second vaccination (***“SARS-CoV-2 specific cellular response following COVID-19 vaccination in patients with chronic lymphocytic leukemia”***, publication IV) but could be enhanced by an additional booster dose (***“SARS-CoV-2-specific cellular response following third COVID-19 vaccination in patients with chronic lymphocytic leukemia”***, publication III). In the patient cohort described in ***“SARS-CoV-2-specific Humoral and T cell Immune Response After Second Vaccination in Liver Cirrhosis and Transplant Patients”***, publication V) it was deciphered that several clinical factors are predictive of a low vaccine response, including age and immunosuppressive drug regimens.

In the manuscript ***“Identification of a spike-specific CD8<sup>+</sup> T cell epitope following vaccination against the Middle East respiratory syndrome coronavirus in humans”***, publication II, we report on a novel CD8<sup>+</sup> T cell epitope detected after MVA-MERS-S vaccination in the two participants of the phase 1a trial positive for the HLA-B\*35:01 allele. This epitope is specific for the MERS-CoV spike and not cross-reactive to other HCoVs. We show that the epitope-specific T cells are polyfunctional and shift towards a memory phenotype over time. The results of the subsequent MVA-MERS-S phase 1b clinical trial, which is still ongoing, are provided in the unpublished results.

## 5. UNPUBLISHED RESULTS

The following chapters describe the unpublished results of this thesis. The results described in chapter 5.1 are related to publication I, showing detailed analyses of T cell responses following SARS-CoV-2 vaccination and infection. Those shown in Figure 18 and Figure 19 were collected and analyzed in collaboration with Vera Brackrock as part of her Master thesis. T cell responses following MVA-MERS-S immunization are described in chapter 5.2. These data are related to a manuscript in preparation by Raadsen et al. describing the safety and humoral immunogenicity of MVA-MERS-S.

### 5.1. SARS-CoV-2 vaccination and infection

#### 5.1.1. SARS-CoV-2-spike-specific T cell response after vaccination or infection

To analyze the T cell immunogenicity of the rMVA-based COVID-19 vaccine candidates, we longitudinally collected blood samples from participants of the MVA-S and MVA-ST phase 1 clinical trials. As a comparison, we also established control cohorts of individuals vaccinated with licensed COVID-19 vaccines, COVID-19 convalescent individuals, and individuals who had a breakthrough infection following COVID-19 vaccination. T cell responses against the SARS-CoV-2 spike were measured using a whole-blood IGRA following the manufacturer's instructions (EUROIMMUN, Lübeck, Germany). An overview of the assay is shown in Figure 16a.

Briefly, lithium-heparin-blood was incubated with SARS-CoV-2 spike antigen for 20 to 24 hours at 37°C and 5% CO<sub>2</sub>. Plasma was then collected after centrifugation and stored at -20°C. IFN- $\gamma$  secretion was measured in plasma using an IFN- $\gamma$  ELISA and quantified in milli international units per ml (mIU/ml) by interpolating from a standard curve using a four-parameter logistic model. Samples outside the standard curve were re-analyzed using a higher dilution. Plasma from unstimulated blood of each sample was used to subtract background IFN- $\gamma$  levels. Stimulation with a mitogen acting as a polyclonal T cell activator served as a positive control. Values below the LLOQ (= 31 mIU/ml) were set to LLOQ/2. Samples with a response above 200 mIU/ml are considered positive per protocol. Samples were collected at baseline before vaccination and at several time points after each vaccination. Time points are labeled according to the time since the last vaccination, as shown in Figure 16b.

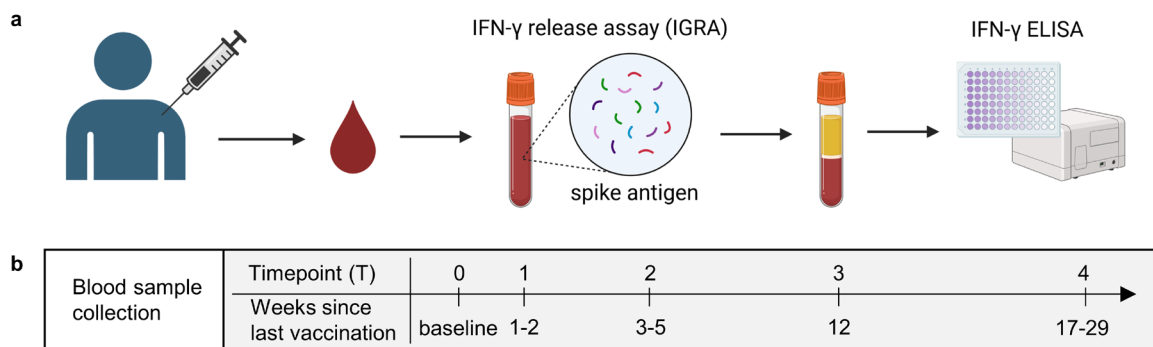


**Figure 16: Study design.** a) Blood samples were collected and stimulated with SARS-CoV-2 spike antigen in a whole-blood IFN- $\gamma$ -release assay (IGRA, Euroimmun). IFN- $\gamma$ -secretion was measured in plasma using an IFN- $\gamma$  ELISA. b) blood sampling schedule: Time points are indicated as weeks since the last vaccination: T0 (baseline), T1 (1-2 weeks), T2 (3-5 weeks), T3 (12 weeks), and T4 (17-29 weeks). This figure was created by Leonie Mayer using BioRender.

Figure 17a shows the results of the three rMVA-based phase 1 clinical trial cohorts. The MVA-S/mRNA cohort received two MVA-S vaccinations followed by two mRNA vaccinations. Participants of the MVA-ST cohort were SARS-CoV-2 naïve and received two vaccinations of MVA-ST. In the mRNA/MVA-ST cohort, one dose of the MVA-ST vaccine was tested as a booster following mRNA vaccination. For a detailed description see study design in chapter 3. Figure 17b shows the control cohorts.

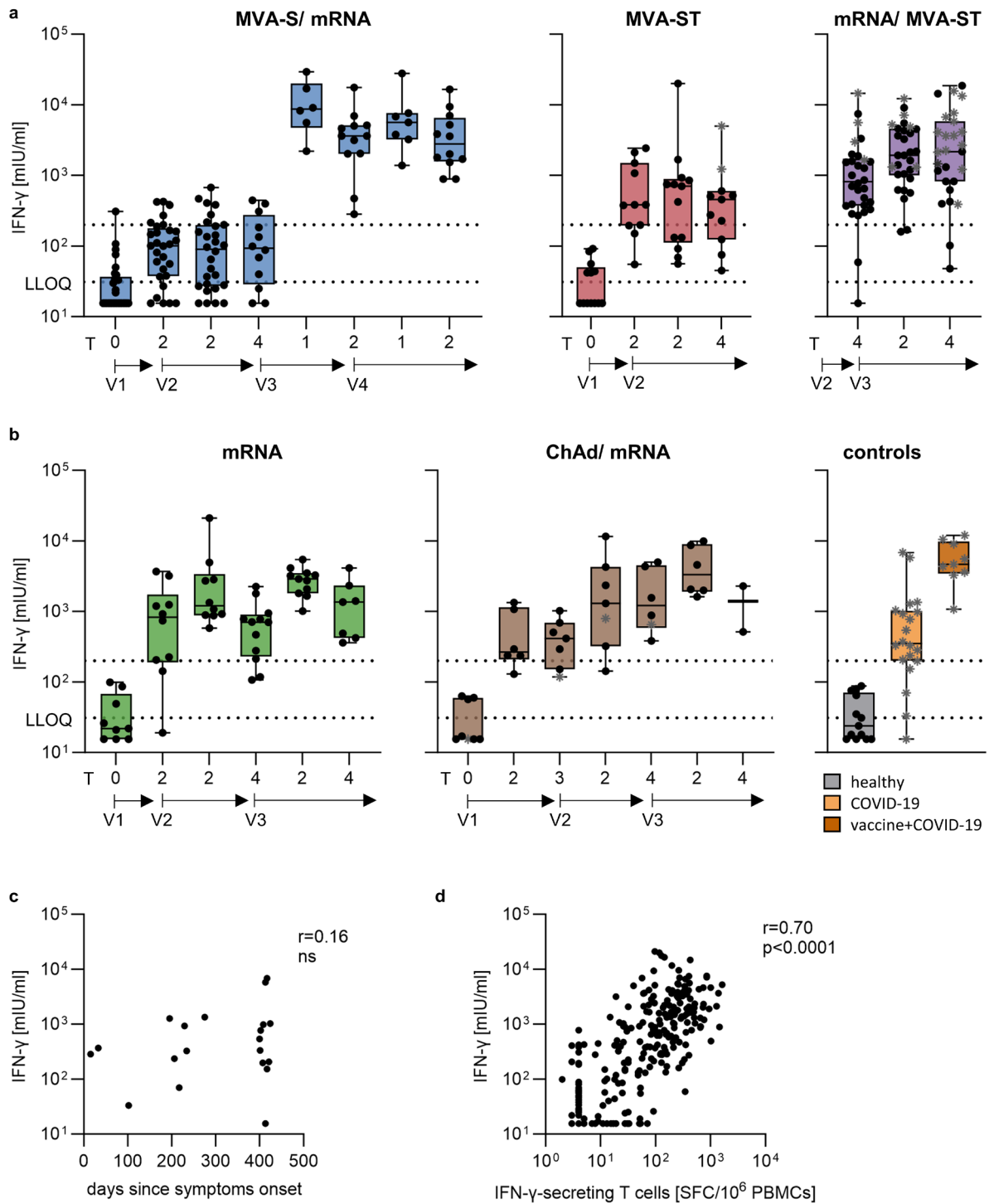


**Figure 17: SARS-CoV-2-S-specific T cell responses following vaccination and infection.** a-d) Vaccinations V1 to V4 are indicated by arrows and time points are indicated as weeks since the last vaccination as outlined in Fig. 18b. T cell responses were measured using a whole-blood IFN- $\gamma$ -release assay (IGRA, Euroimmun). Results are shown as IFN- $\gamma$  secretion levels [mIU/ml]. The dashed lines indicate the LLOQ (= 31 mIU/ml) and the positivity cut-off (= 200 mIU/ml). Time points at which a participant had a positive nucleocapsid antibody test are indicated by grey asterisks. a) Responses in the MVA-S/mRNA (blue), MVA-ST (red), and mRNA/MVA-ST (purple) phase 1 clinical trial cohorts. b) Responses in the mRNA (green), ChAd/mRNA (brown), healthy (grey), COVID-19 (yellow), and vaccine+COVID-19 (orange) control cohorts. c) Correlation of IGRA results with time since symptoms onset in the COVID-19 cohort. d) Correlation of all IGRA results with ELISpot (spot-forming cells (SFC)/ $10^6$  PBMCs) results (shown in published results I). Data are represented as individual data points (b-d). Boxes indicate median  $\pm$  IQR; whiskers are min. to max. (a, b). The correlation coefficients ( $r$ ) and significant  $p$ -values were calculated by two-tailed Spearman correlation with a 95% confidence interval (c, d). This figure was created using GraphPad Prism (v10.0.0).

SARS-CoV-2-spike-specific T cell responses were above the positivity cut-off in 20% (6/30) of participants after two-dose MVA-S vaccination (Figure 17a, left, MVA-S/mRNA, blue, V1 + V2). The response was variable between participants of this cohort (median = 91 mIU/ml; range = 31 to 469 mIU/ml). In the twelve participants who received two additional doses of mRNA vaccine six months following MVA-S vaccination (Figure 17a, left, MVA-S/mRNA, blue, V3 + V4) the T cell response was boosted with peak levels observed one week after the first dose (V3T1 median = 8682 mIU/ml). The median responses in this cohort at time points after the mRNA doses (V3T2 median = 5656 mIU/ml; V4T2 median = 2795 mIU/ml) were higher compared to the corresponding time points in the mRNA control cohort (Figure 17b, left, mRNA, green, V1T2 median = 831 mIU/ml; V2T2 median = 1205 mIU/ml). This may suggest, that MVA-S could prime a T cell response even though it was not very immunogenic when administered alone.

MVA-ST, compared to MVA-S, induced a T cell response at higher median levels (Figure 17a, middle, MVA-ST, red, V2T2 median = 394 mIU/ml). T cell responses were above the positivity cut-off in 62% (8/13) of participants. Median levels after one dose of MVA-ST (V1T2 median = 378 mIU/ml) were comparable with those measured after one dose of ChAd (ChAd/mRNA, brown, V1T2 median = 266 mIU/ml). T cell responses remained detectable 6 months after vaccination (MVA-ST, V2T4 median = 276 mIU/ml) in 80% (8/10) of participants.

Participants of the mRNA/MVA-ST cohort (Figure 17a, right, purple) had highly variable levels of baseline immunity (median V2T4 = 818 mIU/ml; range = 31 to 14545 mIU/ml) before MVA-ST booster vaccination. One dose of MVA-ST could boost T cell responses in this cohort (mRNA/MVA-ST, V3T2 median = 1924 mIU/ml) to comparable levels as measured after V3 in the mRNA cohort (mRNA, V3T2 median = 2092 mIU/ml). When comparing the T cell response between the two control cohorts, it was observed that median responses after one dose mRNA (Figure 17b, left, mRNA, green, V1T2 median = 831 mIU/ml) were higher compared to one dose ChAd (Figure 17b, middle, ChAd/mRNA, brown, V1T2 median = 266 mIU/ml). This difference was not detectable anymore after the second vaccination. The third vaccination with mRNA boosted the T cell response in both cohorts to similar levels (mRNA, V3T2 median = 2902 mIU/ml; ChAd/mRNA, V3T2 median = 3317 mIU/ml). T cell responses remained at high levels 6 months following the third dose.

It is important to note that 18/96 (19%) of participants of the SARS-CoV-2 vaccination cohorts acquired a SARS-CoV-2 infection during the study and that the number of SARS-CoV-2 infections was not distributed equally across cohorts. Prior SARS-CoV-2 exposure was excluded in the MVA-S/mRNA and MVA-ST cohorts by antibody test at the screening visit. We monitored possible SARS-CoV-2 exposures during the study by measuring anti-nucleocapsid antibody titers longitudinally. The data points at which the participants have a positive nucleocapsid antibody test and the time points thereafter are marked by grey asterisks. Note that two participants tested positive at the late follow-up time point in the MVA-ST cohort (Figure 17a, middle, red, V2T4). One participant of the ChAd/mRNA control cohort had a low-positive nucleocapsid test already at baseline but nucleocapsid titers remained very low throughout the study. Four participants of the MVA-ST/mRNA cohort (Figure 17a, right, purple) were already positive at baseline and eleven more participants had SARS-CoV-2 exposures throughout the study. These participants had not been excluded at the screening day because this study arm aimed to test the booster effect of MVA-ST. The high number of SARS-CoV-2 exposures in this cohort, in contrast to the other cohorts, coincides with the high infection rates at the time when this part of the study was conducted (12/2021 – 11/2022).

Notably, the highest median response out of all cohorts was measured in the vaccine+COVID-19 cohort (Figure 17b, right, orange), where participants had a breakthrough infection following two-dose vaccination (median = 4664 mIU/ml). The response in the COVID-19 control cohort was highly variable in magnitude (Figure 17b, right, yellow, median = 327 mIU/ml; range = 31 to 5773 mIU/ml). Some

participants of the COVID-19 control cohorts had responses comparable in magnitude to the vaccinated cohorts, while some had a response not higher than the pre-pandemic healthy controls (Figure 17b, right, grey). Samples of the COVID-19 control cohort were collected from patients at time points ranging from 6 to 424 days since symptoms onset. The magnitude of the response did not correlate with days since symptoms onset (Figure 17c). The results of the IGRA assay showed a significant positive correlation with the results of the SARS-CoV-2-spike-specific IFN- $\gamma$  ELISpot (Figure 17d) used for analyses in the published results (publication I).

### 5.1.2. Longitudinal analysis of epitope-specific CD8+ T cells

To characterize in more detail how the T cell response develops over time, SARS-CoV-2-epitope-specific CD8+ T cells were tracked longitudinally following consecutive exposures through vaccination and infection. These experiments were performed in collaboration with Vera Brackrock as part of her Master thesis. A flow cytometry panel was designed using epitope-loaded tetramers to detect epitope-specific CD8+ T cells and fluorescently-labeled antibodies to measure their activation and memory phenotype (Figure 18a). The previously described HLA-A\*02:01-restricted epitope, S<sub>269-277</sub> (YLQPRTFLL), was used for this analysis<sup>182-185</sup>. Meyer et al. had shown that CD8+ T cells against this epitope could be detected in 98% of COVID-19 convalescent individuals carrying the HLA-A\*02:01 allele, one of the most frequent HLA class I alleles in European Caucasian population<sup>186</sup>. For comparison, T cells against the immunodominant HLA-A\*02:01-restricted epitope LLW (LLWNGPMAV) of the non-structural protein 4b of the yellow fever virus were measured<sup>187</sup>. The live-attenuated yellow fever vaccine, YF-17D, is one of the most successful vaccines, eliciting a long-lived CD8+ T cell response<sup>188</sup>.

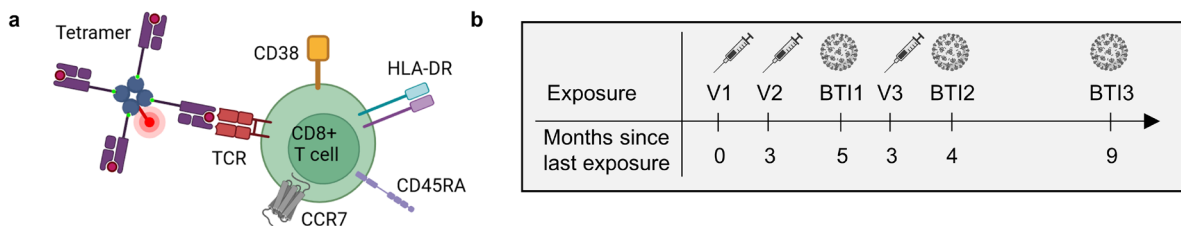


**Figure 18: Study design.** a) Scheme of flow cytometry panel including epitope-specific tetramer, activation, and memory marker. b) Timeline of SARS-CoV-2 spike exposures through vaccinations (V1-V3) and breakthrough infections (BTI1-BTI3) of the study participant. This figure was created using BioRender and Microsoft PowerPoint.

The results provided here describe a two-year follow-up (03/2021-03/2023) of a single healthy individual who had several SARS-CoV-2 exposures as shown in Figure 18b. The study participant received one dose of the ChAdOx1 nCoV-19 vaccine followed by one dose of the BNT162b2 mRNA vaccine against COVID-19 (V1-V2, 12 weeks apart) and then had a SARS-CoV-2 breakthrough infection five months later (BTI). An additional booster dose of the BNT162b2 vaccine (V3) was administered three months following the BTI. The individual then had two additional BTIs, four (BTI2) and 13 (BTI2) months after V3. All BTIs were of mild symptomatic and did not require medical attention as self-reported by the study participant. This individual had been vaccinated with the live-attenuated yellow fever vaccine in the past (12/2016).

Figure 19a shows the frequencies of SARS-CoV-2 spike epitope-specific (S, red) and yellow fever virus epitope-specific (YF, yellow) T cells out of the total CD8+ T cells over time. Time points are denoted as days since last exposure (vaccination (V) or BTI). Flow cytometry plots of spike-specific CD8+ T cells at peak time points following each exposure are shown in Figure 19b. Frequencies denoted next to the tetramer gates refer to the percentage of epitope-specific cells out of the total CD8+ T cells.



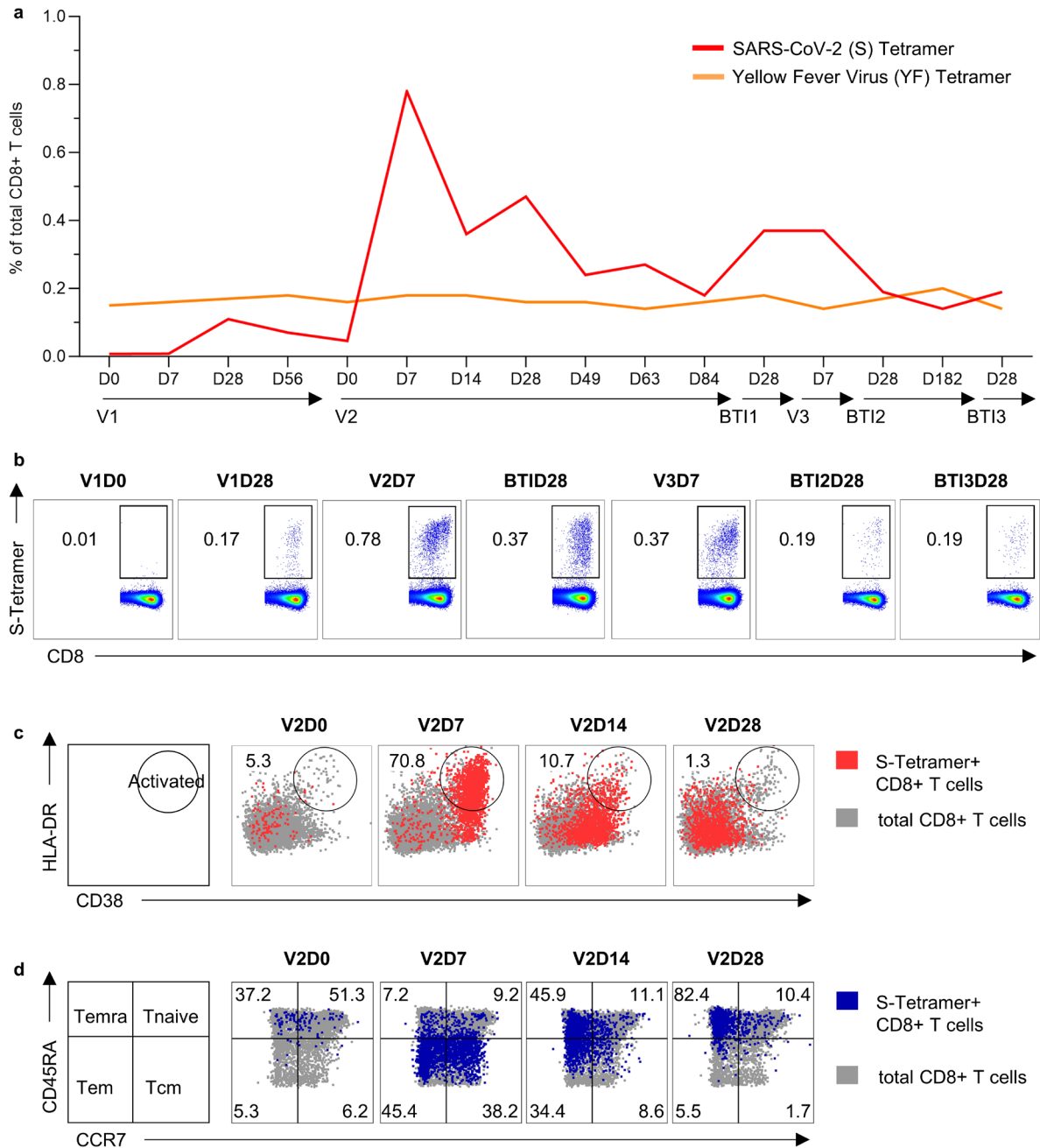


**Figure 19: Epitope-specific CD8+ T cell responses following SARS-CoV-2 vaccination and infection.** a) Longitudinal measurement of SARS-CoV-2 spike-epitope-specific (S, red) compared to yellow fever virus epitope-specific (YF, yellow) CD8+ T cells in an HLA-A\*02 positive individual. Blood samples were collected at baseline and various time points following SARS-CoV-2 vaccination (V1-V3) and breakthrough infections (BT11-BT13). Days refer to the time since the last exposure. Data are represented as a percentage of tetramer-positive cells out of total CD8+ T cells. b) Tetramer staining of SARS-CoV-2-epitope-specific CD8+ T cells at time points of peak response after each exposure (vaccination or breakthrough infection). c) Activation (measured by CD38 and HLA-DR expression) of SARS-CoV-2-epitope-specific cells (red) compared to total CD8+ T cells (grey) before and after V2. Epitope-specific cells are most activated at day 7. Activation returns to baseline by day 28. d) Memory phenotype (measured by CCR7 and CD45RA expression) of SARS-CoV-2-epitope-specific cells (blue) compared to total CD8+ T cells (grey) before and after V2. Epitope-specific cells have a central memory (CCR7+CD45RA-) and effector memory (CCR7-CD45RA-) phenotype at day 7 and shift towards terminally differentiated memory cells (CCR7-CD45RA+) by day 28. This figure was created using FlowJo (v10.9.0), GraphPad Prism (v10.0.0), and Microsoft PowerPoint.

Spike-specific CD8<sup>+</sup> T cells were induced at low levels by the first vaccination and subsequently boosted by the second dose comprising 0.78% of the total CD8<sup>+</sup> T cell pool by V2D7 (Figure 19a, red). The response contracted over time until V2D84 but remained above peak levels seen after the first vaccination. Upon subsequent BTI and V3, the response was boosted again (0.37%) but did not reach peak levels observed after V2. Notably, the frequencies of spike-specific CD8<sup>+</sup> T cells were low (0.19%) after the second and third BTI. As a comparison, yellow fever-specific CD8<sup>+</sup> T cells were tracked (Figure 19a, yellow). They were detectable even five years after the individual had received the yellow fever vaccine (V1D0) and remained stable around 0.2% of the total CD8<sup>+</sup> T cell pool throughout this study.

Since blood samples were obtained at various time points following exposure, it was possible to analyze the change in activation and memory phenotype of the epitope-specific T cells. Figure 19c shows exemplary flow cytometry plots at the time points following the second vaccination (V2). Spike-specific cells (red) had a highly activated profile (CD38+HL-DR+ = 70.8% out of total spike-specific cells) at day 7. At day 14, cells were less activated and returned to basal, non-activated levels by day 28. As shown in Figure 19d, the memory phenotype also changed over time. Spike-specific cells shifted towards an effector (CD45RA-CCR7- = 45.4%) and central memory (CD45RA-CCR7+ = 38.2%) phenotype at day 7 and then progressed towards a terminally differentiated ( $T_{emra}$ ) phenotype (CD45RA+CCR7- = 82.4%) by day 28. Memory and activation marker expression stayed stable over time in the yellow fever-specific cells (data not shown).

In summary, the results described in chapter 5.1 show the differential spike-specific T cell response induced by vaccination with two rMVA-based vaccine candidates, by vaccination with licensed COVID-19 vaccines, and by SARS-CoV-2 infection. The detailed longitudinal tracking of epitope-specific CD8<sup>+</sup> T cells revealed that the activation status and frequency of the spike-specific response are most pronounced after the second vaccination. Vaccine-induced responses are re-activated by subsequent BTIs and a memory pool persists over time. These results provide insights into the changing landscape of SARS-CoV-2 “hybrid immunity” in humans. On the one hand, the IGRA was used which proved to be a useful standardized T cell assay for COVID-19 vaccine trials, while on the other hand, the use of tetramer technology provided more detailed information about the phenotype of the T cell response.

## 5.2. Vaccination against MERS-CoV

### 5.2.1. Longitudinal analysis of T cell responses following MVA-MERS-S vaccination

The immunogenicity of the MVA-MERS-S vaccine candidate against MERS was investigated in a phase 1 clinical trial. Participants were randomized to four different treatment arms receiving prime-boost vaccination with the low dose (LD) or high dose (HD) of MVA-MERS-S and either 28 days (short interval, SI) or 56 days (long interval, LI) apart. All participants received a third booster vaccination eight months later. A placebo arm was included for comparison (see study design in chapter 3.2.2). MERS-CoV-spike-specific T cell responses were measured before and longitudinally after each immunization by IFN- $\gamma$  ELISpot, using a MERS-CoV-spike-specific peptide pool. Responses are measured in spot-forming cells (SFC)/ $10^6$  PBMCs. Only participants recruited at the UKE study site and of the modified intention-to-treat cohort, i.e. those that received all three MVA-MERS-S vaccinations but might have missed a placebo dose, were included in the analysis ( $n = 56$ ). Representative IFN- $\gamma$  ELISpot wells of one participant before and after MVA-MERS-S vaccination are shown in Figure 20a.

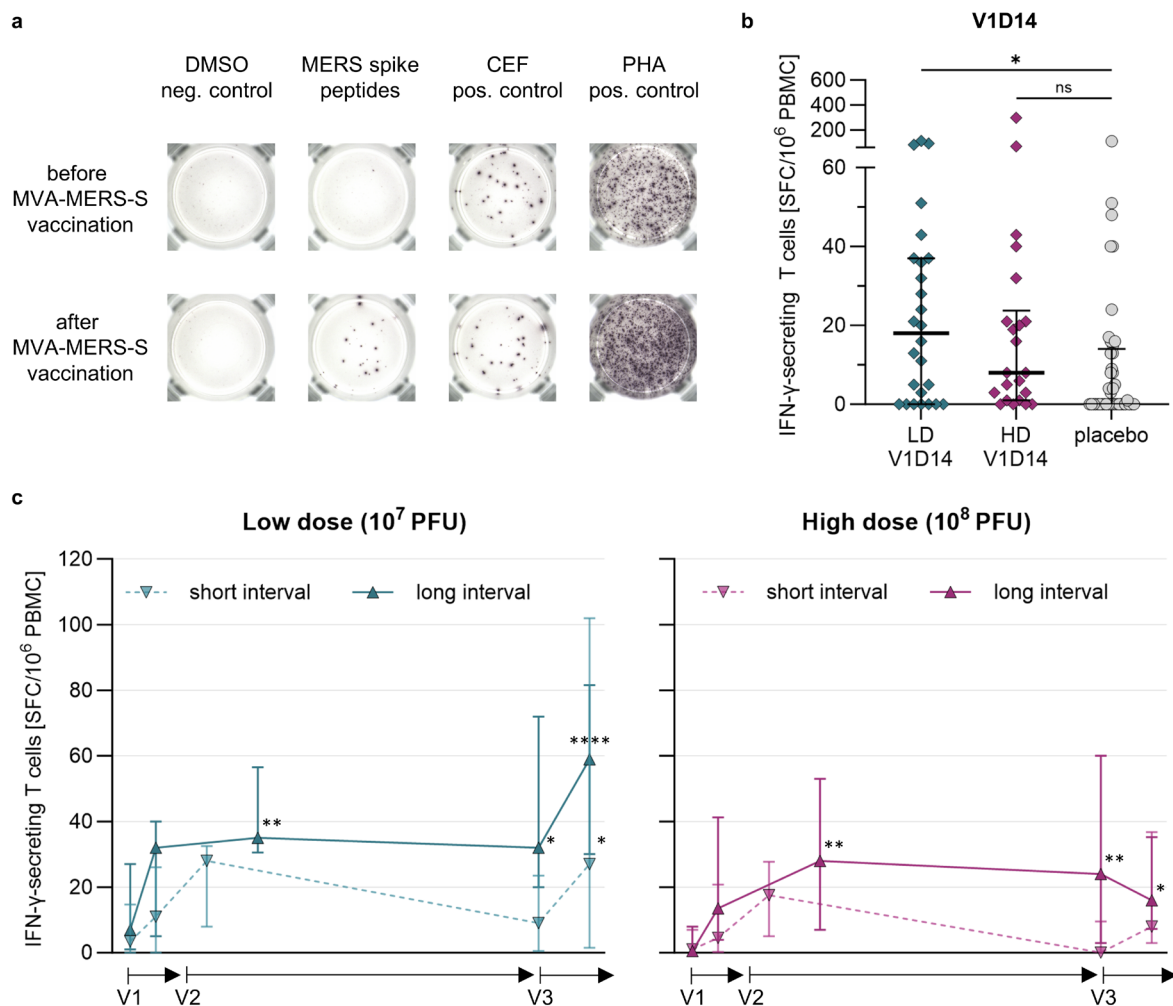


**Figure 20: Spike-specific T cell responses following MVA-MERS-S vaccination.** a) Representative ELISpot wells showing negative control, MERS-CoV spike, CEF peptide, and PHA wells (from left to right) of one participant before and 14 days after MVA-MERS-S vaccination. b) Comparison of T cell responses after first vaccination with the low dose (green) or high dose (purple) MVA-MERS-S or placebo (grey). c) Longitudinal dynamics of the T cell responses in the low dose (left) and high dose (right). Data are represented as individual data points and median  $\pm$  IQR (b) or median  $\pm$  IQR (c). Significant p-values are indicated as calculated by the Kruskal-Wallis test comparing dose groups to placebo (b) or Friedman test comparing time points to baseline within each group (c) and adjusted using Dunn's multiple comparisons test: \* $p < 0.05$ , \*\* $p < 0.01$ , \*\*\* $p < 0.001$ , \*\*\*\* $p < 0.0001$ , ns = not significant. This figure was created using GraphPad Prism (v10.0.0) and Microsoft PowerPoint.

After the first vaccination (Figure 20b), the response in the low dose group (purple) was significantly above the placebo background ( $p = 0.0257$ ), but the median response was low (LD, median = 18 SFC). The response in the high dose group (green) was not significantly above the placebo background.

The analysis of the longitudinal response following all three vaccinations (Figure 20c) shows different dynamics between the treatment arms. The prime-boost vaccination induced a T cell response that reached levels significantly above baseline only in the two long interval groups (LD/LI, median = 35 SFC/ $10^6$  PBMCs,  $p = 0.0061$ ; HD/LI, median = 28 SFC/ $10^6$  PBMCs,  $p = 0.0018$ ). Until D224, median levels remained significantly above baseline in the long interval groups (LD/LI, median = 32 SFC/ $10^6$  PBMCs,  $p = 0.0416$ ; HD/LI, median = 24 SFC/ $10^6$  PBMCs,  $p = 0.0090$ ) and waned to baseline levels in the short interval groups. Third vaccination with the lower dose, regardless of interval, boosted the T cell response significantly above baseline (LD/SI, median = 27 SFC/ $10^6$  PBMCs,  $p = 0.0268$ ; LD/LI, median = 59 SFC/ $10^6$  PBMCs,  $p = <0.0001$ ). The highest response was seen in the LD/LI arm. Third vaccination with the high dose did not boost T cell responses, although the magnitude remained significantly above baseline in the long interval group (HD/LI, median = 16 SFC/ $10^6$  PBMCs,  $p = 0.0054$ ).

Figure 21 shows a direct comparison of T cell responses between treatment arms and placebo at the peak time points following the second and third vaccinations. T cell responses of participants were defined as assay responders if the vaccine response was higher than 26 SFC/ $10^6$  PBMCs (mean of all D0 baseline samples + 2x standard deviation) and two-fold above the respective baseline sample. A trend toward higher responses in both long interval groups was observed after the second vaccination. Here, 75% of the LD/LI cohort and 64% of the HD/LI cohort were assay responders. The response was significantly higher in the LD/LI cohort compared to the placebo cohort ( $p = 0.0007$ ) and the HD/SI cohort ( $p = 0.0393$ ) (Figure 21a). Third vaccination boosted the T cell response especially in the low dose cohorts, with 54% and 69% assay responders, in the LD/SI and LD/LI cohorts, respectively (Figure 21b). In the LD/LI cohort, the response was significantly above placebo ( $p = 0.0050$ ).

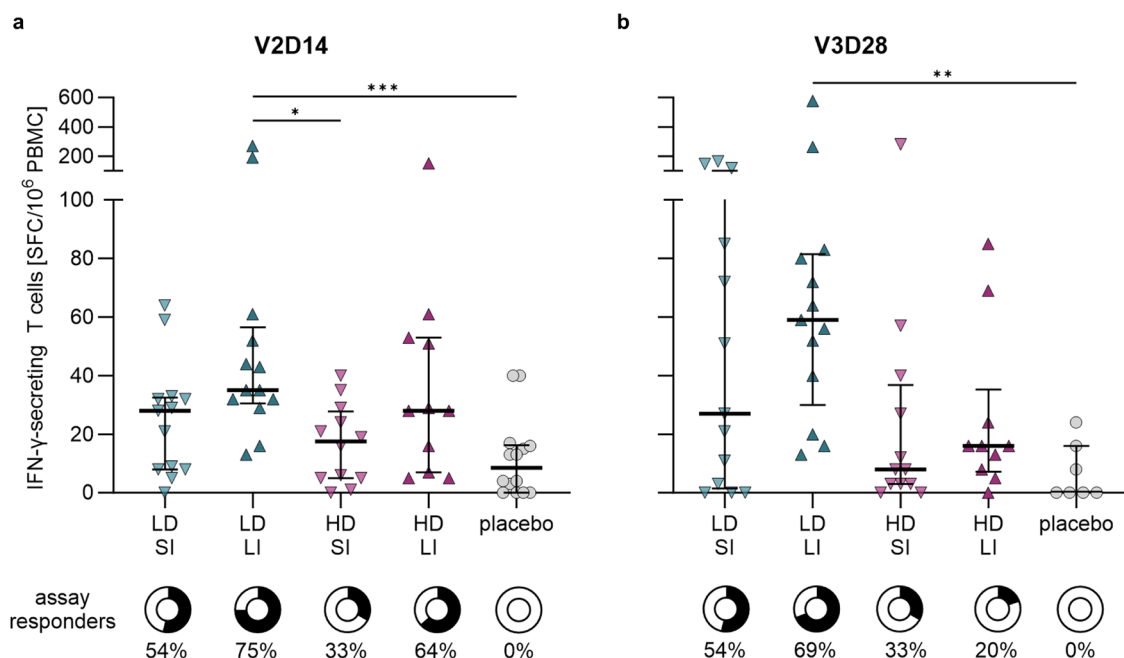


**Figure 21: Comparison of S-specific T cell response at peak time points following MVA-MERS-S vaccination.** Median responses of the different study cohorts were compared after V2 (a) and V3 (b). Assay responders are defined for each participant as  $>26$  SFC (mean of all D0 baseline samples + 2x standard deviation) and two-fold above baseline. Data are represented as individual data points and median  $\pm$  IQR, or as % assay responder out of total  $n$  per cohort (donut charts). Significant  $p$ -values are indicated as calculated by the Kruskal-Wallis test and adjusted using Dunn's multiple comparisons test: \* $p < 0.05$ , \*\* $p < 0.01$ , \*\*\* $p < 0.001$ , \*\*\*\* $p < 0.0001$ . LD = low dose, HD = high dose, SI = short interval, LI = long interval. This figure was created using GraphPad Prism (v10.0.0).

In the LD/SI cohort, responses were highly variable. Third vaccination with the high dose boosted the T cell response to a lesser extent and the percentage of assay responders was also lower, with 33% and 20% of assay responders in the HD/SI and HD/LI groups, respectively.

### 5.2.2. Correlation of T cell and humoral responses following MVA-MERS-S vaccination

Stratifying by dose and interval revealed, that within each group, the response at the different time points following vaccination correlated positively (Figure 22a). Overall, those participants who responded after the first vaccination also responded to the following two vaccinations. Regardless of dose and interval, some participants did not respond to any of the three vaccinations. Next, the T cell analysis was compared to the humoral response, to see if the T cell responders were also antibody responders. Figure 22b shows a correlation matrix of selected time points after vaccination of the long interval group. The same pattern was seen for the short interval group (data not shown). MERS-spike-specific binding IgG (measured by ELISA [IU/ml]), MERS-CoV neutralizing antibodies (VSV-PRNT50 [IU/ml]), and MVA-neutralizing antibodies (MVA-PRNT50 [neutralizing titer]) were measured by collaborators at the EMC Rotterdam, Netherlands, and data were kindly provided by Matthijs Raadsen. Binding IgG and neutralizing antibodies correlated positively with the strongest correlation seen at V3D28. MVA-neutralizing antibodies, a measure of immunity against the vaccine vector, also positively correlated with binding and MERS-neutralizing antibodies. Notably, only a weak, negative correlation was seen between the humoral parameters and the T cell response (Figure 22b).

### 5.2.3. Function and memory phenotype of spike-specific T cell responses

To further characterize the breadth and the functionality of the vaccine-induced T cell response, an intracellular cytokine staining assay was performed. Method details and reagents are described in publication II. In brief, PBMCs were stimulated with peptide pools (2.5 µg/ml) for 7 h at 37°C in the presence of Golgi-Plug, Golgi-Stop, and anti-CD28/CD49 (BD Biosciences). Cells were then stained with antibodies against surface markers and viability dye, and after fixation, with antibodies against the intracellular cytokines, IFN-γ, TNF-α, and IL-2. For each sample, cells incubated with an equimolar amount of DMSO (0.1%) and Phorbol-12-myristate-13-acetate (50 ng/ml), and ionomycin (0.5 µg/ml) served as negative and positive controls, respectively. Samples were measured on a spectral flow cytometer (Cytek Aurora) and analyzed using FlowJo (v.10.8.1.). A representative gating strategy is shown in Figure 23a. Cytokine-secreting memory T cells were identified by excluding CCR7<sup>+</sup>/CD45RO<sup>-</sup> naïve T cells and then gating the individual cytokines on CD4<sup>+</sup> and CD8<sup>+</sup> T cells separately. Results are shown as background (DMSO) subtracted data. To decipher which part of the MERS-CoV spike is most immunogenic, cells were stimulated in separate wells with the individual peptide pools M1-M5 which cover different regions of the spike (Figure 23, blue). Since most participants of the MVA-MERS-S study had a SARS-CoV-2 vaccination or infection during the trial, a peptide pool covering the whole SARS-CoV-2 spike protein was also included (Figure 23, green).

The total CD4<sup>+</sup> (Figure 23b) and CD8<sup>+</sup> (Figure 23c) T cell cytokine responses, as well as cytokine composition (pie charts) of three representative study participants, are shown. These participants were chosen here for comparability as they belonged to the same study arm (LD/LI; Figure 20 and Figure 21) and all had mild COVID-19 between the time points V2D28 and V3D28. The number and timing of SARS-CoV-2 infections and vaccinations varied greatly between participants of the MVA-MERS-S phase 1b trial. Therefore, grouped analyses of all participants would not provide meaningful results and are thus not shown here. The results show, that MVA-MERS-S vaccination induced a T cell response that is not dominated by one peptide pool, but distributed along the whole MERS-CoV spike, and equally of CD4<sup>+</sup> and CD8<sup>+</sup> phenotypes. MERS-CoV-spike-specific CD4<sup>+</sup> responses were highest after the third vaccination, and CD8<sup>+</sup> responses were highest after the second vaccination. Overall, both CD4<sup>+</sup> and CD8<sup>+</sup> SARS-CoV-2-spike-specific responses were preexisting at

V1D0 presumably from previous vaccinations, and increased in higher magnitude compared to MERS-CoV-spike-specific responses after COVID-19 at V3D28. The SARS-CoV-2-spike-specific and MERS-CoV-spike-specific CD4+ and CD8+ T cell response included T cells expressing IFN- $\gamma$ , TNF- $\alpha$ , and IL-2. The CD8+ response was dominated by IFN- $\gamma$ -secreting cells in two participants and by TNF- $\alpha$ -secreting cells in the third participant.

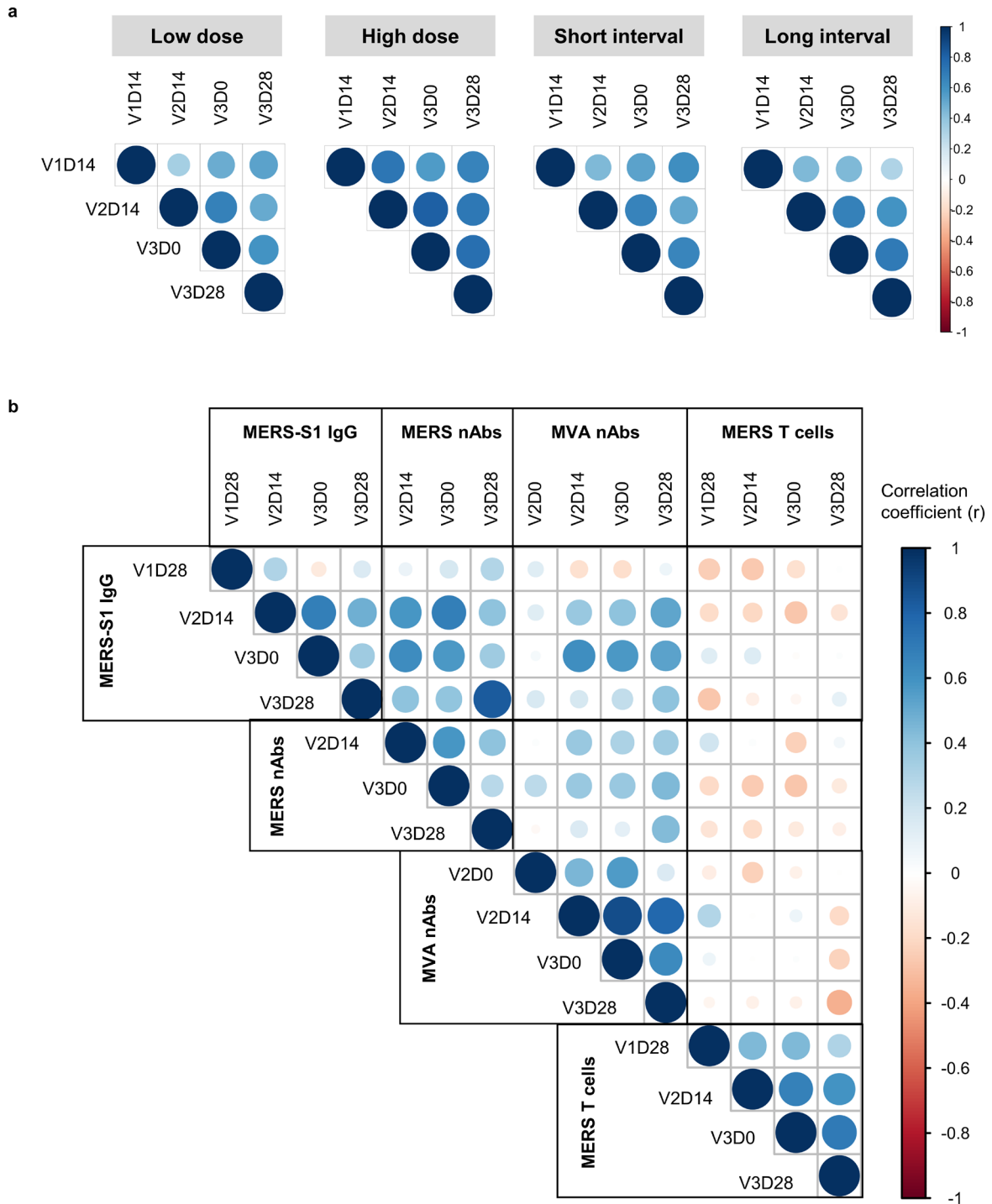


**Figure 22: Correlation of vaccine-induced T cellular and humoral responses.** a) Correlation of the T cell response at different time points stratified by vaccine dose and interval. b) Correlation of MERS-S1 IgG, MERS nAbs, MVA nAbs, and MERS S-specific T cell responses in the long interval group. The correlation coefficients ( $r$ ) as calculated by Spearman correlation, using the R function `corrplot`, are indicated by color (blue = positive correlation, red = negative correlation). nAbs = neutralizing antibodies. This figure was created using R (v4.2.0).

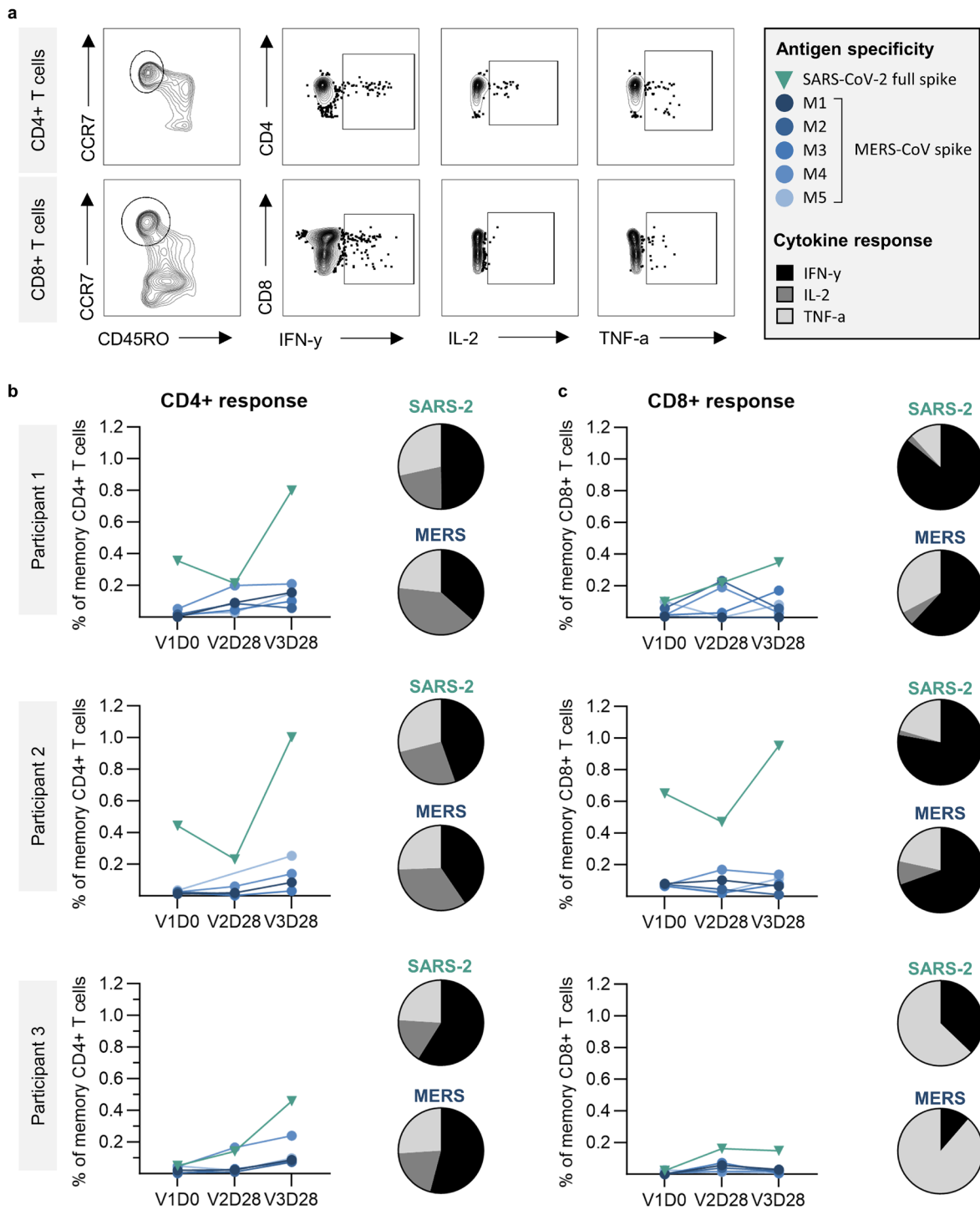


**Figure 23: Cytokine response of memory CD4+ and CD8+ T cells.** a) Intracellular cytokine staining gating strategy of CD4+ and CD8+ memory T cells expressing IFN- $\gamma$  (black), IL-2 (dark grey), or TNF- $\alpha$  (light grey). A peptide pool covering the whole SARS-CoV-2 spike (green), or individual pools M1-M5 covering the MERS-CoV spike (blue) were used for stimulation. b) CD4+ and c) CD8+ T cell response at baseline (V1D0), 28 days after second (V2D28) and 28 days after third (V3D28) MVA-MERS-S vaccination. Pie charts show the composition of total cytokine-secreting cells, either expressing IFN- $\gamma$  (black), IL-2 (dark grey), or TNF- $\alpha$  (light grey). Responses were measured by intracellular cytokine staining, after stimulation with SARS-CoV-2 (green) or MERS-CoV spike peptide pools (blue). The green arrow denotes the time of COVID-19. Data were acquired on the spectral flow cytometer (Cytek Aurora) and analyzed using FlowJo (v.10.8.1.). This figure was created using FlowJo (v10.9.0), GraphPad Prism (v10.0.0), and Microsoft PowerPoint.

#### 5.2.4. Epitope-specific CD8+ T cell responses

In publication II we identified for the first time in humans a MERS-CoV-spike-specific CD8+ T cell epitope<sup>181</sup>. This epitope, namely P19 (GLFPYQGDHGDYVY), was identified in an HLA-A\*03:01/ HLA-B\*35:01 homozygous participant of the MVA-MERS-S phase 1a clinical trial. We showed that P19 likely encodes an HLA-B\*35:01-restricted epitope by epitope prediction and could support this with experimental evidence. Specifically, the only other HLA-B\*35:01-positive individual of the study responded to P19, while those positive for HLA-A\*03:01 did not respond to P19. P19 is located in the S1 subunit of the MERS-CoV spike and in our analysis included in peptide pool M1.

Next, we evaluated if participants of the MVA-MERS-S phase 1b trial also mounted a response to P19. First, all participants of the MVA-MERS-S phase 1b trial were HLA-typed using commercially available A and B locus kits (LABType™ SSO Typing Test, ONE LAMBDA) according to the manufacturer's instructions. HLA-typing was performed at the Institute for Transfusion Medicine (UKE). In total, 11 out of 56 (19.6%) of participants were positive for the HLA-B\*35:01 allele, the HLA class I allele that was shown to restrict the P19 epitope. Next, the T cell response against the P19 peptide as well as against the peptide pools M1-M5 covering the full-length MERS-CoV spike was assessed by IFN- $\gamma$  ELISpot in four HLA-B\*35:01 positive study participants. These individuals were chosen because they had been identified as T cell assay responders following MVA-MERS-S vaccination in the previously described results (see chapter 5.2.1).

Figure 24a shows representative IFN- $\gamma$  ELISpot wells of the DMSO negative control, PHA positive control, P19 peptide stimulation, and M1 pool stimulation. Each row corresponds to one study participant. The HLA-type of each participant is denoted below. Figure 24b shows the frequencies of IFN- $\gamma$ -secreting cells after re-stimulation with the P19 peptide (black) and the peptide pools M1-M5. Notably, three out of the four tested individuals (Participants 4, 5, and 7) responded to the P19 peptide with frequencies ranging from 104 to 208 SFC/10<sup>6</sup> PBMC. In these individuals, the P19 response was comparable in magnitude to the M1-specific response.

In summary, these results show that prime-boost immunization with MVA-MERS-S elicits a robust spike-specific T cell response, particularly when prolonging the time interval between immunizations from 28 days to 56 days. A late third vaccination with the low dose of MVA-MERS-S boosted the T cell response significantly in the LD/LI treatment arm. Notably, the T cell responses did not correlate with the humoral response, which requires further investigation. MVA-MERS-S induced both CD8+ and CD4+ T cell responses that expressed different cytokines and were broadly specific for all peptide pools covering the entire MERS-CoV spike protein. As this trial was performed during the COVID-19 pandemic, participants also generated a SARS-CoV-2-specific response. We identified an immunodominant, MERS-CoV-spike-specific CD8+ T cell epitope, that is not conserved in other HCoVs and will thus be useful for monitoring MERS-CoV-specific responses in populations with pre-existing immunity against other HCoVs.



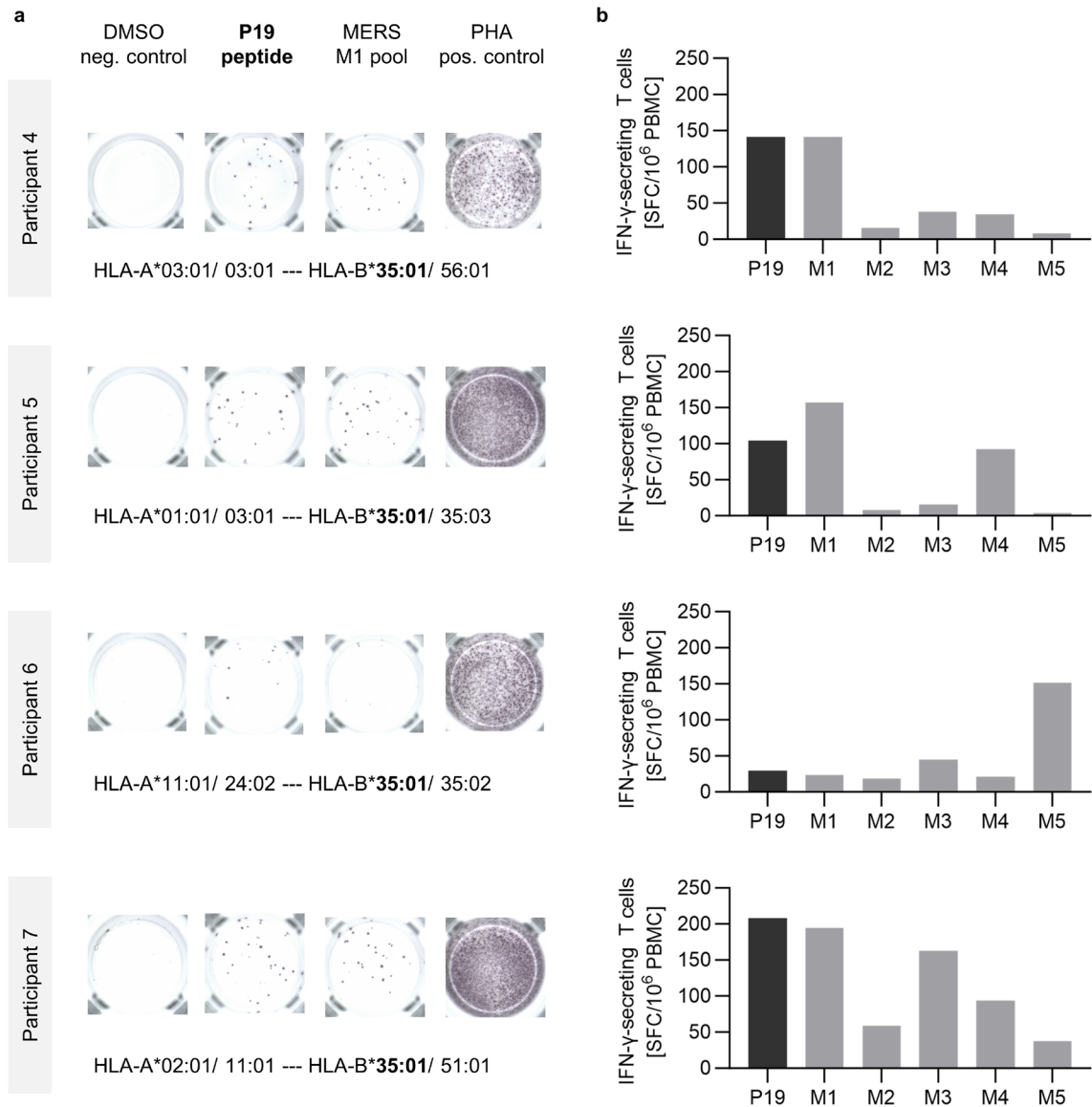


**Figure 24: IFN- $\gamma$  ELISpot of HLA-B\*35:01-positive participants of the MVA-MERS-S phase 1b trial.** a) Representative ELISpot wells showing negative control, P19 peptide, M1 peptide pool, and PHA wells (from left to right) following MVA-MERS-S vaccination in four participants (from top to bottom). HLA-A and HLA-B alleles of each participant are denoted below. b) Bar graphs show the frequencies of T cells specific for the P19-peptide (black) and peptide pools M1-M5 (grey) covering the complete MERS-CoV spike protein. This figure was created using GraphPad Prism (v10.0.0), and Microsoft PowerPoint.

## 6. DISCUSSION

This doctoral thesis set out to investigate the T cell response following vaccination against SARS-CoV-2 and MERS-CoV longitudinally in the context of several phase 1 clinical trials, in comparison to licensed vaccine regimens. Overall, the findings underline several overarching concepts that shape the induction of T cell memory following vaccination. In the following chapters of the discussion, firstly, the immunogenicity of the investigated vaccines is compared. Secondly, the characteristics of the vaccines and vaccination regimens are discussed. Lastly, several host factors are considered.

### 6.1. T cell immunogenicity of rMVA-based vaccine candidates

The rMVA viral vector technology is a promising platform for vaccine development based on several positive attributes, such as its favorable safety profile and large insert capacity. In a heterologous prime-boost regimen, an rMVA-based vaccine has already been licensed against Ebola virus disease. Upon the emergence of SARS-CoV-2, two vaccine candidates using rMVA were developed and tested in humans. Furthermore, a vaccine candidate against MERS is currently in clinical development and shows promise as no licensed vaccines are available against this WHO priority disease to date. The data obtained from our phase 1 clinical trials provide a valuable opportunity to compare the immunogenicity of these vaccine candidates to other candidates in development and those that have already proven efficacious in phase 3 clinical trials. In the following discussion chapters, this comparison is done first for the MVA-MERS-S candidate against MERS and then for the MVA-S and MVA-ST candidates against COVID-19.

#### 6.1.1. The MVA-MERS-S vaccine candidate

MERS is a WHO priority disease, but currently, no licensed vaccines are available. Besides MVA-MERS-S, tested in a phase 1a (published) and a phase 1b (unpublished, ongoing) trial, two other vaccine candidates are currently in clinical development. ChAdOx1 MERS is a viral vector vaccine based on a chimpanzee adenovirus, the same vector that was used to construct the ChAdOx1 nCoV-19 vaccine<sup>189,190</sup>. It was administered to healthy adults as a single-dose regimen by intramuscular injection in two clinical trials conducted in the UK and Saudi Arabia<sup>189,190</sup>. GLS-5300 is a DNA vaccine that was administered to healthy adults in a three-dose regimen (at baseline, week four, and week 12) by intramuscular electroporation in the USA<sup>191,192</sup>. All three vaccine candidates were shown to have an acceptable safety profile and to induce a MERS-CoV-spike-specific immune response, with a trend towards higher binding and neutralizing antibody responses in the high dose groups. A comparison of the T cell response, measured by IFN- $\gamma$  ELISpot, between our MVA-MERS-S phase 1b trial (chapter 5.2.1) and the other published MERS vaccine trials is summarized in Table 1. A direct comparison of these trials is difficult due to differences in experimental setups and the definition of assay responders.

Comparing the two MVA-MERS-S trials, T cell responses were detectable at least at one time point after vaccination in 73% (36/49) of participants in the phase 1b trial compared to 87% (20/23) of participants in the phase 1a trial. This difference may be due to differences in the experimental setups. To be more precise, a single large peptide pool covering the whole spike (316 peptides) was used as a screening assay in the phase 1b trial, whereas in the phase 1a trial, peptides were divided into five pools (79 peptides per pool) that were tested in separate ELISpot wells. When using a larger peptide pool, the final concentration of the individual peptides is lower, which might induce a lower recall response compared to smaller pools with higher concentrations of the individual peptides. On the one hand, the use of five separate pools has the advantage, that responses against different regions of the spike protein can be deciphered. On the other hand, this approach is very resource-consuming, especially with regard to limited PBMC availability. Therefore, a single pool was used for the larger phase 1b trial. An explanation which does not depend on the experimental setup could be that the vaccines used in the two trials are differently immunogenic. Indeed, while they contain the same

vaccine construct, the two vaccines were generated using different manufacturing processes. The vaccine used in the phase 1a trial was produced in chicken embryo fibroblasts (CEF), while the vaccine used in the phase 1b trial was produced in an immortalized cell line (DF-1) to allow for improved upscaling of manufacturing. It is hypothesized that the CEF-produced vaccine contains a higher number of byproducts from the cell line. These products can have immunostimulatory properties<sup>193</sup>. The availability of stimulants that activate the innate immune response directly influences the induction of the T cell response<sup>122</sup>. Future studies are needed to investigate the influence of vaccine production on the immunogenicity of rMVA-based vaccines in humans.

**Table 1: Comparison of T cell responses in MERS vaccine trials.** Results of the MVA-MERS-S 1b trial (unpublished) compared to the results of the published MVA-MERS-S phase 1a trial and those testing the ChAdOx1 MERS and the GLS-5300 DNA vaccine. In all trials, T cell responses were measured by IFN- $\gamma$  ELISpot after re-stimulation with MERS-CoV spike peptide pools. Different experimental setups resulting in different baseline responses and varying definitions of assay responders were used. PFU = plaque-forming units, VP = viral particles, LD = low dose, MD = middle dose, HD = high dose, LI = long interval, SD = standard deviation.

	MVA-MERS-S 1b	MVA-MERS-S 1a	ChAdOx1 MERS	GLS-5300 DNA
<i>Reference</i>	Unpublished results	Koch et al. (2020) <sup>167</sup>	Folegatti et al. (2020) <sup>190</sup>	Modjarrad et al. (2019) <sup>192</sup>
<i>Number of participants</i>	N = 49 (+7 placebos)	N = 23	N = 24	N = 75
<i>Dose groups</i>	LD = $1 \times 10^7$ PFU HD = $1 \times 10^8$ PFU	LD = $1 \times 10^7$ PFU HD = $1 \times 10^8$ PFU	LD = $5 \times 10^9$ VP MD = $2.5 \times 10^{10}$ VP HD = $5 \times 10^{10}$ VP	LD = 0.67 mg MD = 2.0 mg HD = 6.0 mg
<i>Reported T cell results</i>	median against 1 pool	Sum of medians against 5 peptide pools	Sum of means against 13 peptide pools	Sum of means against 5 peptide pools
<i>Definition assay responder</i>	> cut-off (mean of all baseline samples + 2x SD = 26 SFC) and 2x above baseline	> 50 SFC and 4x above baseline	-	> 2x mean of all baseline samples = 141 SFC
<i>% assay responder (N, time point)</i>	73% (36/49, at $\geq 1$ time point); 46% (22/48, V3D28)	87% (20/23, at $\geq 1$ time point)	above baseline in all dose groups	76% (44/58, V3D28)
<i>Baseline response</i>	6 SFC (mean) 1 SFC (median)	20 SFC (median)	~200 SFC (mean)	71 SFC (mean)
<i>Peak response (dose group, time point)</i>	59 SFC (median) (LD, V3D28)	147 SFC (median) (LD, V2D28)	4019 SFC (median) (HD, V1D14)	652 SFC (mean) (LD, V3D28)
<i>Fold-change peak response vs. baseline</i>	9	7	~21	9

When comparing the T cell immunogenicity of MVA-MERS-S with the ChAdOx1 and DNA-based vaccine candidates, the overall dynamics of the responses are similar, but some differences in the magnitude and number of assay responders can be observed. In the GLS-5300 DNA trial, assay responders were defined at a single time point after completion of the GLS-5300 vaccine regimen (=V3D28). At this time point, 76% of participants were assay responders. When applying the same criteria to our MVA-MERS-S phase 1b data set, only 46% (22/48) of participants were assay responders. While these results could suggest that GLS-5300 is more immunogenic in comparison to MVA-MERS-S, it is important to note, that we used a more stringent assay responder definition in our data set, which might account for these differences. In fact, when comparing the magnitude of the response at V3D28, median levels were 9-fold above baseline in both trials. In the ChAdOx1 MERS trial, a cut-off for assay responders was not defined, but the T cell response after vaccination was significantly above baseline in all dose groups. Interestingly, in both, the MVA-MERS-S and GLS-5300 trials, the highest T cell response was observed in the low dose groups, while for the ChAdOx1 MERS trial, the highest response was observed

in the high dose group. Evidence concerning the dose-dependency of vaccine-induced T cell responses is discussed in more detail in chapter 6.2.2.

Overall, it can be summarized that a direct comparison of T cell immunogenicity between the MERS vaccine candidates in humans is difficult since assay setups are not harmonized. The lack of standardized assays is a major challenge in assessing the immunogenicity of vaccine candidates in early-stage clinical trials. This became evident during the COVID-19 pandemic when several vaccine candidates were in development at the same time. Several stakeholders called for the standardization of assays and quality controls to facilitate comparison between studies. In 2020, an international standard for calibrating SARS-CoV-2 neutralizing antibody assays was established and distributed<sup>194</sup>. Nevertheless, no such standard is currently available for assays measuring the cellular immune response. The Coalition of Epidemic Preparedness Innovations (CEPI) is establishing a global network of laboratories to centralize the assessment of COVID-19 vaccine candidates<sup>195</sup>. If successful, such a network should also be considered for assessing vaccine candidates against other infectious diseases, such as MERS.

### **6.1.2. The MVA-S and MVA-ST vaccine candidates**

To overcome the difficulty of comparisons between vaccines due to the lack of standardized cellular assays, we evaluated the immunogenicity of our rMVA-based COVID-19 vaccine candidates, MVA-S and MVA-ST, in direct comparison to the licensed vaccine regimens. Detailed results are described in publication I and chapter 5.1.1. In brief, we recruited two cohorts who received different three-dose vaccination regimens with the licensed ChAd and mRNA-based COVID-19 vaccines as a benchmark. We then analyzed humoral and cellular responses in parallel to the rMVA-based cohorts using the same experimental setups. Furthermore, we used a commercial SARS-CoV-2 spike-specific IGRA T cell assay which was developed during the COVID-19 pandemic and has now been standardized and licensed for research use<sup>196</sup>. We additionally recruited unexposed and COVID-19 convalescent individuals for comparison. With this approach, we were able to compare the immunogenicity of MVA-S and MVA-ST, as well as to put the magnitude of the response into context with licensed vaccine regimens.

Despite providing protective efficacy in pre-clinical models<sup>169</sup>, MVA-S showed only a marginal induction of S1- and RBD-specific antibodies in an interim analysis of the first-in-human trial (publication VI, chapter 5.1.1). The optimized vaccine candidate, MVA-ST, encoding the prefusion-stabilized spike protein was subsequently tested in a phase 1 clinical trial. Our comparative analysis showed that MVA-ST is more immunogenic in humans than MVA-S in terms of spike-specific IgG, B cell, and T cell responses (publication I, chapter 5.1.1). MVA-S elicited a spike-specific T cell response in some individuals, especially after the first dose, but the median response measured by IGRA was 3.5-fold higher after the first MVA-ST vaccination (chapter 5.1.1). The same pattern was observed using the ELISpot assay (publication I). Notably, both candidate vaccines protected animals from disease<sup>168</sup>, underlining the fact that efficacy results from pre-clinical models may have limited transferability to immunogenicity in humans.

In comparison to the licensed vaccines, one dose of MVA-ST induced median T cell responses at comparable magnitude to one dose of the ChAd viral vector vaccine. However, this response was two-fold lower compared to mRNA vaccination. Notably, the response was significantly boosted by the subsequent second mRNA vaccination in our control cohorts. In contrast, the response was not significantly boosted by the second MVA-ST dose in our MVA-ST cohort. Interestingly, one other phase 1 clinical trial of an rMVA-based SARS-CoV-2 vaccine candidate has been published to date and the authors made a similar observation. To briefly introduce the study: Routhu et al. developed a multiantigen rMVA-based vaccine candidate (called COH04S1) expressing the SARS-CoV-2 spike and nucleocapsid antigens<sup>197,198</sup>. Chiuppesi et al. tested the vaccine candidate in a phase 1 clinical trial in

SARS-CoV-2 naïve, healthy adults, receiving one or two doses, 28 days apart, of either  $1 \times 10^7$  (low dose),  $1 \times 10^8$  (middle dose) or  $2.5 \times 10^8$  (high dose) PFU of the vaccine<sup>199</sup>. All study participants seroconverted within 28 days of the second vaccination, as measured by spike-specific IgG ELISA. Notably, T cell responses after the first and second COH04S1 vaccination were induced at comparable levels, and not significantly enhanced by the second dose<sup>199</sup>, as also observed in our MVA-ST trial. These data suggest, that rMVA-based vaccines have a limited capacity to boost the T cell response when used in a homologous prime-boost scheme. How heterologous prime-boost schemes might overcome this is further discussed in chapter 6.3.1.

## 6.2. Vaccine characteristics shaping T cell immunogenicity

Focusing on the T cell response, we observed that various characteristics of the vaccine and vaccination regimen impact immunogenicity. These are discussed in more detail in the following chapters, drawing parallels between the COVID-19 and MERS vaccines analyzed in the published and unpublished results of this thesis. Factors include the spike antigen design (chapter 6.2.1), vaccine dose (chapter 6.2.2), vaccine platform (chapter 6.2.3), the use of heterologous prime-boost regimens (chapter 6.3.1), the time interval between prime and boost vaccinations (chapter 6.3.2), and the potential of re-boosting the T cell response (chapter 6.3.3).

### 6.2.1. Spike antigen design

The spike protein is a major target of the neutralizing antibody response due to its exposure on the viral surface and essential functions in viral entry<sup>200</sup>. It is thus a logical vaccine antigen choice. Indeed, the licensed vaccines against SARS-CoV-2 and those in clinical development against MERS-CoV are all based on the spike protein of these CoVs<sup>90,91,201,202</sup>. However, some structural properties have to be considered when designing the spike protein as a vaccine antigen. The spike protein is metastable in its mature form and can easily undergo conformational changes<sup>193</sup>. When expressed in cells, it is readily cleaved by host proteases triggering the dissociation of the S1 subunit and the irreversible refolding of the S2 subunit into a postfusion conformation. This exposes non-neutralizing epitopes in the S2 subunit while hindering recognition of neutralizing epitopes in the S1 subunit. This phenomenon has also been described for fusion proteins of other viruses such as HIV and RSV<sup>203,204</sup>. Since neutralizing antibodies are important for protection, a structure-based approach has been employed to stabilize the spike protein in its prefusion conformation to preserve neutralizing epitopes<sup>205</sup>.

Initially, prefusion-stabilizing mutations were designed to solve the structures of HCoV spikes by cryo-electron microscopy<sup>15,206,207</sup>. Pallesen et al. introduced two proline substitutions at the beginning of the central helix of the MERS-CoV spike S2 subunit, which sterically hindered refolding and membrane fusion of the spike protein<sup>208</sup>. This design also enhanced the recombinant expression yield and stability of the protein<sup>208</sup>. It was shown that neither receptor binding nor S1/S2 cleavage could induce conformational changes in this prefusion-stabilized construct<sup>209</sup>. Similarly, Wrapp et al. designed a modified SARS-CoV-2 spike sequence that renders the protein in its prefusion-stabilized conformation<sup>15</sup>. This modified spike was used in the licensed COVID-19 mRNA vaccines<sup>82,170</sup>. Notably, the ChAdOx1 vaccine encodes the unmodified, native spike<sup>173</sup>.

Since two versions of our rMVA-based COVID-19 vaccine candidates were constructed and tested in humans, one expressing the native spike (MVA-S) and one expressing the prefusion-stabilized spike (MVA-ST), we had the unplanned but unique opportunity to directly compare the impact of spike antigen conformation on immunogenicity. In our studies comparing the two rMVA-based candidates, we observed a differential bias of the adaptive immune response towards the S1 and S2 subunits of the SARS-CoV-2 spike antigen (publication I). Both vaccine candidates induced an S2-specific response, while the S1-specific response was significantly higher after vaccination with MVA-ST, the vaccine candidate expressing the prefusion-stabilized spike. This bias was reflected in the spike-specific IgG,

B cell, and T cell responses, respectively. A similar pattern was observed in pre-clinical rodent models (publication VI), with enhanced humoral immunogenicity towards the S1 subunit after MVA-ST vaccination and towards the S2 subunit after MVA-S vaccination. Interestingly, rodents mounted similar levels of S1-specific T cell responses, regardless of MVA-S or MVA-ST vaccination. While these results seem in contrast to the S1/S2 T cell bias observed in humans, the results in rodents do not reflect the whole breadth of the response because only a single S1-specific T cell epitope was used in the analysis.

Meyer zu Natrup et al. provided evidence for differential cell surface expression of the native and prefusion stabilized spike delivered by MVA-S or MVA-ST *in vivo* (published results VI)<sup>168</sup>. Immunofluorescent staining of cell lines infected *in vitro* with MVA-S or MVA-ST showed abundant S2 protein expression on the cell surface. In contrast, significantly higher levels of S1 cell surface expression were detected in MVA-ST-infected compared to MVA-S-infected cells. These results suggest that epitopes in the S1 subunit are more readily available for recognition by the immune system *in vivo* when the spike prefusion-stabilized construct is delivered by the vaccine. Interestingly, the MVA-MERS-S vaccine candidate, encoding the native MERS-CoV spike, was shown to be immunogenic, eliciting both, S1- and S2-specific humoral and cellular immune responses, as published previously<sup>167,179,180</sup> and shown in chapter 5.2. This may be explained by intrinsic differences in the stability of the MERS-CoV and SARS-CoV-2 spikes *in vivo*. Örd et al. recently showed that the SARS-CoV-2 spike contains a furin cleavage motif at the S1/S2 cleavage site that is not present in the MERS-CoV spike<sup>210</sup>. Furin is ubiquitously expressed, meaning that the SARS-CoV-2 spike is readily cleaved into the S1 and S2 subunits once expressed, while the MERS-CoV spike remains in its native form, as also demonstrated by Matsuyama et al.<sup>211</sup>

Taken together, our observations in humans, pre-clinical models, and *in vitro* experiments comparing the MVA-S and MVA-ST candidates suggest that the conformation of the spike antigen has important implications for the immunogenicity of vaccine candidates against HCoVs, particularly SARS-CoV-2. How this affects the quality of the immune response requires further investigation but pre-clinical data suggest that the dissociation of the S1 subunit in a non-stabilized spike may induce a higher proportion of non-neutralizing antibodies<sup>193,212,213</sup>. It has been shown previously for RSV in humans<sup>214</sup> and for MERS-CoV in mice<sup>208</sup>, that prefusion-stabilized proteins are superior at inducing neutralizing antibodies since conformational epitopes are exposed on the surface of the prefusion antigen. For T cell responses, theoretically, this conformation of the antigen should be less relevant, as T cells recognize short peptides and do not dependent on the integrity of the three-dimensional structures of the antigen. It may thus be hypothesized that vaccine candidates expressing the native spike can be important for driving T cell responses against the S2 subunit which is highly conserved amongst emerging viral variants. These cross-reactive T cell responses might thus protect against disease from heterologous strains.

### 6.2.2. Vaccine dose

One important goal of early-stage clinical trials is to find the optimal vaccine dose. This is traditionally considered a balancing act between immunogenicity and safety considerations, as lower doses are less reactogenic, but higher doses are often more immunogenic. Since the MVA-MERS-S phase 1b trial consisted of a considerably high participant number for a phase 1 study, it was possible to analyze differences in T cell immunogenicity based on vaccine dose in this trial.

Interestingly, we observed that the median frequency of spike-specific T cells after a single MVA-MERS-S vaccination was higher in the low compared to the high dose (chapter 5.2.1). There was also a trend towards higher responses after the second dose in the low dose cohorts. However, this effect is likely overshadowed by the effect of the different prime-boost time intervals (discussed in

chapter 6.3.2). The difference was clearest after the third vaccination, with a higher median frequency of spike-specific T cells and a higher percentage of assay responders in the low dose cohorts. The same observation was made in the smaller phase 1a trial, with a trend toward higher T cell responses and longer persistence after the second vaccination in the low dose cohort<sup>167</sup>. In the study arm testing MVA-ST as a booster vaccination, we also saw the strongest boosting of T cell responses in the middle dose group (publication I, chapter 5.1.1). Chiuppesi et al. tested three dose levels of a synthetic rMVA-based COVID-19 vaccine candidate in humans and also observed the highest T cell induction in the middle dose<sup>199</sup>. These results show an interesting trend for MVA-based vaccines and are rather unexpected, as generally higher vaccine doses elicit higher immune responses.

Capone et al. tried to address this by performing a dose de-escalation study in humans to test the impact of lowering the rMVA dose in the context of a heterologous prime-boost regimen against Hepatitis C virus (HCV)<sup>215</sup>. Participants received a ChAd-based prime followed by an rMVA-based boost eight weeks later of high ( $2 \times 10^8$  PFU), middle ( $2 \times 10^7$  PFU), or low dose ( $2 \times 10^6$  PFU). Overall, the function, breadth, and magnitude of the HCV-specific T cell response were not impacted when using lower doses of rMVA. Our data, in line with the published results of Capone et al., suggest, that lower doses of rMVA-based vaccines are not inferior, or might even be superior in inducing T cell responses.

Only limited data are available regarding the dose dependency of other vaccines on the T cell response. However, some studies suggest that the above-mentioned observation is not restricted to rMVA-based vaccine regimens. In the phase 1/2 trial of the BNT162b2 vaccine, four different doses ranging from 1 µg to 50 µg were tested. While the antibody response increased with higher doses, no clear dose-dependency of the T cell response was observed. Even the 1 µg dose elicited a robust, Th1-biased T cell response<sup>216</sup>. Low-dose vaccination of the mRNA-1273 vaccine (25 µg) compared to the standard dose (100 µg) resulted in comparable peak CD8+ T cell responses, however, CD4+ T cell responses were 1.4- to 2-fold higher in the standard dose group<sup>217</sup>. Using the ChAd platform in a vaccine candidate against HCV, it was shown that there is no benefit for T cell responses when using doses higher than  $2.5 \times 10^{10}$  viral particles<sup>218</sup>. If and how these results translate into protective efficacy cannot be deciphered by these early-stage trials. Interestingly though, a pooled efficacy analysis of the phase 2/3 trials of the ChAd vaccine revealed that vaccine efficacy was higher in the group that received a low-dose ( $2.2 \times 10^{10}$  viral particles; VE = 90%) compared to a standard dose ( $5 \times 10^{10}$  viral particles; VE = 60%) vaccination<sup>174</sup>. Although this low-dose ChAd vaccination was originally not planned, and the results should be interpreted with caution due to a small sample size in this cohort, the results provide interesting first insights into the relationship between vaccine dose and efficacy.

In contrast to the T cell response, neutralizing antibody responses were most pronounced in the high dose cohorts of our MVA-MERS-S phase 1b trial. These data are consistent with the results of phase 1<sup>219</sup> and phase 2<sup>220</sup> clinical trials testing MVA as a third-generation smallpox vaccine, where seroconversion and total antibody response were higher when using the high vaccine dose ( $1 \times 10^8$  TCID<sub>50</sub>)<sup>221</sup>. The lack of correlation between the humoral and T cell response in our MVA-MERS-S study (chapter 5.2.2) suggests a discordance between these two arms of the immune response. Vaccine studies in humans against influenza and COVID-19 have reported a similar discordance<sup>222,223</sup>.

To decipher why low doses could be beneficial for the induction of a robust T cell response, several immunological reasons are plausible. Studies have previously shown that T cells may require a lower antigen concentration than B cells<sup>224,225</sup> and that concentrations higher than the one required for T cell activation may not result in higher T cell responses<sup>226</sup>. An additional explanation could be that with a low vaccine dose, only high avidity T cells are activated due to competition for the limited available antigen, resulting in an enhanced quality of the T cell response<sup>227</sup>. An excessive antigen load can also lead to tolerance or exhaustion of T cells<sup>228</sup>. Increasing evidence is pointing in the direction that the “more-is-better” line of thinking in vaccination is coming of age and that in addition to dose escalation,

also dose de-escalation studies should be considered in the future<sup>227</sup>. Lower dose vaccination can also have several non-immunological advantages, such as lower reactogenicity, more vaccine doses available, and lower cost per dose. The production of high doses of rMVA-based vaccines is technologically challenging. Thus, the use of lower doses of rMVA-based vaccines specifically would also be more feasible for large-scale vaccination programs.

### 6.2.3. Vaccine platform

One important advantage of mRNA and viral vector-based vaccines, in contrast to subunit vaccines, is that they mimic a natural infection in the sense that antigen is delivered to the interior of the cell where it is presented via the endogenous pathway<sup>97</sup>. Thus, not only CD4+ but also CD8+ T cell responses can be primed efficiently. In our different cohorts, we could observe some differences in the CD4+ and CD8+ T cell bias and the timing of the peak responses between mRNA and viral vector-based vaccines. We saw that vaccination with the licensed COVID-19 vaccine elicited CD4+ T cell responses after the first dose that were boosted by the second dose. CD8+ T cell responses were also induced but only after the second dose (publication I, chapter 5.1.1). This observation was also published in a systems vaccinology analysis of the BNT162b2 vaccine by Arunachalam et al<sup>229</sup>. Both, CD4+ and CD8+ T cell responses were induced by the viral vector-based MVA-MERS-S vaccine candidate in our phase 1b trial (chapter 5.2.3).

In our comparative analysis with the rMVA-based vaccine candidates, we could show that even though the MVA-S vaccine candidate was not immunogenic enough by itself when used as a prime before mRNA vaccination, the polyfunctionality and frequency of cytokine-secreting T cells were enhanced. Most notable was the higher frequency of cytokine-secreting CD8+ T cells after the first mRNA vaccination in the cohort that had previously received MVA-S doses. Zhang et al. performed a comparative immunogenicity analysis of four COVID-19 vaccines, namely the mRNA-1273 and BNT162b2 mRNA vaccines, the Ad26.COVS viral vector vaccine, and the NVX-CoV2373 adjuvanted subunit vaccine<sup>222</sup>. CD8+ T cell responses were similar between the mRNA and viral vector vaccinations. However, CD8+ T cell responses were only detectable in a few participants after NVX-CoV2373 subunit vaccination. Considering the dynamics of the vaccine-induced T cell response, we could also observe some differences between the vaccine platforms in our studies. While the peak frequency of spike-specific T cells was between 7 and 14 days after mRNA and rMVA-based vaccination, the peak was at day 28 after ChAd vaccination.

The differential induction of CD4+ and CD8+ T cells as well as the timing of peak responses might be a result of early innate pathways that are differentially activated by the vaccine platform. Arunachalam et al. showed that the CD8+ T cell response after mRNA vaccination correlated with interferon and antiviral signatures of the innate immune response<sup>229</sup>. Comparison of vector-induced transcriptional responses after Ad- or rMVA-based vaccination revealed that Ad vectors induce genes involved in toll-like receptor (TLR) 2 signaling while rMVA induces greater expression of type 1 IFN genes<sup>230</sup>. Viral vector vaccines, unlike mRNA vaccines, also activate TLR9 which binds dsDNA<sup>231</sup>. Intracellular RNA sensors and components of the inflammasome are activated especially by mRNA vaccines<sup>109</sup>. Differential immunogenicity of the viral vector vaccines may also be impacted by the expression of immune modulators. The MVA genome encodes for several immunomodulatory genes, such as K3L and E3L, that inhibit the activation of interferon-induced proteins of the early host immune response<sup>232,233</sup>. This reduced innate immune activation might dampen the adaptive immune response to the vaccine<sup>233</sup>. Engineering MVA mutants lacking some of these modulators is a growing field of interest, and it has been shown that such mutants improve the immunogenicity of rMVA-based vaccines<sup>234–236</sup>.



### 6.3. Vaccination regimen shaping T cell immunogenicity

Besides the physical characteristics of the vaccine or vaccine platform, the way in which they are used, i.e. the vaccine regimen, has a profound impact on the vaccine-induced immune response. This includes parameters such as the combination of different vaccines in a heterologous prime-boost regimen (chapter 6.3.1), the time interval between vaccine doses (chapter 6.3.2), and the use of additional booster doses (chapter 6.3.3), discussed below.

#### 6.3.1. Heterologous prime-boost

Prime-boost vaccine regimens are necessary when using vaccines based on protein subunits, mRNA, and non-replicating vectors, as these platforms only provide the antigen transiently which is insufficient for generating a potent memory response. This is in contrast to live-attenuated vaccines, which actively replicate and express the antigen over a prolonged period<sup>78</sup>. It has been shown that the memory phenotype and function of vaccine-induced T cells change with the number of immunizations. Responses after booster vaccinations retain effector-like functions and accumulate in non-lymphoid tissues<sup>237</sup>. Using a prime-boost regimen is thought to be beneficial for inducing a long-lived protective response. Prime-boost vaccination can be either homologous, meaning that an identical vaccine is used for prime and boost, or heterologous if a different vaccine is used for the boost<sup>141</sup>.

One theoretical disadvantage of homologous prime-boost vaccination using viral vector platforms is anti-vector immunity. Immune responses induced by the prime vaccination against the vector could limit the immunogenicity of the booster vaccination. These could be for example neutralizing antibodies, that neutralize the viral vector before it can enter cells for the expression of the vaccine antigen<sup>84</sup>. In our phase 1 clinical studies in naïve individuals, homologous prime-boost vaccination with rMVA-based vaccine candidates was tested. Neutralizing antibodies against the rMVA vector were indeed induced at increasing titers by each successive vaccination in the MVA-MERS-S study, however, they correlated positively with MERS-CoV-neutralizing antibody titers (chapter 5.2.2). This suggests, that anti-MVA immunity rather represents a marker of the vaccine response and does not limit the immunogenicity of homologous rMVA-based booster vaccinations. A similar observation of a positive correlation between vector immunity and immunity to the insert was also observed in other studies with viral vector vaccines, e.g. the VSV-EBOV vaccine against Ebola virus disease<sup>238</sup>. However, in the MVA-ST trial it was observed that, while the MVA-ST prime induced a strong T cell response at comparable magnitude to a ChAd prime, the MVA-ST boost only slightly increased the response further (publication I, chapter 5.1.1).

Another rationale for using a heterologous prime-boost approach is that the advantages of individual vaccine platforms can be combined resulting in an additive effect. The first licensed heterologous prime-boost regimen was the Ad26-MVA regimen against Ebola. The Ad26 platform is effective at priming a strong T cell response<sup>190,215</sup>, while the rMVA platform has been shown to enhance the magnitude and breadth of the memory T cell response when used as a boost<sup>239,240</sup>. Swadling et al. showed in an HCV clinical study, that following a ChAd3 prime, an rMVA-boost was superior in inducing a durable, polyfunctional T cell response compared to an Ad6-based boost<sup>218,239</sup>. In our studies rMVA-based vaccines were not combined with an Ad-based vaccine but with mRNA-based vaccination. We could observe enhanced polyfunctionality of the CD4+ T cell response and increased magnitude of the total cytokine-secreting CD8+ T cell response when MVA-S was given before mRNA vaccination. MVA-ST, in turn, was able to boost T cell responses in those with low residual immunity when used as a third vaccination following mRNA-based vaccination (publication I). The ChAd vaccine was originally also licensed as a homologous prime-boost regimen. However, as rare side effects were observed after prime ChAd vaccination, mRNA was more commonly given as a boost in COVID-19 vaccine regimens. A comparative analysis by Barros-Martines et al. showed that heterologous boosting with BNT162b2

was more efficient in inducing a T cell response, particularly IFN- $\gamma$  positive CD8+ T cells, compared to a homologous ChAd boost<sup>241</sup>. Taken together, these data suggest that combining different viral vectors or a viral vector with the mRNA platform in heterologous vaccine regimens can be beneficial for inducing a potent T cell response and should be considered in the design of future trials using rMVA-based vaccines.

### 6.3.2. Prime-boost time interval

Not only the combination of different vaccine platforms in a prime-boost regimen but also the time interval between vaccine doses can have a profound effect on the immune response<sup>242,243</sup>. The time interval between the prime and boost of licensed routine immunization regimens varies from a few weeks to several months. These regimens are mostly based on prior experience and practical constraints but not based on immunological data. Most clinical trials are not designed to assess the impact of different prime-boost intervals on immunogenicity, thus human data is scarce. Rodrigues and Plotkin reviewed the available data from randomized controlled trials that were powered to assess the immunogenicity of different prime-boost intervals<sup>242</sup>. It was shown that longer intervals between prime and boost result in higher antibody titers, as long as the boost is given within 6 months. This data is consistent across vaccines against varicella-zoster, polio, pneumococcal disease, and HPV infection. Unfortunately, there is scarce data on the impact of the interval on the T cell response. This is mainly due to the limitation that T cell responses are usually not assessed in large clinical trials.

The trial design of our MVA-MERS-S phase 1b study provided the unique opportunity to directly assess the impact of the prime-boost interval of a homologous rMVA-based vaccination regimen on vaccine-induced T cell responses. It was observed, that the median frequency of spike-specific T cells after the boost was higher in the cohorts that received the boost after a long interval (56 days) compared to the short interval (28 days). Furthermore, the responses persisted for at least 6 months in the long interval cohorts, while in the short interval cohorts, they decreased to levels not significantly above baseline (chapter 5.2.1).

Human T cell data comparing different intervals of homologous rMVA-based prime-boost regimens are limited to one other clinical trial published by Chiuppesi et al. in 2022<sup>199</sup>. The study tested, amongst other dose levels, a 28-day and 56-day interval of homologous prime-boost vaccination with the low dose ( $1 \times 10^7$  PFU) of a synthetic MVA vaccine expressing the SARS-CoV-2 spike and nucleocapsid antigen. The median frequency of spike-specific T cells (measured by IFN- $\gamma$  ELISpot) was approximately two-fold higher at day 28 after the second vaccination in the 56-day, compared to the 28-day interval, which is in line with our observations in the MVA-MERS-S study. This higher immunogenicity of the long interval was also observed in the humoral response, with a significantly higher increase in neutralizing antibody titers in the 56-day interval group.

The impact of the prime-boost interval was also addressed in two dose-finding studies of the now licensed heterologous prime-boost Ebola vaccine regimen consisting of an Ad26 prime followed by an rMVA boost. A 56-day interval led to a higher induction of binding and neutralizing antibodies compared to the 28-day interval<sup>85,244</sup>. These responses were not further enhanced by an 84-day interval. Overall, T cell responses were less affected, with a trend towards slightly higher median responses in the 28-day interval cohort. These T cell data differ from our results and the aforementioned results published by Chiuppesi et al., which both are for homologous prime-boost regimens. The findings highlight that the T cell response as function of the prime-boost interval also depends on whether the vaccine regimens is homologous or heterologous.

Studies in animal models provide further evidence for a relationship between T cell responses and prime-boost time intervals for vaccination using viral vectors. Natalini et al. analyzed prime-boost intervals in mice using ChAd- and rMVA-based vaccination against the model antigen HIV-1 gag<sup>245</sup>. The

authors showed that an rMVA boost was more effective at day 100 compared to day 30 in boosting HIV-1 gag-specific CD8+ T cells that were primed by ChAd vaccination previously. CD8+ T cells were also more functional, as measured by *in vivo* killing assays. RNA-sequencing revealed an enrichment of genes related to a quiescent, but highly responsive memory T cell signature in the 100-day group. A study testing different combinations of viral vectors encoding the same antigen revealed that reducing the prime-boost interval to two weeks resulted in reduced longevity of CD8+ memory<sup>246</sup>.

Delaying the second COVID-19 vaccine dose was a strategy adopted by many countries during the pandemic to be able to immunize more people in the face of a vaccine shortage. In retrospect, however, it was shown by several observational studies that this delayed dosing interval was also immunologically beneficial. Higher RBD-specific IgG and neutralizing titers were observed when delaying the second BNT162b2 vaccination from 3-6 to 8-16 weeks<sup>247</sup>. In this study, polyfunctional CD4+ and CD8+ T cell responses were also analyzed. Notably, no differences in the magnitude of the T cell response were observed between the short and long interval cohorts. Conversely, in another observational study with a higher participant number, an enrichment of IL-2 expressing CD4+ T cells was measured in the long interval cohort<sup>248</sup>. A pooled analysis of the ChAd clinical trials revealed, that in those who received two standard doses, efficacy was higher in the group with a longer prime-boost interval ( $\geq 12$  weeks interval; VE = 81.3%) than in the group with a short interval ( $< 6$  weeks interval; VE = 55.1%). This was supported by immunogenicity data showing that spike-specific binding IgG titers were higher in the long-interval cohort<sup>174</sup>. Titers of spike-specific binding IgG were even higher when extending the interval between the first and second ChAd vaccination to 45 weeks, as revealed by a sub-study<sup>249</sup>. Unfortunately, T cell responses were not measured.

Overall, a longer time interval for ChAd and mRNA-based vaccinations is beneficial for humoral immunogenicity which translates into higher efficacy. The evidence for T cells is less compelling, but an enhanced response with a longer interval as observed in our MVA-MERS-S trial was also seen in several other studies. One emerging immunological explanation for this is that T cells require sufficient time for recovery between stimulations. Otherwise they enter an exhausted state seen in chronically activated T cells with loss of replicative potential<sup>250</sup>. A study in rMVA-based HCV vaccination showed, that the vaccine-induced T cell pool contracts for at least 14 weeks and continues to differentiate into memory cells for at least 26 weeks post rMVA-boost<sup>218,239</sup>. Overall it is believed, that the re-activation of resting memory T cells is more effective than the re-activation of effector cells. Therefore, a longer time interval is favorable<sup>141</sup>.

### 6.3.3. Re-boosting

Additional booster vaccinations (here referred to as re-boost or late third vaccination) are given in addition to the prime-boost regimen to restore peripheral antibody titers and enhance immune memory<sup>69</sup>. An additional late re-boost was administered to ten participants of the MVA-MERS-S phase 1a study, as a proof-of-concept. Fathi et al.<sup>179</sup> and Weskamm et al.<sup>180</sup> demonstrated that an additional third dose was safe and could boost the immune response considerably. Specifically, antibody and B cell responses were elicited at higher magnitude, had more potent functionality, and persisted for longer, after the late third vaccination compared to after prime-boost vaccination. T cell responses that had waned to undetectable levels were re-boosted to comparable, but not higher, peak levels as seen after prime-boost vaccination<sup>180</sup>. Analyzing the T cell response in the larger MVA-MERS-S phase 1b trial, we could observe that the T cell response could only be boosted in the low dose and not the high dose cohorts (chapter 5.2.1). In the low dose, long interval cohort, the response after re-boost was even two-fold higher compared to after prime-boost.

Although different time intervals of the re-boost were not assessed in the MVA-MERS-S study, data from another rMVA-based re-boosting strategy suggests, that also for the re-boost a long interval is

beneficial. Re-boosting using ChAd and rMVA-based viral vector vaccines was investigated in a phase 1 clinical trial where participants had previously received a ChAd-prime-rMVA-boost regimen against HCV<sup>215,239</sup>. A second cycle of ChAd-rMVA was administered after a short (8 weeks) or long interval (39 to 84 weeks), to improve immunogenicity. A weak expansion of T cell responses was observed when re-boosting was performed after the short interval. In contrast, HCV-specific T cell responses expanded in the long interval group to comparable levels as seen after prime-boost vaccination. The magnitude was the same when using ChAd-rMVA or rMVA alone as a re-boost, highlighting that the interval rather than the use of multiple doses was a critical determinant for successful re-boosting of the T cell response. Furthermore, a larger proportion of T<sub>cm</sub>, which have higher proliferative potential compared to effector T cells, was maintained when re-boosting was delayed to 12-24 weeks<sup>215</sup>. Overall, these data suggest, that a strong T cell recall response is achieved by re-boosting, especially when re-boosting is delayed. Parallels to the interval between prime and boost can be drawn, as overall, the data supports the idea that a longer time interval between vaccinations may allow for responding T cells to fully differentiate into memory cells before getting re-activated by the next vaccine dose.

Notably, when using MVA-ST as a late booster approximately eight months after prime-boost vaccination with an mRNA COVID-19 vaccine, spike-specific T cell responses increased only in some participants. When stratifying participants by low and high baseline T cell levels before MVA-ST vaccination, we could see a significant induction only in the group with a low baseline (publication I, chapter 5.1.1). This finding indicates that not only the time interval but also the amount of residual immunity has a substantial impact on the immunogenicity of re-boosting strategies. In the context of mRNA-based COVID-19 vaccines, an association between lower residual levels and higher fold-induction of antibodies by late booster vaccination was observed. Analyses in mice showed that high residual antibody titers can clear the vaccine antigen via Fc-dependent mechanisms, limiting the immunogenicity of the re-boost<sup>226</sup>.

It may thus be necessary to tailor the timing of re-boost to the speed at which immunity wanes after the prime-boost rather than by a strict time interval. This may be influenced by which vaccine platforms are used or also by intrinsic differences in the human immune response, as each individual responds differently to vaccination. These data support exciting possibilities to generate differential T cell responses by tailoring selected vaccine regimen parameters, particularly, time intervals, dose levels, and combinations of different vaccine platforms can be adjusted to elicit differential T cell responses.

#### **6.4. Host factors affecting T cell immunogenicity**

There is substantial variation in vaccine responses between human individuals. This is reflected in the spread of the immunogenicity data in our clinical trials and is a common topic in human vaccine studies in general. For instance, systems vaccinology approaches of diverse cohorts have shown that antibody responses to yellow fever and influenza vaccination vary by several times<sup>251-253</sup>. Many factors can influence vaccine responses. These include genetic variation, demographic characteristics, underlying disease, perinatal factors, nutrition, concurrent infections, and immunity from previous exposures, as reviewed in detail elsewhere<sup>253</sup>. The factors most relevant to this study are discussed in more detail in the following chapters 6.4.1, 6.4.2, and 6.4.3.

##### **6.4.1. T cells response in patients with underlying disease**

Immunocompromised individuals have been disproportionately affected by the COVID-19 pandemic since they are at increased risk for progression to severe disease after infection<sup>254</sup>. At particular risk are those who suffer from deficiencies in lymphocyte number or function, such as transplant recipients and those patients with hematological cancers. Immunocompromised patients were not included in the initial efficacy trials of COVID-19 vaccines, even though these persons were at highest risk for

severe disease and were expected to benefit the most from vaccination. Nevertheless, immune deficiencies also impair the ability to mount a protective immune response following vaccination.

To contribute to the limited understanding of vaccine responses in these patients at the time, we investigated the COVID-19 vaccine response in prospective cohort studies of immunocompromised populations: patients with chronic lymphocytic leukemia (CLL) and patients with liver cirrhosis (LC) or liver transplant (LT) recipients (publications III, IV, and V). Markedly higher mortality rates due to COVID-19 have been reported in all three patient populations compared to healthy individuals<sup>255-257</sup>. In 2021, several studies confirmed reduced humoral immunogenicity following COVID-19 vaccination in CLL patients<sup>258-260</sup> and preliminary data on limited seroconversion in LT recipients were published<sup>261,262</sup>. However, data on the T cell response in these patients were limited<sup>259</sup>. It has been proposed that cancer patients who have an insufficient antibody response following vaccination may still be protected from disease by an effective cellular response. Ehmsen et al. reported that following mRNA-based COVID-19 vaccination, 92% of solid cancer patients mounted a T cell response as measured by a whole-blood IGRA assay. In patients with underlying hematological cancers, however, a T cell response was only detectable in 45% of patients, but interestingly, among those who were seronegative for antibody responses, 26% still mounted a T cell response<sup>259</sup>.

In our prospective CLL cohort study, we detected binding and neutralizing antibody responses in 38% and 33% of patients after the second COVID-19 vaccination, respectively<sup>176</sup>, in line with previous reports<sup>258-260</sup>. We measured T cell responses using an IFN- $\gamma$  ELISpot and detected a response in 38% of patients. The median response was, however, significantly lower compared to healthy controls (publication IV). Interestingly, most patients showed a discordant response with either antibody seroconversion or a detectable T cell response, and only 15% of patients mounted both antibody and T cell responses. Several months later, in early 2022, Blixt et al. published results similar to our findings on reduced T cell immunogenicity in CLL patients<sup>263</sup>. Since their study cohort was larger, associations with confounding factors could be analyzed. Notably, the lowest vaccine response rate was found in patients who were on active Ibrutinib (a tyrosine kinase inhibitor) treatment. The study by Ehmsen et al. found a statistically significant association between steroid use and lack of T cell response in patients with hematological cancer. While multiple immune mechanisms can be dysfunctional in CLL patients, an accumulation of an abnormal population of B cells is characteristic of the disease<sup>264</sup>. Immunosuppression is a typical feature and the resulting inability to control infections is the leading cause of death in CLL<sup>265</sup>. Tyrosine kinase inhibitors (Ibrutinib) and anti-CD20 antibody (Rituximab) are immune-targeting drugs used in CLL. Both the disease but also the treatment of CLL, contribute to the immunosuppression which could explain the reduced vaccine response in these patients, and calls for adapted vaccination strategies in such patient populations<sup>266</sup>.

In our CLL cohort, we observed a particularly strong T cell response in one patient who had received three vaccinations, which encouraged us to further investigate vaccine responses in these patients after the third COVID-19 vaccine dose. We were able to show that the third vaccination enhanced the antibody and T cell response rate in our cohort<sup>177</sup>. Interestingly, all patients who received a viral vector-based vaccine as the third dose, compared to only one out of three who received an mRNA-based vaccine, showed an increased T cell response (publication III). Since this study was limited by a small sample size and since confounding factors might account for these differences, our data suggest a potential benefit of using heterologous vaccination schemes to enhance T cell responses in CLL patients.

In a large prospective cohort study of LT recipients and LC patients, we also observed reduced immune responses to COVID-19 vaccination and were able to identify predictors of this low response (publication V)<sup>178</sup>. Significantly lower seroconversion rates and median antibody titers compared to healthy controls were observed in LT patients but not in LC patients, suggesting that LC patients did

not have an impaired humoral vaccine response. We measured T cell responses using the whole-blood IGRA assay and saw that T cell responses were detected less frequently in both, LT (37%) and LC (65%) patients compared to healthy controls (100%). Similar to the CLL cohort, discordance between antibody and T cell responses was seen in LT and LC patients. Notably, significantly higher antibody and T cell responses were found in LT patients who received a heterologous vaccination scheme (viral vector- plus mRNA-based) compared to double mRNA-based vaccination. Age, arterial hypertension, diabetes, low B cell count, low estimated globular infiltration rate (eGFR), and several immunosuppressive drug regimens showed to be statistically significant predictors of low vaccine response. Rabinowich et al. reported previously, that age, low eGFR, and several immunosuppressive drugs were negative predictors of antibody responses in LT patients but did not assess T cell responses<sup>262</sup>.

Taken together, our data from the CLL and LT/LC cohort studies contributes to the existing literature on reduced vaccine responses in patients who are immunocompromised due to underlying health conditions or related treatments. The results highlight the need for adapted vaccination strategies to protect this highly vulnerable population from COVID-19 disease. Such studies could include discontinuation of immunosuppressive medication in patients with stable health conditions before vaccination and the use of additional (heterologous) booster doses. Indeed, the CLL cohort study is now continuing to explore additional booster vaccinations in patients who showed no vaccine response.

#### **6.4.2. Demographic factors affecting vaccine response**

It has been described in various settings, that with increasing age, humans are more susceptible to infectious diseases<sup>267–269</sup> and respond less robustly to vaccination<sup>270–272</sup>. This phenomenon is explained by the term “immunosenescence”, the age-related decline of the immune system, which is extensively reviewed elsewhere<sup>273–275</sup>. In terms of the T cell response, this is characterized by a loss of naïve T cells, an accumulation of exhausted memory T cells with less potent effector function, and a loss in TCR diversity<sup>276</sup>. Recent single-cell analyses have revealed, that not all immune pathways and cell populations are uniformly affected by aging<sup>277</sup>. In our LT/LC COVID-19 vaccine study, old age was a negative predictor of vaccine response, irrespective of patient group. In the phase 1 clinical trials of our rMVA-based vaccine candidates, we were not able to assess the effect of age on vaccine response, as these early-stage trials were conducted in healthy adults aged 18 to 64 years. Nevertheless, testing these vaccines in the elderly is important, as morbidity and mortality from infectious diseases affect this age group disproportionately strong. Indeed, a trial testing the ChAdOx1-based MERS vaccine in individuals aged 50 to 70 years is currently ongoing<sup>278</sup>.

Biological sex is another variable that greatly impacts vaccine response. In most vaccine trials investigating sex differences in vaccine responses, females had higher adaptive immune responses that were associated with more differentially expressed genes involved in the early innate response following vaccination<sup>253,279</sup>. Notably, for rMVA vaccines, the opposite has been observed. Using rMVA as a smallpox vaccine, peak neutralizing and binding antibody titers<sup>280</sup>, as well as frequency of vaccine-induced T cells<sup>281</sup> were higher in males compared to females. Dissecting sex differences in vaccine responses using transcriptomic approaches is currently ongoing for the MVA-MERS-S phase 1b study. Hormonal and genetic factors could be responsible for differences in vaccine responses, as discussed in detail elsewhere<sup>279,282–284</sup>.

#### **6.4.3. T cells and HLA-polymorphism**

Arguably the most important genetic factor that dictates differences in the T cell immune response is the polymorphism of the HLA locus. The HLA locus is the most polymorphic region of the human genome<sup>285</sup>. Over 7000 human HLA alleles have been described<sup>286</sup>. HLA alleles determine the number,

as well as the binding affinity of peptides derived from the vaccine antigen. Several studies have predicted and described the viral peptidome of the SARS-CoV-2 virus presented by various HLA alleles and have found that certain HLA types are associated with higher disease susceptibility<sup>287–289</sup>, but less is known about vaccine responses. Population-wide studies and studies in twins have shown associations between certain HLA alleles and cellular vaccine responses<sup>290–293</sup>. Crocchiolo et al. reported that some HLA alleles are overrepresented in a cohort of individuals with a weak antibody response following BNT162b2 vaccination against COVID-19<sup>294</sup>. Barquera et al. mapped the proteome of seven epidemic viruses across more than 400 HLA alleles and found distinct patterns of strong and weak peptide-binding HLA alleles. Interestingly, HLA-A\*02:01, a highly prevalent allele around the world, was amongst the strongest binders against all viruses and the top binder for epidemic HCoVs<sup>287</sup>.

In our study, we longitudinally tracked CD8+ T cells specific for an HLA-A\*02:01-restricted SARS-CoV-2 spike epitope. We observed that CD8+ T cells specific for this SARS-CoV-2 spike epitope comprised up to 0.78% of the total CD8+ response (chapter 5.1.2). In our MERS epitope study, we identified for the first time in humans a MERS-CoV-spike-specific CD8+ T cell epitope that is likely HLA-B\*35:01 restricted (publication II). Notably, we could show that four out of five further HLA-B\*35:01 positive individuals also responded to the epitope following MVA-MERS-S vaccination (chapter 5.2.4). The responding individuals consisted of one individual homozygous for the HLA-B\*35:01 allele and four individuals heterozygous at the HLA-B locus. Cytokine-secreting CD8+ T cells specific for this epitope comprised 0.51% of the total CD8+ memory T cell pool in the homozygous individual, but also reached comparable frequencies in the heterozygous individuals. These data support the notion that even though a large repertoire of epitopes is present after vaccination or infection, some epitopes are highly immunodominant. This immunodominance is likely influenced by intrinsic properties of the epitope and availability together with the HLA type of the host<sup>124</sup>. The HLA restriction of the T cell response is largely responsible for the high variability of immune responses in the human population, which poses an evolutionary advantage. Since each HLA type in combination with the individual TCR repertoire can respond to a different repertoire of peptides, the human population, as a whole, can generate an immune response against virtually any antigen. There are several lines of evidence, that pathogen diversity correlates with HLA variability<sup>295</sup>. From an evolutionary perspective, heterozygotes are on average more broadly protected since they can present a larger variety of epitopes<sup>296</sup>. As HLA allele frequencies are not equally distributed across populations, T cell-based vaccination strategies targeting certain HLA-restricted epitopes should be considered with caution.

## 6.5. From vaccine immunology to T cell correlates of protection

### 6.5.1. Protective T cell responses

Which memory T cell subset mediates protection is not well understood and there is conflicting evidence. Those of central memory phenotype have superior proliferation capacity and may be more important for maintaining long-term memory. In turn, those with an effector memory phenotype may have more rapid effector functionality, especially at the site of infection<sup>297</sup>. Although protective immune responses differ by pathogen and site of infection, some patterns have been observed that are commonly applicable to several viral infections. Human challenge studies have recently gained a lot of interest as they provide excellent opportunities to analyze protective immune responses in humans in detail. As an example, Graham et al. investigated the T cell response in a dengue virus human challenge study, where vaccination with a live-attenuated tetravalent dengue vaccine (DLAV) protected from infection in all participants<sup>298,299</sup>. Following vaccination, CD8+ and CD4+ T cells with a  $T_{em}$  and  $T_{emra}$  memory phenotype predominated<sup>299</sup>. Upon the dengue virus challenge 6 months later, the response was further skewed towards a  $T_{emra}$  phenotype. While this study was not powered to assess correlates of protection, the data suggest that CD4+ and CD8+  $T_{emra}$  contribute to the protective immune response. Further evidence comes from natural dengue infection in a hyperendemic setting,

where a multifunctional CD4+ T<sub>emra</sub> response was associated with protective HLA-DR alleles<sup>300</sup>. Longitudinal tracking of CD8+ T cells following live-attenuated yellow fever vaccination revealed, that long-term memory originates in vaccine-induced T<sub>em</sub> and T<sub>emra</sub> cells that retain an epigenetic fingerprint of their effector memory phenotype<sup>301</sup>. The yellow fever vaccine is considered one of the most effective vaccines and has provided important insights into the mechanisms of vaccine-induced protection, especially the role of CD8+ T cell memory<sup>188,302</sup>.

In our longitudinal analysis of epitope-specific CD8 + T cells following vaccination and infection, we observed that early after vaccination, naïve T cells become activated and develop towards effector and central memory T cells simultaneously (chapter 5.1.2). Over time, the response contracts and persists with a T<sub>emra</sub> phenotype. Several years after yellow fever vaccination, we observed that the pool of memory T cells remained stable, with a portion of the epitope-specific cells re-expressing CCR7, thus having a naïve-like phenotype. We observed the same phenotype of SARS-CoV-2-specific T cells after breakthrough infection. These cells could be T<sub>scm</sub> but this requires further analysis using a more detailed flow cytometry panel. T<sub>scm</sub> represent a recently discovered memory subset with increased proliferative potential and the ability to differentiate into effector, effector memory, or central memory cells<sup>135,303</sup>. This increased fraction of T<sub>scm</sub> has been described by Habel et al. after breakthrough infection, but the clinical significance remains unknown<sup>304</sup>.

### 6.5.2. Role of T cells in protection against COVID-19 and MERS

Deciphering protective immune responses is one of the greatest challenges in the field of vaccinology. If mechanistic correlates of protection were known, it would be more straightforward to develop vaccine strategies that induce protective immune mechanisms<sup>143</sup>. Some lessons on protective immunity can be learned from studying natural infection and applied to vaccine development. The immune response to natural infection is multifaceted and highly dependent on the nature of the pathogen. The contribution of T cells to protection from COVID-19 is reviewed in detail elsewhere<sup>305</sup>. In brief, several parallels can be drawn between the role of T cell immunity in COVID-19 and MERS.

SARS-CoV-2-specific T cell responses have been detected in asymptotically infected individuals who did not seroconvert<sup>182,306,307</sup>. The same has been reported for MERS-CoV-specific T cell responses in abattoir workers with occupational exposure to MERS-CoV<sup>39</sup>. The rapid induction of effector T cells is thought to suppress viral replication before a humoral response can be induced. Spike-specific CD8+ T cells were identified as early as 10 to 12 days after COVID-19 vaccination, when antibodies were barely detectable, yet effective protection was already achieved<sup>90,185</sup>. These results suggest that especially early vaccine-induced protection is mediated by T cells. With the waning of immunity following vaccination and the emergence of viral variants, most people have experienced breakthrough infections. The resulting so-called “hybrid immunity” is hypothesized to provide superior protection from infection compared to vaccination alone<sup>308</sup>. This may be explained by the fact that infection induces immune mediators at the mucosae, the site of viral entry, including tissue-resident T cells. Another reason would be that breakthrough infections broaden the T cell response towards other viral antigens that are not included in the vaccine formulation<sup>309</sup>. Overall, the T cell response wanes more slowly compared to the antibody response and is less prone to viral mutations<sup>99</sup>. The role of T cell immunity in the face of viral variants and closely related viruses is further discussed below.

### 6.5.3. Importance of T cells in protection against viral variants

T cell responses six months after COVID-19 vaccination were less impacted by immune escape of SARS-CoV-2 variants of concern than B cell and antibody responses. It was predicted that 72% of CD4+ and 86% of CD8+ T cell epitopes are conserved between the ancestral strain and the omicron variant<sup>310</sup>. Experimentally, it was confirmed, that the T cell response is highly conserved<sup>310,311</sup>. This is expected since T cells recognize a large pool of short, linear peptides, whereas the humoral response is generally



restricted to fewer immunodominant epitopes that are larger and also dependent on the conservation of the three-dimensional structure. In theory, variants able to evade T cell recognition are also less likely to be selected since MHC molecules are highly polymorphic. The repertoire of T cell epitopes is thus much more individual, while the repertoire of epitopes recognized by the humoral response is much more universal.

#### 6.5.4. Cross-reactive T cell responses to other virus strains

Since the T cell response is more conserved, it could be hypothesized that T cell responses from previous infections with closely related viruses may contribute to protection against newly emerging viruses. Indeed, during the COVID-19 pandemic, data started to accumulate reporting T cell reactivity against SARS-CoV-2 in pre-pandemic samples<sup>312</sup>. Several studies reported reactivity in 20 to 50% of unexposed donors<sup>313–315</sup>. Responses were mainly reactive against various SARS-CoV-2 proteins including the spike<sup>312</sup>. Reactivity was highest against peptide pools that had sequence homology to the common cold HCoVs: HCoV-OC43, HCoV-HKU1, HCoV-NL63, or HCoV-229E<sup>314</sup>. It is expected, that these responses originate from previous infections with HCoVs, as more than 90% of the human population is seropositive for at least three of these HCoVs<sup>316</sup>. Kundu et al. analyzed T cell responses in COVID-19 household contacts and observed that those who did not get infected had higher frequencies of cross-reactive, IL-2-secreting T cells, compared to those who got infected upon exposure. These data suggest a protective role of pre-existing T cells but interpretation should be taken with caution as the sample size in this study was small (n = 52)<sup>317</sup>. Swadling et al. reported pre-existing T cells against the SARS-CoV-2 RNA polymerase in healthcare workers<sup>307</sup>. Analyses of matched samples following SARS-CoV-2 exposure showed an expansion of these pre-existing T cells in the absence of humoral seroconversion. Taken together, these data suggest that cross-reactive T cells might mediate an abortive infection<sup>307,317</sup>. It is important to note, that these pre-existing T cells were mainly reactive to non-spike antigens which are more conserved across HCoVs, arguing for the inclusion of other antigens in vaccine candidates that aim to protect against multiple CoVs.

Cross-reactive T cell responses have been of particular interest in the context of influenza. New influenza strains emerge by antigenic drift and shift and can evade the immune response. In a human challenge study, Wilkinson et al. investigated the adaptive immune response after influenza virus infection<sup>318</sup>. All participants were seronegative for antibodies against the challenge strain, but all had detectable T cell responses against conserved epitopes from previous infections with other strains. The virus was cleared from the respiratory tract by day 7, when antibody responses were not yet detectable. CD4+ and CD8+ T cell responses expanded on average 10-fold by day 7. The frequency of pre-existing T cells, especially CD4+ T cells, correlated inversely with disease duration and severity, suggesting that they contribute to protective immunity<sup>318</sup>. With regard to the 2009 pandemic H1N1 influenza strain, an unusual age distribution of disease severity was observed. Older people had less severe disease compared to the young. This correlated with pre-existing immunity in those people who were old enough to have been exposed to a different H1N1 strain that circulated decades earlier<sup>319,320</sup>. While epidemiological data on HCoV exposure is more scarce compared to data on influenza strains, it is conceivable, and not unlikely, that pre-existing cross-reactive T cell responses may contribute to anti-CoV immunity and might even have an impact on vaccine-induced immunity<sup>312</sup>.

Our large phase 1b clinical trial testing the MVA-MERS-S vaccine candidate was conducted in the middle of the COVID-19 pandemic. This resulted in the unplanned experiment of people being exposed to antigens from two different HCoVs in the same time frame. Indeed, most participants of the study experienced a SARS-CoV-2 infection or were vaccinated against COVID-19 during the trial period. We analyzed the SARS-CoV-2-specific T cell response in parallel to the MERS-CoV-specific response and saw an induction of both (chapter 5.2.3). If there is cross-reactivity between the two responses is yet to be determined in future studies. It could be hypothesized, that previous SARS-CoV-2 specific

exposure could skew the response induced by MVA-MERS-S towards immunodominant, cross-reactive epitopes and potentially diminish responses against MERS-CoV-specific epitopes.

## 6.6. Future Outlook

In summary, this project aimed to investigate the T cell immunogenicity of three novel rMVA-based vaccine candidates against SARS-CoV-2 and MERS-CoV in humans in comparison to licensed vaccines based on the ChAdOx1 and mRNA vaccine platforms. The results highlight the influence of antigen design, vaccine platform, and vaccination regimen, as well as host factors on the T cell response. One strength of this project is the frequent, longitudinal sampling of approximately 170 participants at baseline before and at several time points following vaccination, allowing for a detailed analysis of the T cell dynamics following different vaccine regimens.

### 6.6.1. Systems vaccinology

One major challenge in the field of assessing T cell immunogenicity in clinical trials is the lack of simple, standardized cellular assays. Cellular assays based on PBMC isolation are complex and not feasible in low-resource settings. One promising approach to address this limitation is the use of whole-blood assays, such as the IGRA. We used this assay in our study when it was still in developmental stages and now it is sold as a licensed research product in the context of COVID-19 (chapter 5.1.1). This assay could be further developed for other indications, such as MERS-CoV, to be used for the evaluation of future vaccine candidates. It is important to measure not only humoral but also cellular responses as they are crucial for providing long-term protection against disease. As shown by the results of our MVA-MERS-S phase 1b study and published by others, the humoral and T cell responses do not always correlate. Combining different immunological readouts in a multiplexed approach allows for deciphering signatures of vaccine response. This “systems vaccinology” approach was spearheaded by the analyses of the yellow fever vaccine in the early 2000s<sup>252,321</sup> and has now advanced considerably with new technologies such as multi-omics and single-cell sequencing<sup>229,322</sup>. Detailed signatures of vaccine response would contribute to a better understanding of the mechanisms of actions of vaccines and might be useful to predict vaccine immunogenicity and efficacy. In addition, analysis of the peripheral blood only provides limited insights into the complexity of the vaccine-induced immune response in humans. New methods, such as fine-needle aspirates of draining lymph nodes<sup>323,324</sup> and *in vitro* models of lymphatic tissue, such as tonsil organoids<sup>325,326</sup>, are providing novel insights and will support future vaccine design strategies.

### 6.6.2. Rational vaccine design

Better vaccination strategies can be designed when considering the factors that influence vaccine immunogenicity. Instead of a more empiric trial-and-error approach, vaccines can be designed more rationally based on the target product profile, i.e. the aim of the vaccine. Strategic decisions should include the choice of antigen and its delivery, carefully considering the advantages and disadvantages of the different vaccine platforms<sup>157</sup>. Prime-boost strategies are effective in inducing protective immune responses, but the optimal time interval between doses is yet to be determined. One emerging concept to consider when designing vaccination strategies is “trained immunity” referring to the capacity of the innate immune response to elicit some type of memory. Innate cells, even though they are not part of the adaptive immune system, respond differently to the prime versus boost vaccination and have increased functionality after the second exposure<sup>327</sup>. Epidemiological evidence of trained immunity has been reported for live-attenuated vaccines such as *Bacillus Calmette-Guérin* (BCG), measles, and oral polio, and confirmed in clinical trials<sup>328</sup>. While the underlying mechanisms are mostly unknown, a recent study in mice suggests that this is mediated by a feedback loop between activated T cells and tissue-resident innate cells<sup>329</sup>. Interestingly, evidence of “trained immunity” has also recently been described for the ChAdOx1 nCoV-19 vaccine. Murphy et al. observed sustained

innate activation and metabolic reprogramming of monocytes up to two months after vaccination<sup>330</sup>. These data show, that trained immunity is also relevant for viral vector vaccines. This could be further investigated in the context of our rMVA-based vaccine candidates in the future. How to best harness the potential of trained immunity to optimized vaccination strategies is yet to be determined.

### 6.6.3. Future of the rMVA vaccine platform

Viral vectors are a versatile and modular vaccine platform technology. The rMVA platform has several advantages: It is safe and well tolerated not only in healthy individuals but also in HIV-positive individuals<sup>331,332</sup>, cancer patients<sup>333</sup>, and small children<sup>334</sup>. The MVA genome has a large insert capacity making it an ideal platform for multivalent vaccine design<sup>335</sup>. Nonetheless, the rMVA platform also has some drawbacks, such as the difficulty of producing high doses at a large scale and the lower immunogenicity in humans compared to other platforms, especially mRNA-based vaccines. Immunogenicity of rMVA-based vaccines may be improved by several strategies such as the deletion of immunomodulatory genes in the MVA genome and enhanced expression of recombinant antigens by optimizing promoters<sup>336</sup>. Indeed, a study by Finn et al. showed a causal link between the persistence of recombinant antigen expression and maintenance of CD8+ T cell responses following vaccination<sup>337</sup>. Furthermore, the immunogenicity can be improved by optimizing the vaccine regimen. rMVA-based vaccines seem to be more efficient when used as booster doses, as exemplified by the highly efficacious Ad plus rMVA prime-boost regimen against Ebola<sup>85</sup>. The route of administration also plays an important role. MVA naturally infects the skin, which is highly populated by immune cells<sup>338</sup>. Percutaneous application of rMVA-based vaccines might thus be of advantage. Förster et al. are currently conducting a phase 1 clinical trial applying our MVA-ST candidate against COVID-19 by inhalation. Direct application to the respiratory tract might induce potent mucosal immune responses, which are important for protection against respiratory pathogens<sup>339,340</sup>.

There are several promising rMVA-based vaccine approaches on the horizon. These projects leverage MVA's ability to induce potent cellular responses. An rMVA-based vaccine candidate will be investigated in a multi-center phase 1/2 trial as a therapeutic vaccine for patients chronically infected with Hepatitis B virus (HBV)<sup>341</sup>. After prime-boost vaccination with the subunit HBV vaccine, a booster with a multivalent rMVA-based vaccine coding for the HBV surface antigen, the core antigen, and parts of the HBV polymerase is administered to overcome HBV-specific immune tolerance by the re-activation of cellular responses<sup>342</sup>. rMVA is also being evaluated as a therapeutic anti-tumor vaccine. The efficacy of immunotherapeutic drugs is often limited due to the lack of CD8+ T cells in the tumor. McAuliffe et al. are investigating a prime-boost regimen of ChAdOx1 and rMVA expressing tumor-specific antigens as a therapeutic vaccine against solid tumors<sup>343</sup>. In pre-clinical studies they showed that vaccination promotes CD8+ T cell infiltration into the tumor, which, in combination with immunotherapeutic drugs, induced tumor clearance and improved survival. This vaccination strategy has now proceeded to a phase 1/2 clinical trial in patients with non-small cell lung cancer<sup>344</sup>. These examples highlight that the potential of the rMVA viral vector as a vaccine platform is not limited to its application in vaccine development against EIDs. It will be interesting to see which role rMVA-based vaccines will hold in the future vaccine landscape, potentially also in heterologous vaccination strategies with other vaccine platforms.

## 7. REFERENCES

1. Morens, D. M. & Fauci, A. S. Emerging Pandemic Diseases: How We Got to COVID-19. *Cell* **182**, 1077–1092 (2020).
2. UK Health Security Agency. *Emerging infections: how and why they arise*. <https://www.gov.uk/government/publications/emerging-infections-characteristics-epidemiology-and-global-distribution/emerging-infections-how-and-why-they-arise> (2023).
3. Karesh, W. B. *et al.* Ecology of zoonoses: natural and unnatural histories. *Lancet* **380**, 1936–1945 (2012).
4. Bettis, A. A. *et al.* The global epidemiology of chikungunya from 1999 to 2020: A systematic literature review to inform the development and introduction of vaccines. *PLoS Negl. Trop. Dis.* **16**, e0010069 (2022).
5. Bartholomeeusen, K. *et al.* Chikungunya fever. *Nat. Rev. Dis. Primer* **9**, 1–21 (2023).
6. Cassaniti, I. *et al.* Preliminary results on an autochthonous dengue outbreak in Lombardy Region, Italy, August 2023. *Eurosurveillance* **28**, 2300471 (2023).
7. Gostin, L. O., Lucey, D. & Phelan, A. The Ebola Epidemic: A Global Health Emergency. *JAMA* **312**, 1095–1096 (2014).
8. Fineberg, H. V. Pandemic Preparedness and Response — Lessons from the H1N1 Influenza of 2009. *N. Engl. J. Med.* **370**, 1335–1342 (2014).
9. Afrough, B., Dowall, S. & Hewson, R. Emerging viruses and current strategies for vaccine intervention. *Clin. Exp. Immunol.* **196**, 157–166 (2019).
10. World Health Organization. *An R&D Blueprint for Action to Prevent Epidemics*. <https://www.who.int/publications/m/item/an-r-d-blueprint-for-action-to-prevent-epidemics> (2016).
11. Mehand, M. S., Al-Shorbaji, F., Millett, P. & Murgue, B. The WHO R&D Blueprint: 2018 review of emerging infectious diseases requiring urgent research and development efforts. *Antiviral Res.* **159**, 63–67 (2018).
12. Woo, P. C. Y. *et al.* ICTV Virus Taxonomy Profile: Coronaviridae 2023. *J. Gen. Virol.* **104**, 001843 (2023).
13. V'kovski, P., Kratzel, A., Steiner, S., Stalder, H. & Thiel, V. Coronavirus biology and replication: implications for SARS-CoV-2. *Nat. Rev. Microbiol.* **19**, 155–170 (2021).
14. Li, F. Structure, Function, and Evolution of Coronavirus Spike Proteins. *Annu. Rev. Virol.* **3**, 237–261 (2016).
15. Wrapp, D. *et al.* Cryo-EM structure of the 2019-nCoV spike in the prefusion conformation. *Science* **367**, 1260–1263 (2020).
16. Raghuvamsi, P. V. *et al.* SARS-CoV-2 S protein:ACE2 interaction reveals novel allosteric targets. *eLife* **10**, e63646 (2021).

17. Cai, Y. *et al.* Distinct conformational states of SARS-CoV-2 spike protein. *Science* **369**, 1586–1592 (2020).
18. Woo, P. C. Y. *et al.* Discovery of Seven Novel Mammalian and Avian Coronaviruses in the Genus Deltacoronavirus Supports Bat Coronaviruses as the Gene Source of Alphacoronavirus and Betacoronavirus and Avian Coronaviruses as the Gene Source of Gammacoronavirus and Deltacoronavirus. *J. Virol.* **86**, 3995–4008 (2012).
19. Zhou, P. *et al.* Fatal swine acute diarrhoea syndrome caused by an HKU2-related coronavirus of bat origin. *Nature* **556**, 255–258 (2018).
20. Lin, C.-M., Saif, L. J., Marthaler, D. & Wang, Q. Evolution, antigenicity and pathogenicity of global porcine epidemic diarrhea virus strains. *Virus Res.* **226**, 20–39 (2016).
21. Chen, B. *et al.* Overview of lethal human coronaviruses. *Signal Transduct. Target. Ther.* **5**, 1–16 (2020).
22. Cui, J., Li, F. & Shi, Z.-L. Origin and evolution of pathogenic coronaviruses. *Nat. Rev. Microbiol.* **17**, 181–192 (2019).
23. McIntosh, K., Dees, J. H., Becker, W. B., Kapikian, A. Z. & Chanock, R. M. Recovery in tracheal organ cultures of novel viruses from patients with respiratory disease. *Proc. Natl. Acad. Sci. U. S. A.* **57**, 933–940 (1967).
24. Hamre, D. & Procknow, J. J. A new virus isolated from the human respiratory tract. *Proc. Soc. Exp. Biol. Med.* **121**, 190–193 (1966).
25. van der Hoek, L. *et al.* Identification of a new human coronavirus. *Nat. Med.* **10**, 368–373 (2004).
26. Woo, P. C. Y. *et al.* Characterization and Complete Genome Sequence of a Novel Coronavirus, Coronavirus HKU1, from Patients with Pneumonia. *J. Virol.* **79**, 884–895 (2005).
27. Corman, V. M., Muth, D., Niemeyer, D. & Drosten, C. Hosts and Sources of Endemic Human Coronaviruses. *Adv. Virus Res.* **100**, 163–188 (2018).
28. Gorbalenya, A. E. *et al.* The species Severe acute respiratory syndrome-related coronavirus: classifying 2019-nCoV and naming it SARS-CoV-2. *Nat. Microbiol.* **5**, 536–544 (2020).
29. Drosten, C. *et al.* Identification of a novel coronavirus in patients with severe acute respiratory syndrome. *N. Engl. J. Med.* **348**, 1967–1976 (2003).
30. Zhong, N. S. *et al.* Epidemiology and cause of severe acute respiratory syndrome (SARS) in Guangdong, People’s Republic of China, in February, 2003. *Lancet* **362**, 1353–1358 (2003).
31. World Health Organization. *Summary of probably SARS cases with onset of illness from 1 November 2002 to 31 July 2003.* <https://www.who.int/publications/m/item/summary-of-probable-sars-cases-with-onset-of-illness-from-1-november-2002-to-31-july-2003> (2004)
32. Li, W. *et al.* Angiotensin-converting enzyme 2 is a functional receptor for the SARS coronavirus. *Nature* **426**, 450–454 (2003).
33. de Wit, E., van Doremalen, N., Falzarano, D. & Munster, V. J. SARS and MERS: recent insights into emerging coronaviruses. *Nat. Rev. Microbiol.* **14**, 523–534 (2016).

34. Zaki, A. M., van Boheemen, S., Bestebroer, T. M., Osterhaus, A. D. M. E. & Fouchier, R. A. M. Isolation of a novel coronavirus from a man with pneumonia in Saudi Arabia. *N. Engl. J. Med.* **367**, 1814–1820 (2012).
35. World Health Organization. *MERS situation update, July 2023*. <https://www.emro.who.int/health-topics/mers-cov/mers-outbreaks.html> (2023).
36. Lu, G. *et al.* Molecular basis of binding between novel human coronavirus MERS-CoV and its receptor CD26. *Nature* **500**, 227–231 (2013).
37. Zumla, A., Hui, D. S. & Perlman, S. Middle East respiratory syndrome. *Lancet Lond. Engl.* **386**, 995–1007 (2015).
38. Zhao, J. *et al.* Recovery from the Middle East respiratory syndrome is associated with antibody and T cell responses. *Sci. Immunol.* **2**, eaan5393 (2017).
39. Mok, C. K. P. *et al.* T-cell responses to MERS coronavirus infection in people with occupational exposure to dromedary camels in Nigeria: an observational cohort study. *Lancet Infect. Dis.* **21**, 385–395 (2021).
40. Alhabbab, R. Y. *et al.* Middle East Respiratory Syndrome Coronavirus Infection Elicits Long-lasting Specific Antibody, T and B Cell Immune Responses in Recovered Individuals. *Clin. Infect. Dis.* **76**, e308–e318 (2023).
41. Azhar, E. I. *et al.* Evidence for camel-to-human transmission of MERS coronavirus. *N. Engl. J. Med.* **370**, 2499–2505 (2014).
42. Haagmans, B. L. *et al.* Middle East respiratory syndrome coronavirus in dromedary camels: an outbreak investigation. *Lancet Infect. Dis.* **14**, 140–145 (2014).
43. Kim, K. H., Tandi, T. E., Choi, J. W., Moon, J. M. & Kim, M. S. Middle East respiratory syndrome coronavirus (MERS-CoV) outbreak in South Korea, 2015: epidemiology, characteristics and public health implications. *J. Hosp. Infect.* **95**, 207–213 (2017).
44. Hui, D. S. *et al.* Middle East respiratory syndrome coronavirus: risk factors and determinants of primary, household, and nosocomial transmission. *Lancet Infect. Dis.* **18**, e217–e227 (2018).
45. Wang, C., Horby, P. W., Hayden, F. G. & Gao, G. F. A novel coronavirus outbreak of global health concern. *Lancet* **395**, 470–473 (2020).
46. Lu, R. *et al.* Genomic characterisation and epidemiology of 2019 novel coronavirus: implications for virus origins and receptor binding. *Lancet* **395**, 565–574 (2020).
47. Grifoni, A. *et al.* A Sequence Homology and Bioinformatic Approach Can Predict Candidate Targets for Immune Responses to SARS-CoV-2. *Cell Host Microbe* **27**, 671–680.e2 (2020).
48. Yan, R. *et al.* Structural basis for the recognition of SARS-CoV-2 by full-length human ACE2. *Science* **367**, 1444–1448 (2020).
49. Lamers, M. M. & Haagmans, B. L. SARS-CoV-2 pathogenesis. *Nat. Rev. Microbiol.* **20**, 270–284 (2022).
50. Zhou, H. *et al.* A Review of SARS-CoV2: Compared With SARS-CoV and MERS-CoV. *Front. Med.* **8**, 628370 (2021).

51. Puhach, O., Meyer, B. & Eckerle, I. SARS-CoV-2 viral load and shedding kinetics. *Nat. Rev. Microbiol.* **21**, 147–161 (2023).
52. Lenharo, M. WHO declares end to COVID-19's emergency phase. *Nature* (2023).
53. Cohen, L. E., Spiro, D. J. & Viboud, C. Projecting the SARS-CoV-2 transition from pandemicity to endemicity: Epidemiological and immunological considerations. *PLoS Pathog.* **18**, e1010591 (2022).
54. Koelle, K., Martin, M. A., Antia, R., Lopman, B. & Dean, N. E. The changing epidemiology of SARS-CoV-2. *Science* **375**, 1116–1121 (2022).
55. Markov, P. V. *et al.* The evolution of SARS-CoV-2. *Nat. Rev. Microbiol.* **21**, 361–379 (2023).
56. Li, J., Lai, S., Gao, G. F. & Shi, W. The emergence, genomic diversity and global spread of SARS-CoV-2. *Nature* **600**, 408–418 (2021).
57. Wang, M.-N. *et al.* Longitudinal surveillance of SARS-like coronaviruses in bats by quantitative real-time PCR. *Virologica Sinica* **31**, 78–80 (2016).
58. Hu, B. *et al.* Discovery of a rich gene pool of bat SARS-related coronaviruses provides new insights into the origin of SARS coronavirus. *PLoS Pathog.* **13**, e1006698 (2017).
59. Luo, C.-M. *et al.* Discovery of Novel Bat Coronaviruses in South China That Use the Same Receptor as Middle East Respiratory Syndrome Coronavirus. *J. Virol.* **92**, e00116-18 (2018).
60. Temmam, S. *et al.* Bat coronaviruses related to SARS-CoV-2 and infectious for human cells. *Nature* **604**, 330–336 (2022).
61. Luby, S. P. *et al.* Recurrent Zoonotic Transmission of Nipah Virus into Humans, Bangladesh, 2001–2007. *Emerg. Infect. Dis.* **15**, 1229–1235 (2009).
62. Leroy, E. M. *et al.* Fruit bats as reservoirs of Ebola virus. *Nature* **438**, 575–576 (2005).
63. Towner, J. S. *et al.* Isolation of genetically diverse Marburg viruses from Egyptian fruit bats. *PLoS Pathog.* **5**, e1000536 (2009).
64. Ge, X. *et al.* Metagenomic Analysis of Viruses from Bat Fecal Samples Reveals Many Novel Viruses in Insectivorous Bats in China. *J. Virol.* **86**, 4620–4630 (2012).
65. Poon, L. L. M. *et al.* Identification of a Novel Coronavirus in Bats. *J. Virol.* **79**, 2001–2009 (2005).
66. Ge, X.-Y. *et al.* Isolation and characterization of a bat SARS-like coronavirus that uses the ACE2 receptor. *Nature* **503**, 535–538 (2013).
67. Xiong, Q. *et al.* Close relatives of MERS-CoV in bats use ACE2 as their functional receptors. *Nature* **612**, 748–757 (2022).
68. Strategic Advisory group of Experts on Immunization. *The Global Vaccine Action Plan 2011–2020. Review and lessons learned.* <https://apps.who.int/iris/bitstream/handle/10665/329097/WHO-IVB-19.07-eng.pdf?ua=1> (2019).
69. Pollard, A. J. & Bijker, E. M. A guide to vaccinology: from basic principles to new developments. *Nat. Rev. Immunol.* **21**, 83–100 (2021).

70. World Health Organization. *Global Vaccine Action Plan 2011-2020*. <https://www.who.int/publications/i/item/global-vaccine-action-plan-2011-2020> (2013).
71. Carter, A. *et al.* Modeling the impact of vaccination for the immunization Agenda 2030: Deaths averted due to vaccination against 14 pathogens in 194 countries from 2021 to 2030. *Vaccine* (2023) doi:10.1016/j.vaccine.2023.07.033.
72. World Health Organization. *Immunization Agenda 2030: A Global Strategy To Leave No One Behind*. <https://www.who.int/teams/immunization-vaccines-and-biologicals/strategies/ia2030> (2020).
73. Venkatesan, P. First RSV vaccine approvals. *Lancet Microbe* **4**, e577 (2023).
74. Schneider, M. *et al.* Safety and immunogenicity of a single-shot live-attenuated chikungunya vaccine: a double-blind, multicentre, randomised, placebo-controlled, phase 3 trial. *Lancet* **401**, 2138–2147 (2023).
75. Yue, J. *et al.* The R&D landscape for infectious disease vaccines. *Nat. Rev. Drug Discov.* 867–868 (2023).
76. Kennedy, R. B., Ovsyannikova, I. G., Palese, P. & Poland, G. A. Current Challenges in Vaccinology. *Front. Immunol.* **11**, 1181 (2020).
77. Excler, J.-L., Saville, M., Berkley, S. & Kim, J. H. Vaccine development for emerging infectious diseases. *Nat. Med.* **27**, 591–600 (2021).
78. Siegrist, C.-A. Vaccine Immunology. in *Plotkin's Vaccines* (Elsevier, 2008).
79. Cid, R. & Bolívar, J. Platforms for Production of Protein-Based Vaccines: From Classical to Next-Generation Strategies. *Biomolecules* **11**, 1072 (2021).
80. Donaldson, B., Lateef, Z., Walker, G. F., Young, S. L. & Ward, V. K. Virus-like particle vaccines: immunology and formulation for clinical translation. *Expert Rev. Vaccines* **17**, 833–849 (2018).
81. van Riel, D. & de Wit, E. Next-generation vaccine platforms for COVID-19. *Nat. Mater.* **19**, 810–812 (2020).
82. Corbett, K. S. *et al.* SARS-CoV-2 mRNA vaccine design enabled by prototype pathogen preparedness. *Nature* **586**, 567–571 (2020).
83. Bellino, S. COVID-19 vaccines approved in the European Union: current evidence and perspectives. *Expert Rev. Vaccines* **20**, 1195–1199 (2021).
84. Travieso, T., Li, J., Mahesh, S., Mello, J. D. F. R. E. & Blasi, M. The use of viral vectors in vaccine development. *Npj Vaccines* **7**, 1–10 (2022).
85. Pollard, A. J. *et al.* Safety and immunogenicity of a two-dose heterologous Ad26.ZEBOV and MVA-BN-Filo Ebola vaccine regimen in adults in Europe (EBOVAC2): a randomised, observer-blind, participant-blind, placebo-controlled, phase 2 trial. *Lancet Infect. Dis.* **21**, 493–506 (2021).
86. Sadoff, J. *et al.* Safety and Efficacy of Single-Dose Ad26.COVS.2.S Vaccine against Covid-19. *N. Engl. J. Med.* **384**, 2187–2201 (2021).



87. Folegatti, P. M. *et al.* Safety and immunogenicity of the ChAdOx1 nCoV-19 vaccine against SARS-CoV-2: a preliminary report of a phase 1/2, single-blind, randomised controlled trial. *Lancet* **396**, 467–478 (2020).
88. Henao-Restrepo, A. M. *et al.* Efficacy and effectiveness of an rVSV-vectored vaccine in preventing Ebola virus disease: final results from the Guinea ring vaccination, open-label, cluster-randomised trial (Ebola Ça Suffit!). *Lancet* **389**, 505–518 (2017).
89. Sahin, U., Karikó, K. & Türeci, Ö. mRNA-based therapeutics — developing a new class of drugs. *Nat. Rev. Drug Discov.* **13**, 759–780 (2014).
90. Polack, F. P. *et al.* Safety and Efficacy of the BNT162b2 mRNA Covid-19 Vaccine. *N. Engl. J. Med.* **383**, 2603–2615 (2020).
91. Baden, L. R. *et al.* Efficacy and Safety of the mRNA-1273 SARS-CoV-2 Vaccine. *N. Engl. J. Med.* **384**, 403–416 (2020).
92. Chaudhary, N., Weissman, D. & Whitehead, K. A. mRNA vaccines for infectious diseases: principles, delivery and clinical translation. *Nat. Rev. Drug Discov.* **20**, 817–838 (2021).
93. Karikó, K. *et al.* Incorporation of Pseudouridine Into mRNA Yields Superior Nonimmunogenic Vector With Increased Translational Capacity and Biological Stability. *Mol. Ther.* **16**, 1833–1840 (2008).
94. Linares-Fernández, S., Lacroix, C., Exposito, J.-Y. & Verrier, B. Tailoring mRNA Vaccine to Balance Innate/Adaptive Immune Response. *Trends Mol. Med.* **26**, 311–323 (2020).
95. Barbier, A. J., Jiang, A. Y., Zhang, P., Wooster, R. & Anderson, D. G. The clinical progress of mRNA vaccines and immunotherapies. *Nat. Biotechnol.* **40**, 840–854 (2022).
96. Pulendran, B. & Ahmed, R. Immunological mechanisms of vaccination. *Nat. Immunol.* **12**, 509–517 (2011).
97. Liu, M. A. Immunologic basis of vaccine vectors. *Immunity* **33**, 504–515 (2010).
98. Akira, S., Uematsu, S. & Takeuchi, O. Pathogen Recognition and Innate Immunity. *Cell* **124**, 783–801 (2006).
99. Abbas, A. K. Properties and Overview of Immune Responses. in *Cellular and Molecular Immunology* (Elsevier Health Sciences, 2021).
100. Querec, T. *et al.* Yellow fever vaccine YF-17D activates multiple dendritic cell subsets via TLR2, 7, 8, and 9 to stimulate polyvalent immunity. *J. Exp. Med.* **203**, 413–424 (2006).
101. Koyama, S. *et al.* Differential role of TLR- and RLR-signaling in the immune responses to influenza A virus infection and vaccination. *J. Immunol.* **179**, 4711–4720 (2007).
102. Pulendran, B., S. Arunachalam, P. & O’Hagan, D. T. Emerging concepts in the science of vaccine adjuvants. *Nat. Rev. Drug Discov.* **20**, 454–475 (2021).
103. Eisenbarth, S. C., Colegio, O. R., O’Connor, W., Sutterwala, F. S. & Flavell, R. A. Crucial role for the Nalp3 inflammasome in the immunostimulatory properties of aluminium adjuvants. *Nature* **453**, 1122–1126 (2008).

104. Marrack, P., McKee, A. S. & Munks, M. W. Towards an understanding of the adjuvant action of aluminium. *Nat. Rev. Immunol.* **9**, 287–293 (2009).
105. Lal, H. *et al.* Efficacy of an adjuvanted herpes zoster subunit vaccine in older adults. *N. Engl. J. Med.* **372**, 2087–2096 (2015).
106. Garçon, N. & Di Pasquale, A. From discovery to licensure, the Adjuvant System story. *Hum. Vaccines Immunother.* **13**, 19–33 (2017).
107. Didierlaurent, A. M. *et al.* AS04, an aluminum salt- and TLR4 agonist-based adjuvant system, induces a transient localized innate immune response leading to enhanced adaptive immunity. *J. Immunol.* **183**, 6186–6197 (2009).
108. O’Hagan, D. T., Ott, G. S., De Gregorio, E. & Seubert, A. The mechanism of action of MF59 - an innately attractive adjuvant formulation. *Vaccine* **30**, 4341–4348 (2012).
109. Pardi, N., Hogan, M. J., Porter, F. W. & Weissman, D. mRNA vaccines — a new era in vaccinology. *Nat. Rev. Drug Discov.* **17**, 261–279 (2018).
110. McCann, N., O’Connor, D., Lambe, T. & Pollard, A. J. Viral vector vaccines. *Curr. Opin. Immunol.* **77**, 102210 (2022).
111. Rhee, E. G. *et al.* Multiple Innate Immune Pathways Contribute to the Immunogenicity of Recombinant Adenovirus Vaccine Vectors. *J. Virol.* **85**, 315–323 (2011).
112. Iwasaki, A. & Medzhitov, R. Regulation of adaptive immunity by the innate immune system. *Science* **327**, 291–295 (2010).
113. Coffman, R. L., Sher, A. & Seder, R. A. Vaccine adjuvants: putting innate immunity to work. *Immunity* **33**, 492–503 (2010).
114. Abbas, A. K. Antigen Presentation to T Lymphocytes and the Functions of MHC Molecules. in *Cellular and Molecular Immunology* (Elsevier Health Sciences, 2021).
115. Abbas, A. K. B Cell Activation and Antibody Production. in *Cellular and Molecular Immunology* (Elsevier Health Sciences, 2021).
116. Akkaya, M., Kwak, K. & Pierce, S. K. B cell memory: building two walls of protection against pathogens. *Nat. Rev. Immunol.* **20**, 229–238 (2020).
117. Park, J.-E. *et al.* A cell atlas of human thymic development defines T cell repertoire formation. *Science* **367**, eaay3224 (2020).
118. Kappes, D. J., He, X. & He, X. CD4-CD8 lineage commitment: an inside view. *Nat. Immunol.* **6**, 761–766 (2005).
119. Karimi, M. M. *et al.* The order and logic of CD4 versus CD8 lineage choice and differentiation in mouse thymus. *Nat. Commun.* **12**, 99 (2021).
120. La Gruta, N. L., Gras, S., Daley, S. R., Thomas, P. G. & Rossjohn, J. Understanding the drivers of MHC restriction of T cell receptors. *Nat. Rev. Immunol.* **18**, 467–478 (2018).
121. Watkins, T. S. & Miles, J. J. The human T-cell receptor repertoire in health and disease and potential for omics integration. *Immunol. Cell Biol.* **99**, 135–145 (2021).

122. Pulendran, B. & Ahmed, R. Translating Innate Immunity into Immunological Memory: Implications for Vaccine Development. *Cell* **124**, 849–863 (2006).
123. Pishesha, N., Harmand, T. J. & Ploegh, H. L. A guide to antigen processing and presentation. *Nat. Rev. Immunol.* **22**, 751–764 (2022).
124. Wieczorek, M. *et al.* Major Histocompatibility Complex (MHC) Class I and MHC Class II Proteins: Conformational Plasticity in Antigen Presentation. *Front. Immunol.* **8**, 292 (2017).
125. Lee, W. & Suresh, M. Vaccine adjuvants to engage the cross-presentation pathway. *Front. Immunol.* **13**, 940047 (2022).
126. Embgenbroich, M. & Burgdorf, S. Current Concepts of Antigen Cross-Presentation. *Front. Immunol.* **9**, (2018).
127. Kaech, S. M., Wherry, E. J. & Ahmed, R. Effector and memory T-cell differentiation: implications for vaccine development. *Nat. Rev. Immunol.* **2**, 251–262 (2002).
128. Robinson, H. L. & Amara, R. R. T cell vaccines for microbial infections. *Nat. Med.* **11**, 25–32 (2005).
129. Lagattuta, K. A. *et al.* Repertoire analyses reveal T cell receptor sequence features that influence T cell fate. *Nat. Immunol.* **23**, 446–457 (2022).
130. Sun, L., Su, Y., Jiao, A., Wang, X. & Zhang, B. T cells in health and disease. *Signal Transduct. Target. Ther.* **8**, 1–50 (2023).
131. Abbas, A. K. Differentiation and Functions of CD4+ Effector T Cells. in *Cellular and Molecular Immunology* (Elsevier Health Sciences, 2021).
132. Walker, J. A. & McKenzie, A. N. J. TH2 cell development and function. *Nat. Rev. Immunol.* **18**, 121–133 (2018).
133. Abbas, A. K. Differentiation and Functions of CD8+ Effector T Cells. in *Cellular and Molecular Immunology* (Elsevier Health Sciences, 2021).
134. Farber, D. L., Yudanin, N. A. & Restifo, N. P. Human memory T cells: generation, compartmentalization and homeostasis. *Nat. Rev. Immunol.* **14**, 24–35 (2014).
135. Gattinoni, L., Speiser, D. E., Lichterfeld, M. & Bonini, C. T memory stem cells in health and disease. *Nat. Med.* **23**, 18–27 (2017).
136. Zehn, D., Thimme, R., Lugli, E., de Almeida, G. P. & Oxenius, A. ‘Stem-like’ precursors are the fount to sustain persistent CD8+ T cell responses. *Nat. Immunol.* **23**, 836–847 (2022).
137. Buggert, M., Price, D. A., Mackay, L. K. & Betts, M. R. Human circulating and tissue-resident memory CD8+ T cells. *Nat. Immunol.* **24**, 1076–1086 (2023).
138. Klonowski, K. D. *et al.* Dynamics of blood-borne CD8 memory T cell migration in vivo. *Immunity* **20**, 551–562 (2004).
139. Masopust, D., Vezys, V., Marzo, A. L. & Lefrançois, L. Preferential localization of effector memory cells in nonlymphoid tissue. *Science* **291**, 2413–2417 (2001).
140. Cano-Gamez, E. *et al.* Single-cell transcriptomics identifies an effectorness gradient shaping the response of CD4+ T cells to cytokines. *Nat. Commun.* **11**, 1801 (2020).

141. Woodland, D. L. Jump-starting the immune system: prime–boosting comes of age. *Trends Immunol.* **25**, 98–104 (2004).
142. Shim, E. & Galvani, A. P. Distinguishing vaccine efficacy and effectiveness. *Vaccine* **30**, 6700–6705 (2012).
143. Plotkin, S. A. Correlates of Protection Induced by Vaccination. *Clin. Vaccine Immunol.* **17**, 1055–1065 (2010).
144. Mason, R. A., Tauraso, N. M., Spertzel, R. O. & Ginn, R. K. Yellow fever vaccine: direct challenge of monkeys given graded doses of 17D vaccine. *Appl. Microbiol.* **25**, 539–544 (1973).
145. Goncalvez, A. P. *et al.* Humanized Monoclonal Antibodies Derived from Chimpanzee Fabs Protect against Japanese Encephalitis Virus In Vitro and In Vivo. *J. Virol.* **82**, 7009–7021 (2008).
146. Kreil, T. R., Burger, I., Bachmann, M., Fraiss, S. & Eibl, M. M. Antibodies protect mice against challenge with tick-borne encephalitis virus (TBEV)-infected macrophages. *Clin. Exp. Immunol.* **110**, 358–361 (1997).
147. Gilbert, P. B. *et al.* Immune correlates analysis of the mRNA-1273 COVID-19 vaccine efficacy clinical trial. *Science* **375**, 43–50 (2022).
148. Feng, S. *et al.* Correlates of protection against symptomatic and asymptomatic SARS-CoV-2 infection. *Nat. Med.* **27**, 2032–2040 (2021).
149. Wahl, I. & Wardemann, H. Sterilizing immunity: Understanding COVID-19. *Immunity* **55**, 2231–2235 (2022).
150. Sarkar, J. K., Mitra, A. C. & Mukherjee, M. K. The minimum protective level of antibodies in smallpox. *Bull. World Health Organ.* **52**, 307–311 (1975).
151. Benhnia, M. R.-E.-I. *et al.* Redundancy and Plasticity of Neutralizing Antibody Responses Are Cornerstone Attributes of the Human Immune Response to the Smallpox Vaccine. *J. Virol.* **82**, 3751–3768 (2008).
152. Amanna, I. J., Slifka, M. K. & Crotty, S. Immunity and immunological memory following smallpox vaccination. *Immunol. Rev.* **211**, 320–337 (2006).
153. Treanor, J. & Wright, P. F. Immune correlates of protection against influenza in the human challenge model. *Dev. Biol.* **115**, 97–104 (2003).
154. McElhaney, J. E. *et al.* Granzyme B: Correlates with protection and enhanced CTL response to influenza vaccination in older adults. *Vaccine* **27**, 2418–2425 (2009).
155. Bunde, T. *et al.* Protection from cytomegalovirus after transplantation is correlated with immediate early 1–specific CD8 T cells. *J. Exp. Med.* **201**, 1031–1036 (2005).
156. Arvin, A. M. Humoral and cellular immunity to varicella-zoster virus: an overview. *J. Infect. Dis.* **197**, 58–60 (2008).
157. Schijns, V. *et al.* Rational Vaccine Design in Times of Emerging Diseases: The Critical Choices of Immunological Correlates of Protection, Vaccine Antigen and Immunomodulation. *Pharmaceutics* **13**, 501 (2021).

158. Mahnel, H. & Mayr, A. [Experiences with immunization against orthopox viruses of humans and animals using vaccine strain MVA. *Berl. Munch. Tierarztl. Wochenschr.* **107**, 253–256 (1994).
159. Volz, A. & Sutter, G. Modified Vaccinia Virus Ankara: History, Value in Basic Research, and Current Perspectives for Vaccine Development. *Adv. Virus Res.* **97**, 187–243 (2017).
160. Mayr, A. [Historical review of smallpox, the eradication of smallpox and the attenuated smallpox MVA vaccine. *Berl. Munch. Tierarztl. Wochenschr.* **112**, 322–328 (1999).
161. EMA recommends approval of Imvanex for the prevention monkeypox disease. *European Medicines Agency* <https://www.ema.europa.eu/en/news/ema-recommends-approval-imvanex-prevention-monkeypox-disease> (2022).
162. Orlova, O. V., Glazkova, D. V., Bogoslovskaya, E. V., Shipulin, G. A. & Yudin, S. M. Development of Modified Vaccinia Virus Ankara-Based Vaccines: Advantages and Applications. *Vaccines* **10**, 1516 (2022).
163. Woolsey, C. & Geisbert, T. W. Current state of Ebola virus vaccines: A snapshot. *PLoS Pathog.* **17**, e1010078 (2021).
164. Song, F. *et al.* Middle East Respiratory Syndrome Coronavirus Spike Protein Delivered by Modified Vaccinia Virus Ankara Efficiently Induces Virus-Neutralizing Antibodies. *J. Virol.* **87**, 11950–11954 (2013).
165. Volz, A. *et al.* Protective Efficacy of Recombinant Modified Vaccinia Virus Ankara Delivering Middle East Respiratory Syndrome Coronavirus Spike Glycoprotein. *J. Virol.* **89**, 8651–8656 (2015).
166. Haagmans, B. L. *et al.* An orthopoxvirus-based vaccine reduces virus excretion after MERS-CoV infection in dromedary camels. *Science* **351**, 77–81 (2016).
167. Koch, T. *et al.* Safety and immunogenicity of a modified vaccinia virus Ankara vector vaccine candidate for Middle East respiratory syndrome: an open-label, phase 1 trial. *Lancet Infect. Dis.* **20**, 827–838 (2020).
168. Meyer Zu Natrup, C. *et al.* Stabilized recombinant SARS-CoV-2 spike antigen enhances vaccine immunogenicity and protective capacity. *J. Clin. Invest.* **132**, e159895 (2022).
169. Tscherne, A. *et al.* Immunogenicity and efficacy of the COVID-19 candidate vector vaccine MVA-SARS-2-S in preclinical vaccination. *Proc. Natl. Acad. Sci. U. S. A.* **118**, e2026207118 (2021).
170. Vogel, A. B. *et al.* BNT162b vaccines protect rhesus macaques from SARS-CoV-2. *Nature* **592**, 283–289 (2021).
171. Corbett, K. S. *et al.* Evaluation of the mRNA-1273 Vaccine against SARS-CoV-2 in Nonhuman Primates. *N. Engl. J. Med.* **383**, 1544–1555 (2020).
172. Dicks, M. D. J. *et al.* A Novel Chimpanzee Adenovirus Vector with Low Human Seroprevalence: Improved Systems for Vector Derivation and Comparative Immunogenicity. *PLOS ONE* **7**, e40385 (2012).
173. van Doremalen, N. *et al.* ChAdOx1 nCoV-19 vaccine prevents SARS-CoV-2 pneumonia in rhesus macaques. *Nature* **586**, 578–582 (2020).

174. Voysey, M. *et al.* Single-dose administration and the influence of the timing of the booster dose on immunogenicity and efficacy of ChAdOx1 nCoV-19 (AZD1222) vaccine: a pooled analysis of four randomised trials. *Lancet* **397**, 881–891 (2021).
175. Rotshild, V., Hirsh-Racah, B., Miskin, I., Muszkat, M. & Matok, I. Comparing the clinical efficacy of COVID-19 vaccines: a systematic review and network meta-analysis. *Sci. Rep.* **11**, 22777 (2021).
176. Mellinghoff, S. C. *et al.* SARS-CoV-2 specific cellular response following COVID-19 vaccination in patients with chronic lymphocytic leukemia. *Leukemia* **36**, 562–565 (2022).
177. Mellinghoff, S. C. *et al.* SARS-CoV-2-specific cellular response following third COVID-19 vaccination in patients with chronic lymphocytic leukemia. *Haematologica* **107**, 2480–2484 (2022).
178. Ruether, D. F. *et al.* SARS-CoV2-specific Humoral and T-cell Immune Response After Second Vaccination in Liver Cirrhosis and Transplant Patients. *Clin. Gastroenterol. Hepatol.* **20**, 162–172 (2022).
179. Fathi, A. *et al.* Increased neutralization and IgG epitope identification after MVA-MERS-S booster vaccination against Middle East respiratory syndrome. *Nat. Commun.* **13**, 4182 (2022).
180. Weskamm, L. M. *et al.* Persistence of MERS-CoV-spike-specific B cells and antibodies after late third immunization with the MVA-MERS-S vaccine. *Cell Rep. Med.* **3**, 100685 (2022).
181. Harrer, C. E. *et al.* Identification of a spike-specific CD8+ T cell epitope following vaccination against the Middle East respiratory syndrome coronavirus in humans. *J. Infect. Dis.* **jiad612** (2024) doi:10.1093/infdis/jiad612.
182. Sekine, T. *et al.* Robust T Cell Immunity in Convalescent Individuals with Asymptomatic or Mild COVID-19. *Cell* **183**, 158-168.e14 (2020).
183. Shomuradova, A. S. *et al.* SARS-CoV-2 Epitopes Are Recognized by a Public and Diverse Repertoire of Human T Cell Receptors. *Immunity* **53**, 1245-1257.e5 (2020).
184. Sahin, U. *et al.* BNT162b2 vaccine induces neutralizing antibodies and poly-specific T cells in humans. *Nature* **595**, 572–577 (2021).
185. Oberhardt, V. *et al.* Rapid and stable mobilization of CD8+ T cells by SARS-CoV-2 mRNA vaccine. *Nature* **597**, 268–273 (2021).
186. Meyer, S. *et al.* Prevalent and immunodominant CD8 T cell epitopes are conserved in SARS-CoV-2 variants. *Cell Rep.* **42**, 111995 (2023).
187. Bovay, A. *et al.* Identification of a superagonist variant of the immunodominant Yellow fever virus epitope NS4b 214-222 by combinatorial peptide library screening. *Mol. Immunol.* **125**, 43–50 (2020).
188. Pulendran, B. Learning immunology from the yellow fever vaccine: innate immunity to systems vaccinology. *Nat. Rev. Immunol.* **9**, 741–747 (2009).
189. Bosaeed, M. *et al.* Safety and immunogenicity of ChAdOx1 MERS vaccine candidate in healthy Middle Eastern adults (MERS002): an open-label, non-randomised, dose-escalation, phase 1b trial. *Lancet Microbe* **3**, e11–e20 (2022).

190. Folegatti, P. M. *et al.* Safety and immunogenicity of a candidate Middle East respiratory syndrome coronavirus viral-vectored vaccine: a dose-escalation, open-label, non-randomised, uncontrolled, phase 1 trial. *Lancet Infect. Dis.* **20**, 816–826 (2020).
191. Muthumani, K. *et al.* A synthetic consensus anti-spike protein DNA vaccine induces protective immunity against Middle East respiratory syndrome coronavirus in nonhuman primates. *Sci. Transl. Med.* **7**, 301ra132 (2015).
192. Modjarrad, K. *et al.* Safety and immunogenicity of an anti-Middle East respiratory syndrome coronavirus DNA vaccine: a phase 1, open-label, single-arm, dose-escalation trial. *Lancet Infect. Dis.* **19**, 1013–1022 (2019).
193. Heinz, F. X. & Stiasny, K. Distinguishing features of current COVID-19 vaccines: knowns and unknowns of antigen presentation and modes of action. *Npj Vaccines* **6**, 1–13 (2021).
194. Knezevic, I. *et al.* WHO International Standard for evaluation of the antibody response to COVID-19 vaccines: call for urgent action by the scientific community. *Lancet Microbe* **3**, e235–e240 (2022).
195. Kumar, A., Bernasconi, V., Manak, M., de Almeida Aranha, A. P. & Kristiansen, P. A. The CEPI centralised laboratory network: supporting COVID-19 vaccine development. *Lancet* **397**, 2148–2149 (2021).
196. Huzly, D. *et al.* Accuracy and real life performance of a novel interferon- $\gamma$  release assay for the detection of SARS-CoV2 specific T cell response. *J. Clin. Virol.* **148**, 105098 (2022).
197. Routhu, N. K. *et al.* A modified vaccinia Ankara vector-based vaccine protects macaques from SARS-CoV-2 infection, immune pathology, and dysfunction in the lungs. *Immunity* **54**, 542–556.e9 (2021).
198. Routhu, N. K. *et al.* A modified vaccinia Ankara vaccine expressing spike and nucleocapsid protects rhesus macaques against SARS-CoV-2 Delta infection. *Sci. Immunol.* **7**, eabo0226 (2022).
199. Chiappesi, F. *et al.* Safety and immunogenicity of a synthetic multiantigen modified vaccinia virus Ankara-based COVID-19 vaccine (COH04S1): an open-label and randomised, phase 1 trial. *Lancet Microbe* **3**, e252–e264 (2022).
200. Liu, L. *et al.* Potent neutralizing antibodies against multiple epitopes on SARS-CoV-2 spike. *Nature* **584**, 450–456 (2020).
201. Choi, J.-A. & Kim, J.-O. Middle East Respiratory Syndrome coronavirus vaccine development: updating clinical studies using platform technologies. *J. Microbiol.* **60**, 238–246 (2022).
202. Voysey, M. *et al.* Safety and efficacy of the ChAdOx1 nCoV-19 vaccine (AZD1222) against SARS-CoV-2: an interim analysis of four randomised controlled trials in Brazil, South Africa, and the UK. *Lancet* **397**, 99–111 (2020).
203. McLellan, J. S. *et al.* Structure-Based Design of a Fusion Glycoprotein Vaccine for Respiratory Syncytial Virus. *Science* **342**, 592–598 (2013).
204. Frey, G. *et al.* Distinct conformational states of HIV-1 gp41 are recognized by neutralizing and non-neutralizing antibodies. *Nat. Struct. Mol. Biol.* **17**, 1486–1491 (2010).

205. Hsieh, C.-L. *et al.* Structure-based design of prefusion-stabilized SARS-CoV-2 spikes. *Science* **369**, 1501–1505 (2020).
206. Park, Y.-J. *et al.* Structures of MERS-CoV spike glycoprotein in complex with sialoside attachment receptors. *Nat. Struct. Mol. Biol.* **26**, 1151–1157 (2019).
207. Li, Z. *et al.* The human coronavirus HCoV-229E S-protein structure and receptor binding. *eLife* **8**, e51230 (2019).
208. Pallesen, J. *et al.* Immunogenicity and structures of a rationally designed prefusion MERS-CoV spike antigen. *Proc. Natl. Acad. Sci.* **114**, E7348–E7357 (2017).
209. Kirchdoerfer, R. N. *et al.* Stabilized coronavirus spikes are resistant to conformational changes induced by receptor recognition or proteolysis. *Sci. Rep.* **8**, 15701 (2018).
210. Örd, M., Faustova, I. & Loog, M. The sequence at Spike S1/S2 site enables cleavage by furin and phospho-regulation in SARS-CoV2 but not in SARS-CoV1 or MERS-CoV. *Sci. Rep.* **10**, 16944 (2020).
211. Matsuyama, S. *et al.* Middle East Respiratory Syndrome Coronavirus Spike Protein Is Not Activated Directly by Cellular Furin during Viral Entry into Target Cells. *J. Virol.* **92**, e00683-18 (2018).
212. Bos, R. *et al.* Ad26 vector-based COVID-19 vaccine encoding a prefusion-stabilized SARS-CoV-2 Spike immunogen induces potent humoral and cellular immune responses. *Npj Vaccines* **5**, 1–11 (2020).
213. Amanat, F. *et al.* Introduction of Two Prolines and Removal of the Polybasic Cleavage Site Lead to Higher Efficacy of a Recombinant Spike-Based SARS-CoV-2 Vaccine in the Mouse Model. *mBio* **12**, 10–1128 (2021).
214. Crank, M. C. *et al.* A proof of concept for structure-based vaccine design targeting RSV in humans. *Science* **365**, 505–509 (2019).
215. Capone, S. *et al.* Optimising T cell (re)boosting strategies for adenoviral and modified vaccinia Ankara vaccine regimens in humans. *NPJ Vaccines* **5**, 94 (2020).
216. Sahin, U. *et al.* COVID-19 vaccine BNT162b1 elicits human antibody and TH1 T cell responses. *Nature* **586**, 594–599 (2020).
217. Mateus, J. *et al.* Low-dose mRNA-1273 COVID-19 vaccine generates durable memory enhanced by cross-reactive T cells. *Science* **374**, eabj9853 (2021).
218. Barnes, E. *et al.* Novel adenovirus-based vaccines induce broad and sustained T cell responses to HCV in man. *Sci. Transl. Med.* **4**, 115ra1 (2012).
219. Vollmar, J. *et al.* Safety and immunogenicity of IMVAMUNE, a promising candidate as a third generation smallpox vaccine. *Vaccine* **24**, 2065–2070 (2006).
220. von Krempelhuber, A. *et al.* A randomized, double-blind, dose-finding Phase II study to evaluate immunogenicity and safety of the third generation smallpox vaccine candidate IMVAMUNE®. *Vaccine* **28**, 1209–1216 (2010).
221. Nave, L. *et al.* Immunogenicity and Safety of Modified Vaccinia Ankara (MVA) Vaccine—A Systematic Review and Meta-Analysis of Randomized Controlled Trials. *Vaccines* **11**, 1410 (2023).



222. Zhang, Z. *et al.* Humoral and cellular immune memory to four COVID-19 vaccines. *Cell* **185**, 2434–2451.e17 (2022).
223. Co, M. D. T. *et al.* Discordance between antibody and T cell responses in recipients of trivalent inactivated influenza vaccine. *Vaccine* **26**, 1990–1998 (2008).
224. Bhattacharyya, M. *et al.* Regulation of CD4 T cells and their effects on immunopathological inflammation following viral infection. *Immunology* **152**, 328–343 (2017).
225. West, E. E. *et al.* Tight Regulation of Memory CD8+ T Cells Limits Their Effectiveness during Sustained High Viral Load. *Immunity* **35**, 285–298 (2011).
226. Dangi, T. *et al.* Pre-existing immunity modulates responses to mRNA boosters. *Cell Rep.* **42**, 112167 (2023).
227. Billeskov, R., Beikzadeh, B. & Berzofsky, J. A. The effect of antigen dose on T cell-targeting vaccine outcome. *Hum. Vaccines Immunother.* **15**, 407–411 (2018).
228. Schietinger, A. & Greenberg, P. D. Tolerance and Exhaustion: Defining Mechanisms of T cell Dysfunction. *Trends Immunol.* **35**, 51–60 (2014).
229. Arunachalam, P. S. *et al.* Systems vaccinology of the BNT162b2 mRNA vaccine in humans. *Nature* **596**, 410–416 (2021).
230. Sheerin, D., Dold, C., O'Connor, D., Pollard, A. J. & Rollier, C. S. Distinct patterns of whole blood transcriptional responses are induced in mice following immunisation with adenoviral and poxviral vector vaccines encoding the same antigen. *BMC Genomics* **22**, 777 (2021).
231. Teijaro, J. R. & Farber, D. L. COVID-19 vaccines: modes of immune activation and future challenges. *Nat. Rev. Immunol.* **21**, 195–197 (2021).
232. Hornemann, S. *et al.* Replication of Modified Vaccinia Virus Ankara in Primary Chicken Embryo Fibroblasts Requires Expression of the Interferon Resistance Gene E3L. *J. Virol.* **77**, 8394 (2003).
233. Kaynarcalidan, O., Moreno Mascaraque, S. & Drexler, I. Vaccinia Virus: From Crude Smallpox Vaccines to Elaborate Viral Vector Vaccine Design. *Biomedicines* **9**, 1780 (2021).
234. Pérez, P. *et al.* Deletion of Vaccinia Virus A40R Gene Improves the Immunogenicity of the HIV-1 Vaccine Candidate MVA-B. *Vaccines* **8**, 70 (2020).
235. Holgado, M. P. *et al.* Deletion of A44L, A46R and C12L Vaccinia Virus Genes from the MVA Genome Improved the Vector Immunogenicity by Modifying the Innate Immune Response Generating Enhanced and Optimized Specific T-Cell Responses. *Viruses* **8**, 139 (2016).
236. Rehm, K. E. & Roper, R. L. Deletion of the A35 Gene from Modified Vaccinia Virus Ankara Increases Immunogenicity and Isotype Switching. *Vaccine* **29**, 3276–3283 (2011).
237. Masopust, D., Ha, S.-J., Vezys, V. & Ahmed, R. Stimulation History Dictates Memory CD8 T Cell Phenotype: Implications for Prime-Boost Vaccination<sup>1</sup>. *J. Immunol.* **177**, 831–839 (2006).
238. Poetsch, J. H. *et al.* Detectable Vesicular Stomatitis Virus (VSV)–Specific Humoral and Cellular Immune Responses Following VSV–Ebola Virus Vaccination in Humans. *J. Infect. Dis.* **219**, 556–561 (2019).

239. Swadling, L. *et al.* A Human Vaccine Strategy Based On Chimpanzee Adenoviral and MVA Vectors That Primes, Boosts and Sustains Functional HCV Specific T-Cell Memory. *Sci. Transl. Med.* **6**, 261ra153 (2014).
240. Ewer, K. *et al.* A Monovalent Chimpanzee Adenovirus Ebola Vaccine Boosted with MVA. *N. Engl. J. Med.* **374**, 1635–1646 (2016).
241. Barros-Martins, J. *et al.* Immune responses against SARS-CoV-2 variants after heterologous and homologous ChAdOx1 nCoV-19/BNT162b2 vaccination. *Nat. Med.* **27**, 1525–1529 (2021).
242. Rodrigues, C. M. C. & Plotkin, S. A. The influence of interval between doses on response to vaccines. *Vaccine* **39**, 7123–7127 (2021).
243. Plotkin, S., Orenstein, W., Offit, P. & Edwards, K. *Plotkin's Vaccines*. (Elsevier, 2017).
244. Barry, H. *et al.* Safety and immunogenicity of 2-dose heterologous Ad26.ZEBOV, MVA-BN-Filo Ebola vaccination in healthy and HIV-infected adults: A randomised, placebo-controlled Phase II clinical trial in Africa. *PLoS Med.* **18**, e1003813 (2021).
245. Natalini, A. *et al.* Improved memory CD8 T cell response to delayed vaccine boost is associated with a distinct molecular signature. *Front. Immunol.* **14**, (2023).
246. Thompson, E. A., Beura, L. K., Nelson, C. E., Anderson, K. G. & Vezys, V. Shortened Intervals during Heterologous Boosting Preserve Memory CD8 T Cell Function but Compromise Longevity. *J. Immunol.* **196**, 3054–3063 (2016).
247. Hall, V. G. *et al.* Delayed-interval BNT162b2 mRNA COVID-19 vaccination enhances humoral immunity and induces robust T cell responses. *Nat. Immunol.* **23**, 380–385 (2022).
248. Payne, R. P. *et al.* Immunogenicity of standard and extended dosing intervals of BNT162b2 mRNA vaccine. *Cell* **184**, 5699-5714.e11 (2021).
249. Flaxman, A. *et al.* Reactogenicity and immunogenicity after a late second dose or a third dose of ChAdOx1 nCoV-19 in the UK: a substudy of two randomised controlled trials (COV001 and COV002). *Lancet* **398**, 981–990 (2021).
250. Natalini, A. *et al.* Durable CD8 T Cell Memory against SARS-CoV-2 by Prime/Boost and Multi-Dose Vaccination: Considerations on Inter-Dose Time Intervals. *Int. J. Mol. Sci.* **23**, 14367 (2022).
251. Nakaya, H. I. *et al.* Systems Analysis of Immunity to Influenza Vaccination across Multiple Years and in Diverse Populations Reveals Shared Molecular Signatures. *Immunity* **43**, 1186–1198 (2015).
252. Querec, T. D. *et al.* Systems biology approach predicts immunogenicity of the yellow fever vaccine in humans. *Nat. Immunol.* **10**, 116–125 (2009).
253. Zimmermann, P. & Curtis, N. Factors That Influence the Immune Response to Vaccination. *Clin. Microbiol. Rev.* **32**, e00084-18 (2019).
254. Antinori, A. & Bausch-Jurken, M. The Burden of COVID-19 in the Immunocompromised Patient: Implications for Vaccination and Needs for the Future. *J. Infect. Dis.* **228**, S4–S12 (2023).
255. Chatzikonstantinou, T. *et al.* COVID-19 severity and mortality in patients with CLL: an update of the international ERIC and Campus CLL study. *Leukemia* **35**, 3444–3454 (2021).

256. Webb, G. J. *et al.* Outcomes following SARS-CoV-2 infection in liver transplant recipients: an international registry study. *Lancet Gastroenterol. Hepatol.* **5**, 1008–1016 (2020).
257. Marjot, T. *et al.* Outcomes following SARS-CoV-2 infection in patients with chronic liver disease: An international registry study. *J. Hepatol.* **74**, 567–577 (2021).
258. Herishanu, Y. *et al.* Efficacy of the BNT162b2 mRNA COVID-19 vaccine in patients with chronic lymphocytic leukemia. *Blood* **137**, 3165–3173 (2021).
259. Ehmsen, S. *et al.* Antibody and T cell immune responses following mRNA COVID-19 vaccination in patients with cancer. *Cancer Cell* **39**, 1034–1036 (2021).
260. Parry, H. *et al.* Antibody responses after first and second Covid-19 vaccination in patients with chronic lymphocytic leukaemia. *Blood Cancer J.* **11**, 1–8 (2021).
261. Boyarsky, B. J. *et al.* Antibody Response to 2-Dose SARS-CoV-2 mRNA Vaccine Series in Solid Organ Transplant Recipients. *JAMA* **325**, 2204–2206 (2021).
262. Rabinowich, L. *et al.* Low immunogenicity to SARS-CoV-2 vaccination among liver transplant recipients. *J. Hepatol.* **75**, 435–438 (2021).
263. Blixt, L. *et al.* T-cell immune responses following vaccination with mRNA BNT162b2 against SARS-CoV-2 in patients with chronic lymphocytic leukemia: results from a prospective open-label clinical trial. *Haematologica* **107**, 1000–1003 (2022).
264. Shadman, M. Diagnosis and Treatment of Chronic Lymphocytic Leukemia: A Review. *JAMA* **329**, 918–932 (2023).
265. Forconi, F. & Moss, P. Perturbation of the normal immune system in patients with CLL. *Blood* **126**, 573–581 (2015).
266. Bewarder, M., Stilgenbauer, S., Thurner, L. & Kaddu-Mulindwa, D. Current Treatment Options in CLL. *Cancers* **13**, 2468 (2021).
267. Wroe, P. C. *et al.* Aging Population and Future Burden of Pneumococcal Pneumonia in the United States. *J. Infect. Dis.* **205**, 1589–1592 (2012).
268. Gordon, A. & Reingold, A. The Burden of Influenza: a Complex Problem. *Curr. Epidemiol. Rep.* **5**, 1–9 (2018).
269. Johnson, R. W. *et al.* The impact of herpes zoster and post-herpetic neuralgia on quality-of-life. *BMC Med.* **8**, 37 (2010).
270. Rondy, M. *et al.* Effectiveness of influenza vaccines in preventing severe influenza illness among adults: A systematic review and meta-analysis of test-negative design case-control studies. *J. Infect.* **75**, 381–394 (2017).
271. Tseng, H. F. *et al.* Declining Effectiveness of Herpes Zoster Vaccine in Adults Aged  $\geq 60$  Years. *J. Infect. Dis.* **213**, 1872–1875 (2016).
272. Wagner, A. *et al.* Age-related differences in humoral and cellular immune responses after primary immunisation: indications for stratified vaccination schedules. *Sci. Rep.* **8**, 9825 (2018).
273. Crooke, S. N., Ovsyannikova, I. G., Poland, G. A. & Kennedy, R. B. Immunosenescence and human vaccine immune responses. *Immun. Ageing* **16**, 25 (2019).

274. Rodriguez, I. J. *et al.* Immunosenescence Study of T Cells: A Systematic Review. *Front. Immunol.* **11**, 604591 (2021).
275. Boraschi, D. *et al.* The Gracefully Aging Immune System. *Sci. Transl. Med.* **5**, 185ps8-185ps8 (2013).
276. Mittelbrunn, M. & Kroemer, G. Hallmarks of T cell aging. *Nat. Immunol.* **22**, 687–698 (2021).
277. Mogilenko, D. A., Shchukina, I. & Artyomov, M. N. Immune ageing at single-cell resolution. *Nat. Rev. Immunol.* **22**, 484–498 (2022).
278. University of Oxford. *Oxford and Liverpool scientists launch new vaccine trial for Middle East Respiratory Syndrome (MERS)*. <https://www.ox.ac.uk/news/2023-09-18-oxford-and-liverpool-scientists-launch-new-vaccine-trial-middle-east-respiratory-0> (2023).
279. Klein, S. L., Jedlicka, A. & Pekosz, A. The Xs and Y of immune responses to viral vaccines. *Lancet Infect. Dis.* **10**, 338–349 (2010).
280. Troy, J. D., Hill, H. R., Ewell, M. G. & Frey, S. E. Sex Difference in Immune Response to Vaccination: A Participant-Level Meta-Analysis of Randomized Trials of IMVAMUNE® Smallpox Vaccine. *Vaccine* **33**, 5425–5431 (2015).
281. Haralambieva, I. H. *et al.* Race and Sex-Based Differences in Cytokine Immune Responses to Smallpox Vaccine in Healthy Individuals. *Hum. Immunol.* **74**, 1263–1266 (2013).
282. Fathi, A., Addo, M. M. & Dahlke, C. Sex Differences in Immunity: Implications for the Development of Novel Vaccines Against Emerging Pathogens. *Front. Immunol.* **11**, 601170 (2021).
283. Klein, S. L. & Flanagan, K. L. Sex differences in immune responses. *Nat. Rev. Immunol.* **16**, 626–638 (2016).
284. Flanagan, K. L., Fink, A. L., Plebanski, M. & Klein, S. L. Sex and Gender Differences in the Outcomes of Vaccination over the Life Course. *Annu. Rev. Cell Dev. Biol.* **33**, 577–599 (2017).
285. Sewell, A. K. Why must T cells be cross-reactive? *Nat. Rev. Immunol.* **12**, 669–677 (2012).
286. Robinson, J. *et al.* The IMGT/HLA database. *Nucleic Acids Res.* **41**, D1222–D1227 (2013).
287. Barquera, R. *et al.* Binding affinities of 438 HLA proteins to complete proteomes of seven pandemic viruses and distributions of strongest and weakest HLA peptide binders in populations worldwide. *HLA* **96**, 277–298 (2020).
288. Pretti, M. A. M. *et al.* Class I HLA Allele Predicted Restricted Antigenic Coverages for Spike and Nucleocapsid Proteins Are Associated With Deaths Related to COVID-19. *Front. Immunol.* **11**, 565730 (2020).
289. Nguyen, A. *et al.* Human Leukocyte Antigen Susceptibility Map for Severe Acute Respiratory Syndrome Coronavirus 2. *J. Virol.* **94**, e00510-20 (2020).
290. Tan, P.-L., Jacobson, R. M., Poland, G. A., Jacobsen, S. J. & Pankratz, V. S. Twin studies of immunogenicity — determining the genetic contribution to vaccine failure. *Vaccine* **19**, 2434–2439 (2001).

291. Ovsyannikova, I. G. *et al.* Human Leukocyte Antigen and Cytokine Receptor Gene Polymorphisms Associated With Heterogeneous Immune Responses to Mumps Viral Vaccine. *Pediatrics* **121**, e1091–e1099 (2008).
292. Gelder, C. M. *et al.* Associations between Human Leukocyte Antigens and Nonresponsiveness to Influenza Vaccine. *J. Infect. Dis.* **185**, 114–117 (2002).
293. Ovsyannikova, I. G. *et al.* HLA haplotype and supertype associations with cellular immune responses and cytokine production in healthy children after rubella vaccine. *Vaccine* **27**, 3349–3358 (2009).
294. Crocchiolo, R. *et al.* Polymorphism of the HLA system and weak antibody response to BNT162b2 mRNA vaccine. *HLA* **99**, 183–191 (2022).
295. Meyer, D., C. Aguiar, V. R., Bitarello, B. D., C. Brandt, D. Y. & Nunes, K. A genomic perspective on HLA evolution. *Immunogenetics* **70**, 5–27 (2018).
296. Markov, P. V. & Pybus, O. G. Evolution and Diversity of the Human Leukocyte Antigen(HLA). *Evol. Med. Public Health* **2015**, 1 (2015).
297. Seder, R. A., Darrah, P. A. & Roederer, M. T-cell quality in memory and protection: implications for vaccine design. *Nat. Rev. Immunol.* **8**, 247–258 (2008).
298. Kirkpatrick, B. D. *et al.* The live attenuated dengue vaccine TV003 elicits complete protection against dengue in a human challenge model. *Sci. Transl. Med.* **8**, 330ra36 (2016).
299. Graham, N. *et al.* Rapid Induction and Maintenance of Virus-Specific CD8+ TEMRA and CD4+ TEM Cells Following Protective Vaccination Against Dengue Virus Challenge in Humans. *Front. Immunol.* **11**, 479 (2020).
300. Weiskopf, D. *et al.* Dengue virus infection elicits highly polarized CX3CR1+ cytotoxic CD4+ T cells associated with protective immunity. *Proc. Natl. Acad. Sci. U. S. A.* **112**, E4256–E4263 (2015).
301. Akondy, R. S. *et al.* Origin and differentiation of human memory CD8 T cells after vaccination. *Nature* **552**, 362–367 (2017).
302. Ahmed, R. & Akondy, R. S. Insights into human CD8(+) T-cell memory using the yellow fever and smallpox vaccines. *Immunol. Cell Biol.* **89**, 340–345 (2011).
303. Wang, Y. *et al.* Stem cell-like memory T cells: The generation and application. *J. Leukoc. Biol.* **110**, 1209–1223 (2021).
304. Habel, J. R. *et al.* Suboptimal SARS-CoV-2-specific CD8+ T cell response associated with the prominent HLA-A\*02:01 phenotype. *Proc. Natl. Acad. Sci.* **117**, 24384–24391 (2020).
305. Kent, S. J. *et al.* Disentangling the relative importance of T cell responses in COVID-19: leading actors or supporting cast? *Nat. Rev. Immunol.* **22**, 387–397 (2022).
306. Le Bert, N. *et al.* Highly functional virus-specific cellular immune response in asymptomatic SARS-CoV-2 infection. *J. Exp. Med.* **218**, e20202617 (2021).
307. Swadling, L. *et al.* Pre-existing polymerase-specific T cells expand in abortive seronegative SARS-CoV-2. *Nature* **601**, 110–117 (2022).

308. Goldberg, Y. *et al.* Protection and Waning of Natural and Hybrid Immunity to SARS-CoV-2. *N. Engl. J. Med.* **386**, 2201–2212 (2022).
309. Bertoletti, A., Le Bert, N. & Tan, A. T. SARS-CoV-2-specific T cells in the changing landscape of the COVID-19 pandemic. *Immunity* **55**, 1764–1778 (2022).
310. Tarke, A. *et al.* SARS-CoV-2 vaccination induces immunological T cell memory able to cross-recognize variants from Alpha to Omicron. *Cell* **185**, 847-859.e11 (2022).
311. Liu, J. *et al.* Vaccines elicit highly conserved cellular immunity to SARS-CoV-2 Omicron. *Nature* **603**, 493–496 (2022).
312. Sette, A. & Crotty, S. Pre-existing immunity to SARS-CoV-2: the knowns and unknowns. *Nat. Rev. Immunol.* **20**, 457–458 (2020).
313. Grifoni, A. *et al.* Targets of T Cell Responses to SARS-CoV-2 Coronavirus in Humans with COVID-19 Disease and Unexposed Individuals. *Cell* **181**, 1489-1501.e15 (2020).
314. Braun, J. *et al.* SARS-CoV-2-reactive T cells in healthy donors and patients with COVID-19. *Nature* **587**, 270–274 (2020).
315. Le Bert, N. *et al.* SARS-CoV-2-specific T cell immunity in cases of COVID-19 and SARS, and uninfected controls. *Nature* **584**, 457–462 (2020).
316. Gorse, G. J., Patel, G. B., Vitale, J. N. & O'Connor, T. Z. Prevalence of Antibodies to Four Human Coronaviruses Is Lower in Nasal Secretions than in Serum. *Clin. Vaccine Immunol.* **17**, 1875–1880 (2010).
317. Kundu, R. *et al.* Cross-reactive memory T cells associate with protection against SARS-CoV-2 infection in COVID-19 contacts. *Nat. Commun.* **13**, 80 (2022).
318. Wilkinson, T. M. *et al.* Preexisting influenza-specific CD4+ T cells correlate with disease protection against influenza challenge in humans. *Nat. Med.* **18**, 274–280 (2012).
319. Greenbaum, J. A. *et al.* Pre-existing immunity against swine-origin H1N1 influenza viruses in the general human population. *Proc. Natl. Acad. Sci.* **106**, 20365–20370 (2009).
320. Hancock, K. *et al.* Cross-Reactive Antibody Responses to the 2009 Pandemic H1N1 Influenza Virus. *N. Engl. J. Med.* **361**, 1945–1952 (2009).
321. Pulendran, B. Systems vaccinology: Probing humanity's diverse immune systems with vaccines. *Proc. Natl. Acad. Sci.* **111**, 12300–12306 (2014).
322. Wimmers, F. & Pulendran, B. Emerging technologies for systems vaccinology — multi-omics integration and single-cell (epi)genomic profiling. *Curr. Opin. Immunol.* **65**, 57–64 (2020).
323. Mudd, P. A. *et al.* SARS-CoV-2 mRNA vaccination elicits a robust and persistent T follicular helper cell response in humans. *Cell* **185**, 603-613.e15 (2022).
324. Turner, J. S. *et al.* SARS-CoV-2 mRNA vaccines induce persistent human germinal centre responses. *Nature* **596**, 109–113 (2021).
325. Wagar, L. E. Human immune organoids: a tool to study vaccine responses. *Nat. Rev. Immunol.* **23**, 699–699 (2023).

326. Wagar, L. E. *et al.* Modeling human adaptive immune responses with tonsil organoids. *Nat. Med.* **27**, 125–135 (2021).
327. Palgen, J.-L. *et al.* Optimize Prime/Boost Vaccine Strategies: Trained Immunity as a New Player in the Game. *Front. Immunol.* **12**, (2021).
328. de Bree, L. C. J. *et al.* Non-specific effects of vaccines: Current evidence and potential implications. *Semin. Immunol.* **39**, 35–43 (2018).
329. Lee, A. *et al.* BCG vaccination stimulates integrated organ immunity by feedback of the adaptive immune response to imprint prolonged innate antiviral resistance. *Nat. Immunol.* **25**, 41–53 (2023).
330. Murphy, D. M. *et al.* Trained immunity is induced in humans after immunization with an adenoviral vector COVID-19 vaccine. *J. Clin. Invest.* **133**, e162581.
331. Overton, E. T. *et al.* Safety and Immunogenicity of Modified Vaccinia Ankara-Bavarian Nordic Smallpox Vaccine in Vaccinia-Naive and Experienced Human Immunodeficiency Virus-Infected Individuals: An Open-Label, Controlled Clinical Phase II Trial. *Open Forum Infect. Dis.* **2**, ofv040 (2015).
332. Greenberg, R. N. *et al.* Safety, Immunogenicity, and Surrogate Markers of Clinical Efficacy for Modified Vaccinia Ankara as a Smallpox Vaccine in HIV-Infected Subjects. *J. Infect. Dis.* **207**, 749–758 (2013).
333. Harrop, R., Shingler, W., Kelleher, M., de Belin, J. & Treasure, P. Cross-trial analysis of immunologic and clinical data resulting from phase I and II trials of MVA-5T4 (TroVax) in colorectal, renal, and prostate cancer patients. *J. Immunother.* **33**, 999–1005 (2010).
334. Harris, S. A. *et al.* Process of Assay Selection and Optimization for the Study of Case and Control Samples from a Phase IIb Efficacy Trial of a Candidate Tuberculosis Vaccine, MVA85A. *Clin. Vaccine Immunol.* **21**, 1005 (2014).
335. Sutter, G. & Moss, B. Nonreplicating vaccinia vector efficiently expresses recombinant genes. *Proc. Natl. Acad. Sci. U. S. A.* **89**, 10847–10851 (1992).
336. García-Arriaza, J. & Esteban, M. Enhancing poxvirus vectors vaccine immunogenicity. *Hum. Vaccines Immunother.* **10**, 2235–2244 (2014).
337. Finn, J. D. *et al.* Persistence of Transgene Expression Influences CD8<sup>+</sup> T-Cell Expansion and Maintenance following Immunization with Recombinant Adenovirus. *J. Virol.* **83**, 12027–12036 (2009).
338. Meseda, C. A., Atukorale, V., Kuhn, J., Schmeisser, F. & Weir, J. P. Percutaneous Vaccination as an Effective Method of Delivery of MVA and MVA-Vectored Vaccines. *PloS One* **11**, e0149364 (2016).
339. Förster, R., Fleige, H. & Sutter, G. Combating COVID-19: MVA Vector Vaccines Applied to the Respiratory Tract as Promising Approach Toward Protective Immunity in the Lung. *Front. Immunol.* **11**, (2020).
340. Bošnjak, B. *et al.* Intranasal Delivery of MVA Vector Vaccine Induces Effective Pulmonary Immunity Against SARS-CoV-2 in Rodents. *Front. Immunol.* **12**, (2021).

341. About TherVacB: New Concept to fight Chronic Hepatitis B. <https://www.thervacb.eu/the-project/> (2020).
342. Backes, S. *et al.* Protein-prime/modified vaccinia virus Ankara vector-boost vaccination overcomes tolerance in high-antigenemic HBV-transgenic mice. *Vaccine* **34**, 923–932 (2016).
343. McAuliffe, J. *et al.* Heterologous prime-boost vaccination targeting MAGE-type antigens promotes tumor T-cell infiltration and improves checkpoint blockade therapy. *J. Immunother. Cancer* **9**, e003218 (2021).
344. Van den Eynde, B. J. Cancer Research UK dose first patient in phase I/IIa trial of lung cancer immunotherapy vaccine | Cancer Research Horizons. *First patient dosed in phase I/IIa trial of lung cancer immunotherapy vaccine* <https://www.ludwig.ox.ac.uk/news/first-patient-dosed-in-phase-i-ii-a-trial-of-lung-cancer-immunotherapy-vaccine>.



## 8. ACKNOWLEDGEMENTS

I would like to thank Prof. Dr. med. Marylyn M. Addo for the supervision and for giving me the opportunity to conduct my doctoral studies in her institute. Her scientific insights, encouragement to attend conferences and courses, and her enthusiastic and supportive supervision have made this a very interesting and rewarding experience.

I would like to thank Prof. Dr. med. Jonas Schmidt-Chanasit for evaluating my thesis and providing an important external, scientific perspective to my doctoral thesis.

I would like to thank Dr. Christine Dahlke for encouraging me to join the team and for her scientific and personal mentoring. I want to thank Dr. med. Anahita Fathi, for her important contributions to the clinical trials, the fruitful discussions, and her critical review of the results presented in this thesis. Thanks to Dr. med. Maria Mackroth, for her guidance as a co-supervisor at the BNITM.

I am very grateful to Dr. Marie Weskamm, for the joint projects and manuscripts, the discussions of experiments and data, and the exchange of ideas. Thanks to Caroline E. Harrer for the great T cell collaboration across the Atlantic Ocean and Dr. med. Sibylle C. Mellinshoff for the joined CLL projects.

A special thanks goes to My Linh, who spent numerous hours with me in the lab and helped me with many of the experiments presented in this thesis.

I am also grateful for the rewarding experience of mentoring two excellent Master students, Jana Kochmann and Vera Brackrock, who have contributed to the results of this thesis.

I would like to thank the whole IIRVD team, including current and former members: Alena Sendzik, Alina Grefe, Claudia Schlesner, Cordula Grüttner, Dominik Hillesheim, Dr. Etienne Bartels, Golda Schaub, Dr. med. Hanna-Marie Weichel, Ilka Grewe, Laura Rübenacker, Maher Almahfoud, Maren Sandkuhl, Marie-Louise Dieck, Dr. Maya Kono, Dr. Melanie Richter, Monika Friedrich, Monika Rottstegge, M Saleh Yunus, Niclas Rénevier, Paulina Tarnow, PD Dr. med. Robin Kobbe, Ruben Baumann, Stefanie Gräfe, Stephanie Petereit, Dr. Susanne Ziegler, Dr. Svenja Hardtke, Dr. Tamara Zoran, Dr. med. Till Koch, Dr. Toni L. Meister, Valentin Bärreiter, Yashin Simsek, and all mentioned above, for creating such a friendly work environment and for the great teamwork!

I also extend my gratitude to everyone involved in the MVA-based vaccine projects at the German Center for Infection Research, the Clinical Trial Center North, the Ludwig Maximilian University of Munich, the Philipps University of Marburg, and the Erasmus Medical Center Rotterdam, and to all study participants, as without their dedication, clinical vaccine development would not be possible.

A special mention goes to the coordinators and colleagues of the Erasmus Mundus Joint Master in Leading International Vaccinology Education (LIVE), who have sparked my passion for vaccine development.

I would like to thank my friends and family, especially Vinnycius Pereira, Zuzanna Piwowarska, Emil Vergara, and Rodrigo Arcoverde for their scientific and emotional support, Marie Godow and Lasse Seddig who made me feel at home in Hamburg, my brothers Simon and David Mayer who are on my team since day one, and my partner David Garthe who I can always count on.

Finally, I want to thank my parents, Carola and Stefan Mayer, for their unconditional and constant support. Without them, none of this would have been possible.

9. EIDESSTATTLICHE VERSICHERUNG – DECLARATION ON OATH

Hiermit erkläre ich an Eides statt, dass ich die vorliegende Dissertationsschrift selbst verfasst und keine anderen als die angegebenen Quellen und Hilfsmittel benutzt habe.

I hereby declare, on oath, that I have written the present dissertation by my own and have not used other than the acknowledged resources and aids.

A handwritten signature in blue ink, appearing to read 'L. Mayer', with a long horizontal stroke extending to the right.

Leonie Mayer

Hamburg / 11.01.2024

## 10. PUBLICATIONS

**I. MVA-based vaccine candidates encoding the native or prefusion-stabilized SARS-CoV-2 spike protein reveal differential immunogenicity in humans**

**Leonie Mayer\***, Leonie M. Weskamm\*, Anahita Fathi, Maya Kono, Jasmin Heidepriem, Verena Krähling, Sibylle C. Mellinshoff, My Linh Ly, Monika Friedrich, Svenja Hardtke, Saskia Borregaard, Thomas Hesterkamp, Felix F. Loeffler, the MVA-SARS-2 Study Group, Asisa Volz, Gerd Sutter, Stephan Becker, Christine Dahlke, Marylyn M. Addo

\*These authors contributed equally.

Accepted manuscript in *npj Vaccines* (12 December 2023)

## ARTICLE OPEN



## MVA-based vaccine candidates encoding the native or prefusion-stabilized SARS-CoV-2 spike reveal differential immunogenicity in humans

Leonie Mayer<sup>1,2,3,16</sup>✉, Leonie M. Weskamm<sup>1,2,3,16</sup>, Anahita Fathi<sup>1,2,3,4</sup>, Maya Kono<sup>1,2,3</sup>, Jasmin Heidepriem<sup>5</sup>, Verena Krähling<sup>6,7</sup>, Sibylle C. Mellinshoff<sup>8,9</sup>, My Linh Ly<sup>1,2,3</sup>, Monika Friedrich<sup>1,2,3</sup>, Svenja Hardtke<sup>1,2,3</sup>, Saskia Borregaard<sup>10</sup>, Thomas Hestekamp<sup>11</sup>, Felix F. Loeffler<sup>5</sup>, Asisa Volz<sup>12,13</sup>, Gerd Sutter<sup>14,15</sup>, Stephan Becker<sup>6,7</sup>, Christine Dahlke<sup>1,2,3,16</sup> and Marylyn M. Addo<sup>1,2,3,16</sup>✉

In response to the COVID-19 pandemic, multiple vaccines were developed using platforms, such as viral vectors and mRNA technology. Here, we report humoral and cellular immunogenicity data from human phase 1 clinical trials investigating two recombinant Modified Vaccinia virus Ankara vaccine candidates, MVA-SARS-2-S and MVA-SARS-2-ST, encoding the native and the prefusion-stabilized SARS-CoV-2 spike protein, respectively. MVA-SARS-2-ST was more immunogenic than MVA-SARS-2-S, but both were less immunogenic compared to licensed mRNA- and ChAd-based vaccines in SARS-CoV-2 naïve individuals. In heterologous vaccination, previous MVA-SARS-2-S enhanced T cell functionality and MVA-SARS-2-ST boosted the frequency of T cells and S1-specific IgG levels when used as a third vaccination. While the vaccine candidate containing the prefusion-stabilized spike elicited predominantly S1-specific responses, immunity to the candidate with the native spike was skewed towards S2-specific responses. These data demonstrate how the spike antigen conformation, using the same viral vector, directly affects vaccine immunogenicity in humans.

npj Vaccines \_#####\_; <https://doi.org/10.1038/s41541-023-00801-z>

## INTRODUCTION

Severe acute respiratory syndrome coronavirus 2 (SARS-CoV-2) causing coronavirus disease 2019 (COVID-19) has led to significant morbidity and mortality, which was alleviated by the rapid availability of effective vaccines<sup>1–4</sup>. The accelerated development of COVID-19 vaccines was, in part, possible because vaccine platforms such as mRNA and viral vectors were optimized prior to the pandemic and were quickly adjusted to encode a new antigen upon the emergence of SARS-CoV-2<sup>5</sup>.

One promising vaccine platform against emerging viruses is the recombinant Modified Vaccinia virus Ankara (rMVA), an attenuated poxviral vector that efficiently infects, but cannot replicate, in human cells. While non-recombinant MVA is a licensed vaccine against smallpox and monkeypox, the rMVA viral vector platform was recently approved in a heterologous prime-boost regimen against Ebola (Mvabea) and has been investigated in various clinical trials, including an rMVA-based multivalent RSV vaccine currently undergoing phase III efficacy testing<sup>6–8</sup>. Clinical trials using MVA have included immunocompromised patients and infants, providing extensive favorable safety data<sup>9,10</sup>. Using the rMVA platform, two vaccine candidates against COVID-19 were developed<sup>11,12</sup>, leveraging prior experience with an rMVA-based

vaccine candidate (MVA-MERS-S) against *Middle East respiratory syndrome* (MERS), which encodes the native, full-length MERS-CoV spike (S)-protein, and was shown to be safe and immunogenic in a first-in-human phase 1 clinical trial<sup>13–15</sup>. The S-protein of *Betacoronaviruses* consists of the S1 subunit binding the host cell receptor and the S2 subunit, which mediates fusion with the cell membrane upon S1/S2 cleavage. Both subunits are important targets for antibodies that can interfere with virus entry, thus making the S-protein a promising vaccine antigen<sup>16–18</sup>.

MVA-SARS-2-S (MVA-S) encodes the native, full-length SARS-CoV-2 S-protein. MVA-SARS-2-ST (MVA-ST) encodes a modified S-protein with two proline amino acid substitutions in the S2 subunit and additional mutations to inactivate the S1/S2 cleavage site. These modifications render the S-protein in a prefusion-stabilized conformation that is not cleaved into S1 and S2 subunits, but anchored on the membrane of MVA-ST-infected cells<sup>12</sup>. Both vaccine candidates showed protective efficacy in mice and hamsters<sup>11,12</sup> and proceeded to evaluation in phase 1 clinical trials in October 2020 (MVA-S, ClinicalTrials.gov: NCT04569383) and July 2021 (MVA-ST, ClinicalTrials.gov: NCT04895449), respectively (see Supplementary Note 1 for details). MVA-S and MVA-ST were administered to SARS-CoV-2 naïve individuals in a two-dose immunization schedule,

<sup>1</sup>Institute for Infection Research and Vaccine Development (IIRVD), University Medical Centre Hamburg-Eppendorf, Hamburg, Germany. <sup>2</sup>Department for Clinical Immunology of Infectious Diseases, Bernhard Nocht Institute for Tropical Medicine, Hamburg, Germany. <sup>3</sup>German Centre for Infection Research, Partner Site Hamburg-Lübeck-Borstel-Riems, Hamburg, Germany. <sup>4</sup>First Department of Medicine, Division of Infectious Diseases, University Medical Centre Hamburg-Eppendorf, Hamburg, Germany. <sup>5</sup>Department of Biomolecular Systems, Max Planck Institute of Colloids and Interfaces, Potsdam, Germany. <sup>6</sup>Institute for Virology, Philipps University Marburg, Marburg, Germany. <sup>7</sup>German Centre for Infection Research, Partner Site Gießen-Marburg-Langen, Marburg, Germany. <sup>8</sup>Faculty of Medicine and University Hospital of Cologne, Department I of Internal Medicine, Centre for Integrated Oncology Aachen Bonn Cologne Düsseldorf (CIO ABCD), German CLL Group (GCLLSG), University of Cologne, Cologne, Germany. <sup>9</sup>German Centre for Infection Research, Partner Site Bonn-Cologne, Cologne, Germany. <sup>10</sup>Clinical Trial Center North GmbH & Co. KG, Hamburg, Germany. <sup>11</sup>German Centre for Infection Research, Translational Project Management Office, Brunswick, Germany. <sup>12</sup>Institute of Virology, University of Veterinary Medicine Hannover, Foundation, Hanover, Germany. <sup>13</sup>German Centre for Infection Research, Partner Site Hannover-Brunswick, Hanover, Germany. <sup>14</sup>Division of Virology, Department of Veterinary Sciences, Institute for Infectious Diseases and Zoonoses, LMU Munich, Munich, Germany. <sup>15</sup>German Centre for Infection Research, Partner Site Munich, Munich, Germany. <sup>16</sup>These authors contributed equally: Leonie Mayer, Leonie M. Weskamm, Christine Dahlke, Marylyn M. Addo. ✉email: [lmayer@uke.de](mailto:lmayer@uke.de); [m.addo@uke.de](mailto:m.addo@uke.de)

28 days apart. Additionally, MVA-ST was investigated as a one-dose booster vaccination for mRNA-vaccinated individuals.

To comparatively evaluate the immunogenicity of the rMVA-based COVID-19 vaccine candidates, we included the first three COVID-19 vaccines licensed in the EU in the analysis. BNT162b2 (Comirnaty) and mRNA-1273 (Spikevax), here referred to as mRNA, encode a prefusion-stabilized SARS-CoV-2 S-protein with the native S1/S2 cleavage site<sup>19–21</sup>. ChAdOx1 nCov-19 (Vaxzevria), here referred to as ChAd, is a viral vector vaccine based on a replication-deficient chimpanzee adenovirus encoding the native, full-length SARS-CoV-2 S-protein<sup>22,23</sup>. The high efficacy of the mRNA and ChAd vaccines against symptomatic COVID-19 has been associated with high titers of S-specific binding immunoglobulin G (IgG) and neutralizing antibodies<sup>24,25</sup>. However, no distinct correlate of protection has been defined, and the underlying mechanisms leading to and maintaining protection remain elusive. Important parameters, such as memory B and T cells that contribute to long-term immune memory, are often not part of primary analyses<sup>26–29</sup>.

To investigate the immunogenicity of the two rMVA-based vaccine candidates in comparison to the licensed mRNA and ChAd vaccines in humans, peripheral blood samples were collected prior to and at multiple defined time points after vaccination, allowing for a comprehensive and longitudinal comparison of the immune response in individuals receiving five different vaccination regimens. We specifically analyzed S1- and S2-specific antibody isotypes and IgG subclasses, and identified potential IgG epitopes. In addition, we performed a longitudinal analysis of S-specific B cells as well as the magnitude and cytokine profile of S-specific T cells. Our findings highlight distinct S1- and S2-specific characteristics of the adaptive immune response induced by the same viral vector platform but encoding different conformations of the S-antigen, which is an important approach to inform future antigen design.

## RESULTS

To gain insight into the humoral and cellular immune responses induced by two novel rMVA-based COVID-19 vaccine candidates encoding different conformations of the S-protein, we evaluated immunogenicity in three cohorts receiving MVA-S (native S) or MVA-ST (prefusion-stabilized S) in combination with licensed vaccines (MVA-S/mRNA (blue), MVA-ST (red), and mRNA/MVA-ST cohorts (purple)). For comparison, we recruited two control cohorts vaccinated with the licensed ChAd and mRNA vaccines (mRNA (green) and ChAd/mRNA (brown) cohorts). Only participants without SARS-CoV-2 infections before and during the entire study period were included in this analysis (as detailed in the methods section). A detailed description of the vaccine regimens and antigens is shown in Fig. 1a. Participant demographics and time intervals between vaccinations are shown in Supplementary Tables 1 and 2 and Supplementary Fig. 1. Peripheral blood samples were collected longitudinally at T0 (baseline before vaccination), T1 (1–2 weeks), T2 (3–5 weeks), T3 (12 weeks), and T4 (17–29 weeks) post vaccination (Fig. 1a; Supplementary Table 3), with weeks referring to the time since the last vaccination (V1–V4). In total, blood samples were obtained from 76 donors, longitudinally (Supplementary Fig. 1). We longitudinally measured antigen-specific serum antibodies and performed several phenotypic B and T cell assays, as described in Fig. 1b. Sample sizes of each analysis and timepoint, and statistics of the following paragraphs are indicated in Supplementary Tables 4 and 12.

### S1/S2-specific IgG response induced by MVA-S and MVA-ST immunization

First, plasma antibodies against the S1 and S2 subunits of the S-protein were measured longitudinally using a bead-based

multiplex immunoassay to quantify the relative antibody response based on the median fluorescence intensity (MFI). Here, we highlight the S1- and S2-specific IgG responses (Fig. 2). IgM and IgA responses are shown in Supplementary Fig. 2.

The dynamics of the IgG response for the five different cohorts are shown in Fig. 2a. S1-specific IgG (solid line) was undetectable, whereas S2-specific IgG (dashed line) was present at baseline (T0) in all cohorts. Two immunizations using the MVA-S vaccine candidate (MVA-S/mRNA cohort) induced S1-specific IgG (median fold change (mfc) [MFI] = 3.5;  $p = 0.0104$ ) and S2-specific IgG (mfc [MFI] = 8.2;  $p = 0.0012$ ) above baseline. S1-specific IgG waned over a period of six months to baseline levels (mfc [MFI] = 1, ns), whereas S2-specific IgG was maintained significantly above baseline (mfc [MFI] = 4.3;  $p = 0.0030$ ). Following subsequent mRNA vaccination, both S1- and S2-specific IgG were rapidly boosted, and thereafter followed similar dynamics compared to the control cohorts (see green and brown cohorts in Fig. 2a). In comparison, two vaccinations with MVA-ST (MVA-ST cohort) induced S2-specific IgG (mfc [MFI] = 7.2,  $p = 0.0005$ ) with a similar fold-change as MVA-S but led to a more robust induction of S1-specific IgG (mfc [MFI] = 509.9;  $p = 0.0005$ ) compared to baseline. When using MVA-ST as a third vaccination in previously mRNA vaccinated (mRNA/MVA-ST cohort), the fold-induction of S1- and S2-specific IgG levels above baseline before third vaccination was low (S1: mfc [MFI] = 1.2,  $p = 0.0007$ ; S2: mfc [MFI] = 1.2,  $p = 0.0018$ ). In comparison, the fold-induction of IgG levels after third mRNA vaccination was higher and reached similar levels as seen after second vaccination, both in the mRNA cohort (S1: mfc [MFI] = 3.7,  $p = 0.0421$ ; S2: mfc [MFI] = 2.5,  $p = 0.0421$ ) and the ChAd/mRNA cohort (S1: mfc [MFI] = 2.9, ns; S2: mfc [MFI] = 2.8, ns).

To analyze differences in the specificity of the antibody response towards the S1 or S2 subunit, we directly compared the median MFI (mMFI) IgG levels at the time points of the peak response between the different cohorts). Figure 2b depicts the IgG level at V2T1, where MVA-ST-induced significantly higher S1-specific IgG levels (mMFI = 2704) compared to MVA-S (mMFI = 18;  $p < 0.0001$ ), but lower compared to mRNA (mMFI = 19295,  $p < 0.0001$ ) and ChAd/mRNA (mMFI = 14558,  $p = 0.0006$ ). In contrast, S2-specific IgG was induced at similar levels by MVA-S (mMFI = 2296) and MVA-ST (mMFI = 1697, ns). The S2-specific IgG response after MVA-S vaccination was significantly lower compared to those of the mRNA (mMFI = 13186;  $p < 0.0001$ ) and ChAd/mRNA (mMFI = 12160,  $p = 0.0008$ ) control cohorts. In Fig. 2c, we compared the time point V3T2 of the MVA-S/mRNA cohort to the time point V1T2 of the mRNA control cohort (both corresponding to T2 after the first mRNA vaccination) to determine whether previous MVA-S vaccination had an effect on the IgG response induced by subsequent mRNA vaccination. At this time point, S2-specific IgG was significantly higher in the MVA-S/mRNA compared to the mRNA cohort (MVA-S/mRNA: mMFI = 17071; mRNA: mMFI = 7468,  $p = 0.0014$ ). S1-specific IgG levels of the MVA-S/mRNA cohort (mMFI = 10687) also tended to be higher than those of the mRNA cohort (mMFI = 6590, ns).

Next, we evaluated the IgG response following third vaccination by stratifying the MVA-ST cohort based on dose (Fig. 2d) and pre-boosting IgG levels (Fig. 2e). Comparable inductions were observed in the middle-dose (mfc [MFI] = 1.6,  $p = 0.0285$ ) and high-dose groups (mfc [MFI] = 1.5, ns), and a lower induction in the low-dose group (mfc [MFI] = 1.2, ns). Notably, there was significant S1-specific IgG induction in individuals with low baseline levels before MVA-ST booster vaccination ( $p = 0.0006$ ), but not in those with a high baseline, regardless of the MVA-ST dose group (Fig. 2e).

Of the 257 samples analyzed by bead-based immunoassay, a total of 228 samples across all cohorts were additionally analyzed by SARS-CoV-2 virus neutralization test (VNT<sub>100</sub>). Neutralization capacity strongly correlated with the levels of S1-specific IgG

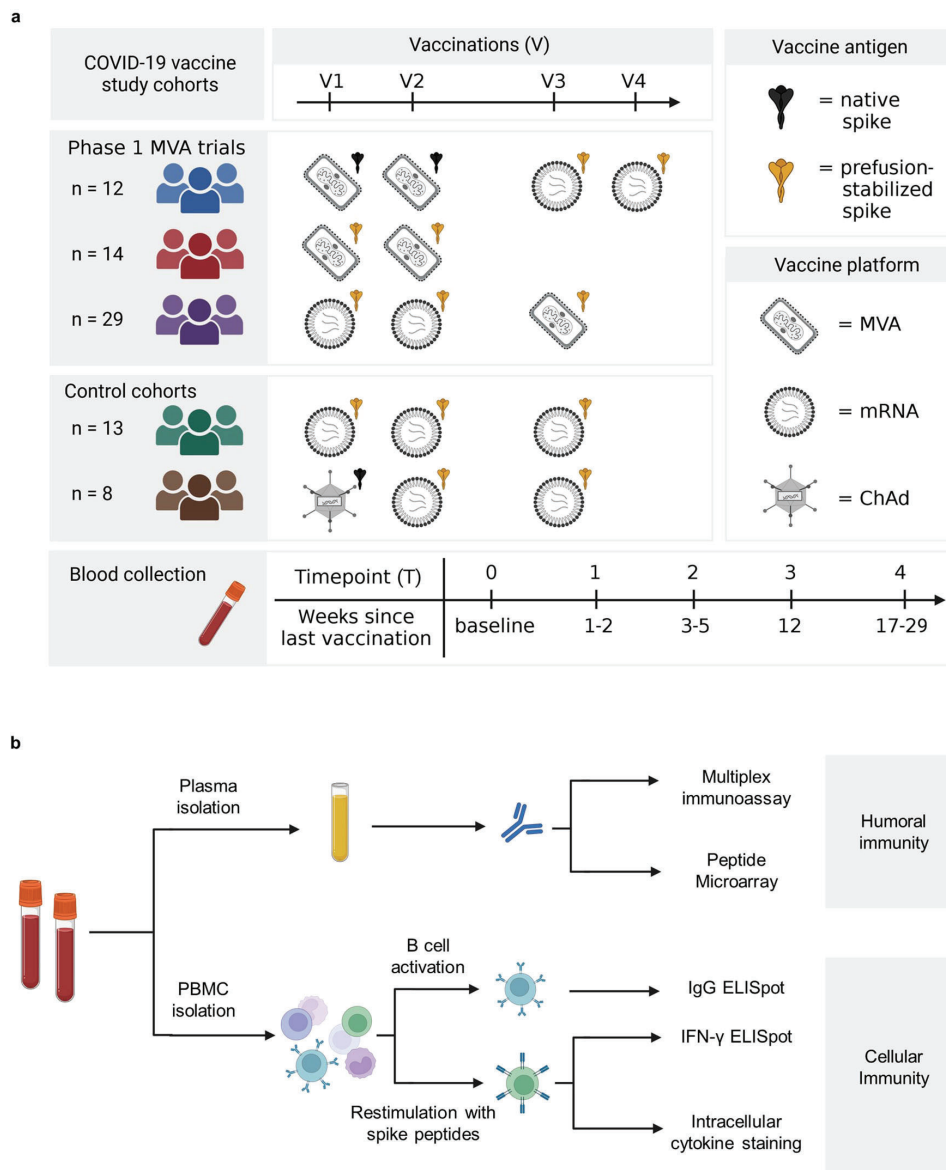


**Fig. 1 Study design.** **a** Participants of five study cohorts received up to four vaccinations (V1 to V4) with different COVID-19 vaccines. The vaccines administered in this study include the two experimental rMVA-based vaccine candidates MVA-SARS-2-S (MVA-S) and MVA-SARS-2-ST (MVA-ST), as well as the licensed vaccines BNT162b2 and mRNA-1273 (together referred to as mRNA) and ChAdOx1 nCov-19 (ChAd). The different vaccines encode either the native spike protein (black) or the prefusion-stabilized spike (yellow). Blood samples were collected at different time points after vaccination, labeled as T0 (baseline), T1 (1–2 weeks), T2 (3–5 weeks), T3 (12 weeks), and T4 (17–29 weeks), referring to the time since last vaccination (V1–V4). **b** The humoral and cellular immune response was analyzed using different assays. See Supplementary Tables 4–8 for detailed number of samples and analyzed time points by assay and study cohort.

( $r = 0.8991$ ,  $p < 0.0001$ ), and to a lesser extent with S2-specific IgG ( $r = 0.7830$ ,  $p < 0.0001$ ) (Fig. 2f). Correlations of neutralizing capacity with S1- and S2-specific IgG responses are stratified by cohort in Supplementary Fig. 3.

#### Dynamics of IgG subclasses and identification of immunogenic S1/S2-specific B cell epitopes

We longitudinally analyzed the S1- (top panel) and S2- (bottom panel) specific IgG1-IgG4 responses using the bead-based multiplex immunoassay (Fig. 3a). Primary vaccination with MVA-ST, mRNA, and ChAd mainly induced IgG1 and IgG3, which were boosted by subsequent vaccinations. Overall, both IgG1 and IgG3

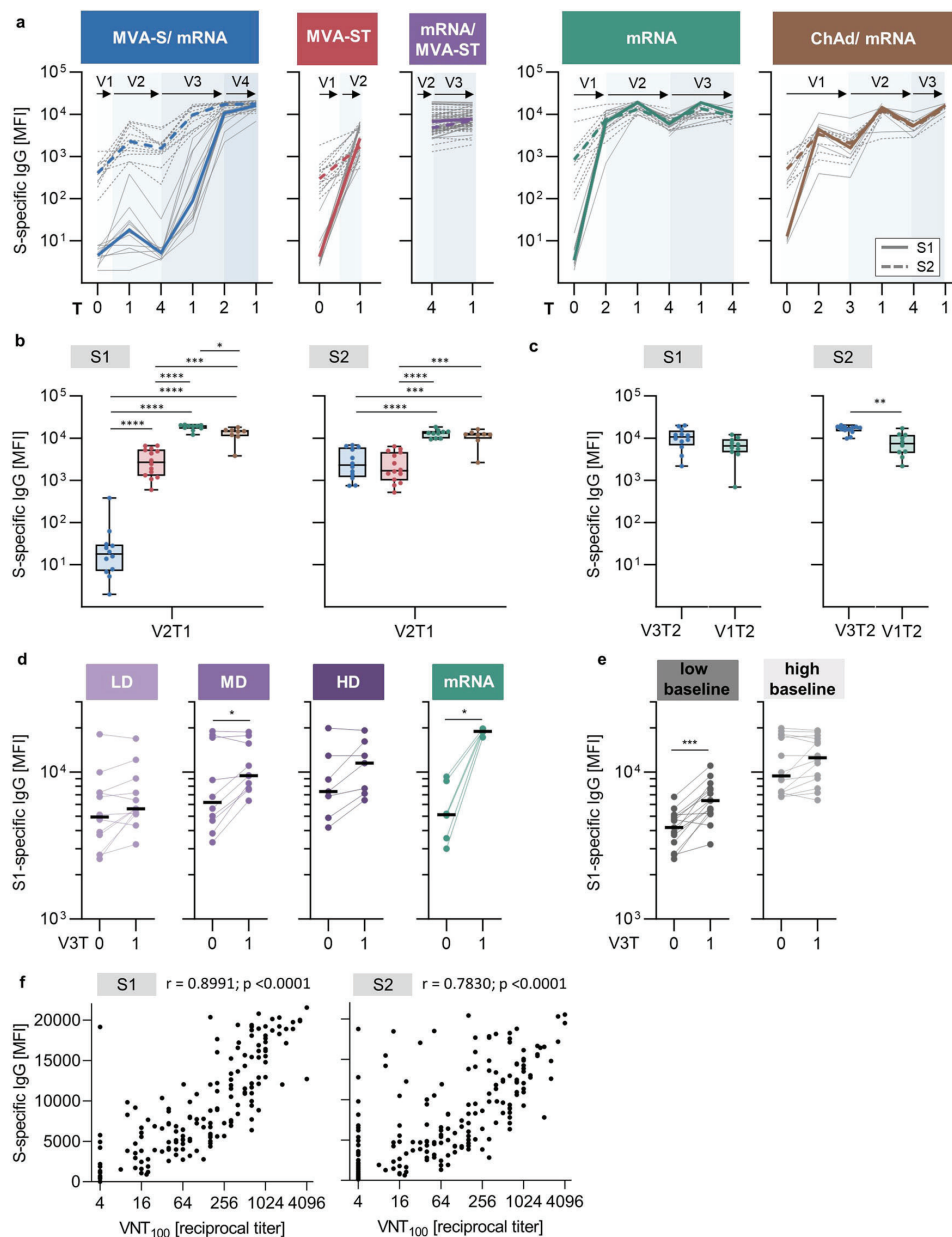


**Fig. 2** S1/S2-specific IgG response induced by MVA-S and MVA-ST immunization. **a** S1 (continuous line)- and S2 (dashed line)- specific IgG responses measured at baseline and longitudinally after each vaccination. Colored lines depict median MFI (measured by bead-based multiplex immunoassay, mean of technical duplicates). Gray lines show dynamics of individual study participants. Vaccinations V1 to V4 are indicated by arrows. **b** S1- (left) and S2- (right) specific IgG levels induced by two doses of MVA-S (blue) or MVA-ST (red) at V2T1 in comparison to the control cohorts (green and brown). **c** S1- (left) and S2- (right) specific IgG levels after first mRNA vaccination in the MVA-S/mRNA cohort (blue; V3T2) in comparison to the mRNA control cohort (green; V1T2). **d**, **e** S1-specific IgG levels induced by third vaccination with MVA-ST divided into **(d)** dose groups (purple; LD = low dose, MD = middle dose, HD = high dose) compared to mRNA (green) or by **(e)** low ( $\leq$ median V3T0; left) and high baseline ( $>$ median V3T0; right). Data are represented as median  $\pm$  IQR (**b**, **c**) or individual data points and median (**d**, **e**). **f** Spearman correlation of serum neutralizing capacity (measured by SARS-CoV-2 virus neutralization test, VNT<sub>100</sub>) with S1- (left) and S2- (right) specific IgG,  $n = 228$ . Significant  $p$ -values are indicated as calculated by two-tailed Mann–Whitney  $U$  test (**b**, **c**) or Wilcoxon matched-pairs signed rank test (**d**, **e**) and adjusted for multiple comparisons using a Benjamini & Hochberg correction: \* $p < 0.05$ , \*\* $p < 0.01$ , \*\*\* $p < 0.001$ , \*\*\*\* $p < 0.0001$ . Time points after vaccination are indicated as T0 (baseline), T1 (1–2 weeks), T2 (3–5 weeks), T3 (12 weeks), and T4 (17–29 weeks) (**a**, **b**, **c**, **d**, **e**).  $P$  values and sample sizes are indicated in Supplementary Tables 9 and 4 and 8.

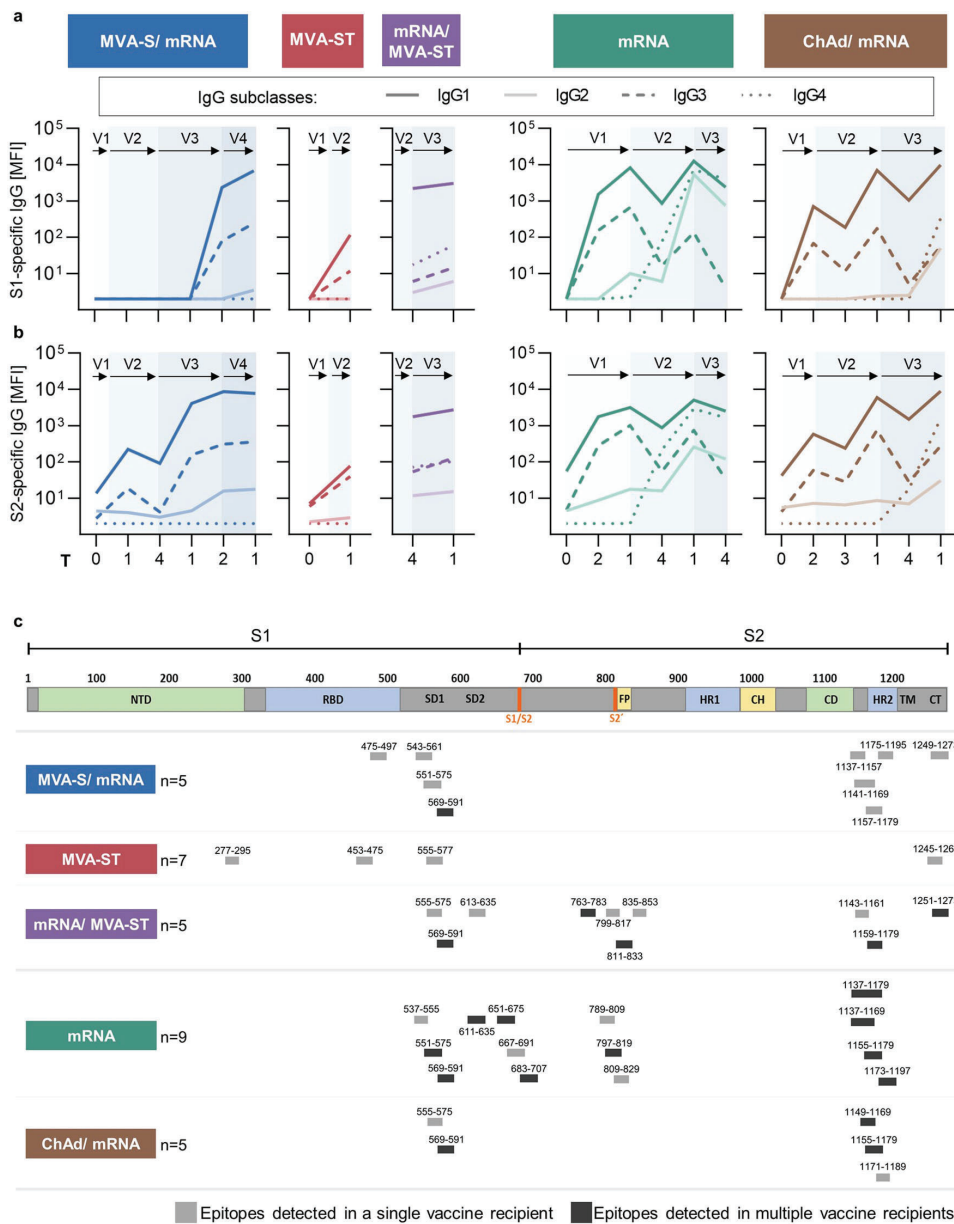


**Fig. 3 Dynamics of IgG subclasses and identification of immunogenic S1/S2-specific B cell epitopes.** **a** S1- (top) and S2- (bottom) specific IgG subclasses of the different study cohorts measured at baseline and longitudinally after each vaccination. Median MFIs (measured by bead-based multiplex immunoassay, mean of technical duplicates) of IgG1-4 are shown as differently dotted lines. Vaccinations V1 to V4 are indicated by arrows and time points after vaccination are indicated as T0 (baseline), T1 (1–2 weeks), T2 (3–5 weeks), T3 (12 weeks), and T4 (17–29 weeks). **b** Schematic representation of immunogenic B cell epitopes measured on peptide microarrays and identified by increased fluorescent intensity (as arbitrary fluorescence units, AFU) in the five study cohorts in one (gray) or multiple (black) individuals, aligned to a schematic depiction of the S-protein<sup>18</sup>. Positive epitope binding was defined as >400 mean AFU of three successive peptides and 2.5-fold above baseline before first vaccination (if available). Time points analyzed after vaccination: mRNA (V2:T1), ChAd/mRNA (V2:T1; V3:T1), MVA-S/ mRNA (V2:T1; V4:T1), MVA-ST (V2:T1), mRNA/MVA-ST (V3:T0; V3:T1). (NTD: N-terminal domain, RBD receptor-binding domain, SD1, SD2 subdomain 1 and 2, S1/S2 S1/S2 cleavage site, S2' S2' cleavage site, FP fusion peptide, HR1 heptad repeat 1, CH central helix, CD connector domain, HR2 heptad repeat 2, TM transmembrane domain, CT cytoplasmic tail). Sample sizes are indicated in Supplementary Tables 4–8.



followed kinetics similar to that observed for total IgG (Fig. 2a). Notably, the IgG2 and IgG4 subclasses were only induced in the mRNA and ChAd/mRNA control cohorts, where they were first detectable after the second dose of mRNA vaccination, which corresponds to V2 in the mRNA cohort and V3 in the ChAd/mRNA cohort. The IgG2 and IgG4 responses were further boosted after the third mRNA vaccination in the mRNA cohort (Fig. 3a).

To further investigate epitope specificity of the humoral response, we analyzed IgG and IgA binding to S-specific peptides using microarrays. Heatmaps of all cohorts depicting antibody binding measured in arbitrary fluorescent units (AFU) are shown in Supplementary Data 1. Vaccine-induced responses were defined by comparing the AFU after vaccination with the baseline. We did not detect a change in the binding of IgA antibodies to linear S-specific epitopes after vaccination compared to the baseline (Supplementary Data 1). IgG binding to S-specific epitopes was detected in all cohorts after vaccination (Fig. 3b). As shown in Supplementary Data 1, the epitope breadth varies, depending on the grouping of epitopes and the number of participants analyzed per cohort. Immunogenic regions within SARS-CoV-2 S, in which vaccine recipients from several cohorts showed antibody binding, were identified in the S1 subunit (amino acids (AA) 537-635) and in the S2 subunit (AA 763-853, AA 1137-1159). One region in the S1/S2 junction (AA 651-707) was identified only in the mRNA cohort. Notably, epitopes in the cytoplasmic tail of the S2 subunit (AA 1245-1273) were detected only in the cohorts that had received an MVA-based vaccination.

#### Longitudinal analysis of S1/S2-specific B cell responses induced by MVA-S and MVA-ST immunization

To evaluate whether the observed S1/S2 bias within the antibody response (see Fig. 2) was also reflected in the cellular response, we characterized the B cellular immune response using an antigen-specific IgG enzyme-linked immunosorbent assay (ELISpot) assay (Fig. 4). B cells specific for the S1 and S2 subunits were quantified as IgG spot-forming cells (SFC) per million peripheral blood mononuclear cells (PBMCs), and total IgG-secreting B cells served as a positive control.

In the MVA-S/mRNA cohort, a slight induction of S1-specific B cells (S1: mfc [SFC] = 1.5,  $p = 0.0298$ ) and a more pronounced induction of S2-specific B cells (S2: mfc [SFC] = 7.8,  $p = 0.0018$ ) above baseline levels were observed after two MVA-S vaccinations (V2T1) (Fig. 4a). This observation was consistent with the IgG response (see Fig. 2a). Notably, S2-specific B cells expanded more rapidly after the first mRNA vaccination in this cohort compared to the mRNA control cohort, while S1-specific B cells followed similar dynamics. Vaccination with two doses of MVA-ST induced S1- and S2-specific B cells significantly above baseline, but both at low levels (S1: mfc [SFC] = 2.2,  $p = 0.0156$ ; S2: mfc [SFC] = 2.5,  $p = 0.0078$ ). The fold induction of S1- and S2-specific B cells was also low after the first immunization using mRNA (S1: mfc [SFC] = 5.4,  $p = 0.0201$ ; S2: mfc [SFC] = 3.2,  $p = 0.0419$ ) or ChAd (S1: mfc [SFC] = 3.5,  $p = 0.0170$ ; S2: mfc [SFC] = 7.2,  $p = 0.0419$ ), but was further increased after the second dose in the mRNA (S1: mfc [SFC] = 33.1,  $p = 0.0066$ ; S2: mfc [SFC] = 13.1,  $p = 0.0156$ ) and ChAd/mRNA (S1: mfc [SFC] = 115.8,  $p = 0.0170$ ; S2: mfc [SFC] = 82.5,  $p = 0.0170$ ) control cohorts. The frequency of S1- and S2-specific B cells did not increase following MVA-ST as a third vaccination (mRNA/MVA-ST cohort) (S1: mfc [SFC] = 1; S2: mfc [SFC] = 1). In contrast, a third mRNA vaccination boosted the B cell response in the mRNA (S1: mfc [SFC] = 8.8; S2: mfc [SFC] = 5.8) and ChAd/mRNA (S1: mfc [SFC] = 5.0; S2: mfc [SFC] = 7.3) control cohorts, but this did not reach statistical significance.

After the primary vaccination series at V2T1, an S1/S2 bias was observed for B cells (Fig. 4b), similar to that detected for IgG (Fig. 2b). S1-specific B cell frequencies were higher, although not significantly, after MVA-ST (median = 13 SFC) than after MVA-S

vaccination (median = 10 SFC), but significantly lower than in the mRNA (median = 371 SFC,  $p = 0.0004$ ) and ChAd/mRNA (median = 316 SFC,  $p < 0.0008$ ) control cohorts. In contrast, S2-specific B cells were induced at significantly higher frequencies by MVA-S (median = 25 SFC) compared to MVA-ST (median = 14 SFC,  $p = 0.0228$ ). The S2-specific B cell response after MVA-S vaccination was still significantly lower than that in the mRNA (median = 122 SFC,  $p = 0.0017$ ) and ChAd/mRNA (median = 191 SFC,  $p = 0.0005$ ) control cohorts. Looking at the effect of primary MVA-S vaccination on subsequent mRNA vaccination, the induction of S2-specific B cells was significantly higher in the MVA-S/mRNA cohort (V3T2: median = 138 SFC) compared to primary vaccination in the mRNA cohort (V1T2: median = 19 SFC,  $p = 0.0008$ ) (Fig. 4c), whereas S1-specific responses did not show a significant difference. We also evaluated the S1-specific B cell response following third MVA-ST vaccination stratified by dose (Fig. 4d) and pre-boosting B cell levels (Fig. 4e). In contrast to the IgG response, no significant induction was observed regardless of the dose group and baseline levels.

#### Longitudinal analysis of S1/S2-specific T cell responses induced by MVA-S and MVA-ST immunization

It is strongly suggested that T cells contribute significantly to vaccine-induced immunity and protection. Here, the S-specific T cell dynamics following vaccination were analyzed by IFN- $\gamma$  ELISpot assay, as shown in Fig. 5a for the different cohorts. PBMCs were stimulated with an overlapping peptide (OLP) pool consisting of four individual pools (M1-M4) spanning the entire SARS-CoV-2 S-protein (Fig. 5b), with M1-M2 corresponding predominantly to S1 and M3-M4 to S2. The results were quantified as IFN- $\gamma$ -secreting SFC per million PBMCs. Representative ELISpot wells are shown in Fig. 5b. To confirm the T cell results in an independent assay, we used a commercial whole-blood IFN- $\gamma$  release T cell assay. The results correlated with those of the IFN- $\gamma$  ELISpot assay (Spearman  $r = 0.7$ ;  $p < 0.0001$ ), providing additional evidence for the robustness of the methods (Fig. 5c).

Although MVA-S induced a detectable T cell response in some participants, the mfc at the time point of peak response (V1T2) was not significantly higher than that at baseline (mfc [SFC] = 1, ns) (Fig. 5a). Upon subsequent mRNA vaccination in this cohort, S-specific T cell frequencies were boosted 22-fold above baseline, as early as one week after the first mRNA vaccination. In contrast to MVA-S, one dose of MVA-ST induced a T cell response significantly above baseline (mfc [SFC] = 2.4,  $p = 0.0249$ ), which was comparable to one dose of mRNA (mfc [SFC] = 2.9) but lower than that of ChAd (mfc [SFC] = 9.7). When used as a third vaccination in previously mRNA-vaccinated individuals, MVA-ST significantly boosted the T cell response above the baseline (mfc [SFC] = 1.7,  $p = 0.0012$ ). These results are comparable to a third mRNA vaccination where the T cell response was boosted (mfc [SFC] = 2.0, ns) but not above the peak levels seen after the second vaccination.

Peak responses at V2T1 were directly compared between the different cohorts, revealing that MVA-ST induced a significantly higher T cell response than MVA-S (MVA-ST = 65 SFC; MVA-S = 4 SFC,  $p = 0.0021$ ) (Fig. 5d). However, this response was significantly lower compared to the control cohorts (mRNA = 356 SFC,  $p = 0.0021$ ; ChAd/mRNA = 306 SFC,  $p = 0.0023$ ). We then analyzed the T cell response to the two S subunits by evaluating the response to the four OLP pools separately. The pools M1-M2 mainly cover the S1 and M3-M4 the S2 subunit. MVA-S induced a T cell response that was biased towards the S2 subunit after first vaccination. This bias was not observed after the second MVA-S vaccination, where the response was overall low. MVA-ST induced an S1-biased response, that was most pronounced after the second MVA-ST vaccination (Fig. 5e). The same pattern was reflected in the IgG and B cell responses, suggesting a

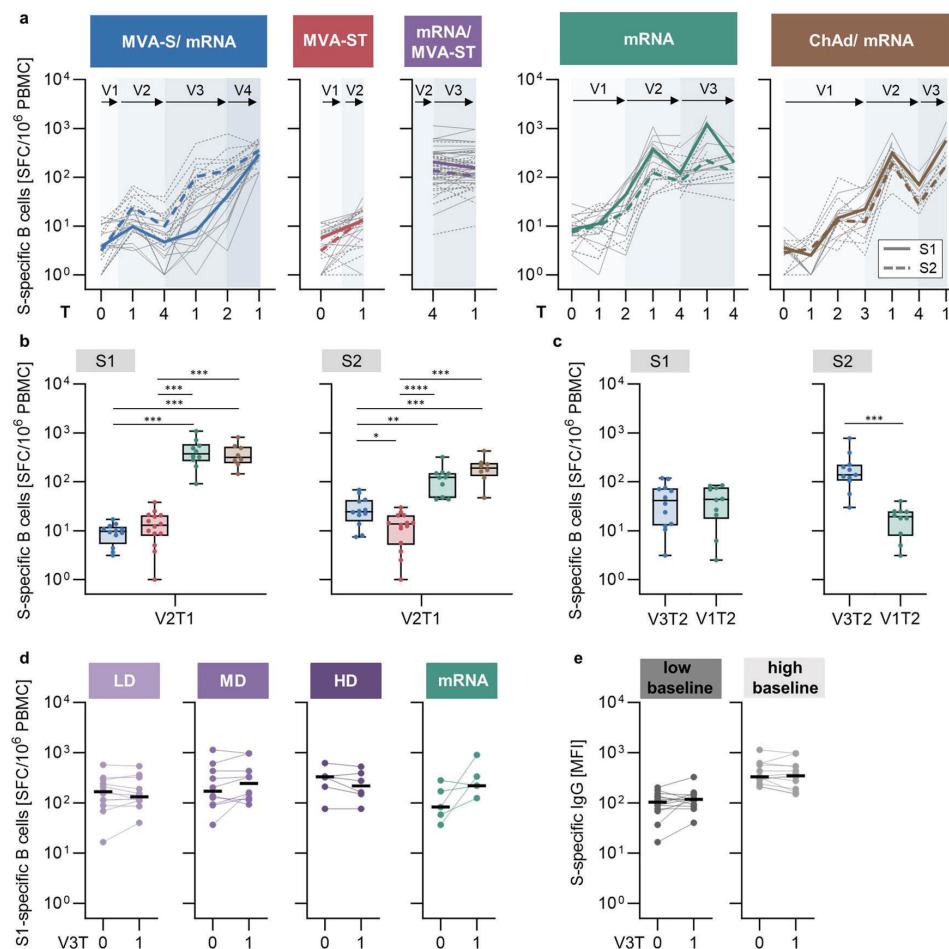


**Fig. 4** Longitudinal analysis of S1/S2-specific B cell responses induced by MVA-S and MVA-ST immunization. **a** Frequencies of IgG-secreting B cells shown as SFC/10<sup>6</sup> PBMCs (mean of technical duplicates) measured by IgG ELISpot. Colored lines depict median S1 (continuous line)- and S2 (dashed line)-specific responses for each cohort. Gray lines show the dynamics of individual participants. **b** S1- (left) and S2- (right) specific IgG-secreting B cells induced by two doses MVA-S (blue) or MVA-ST (red) at V2T1 in comparison to the control cohorts (green and brown). **c** S1- (left) and S2- (right) specific IgG-secreting B cells after first mRNA vaccination in the MVA-S/mRNA cohort (blue; V3T2) in comparison to first vaccination in the mRNA control cohort (green; V1T2). S1-specific IgG-secreting B cells induced by third vaccination with MVA-ST divided into **(d)** dose groups (purple; LD = low dose, MD = middle dose, HD = high dose) compared to mRNA (green) or by **(e)** low (<median V3T0; left) and high baseline (>median V3T0; right). Data are represented as median ± IQR (**b, c**) or individual data points and median (**d, e**). Significant *p* values are indicated as calculated by two-tailed Mann–Whitney-U test (**b, c**) or Wilcoxon matched-pairs signed rank test (**d, e**) and adjusted for multiple comparisons using a Benjamini & Hochberg correction: \**p* < 0.05, \*\**p* < 0.01, \*\*\**p* < 0.001, \*\*\*\**p* < 0.0001 (**b, c**). Time points after vaccination are indicated as T0 (baseline), T1 (1–2 weeks), T2 (3–5 weeks), T3 (12 weeks), and T4 (17–29 weeks) (**a, b, c**). *P* values and sample sizes are indicated in Supplementary Tables 10 and 4–8.

dependence on S-protein conformation. S1- and S2-specific T cells were induced at comparable frequencies in the control cohorts.

To evaluate whether previous MVA-S vaccination affected the resulting T cell response, we directly compared S-specific T cell frequencies at the peak time point after the first

mRNA vaccination in the MVA-S/mRNA (V3T1) and mRNA (V1T1) cohorts (Fig. 5f). The IFN- $\gamma$  T cell response was significantly higher in the MVA-S/mRNA cohort (MVA-S/mRNA = 213 SFC) than in the mRNA control cohort (mRNA = 74 SFC, *p* = 0.0211). When using MVA-ST as a third vaccination, a significant increase above baseline before third vaccination was only seen in the middle-dose group (*p* = 0.0093), with a higher fold-change compared to

the other dose groups (LD:mfc [SFC] = 1.1; MD:mfc [SFC] = 2.7; HD mfc [SFC] = 2.0) (Fig. 5g). Notably, the ability of MVA-ST to boost the T cell response was dependent on the baseline levels before the third vaccination, similar to the IgG response shown in Fig. 2e. A significant induction of the T cell response was only observed in participants with low baseline levels (*p* = 0.0012), in contrast to those with a high baseline (Fig. 5h).

#### Enhanced T cell polyfunctionality after previous MVA-S immunization

The polyfunctionality of S-specific memory T cells was assessed 3–5 weeks after two-dose mRNA vaccination, corresponding to V3

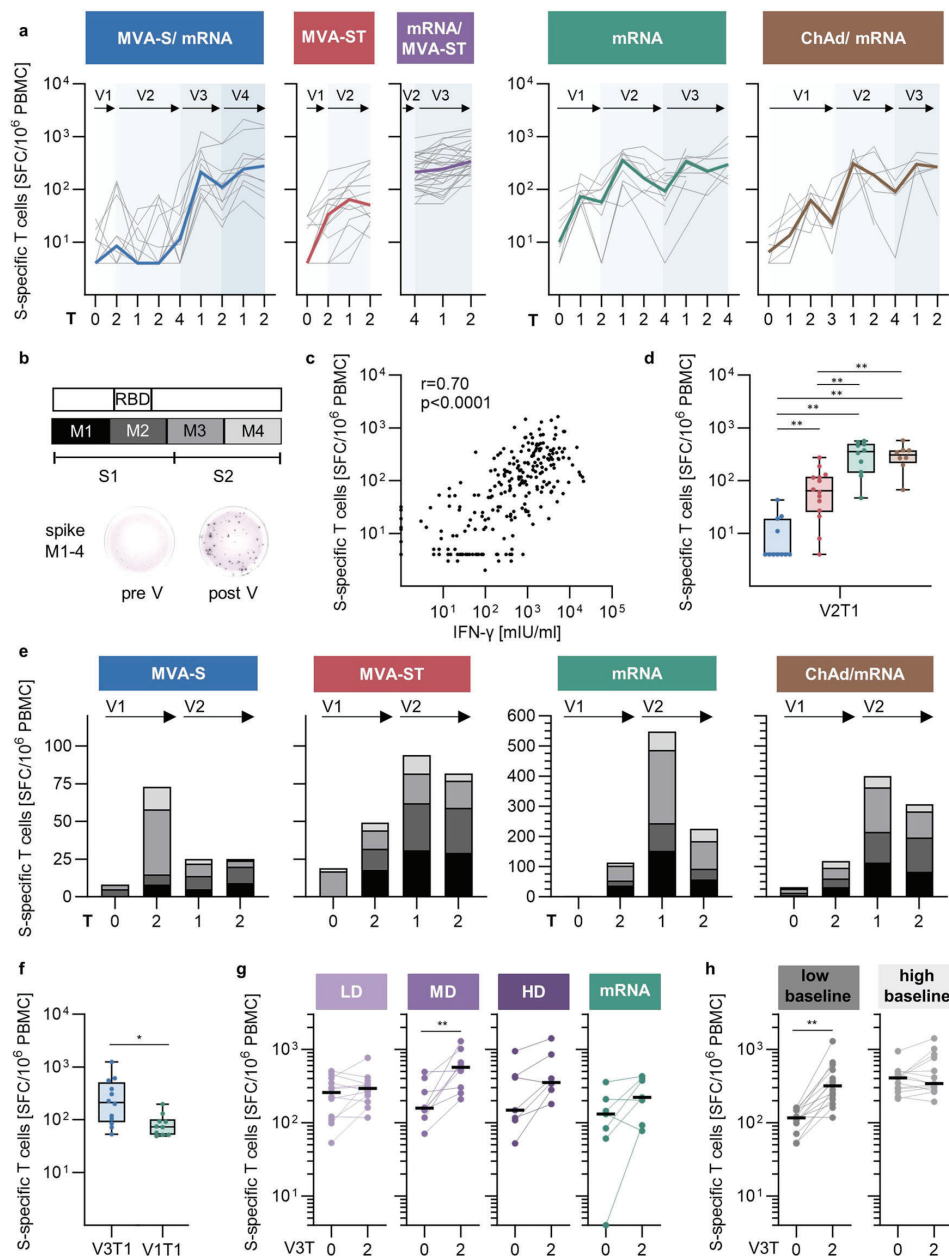


**Fig. 5** Longitudinal analysis of S1/S2-specific T cell responses induced by MVA-S and MVA-ST immunization. **a** Frequencies of IFN- $\gamma$ -producing T cells (SFC/10<sup>6</sup> PBMCs; mean of technical triplicates) measured by ELISpot. Colored lines depict median responses, gray lines show the dynamics of individual participants. **b** Schematic of the peptide pools M1-4 resembling the spike S1 and S2. Representative ELISpot wells pre (left) and post vaccination (right). **c** Spearman correlation of ELISpot and IFN- $\gamma$  release assay. T cell response induced by two doses MVA-S (blue) or MVA-ST (red) at (d) V2T1 or (e) against individual peptide pools M1-M4 compared to the control cohorts (green and brown). **f** T cell responses after first mRNA vaccination in the MVA-S/mRNA cohort (blue; V3T1) compared to the mRNA control cohort (green; V1T1). T cell responses induced by third vaccination with MVA-ST divided into (g) dose groups (LD = low dose, MD = middle dose, HD = high dose) compared to mRNA (green) or by (h) low ( $\leq$  median V3T0; left) and high baseline ( $>$  median V3T0; right). Data are represented as median  $\pm$  IQR (d, f), sum of medians (e), or individual data points and median (g, h). Significant  $p$  values are indicated as calculated by two-tailed Mann-Whitney  $U$  test (d, f) or Wilcoxon matched-pairs signed rank test (g, h) and adjusted for multiple comparisons using a Benjamini & Hochberg correction: \* $p < 0.05$ , \*\* $p < 0.01$ , \*\*\* $p < 0.001$ , \*\*\*\* $p < 0.0001$ . Time points after vaccination are indicated as T0 (baseline), T1 (1–2 weeks), T2 (3–5 weeks), T3 (12 weeks), and T4 (17–29 weeks) (a, d, e, f, g, h).  $P$  values and sample sizes are indicated in Supplementary Tables 11 and 4–8.

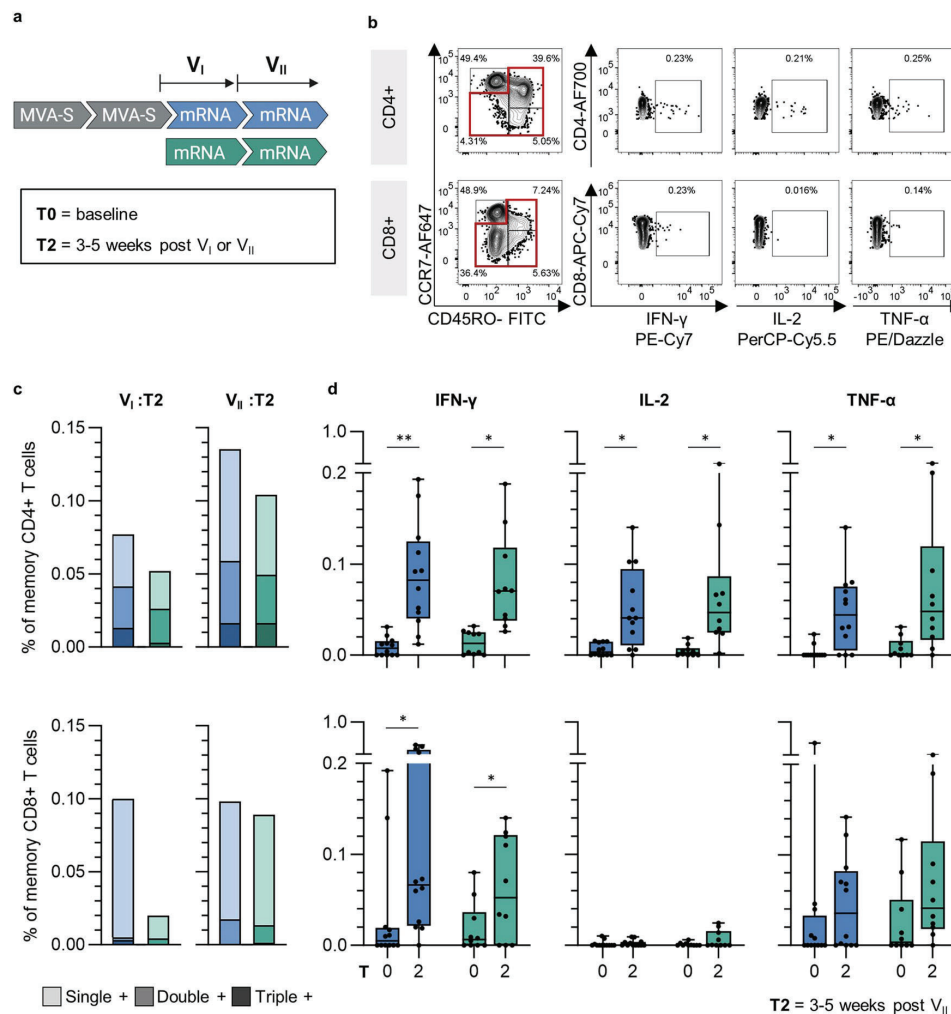


**Fig. 6 Enhanced T cell polyfunctionality after previous MVA-S immunization.** **a** Analyzed study cohorts and time points: MVA-S/mRNA (blue) and mRNA (green) were analyzed at baseline (T0) and time points after first and second vaccination with licensed mRNA vaccines, referred to as  $V_I$  and  $V_{II}$  (T2). **b** Representative gating strategy of cytokine-secreting CD4<sup>+</sup> (top) and CD8<sup>+</sup> (bottom) memory T cells after stimulation with overlapping peptide pools covering the S-protein. **c** Median frequencies of single positive (IFN- $\gamma$ <sup>+</sup> or IL-2<sup>+</sup> or TNF- $\alpha$ <sup>+</sup>), double positive (IFN- $\gamma$ <sup>+</sup> IL-2<sup>+</sup> TNF- $\alpha$ <sup>+</sup> or IFN- $\gamma$ <sup>+</sup> IL-2<sup>+</sup> TNF- $\alpha$ <sup>+</sup> or IFN- $\gamma$ <sup>+</sup> IL-2<sup>+</sup> TNF- $\alpha$ <sup>+</sup>), and triple positive (IFN- $\gamma$ <sup>+</sup> IL-2<sup>+</sup> TNF- $\alpha$ <sup>+</sup>) T cells out of total CD4<sup>+</sup> (top) and CD8<sup>+</sup> (bottom) memory T cells. Results were obtained by Boolean gating of the cytokine gates shown in **(b)**. **d** Frequencies of IFN- $\gamma$ , IL-2, and TNF- $\alpha$ -positive T cells out of total CD4<sup>+</sup> (top) and CD8<sup>+</sup> (bottom) memory T cells at baseline and time point T2 post  $V_I$  and  $V_{II}$ . Data are represented as individual data points and median  $\pm$  IQR. Significant *p* values are indicated as calculated by two-tailed Wilcoxon matched-pairs signed rank test and adjusted for multiple comparisons using a Benjamini & Hochberg correction: \**p* < 0.05, \*\**p* < 0.01, \*\*\**p* < 0.001, \*\*\*\**p* < 0.0001. *P* values and sample sizes are indicated in Supplementary Tables 12 and 4–8.

and V4 in the MVA-S/mRNA cohort and V1 and V2 in the mRNA cohort, respectively (Fig. 6a). Intracellular cytokine staining was used to analyze the production of IFN- $\gamma$ , interleukin-2 (IL-2) and tumor necrosis factor alpha (TNF- $\alpha$ ) by CD4<sup>+</sup> and CD8<sup>+</sup> T cells (gating is shown in Fig. 6b and Supplementary Fig. 4).

The median frequency (mfr) of total cytokine-producing CD4<sup>+</sup> T cells was highest in the MVA-S/mRNA cohort, both after the first and second mRNA vaccinations (Fig. 6c). The mfr of polyfunctional CD4<sup>+</sup> memory T cells expressing all three cytokines was also higher in the MVA-S/mRNA cohort than the mRNA cohort after the first mRNA vaccination (MVA-S/mRNA: mfr = 0.013%; mRNA: mfr = 0.003%) and comparable between both cohorts post second

mRNA vaccination (MVA-S/mRNA: mfr = 0.017%; mRNA: mfr = 0.017%). IFN- $\gamma$ , IL-2- and TNF- $\alpha$ -producing CD4<sup>+</sup> memory T cells were significantly above baseline in both cohorts (Fig. 6d).

The S-specific cytokine-producing CD8<sup>+</sup> memory T cell response was less pronounced than the CD4<sup>+</sup> response. The memory CD8<sup>+</sup> T cell response was dominated by cells expressing a single cytokine, with a low frequency of polyfunctional CD8<sup>+</sup> cells in both cohorts (Fig. 6c). Notably, a higher mfr of total cytokine-producing CD8<sup>+</sup> memory T cells was observed already after the first mRNA vaccination in the MVA-S/mRNA cohort (mfr = 0.1%) compared to the mRNA cohort (mfr = 0.02%). A

significant induction of IFN- $\gamma$ -producing CD8<sup>+</sup> memory T cells was observed in the MVA-S/mRNA and mRNA cohorts (Fig. 6d).

Overall, our longitudinal analyses indicated that MVA-ST, which encodes the prefusion-stabilized S, is more immunogenic than MVA-S, which encodes the native S, in SARS-CoV-2 naïve individuals. Both vaccine candidates are less immunogenic than the licensed ChAd and mRNA vaccines. Detailed measurement of humoral and cellular immune parameters revealed a bias towards the S2 subunit after MVA-S vaccination, in contrast to a bias towards the S1 subunit after MVA-ST vaccination, which is reflected in the IgG, B cell, and T cell responses. Despite the lower immunogenicity of MVA-S alone, it showed a recall response of the humoral response and polyfunctional T cells upon subsequent mRNA vaccination.

## DISCUSSION

The recent COVID-19 pandemic has led to unprecedented global efforts toward vaccine development. Several vaccine candidates have been licensed, and a multitude of vaccine candidates are still in different stages of development. Here, we report a comparative study of two rMVA-based vaccine candidates that were tested as primary immunization series and as a booster vaccination in consecutive phase 1 first-in-human clinical trials. While the investigated vaccine candidates share identical rMVA viral vector backbones, MVA-S encodes the native S-protein, and MVA-ST was optimized to code for a prefusion-stabilized S-protein. Our comparative analysis of MVA-S and MVA-ST provided the opportunity to directly investigate the impact of different S-protein conformations on the vaccine-induced immune response in humans. Two key distinctions were observed: 1) MVA-ST was shown to be more immunogenic than MVA-S, but less immunogenic compared to licensed vaccines, and 2) a differential skewing of the humoral and cellular immune response towards the S1 and S2 subunits after rMVA-based vaccination was observed.

MVA-S and MVA-ST vaccination induced detectable S-specific immune responses, including IgG, B, and T cells, in seronegative individuals, but MVA-S was overall less immunogenic. An mRNA booster dose following two MVA-S vaccinations led to an early induction of S2-specific IgG and B cells, IFN- $\gamma$ -producing T cells and an overall higher frequency of polyfunctional T cells compared to the control cohort only vaccinated with mRNA. This observation may indicate a priming effect of MVA-S, resulting in a recall response of immune memory upon mRNA vaccination despite the low immunogenicity of MVA-S when administered alone. To date, clinical data from another MVA-based COVID-19 vaccine candidate have been published by Routhu et al. Their synthetic MVA-based vaccine candidate encoding a prefusion-stabilized S-protein similar to our MVA-ST, in combination with the nucleocapsid antigen, was tested as a prime-boost schedule in a phase 1 clinical trial<sup>30–32</sup>. Since different assays were used, immunogenicity cannot be compared directly to our studies. However, the early induction of a T cell response after the first dose and the subsequent induction of the humoral response after the second dose showed similar dynamics to those observed for our MVA-ST vaccine.

Analysis of the specificity of the immune response induced by MVA-S and MVA-ST revealed a differential bias towards the S1 and S2 subunits of the S-protein: Both MVA-S and MVA-ST increased the S2-specific IgG levels that were already detectable at baseline, possibly as a result of cross-reactive antibodies and memory cells from previous infections with common cold coronaviruses, as has been suggested previously<sup>33–35</sup>. In contrast, S1-specific IgG was elicited at significantly higher levels following MVA-ST vaccination. In line with this, the T cell response was also biased towards the S2 subunit by MVA-S and towards the S1 subunit by MVA-ST vaccination. A similar pattern was observed in preclinical rodent

studies. Even though S-specific seroconversion was reached in all mice regardless of MVA-S or MVA-ST vaccination, significantly lower S1-specific IgG titers were observed in the MVA-S-vaccinated group, whereas S2-specific titers were comparable<sup>12</sup>. These results are likely explained by the differential cell surface expression of native and prefusion-stabilized S-proteins, as shown in *in vitro* experiments<sup>12</sup>. Across all cohorts, serum neutralization capacity showed a stronger correlation with S1- compared to S2-specific IgG, in line with the previous finding that the RBD-containing S1 subunit is the main target of SARS-CoV-2 neutralizing antibodies<sup>36</sup>.

Based on this bias towards the S1 or S2 subunit, which is especially prominent in the IgG response, we studied the vaccine-induced IgG subclasses and epitope specificity in more detail. We observed induction of the pro-inflammatory and highly functional IgG1 and IgG3 subclasses against S1 and S2 in all cohorts, irrespective of vaccination scheme, which is in line with the results of licensed mRNA and ChAd vaccines and our own previous data for MVA-MERS-S<sup>14,37–39</sup>. In contrast, IgG2 and IgG4, both generally associated with low functional potency, were detectable only after the second mRNA dose in our control cohorts and not in the MVA cohorts. Similar observations were recently reported by Irgang et al.<sup>40</sup> The prolonged germinal center reaction described after mRNA vaccination may result in a continuous class switch recombination towards anti-inflammatory IgG4<sup>41,42</sup>. However, the clinical relevance of this phenomenon remains poorly understood and requires further investigation. We detected linear IgG epitopes that were predominantly localized outside of the receptor-binding domain (RBD) in the C-terminal part of the S1 subunit and along the S2 subunit across all study cohorts. Half of the identified immunogenic regions were recognized by more than one vaccine recipient. Notably, we identified an immunogenic region in the S2 domain (AA 763–853) that contains the epitope specificity (AA 814–826) of a recently described neutralizing antibody with pan-coronavirus reactivity<sup>43</sup>. We also revealed one immunogenic region in the C-terminal transmembrane domain of S2 (AA 1245–1273), which was only detected in the cohorts that had received at least one MVA vaccination. While the S1 subunit contains the RBD and has been shown to be the main target of SARS-CoV-2 neutralizing antibodies, antibodies targeting epitopes in the more conserved S2 subunit may contribute to the protection against SARS-CoV-2 variants and other human coronaviruses, especially if pre-existing cellular memory is present<sup>35,36,44</sup>. Whether the induction of functional IgG responses against immunogenic regions in the S2 subunit provides targets for pan-coronavirus vaccines needs to be evaluated in future studies.

In a comparative analysis with the mRNA and ChAd vaccines, our data suggest that neither rMVA-based candidate reached the immunogenicity elicited by these licensed vaccines. This is particularly interesting for the comparison of the viral vector-based vaccines as they show similar immunogenicity in pre-clinical models<sup>45</sup>. It could be hypothesized that the higher dose of ChAd ( $5 \times 10^{10}$  viral particles) but also the differential molecular mechanisms of the viral vectors may explain this differential immunogenicity. The MVA genome encodes for several immunomodulatory genes that inhibit innate immune pathways, which may dampen the adaptive immune response<sup>46,47</sup>. Combining viral vectors with mRNA-based vaccines in a heterologous prime-boost schedule may be advantageous in humans<sup>22</sup>. Indeed, Barros-Martins et al. showed that individuals who received a heterologous ChAd/mRNA vaccination compared to a homologous ChAd/ChAd schedule showed stronger antibody responses<sup>48</sup>. This may also apply to combining MVA-ST with an mRNA boost. Notably, the T cell response elicited by a two-dose MVA-ST vaccination was comparable in magnitude to that elicited by one dose of ChAd or mRNA vaccine. MVA-ST also induced similar T cell frequencies to mRNA when used as a third vaccination. The ability of the MVA platform to efficiently induce T cell responses has

been demonstrated for other rMVA-based vaccines<sup>49,50</sup>. Recent follow-up data from our MVA-MERS-S trial demonstrated that a third immunization up to 12 months after the primary vaccination series could enhance the magnitude and persistence of spike-specific antibodies and memory B cells<sup>14,15</sup>. Since the residual S-specific immune response from the two prior mRNA vaccinations negatively impacted the boosting capacity, regardless of the platform used, we were unable to measure the same late booster effect on the humoral response as seen in the MVA-MERS-S trial. The phenomenon of baseline dependency has been reported in observational studies of booster vaccinations using licensed vaccines against several pathogens<sup>51</sup>. Together, these data support the potential of using rMVA-based vaccines as booster vaccinations but also highlight the importance of an optimized time interval between immunizations and the advantage of heterologous vaccination schedules<sup>14,15,23</sup>.

The longitudinal blood sampling of each study participant represents a key strength of our study. However, the frequent blood sampling also limited the blood volume per sampling time point which made further analyses, such as deconvoluting the T cell response, not feasible. Another limitation of our study is the small size of some of the cohorts, resulting in a limited power of statistical tests. Nonetheless, the data reported in our manuscript provide a detailed longitudinal investigation of different vaccine regimens, yielding important insights into the impact of the platform, schedule, and antigen conformation on vaccine-induced immune responses. We showed that the immunogenicity of rMVA-based COVID-19 vaccine candidates in humans can be enhanced by conformational changes in the S-protein. Studies such as the one presented here add to a more comprehensive understanding of the strengths and limitations of rMVA vector technology in comparison to other vaccine platforms. However, critical knowledge gaps, such as the correlates of protection for rMVA-based vaccines, remain to be addressed. A phase 1 clinical study investigating MVA-SARS-ST administered by inhalation (ClinicalTrials.gov: NCT05226390) is currently ongoing and may yield critical insights into the safety and immunogenicity of MVA targeting the respiratory mucosal layer<sup>52</sup>.

## METHODS

### Vaccines

MVA-SARS-2-S (MVA-S) is a vaccine candidate based on rMVA, encoding the native full-length S-protein of SARS-CoV-2<sup>11</sup>. MVA-SARS-2-ST (MVA-ST) is an optimized version of MVA-S that encodes a pre-fusion-stabilized S protein with an inactivated S1/S2 furin cleavage site, as described by Natrup et al.<sup>12</sup>. BNT162b2 (Comirnaty) and mRNA-1273 (Spikevax), here referred to as mRNA, are licensed vaccines consisting of nucleoside-modified mRNA encoding the prefusion-stabilized S-protein, formulated in lipid-nanoparticles<sup>1,4</sup>. ChAdOx1 nCoV-19 Vaxzevria, herein referred to as ChAd, is a licensed vaccine based on the modified chimpanzee adenovirus ChAdOx1 vector, encoding the full-length S-protein and a tissue plasminogen activator leader sequence<sup>22</sup>.

### Study approval

The following phase 1 clinical trials were reviewed and approved by the National Competent Authority (Paul-Ehrlich-Institute, EudraCT numbers 2020-003875-16; 2021-000548-23) and the Ethics Committee of the Hamburg Medical Association (reference numbers 2020-10164-AMG-ff; 2021-100621-AMG-ff), conducted under the sponsorship of the University Medical Center Hamburg-Eppendorf (Hamburg, Germany) in accordance with ICH-GCP and the EU directives 2001/20/EC and 2001/83/EC, and are registered at ClinicalTrials.gov. (NCT04569383; NCT04895449). The Ethics Committee of the Hamburg Medical Association

approved the clinical study with licensed vaccines (reference number: 2020-10376-BO-ff). Written informed consent was obtained from all participants.

### Study design

NCT04569383 is a phase 1 clinical trial to evaluate the MVA-SARS-2-S vaccine candidate in 30 seronegative individuals divided into two ascending dose groups. Participants received two single injections 28 days apart, either a low dose of  $1 \times 10^7 \pm 0.5$  log IU ( $N = 15$ ) or a high dose of  $1 \times 10^8 \pm 0.5$  log IU ( $N = 15$ ). The MVA-S/mRNA cohort is a subgroup of this trial ( $N = 12$ ), which received two doses of the BNT162b2 vaccine 21 days apart, at least six months after the last MVA-SARS-2-S vaccination.

NCT04895449 is a phase 1b clinical trial to evaluate the MVA-SARS-2-ST vaccine candidate in seronegative individuals (Part A) and in individuals who had previously received two doses of the BNT162b2 vaccine (Part B). In Part A, participants received two single injections 28 days apart, either a low dose of  $1 \times 10^7 \pm 0.5$  log IU ( $N = 8$ ) or a middle dose of  $5 \times 10^7 \pm 0.5$  log IU ( $N = 7$ ). In Part B, participants received a single injection of low dose  $1 \times 10^7 \pm 0.5$  log IU ( $N = 12$ ), middle dose  $5 \times 10^7 \pm 0.5$  log IU ( $N = 10$ ), or high dose  $1 \times 10^8 \pm 0.5$  log IU ( $N = 8$ ) MVA-SARS-2-ST at least six months after their last BNT162b2 vaccination. Here, the MVA-ST cohort refers to Part A, whereas the mRNA/MVA-ST cohort refers to Part B of this study (Fig. 1A).

The mRNA and ChAd/mRNA study cohorts consisted of participants who received two doses of mRNA vaccine (21 or 28 days apart) or one dose ChAd plus one dose mRNA (84 days apart), respectively, and a booster vaccination of mRNA after six months. The studies were conducted at the University Medical Center Hamburg-Eppendorf.

### Exclusion criteria

For the phase 1 clinical trials testing the MVA-based vaccine candidates (MVA-S/mRNA; MVA-ST; mRNA/MVA-ST cohorts), SARS-CoV-2 exposure prior to the study was an exclusion criterion. Individuals with a positive SARS-CoV-2 PCR in medical history (MVA-S/mRNA; MVA-ST; mRNA/MVA-ST cohorts) and/or positive SARS-CoV-2 antibody test at screening day (MVA-S/mRNA; MVA-ST cohorts) were not included in the clinical trials. Additionally, active SARS-CoV-2 infection on screening day was excluded by PCR (MVA-S/mRNA) or antigen test followed by PCR if positive (MVA-ST; mRNA/MVA-ST). Participants of these phase 1 clinical trials were instructed to report clinical evidence of COVID-19-like symptoms to the study site per study protocol. In these cases, participants were diagnosed by SARS-CoV-2-specific PCR. Study participants who acquired a SARS-CoV-2 infection during the study were excluded from the immunogenicity analyses of this manuscript.

For the control cohorts (mRNA; ChAd/mRNA) only individuals without prior SARS-CoV-2 exposure (self-reported) were included. Upon inclusion, participants were instructed to report clinical evidence of COVID-19-like symptoms or positive SARS-CoV-2 antigen and/or PCR test results. If participants acquired a SARS-CoV-2 infection, immunogenicity time points thereafter were excluded from the analyses of this manuscript.

### Blood sampling

A total of 452 peripheral blood samples were obtained from 75 donors. The blood sample collection schedule and the number of samples for each individual are shown in Supplementary Fig. 1. Blood was collected at T0 (baseline before vaccination), T1 (1–2 weeks), T2 (3–5 weeks), T3 (12 weeks), and T4 (17–29 weeks) post vaccination. Weeks refers to the time since the last vaccination. The exact time intervals between vaccinations and blood collections are shown in Supplementary Tables 2 and 3.

### PBMC and plasma isolation

Whole blood was collected in EDTA vacutainers. After centrifugation, plasma was removed and stored at  $-80^{\circ}\text{C}$ . PBMCs were isolated by density-gradient centrifugation using Ficoll-Histopaque (Sigma) or SepMate™ (Stemcell), cryopreserved, and stored in liquid nitrogen. Serum was collected using Gel monovettes with clotting activators, and stored at  $-20^{\circ}\text{C}$ . Additionally, whole blood was collected in lithium heparin monovettes and used for the IGRA assay within 10 h after collection.

### Bead-based multiplex immunoassay

A bead-based multiplex immunoassay was used to separately measure plasma antibody isotypes and IgG subclasses directed against the S1 and S2 subunits of the SARS-CoV-2S-protein. For the detection of IgM, IgA and IgG isotypes, the MILLIPLEx® SARS-CoV-2 Antigen Panel 1 IgM/IgA/IgG kits (Merck KGaA) were used according to the manufacturer's instructions with adjusted concentrations of detection antibodies. Briefly, magnetic beads coated with SARS-CoV-2 S1 and S2 antigens were added to a black, clear-bottom 96 well plate for each isotype. Plasma samples were added at a final dilution of 1:600 and plates were incubated on a plate shaker at 650 rpm at room temperature (RT) for 2 h. After washing, 45  $\mu\text{l}$  of PE-anti-human IgG (#HC19-PEIGG), IgA (#HC19-PEIGA), or IgM (#HC19-PEIGM) conjugate was added to each well and incubated on a plate shaker at 650 rpm at RT for 1.5 h. After another washing step, the beads were resuspended in 150  $\mu\text{l}$  of sheath fluid per well and stored overnight at  $4^{\circ}\text{C}$ . The plates were analyzed the next day using a Bio-Plex™ 200 system. For the detection of IgG subclasses, the MILLIPLEx® SARS-CoV-2 Antigen Panel 1 IgG kit (Merck KGaA) was used as described above, but detection antibodies were substituted with PE-conjugated antibodies specific to IgG1-4 (#SBA-9052-09, #SBA-9070-09, #SBA-9210-09, #SBA-9200-09; SouthernBiotech), added at a concentration of 0.65  $\mu\text{g}/\text{ml}$  in 80  $\mu\text{l}$  per well. For each isotype and subclass, wells without plasma samples were measured as controls for non-specific background signals and subtracted from the measured sample values. MFI values less than 2 were set to 2. The results are shown as the mean of duplicate wells.

### SARS-CoV-2 VNT<sub>100</sub>

The serum neutralization capacity against SARS-CoV-2 was assessed by VNT<sub>100</sub> (virus neutralization test) as described previously<sup>53</sup>. Briefly, vaccinee serum samples were heat-inactivated for 30 min at  $56^{\circ}\text{C}$  and diluted in a two-fold dilution series (1:4–1:512) in 96-well cell culture plates, followed by addition of 100 plaque-forming units (PFU) of SARS-CoV-2 (German isolate BavPat1/2020; European Virus Archive Global #026 V-03883 (Genbank: MZ558051.1)). After 1 h of incubation at  $37^{\circ}\text{C}$ , 20,000 Vero C1008 cells (ATCC, Cat. no. CRL-1586, RRID: CVCL\_0574) were added. Cytopathic effects were evaluated at day 4 post infection. Neutralization was defined as the absence of cytopathic effects, and the reciprocal neutralization titer was calculated from the highest serum dilution without cytopathic effects as a geometric mean based on three replicates. The lower limit of detection is a reciprocal titer of 8, corresponding to the first dilution of the respective serum.

### IgG ELISpot assay

SARS-CoV-2 S-specific B cells were analyzed using IgG ELISpot. To activate antibody secretion from B cells, PBMCs at a concentration of  $2 \times 10^6/\text{ml}$  in R10 medium [RPMI 1640 (Sigma) supplemented with 10% fetal bovine serum (FBS) and 1% streptomycin/penicillin] containing 1% HEPES (Thermo Fisher Scientific), were stimulated with 0.5  $\mu\text{g}/\text{ml}$  Resiquimod (R848, Mabtech) and 5 ng/ml interleukin-2 (IL-2, Mabtech) for  $75 \pm 1$  h at  $37^{\circ}\text{C}$  and 5%  $\text{CO}_2$ .

PVDF-MultiScreen-IP plates (Millipore) were treated with 35% ethanol and coated with anti-IgG capture antibody (15  $\mu\text{g}/\text{ml}$ ; #3850-2 A; Mabtech). After blocking with R10 containing 1% HEPES, pre-stimulated PBMCs were added to the wells at different concentrations and incubated for 16 h at  $37^{\circ}\text{C}$  and 5%  $\text{CO}_2$ . For the positive control (total IgG-secreting B cells),  $1 \times 10^4$  PBMCs were added per well, whereas numbers between  $1 \times 10^4$  and  $8 \times 10^5$  cells were used for the antigen-specific assay, depending on the time point post-vaccination. Biotinylated SARS-CoV-2 S-protein S1 or S2 subunit (S1: 0.1  $\mu\text{g}/\text{ml}$ , S2: 0.2  $\mu\text{g}/\text{ml}$ ; SinoBiological) and anti-IgG detection antibody (1  $\mu\text{g}/\text{ml}$ ; #3850-2A; Mabtech) were added to detect antigen-specific and total IgG-secreting B cells, respectively. For spot development, streptavidin-ALP and BCIP/NBT-plus substrate solutions (Mabtech) were used according to the manufacturer's protocol. The plates were analyzed using an AID ELISpot Reader System (AID GmbH). All samples were measured in duplicate and the mean was used for further analysis. Results below the LLOD (2 SFC/ $10^6$  PBMCs) were set to 1 SFC/ $10^6$  PBMCs.

### Peptide microarrays

To identify linear B cell epitopes in the S protein, we screened the sera of study participants using high-density peptide microarrays as described in<sup>54</sup>. The sequence of the SARS-CoV-2S protein (GenBank ID: MN908947.3) consisting of 1273 AA was mapped as a total of 634 overlapping 15-mer peptides with a lateral shift of two AA on peptide microarrays obtained from PEPperPRINT GmbH (Heidelberg, Germany). Serum samples were incubated on the arrays at 1:200 dilution, and IgG antibody interactions were then detected with fluorescently labeled secondary antibodies and quantified in arbitrary fluorescence units (AFU). Epitope binding was defined as positive if the mean AFU of three successive peptides was higher than 400 and 2.5-fold above the baseline before vaccination (if available).

### IFN- $\gamma$ ELISpot assay

SARS-CoV-2 S-specific T cells were analyzed using the Human IFN- $\gamma$  ELISpotPLUS (ALP) kit (Mabtech). After overnight resting in R10 containing 1% HEPES, PBMCs were seeded at  $1.25 \times 10^5$  cells/well in PVDF-MultiScreen-IP plates, pre-coated with anti-IFN- $\gamma$ -mAb 1-D1K (#34206; Mabtech). Cells were then stimulated with a peptide pool (15-mers overlapping by 11 amino acids; Supplementary Data 2) spanning the SARS-CoV-2 S protein sequence (GenBank ID: MN908947.3) (2.5  $\mu\text{g}/\text{ml}$  in 0.1% dimethyl sulfoxide (DMSO); JPT Peptide Technologies) for 16 h at  $37^{\circ}\text{C}$  and 5%  $\text{CO}_2$ . An equimolar concentration of DMSO was used as a negative control. Phytohemagglutinin (PHA) (1  $\mu\text{g}/\text{ml}$ ; Sigma) and CMV/EBV/Influenza (CEF) peptide pool (2  $\mu\text{g}/\text{ml}$ ; JPT Peptide Technologies) were used as positive control stimulations. Plates were then incubated with biotinylated anti-IFN- $\gamma$  (1  $\mu\text{g}/\text{ml}$  in PBS-0.5% FCS; clone mAb-7B6-1; #331010; Mabtech) for 2 h, followed by streptavidin-ALP (1:1000 in PBS-0.5% FCS; Mabtech) for 1 h at room temperature. Plates were developed using a substrate solution (BCIP/NBT; Mabtech). Spots were counted using an AID ELISpot Reader System (AID GmbH). Results are reported as spot-forming cells (SFC) per million PBMCs, calculated by subtracting the mean count of triplicate negative control wells from the mean count of duplicate peptide-stimulated wells. Results were normalized to the total reactive T cells of each participant, using PHA stimulation as a positive control. Results below the LLOD (8 SFC/ $10^6$  PBMCs) were set to 4 SFC/ $10^6$  PBMCs.

### IFN- $\gamma$ release T cell assay

IFN- $\gamma$  secretion by S-specific T cells was analyzed in whole blood using a commercial, standardized IFN- $\gamma$  release T cell assay (ET 2606-3003, Euroimmun, Lübeck, Germany). After a 20- to 24-h

stimulation, IFN- $\gamma$  was measured in the plasma using an IFN- $\gamma$  ELISA (EQ 6841-9601, Euroimmun, Lübeck, Germany) according to the manufacturer's instructions. IFN- $\gamma$  secretion was quantified using a 5PL sigmoidal standard curve, and data are shown as background subtracted concentrations using an unstimulated control for each sample. Samples outside the standard curve were repeated at higher dilutions.

#### Intracellular cytokine staining (ICS) assay

After overnight resting, PBMCs were stimulated with 5 peptides (2.5  $\mu$ g/ml) for 7 h at 37 °C in the presence of Golgi-Plug, Golgi-Stop, and anti-CD28/CD49 (1:100; #9035982; BD Biosciences) in 96-well V-bottom plates (Sarstedt). For each sample, cells incubated with an equimolar amount of DMSO (0.1%) and Phorbol-12-myristate-13-acetate (50 ng/ml), and ionomycin (0.5  $\mu$ g/ml) served as negative and positive controls, respectively. Cells were then washed and stained with an antibody mix of anti-CD3-BUV395 (1:100; #564001; BD Biosciences), anti-CD4-AF700 (1:50; #300526; BioLegend), anti-CD19-BV510 (1:100; #302242; BioLegend), anti-CD14-BV510 (1:100; #301842; BioLegend), anti-CD8-APC-Cy7 (1:100; #344714; BioLegend), anti-CCR7-AF647 (1:50; #353218; BioLegend), anti-CD45RO-FITC (1:33; #304242; BioLegend), and Zombie Aqua™ Fixable Viability Kit (1:500; #423101; BioLegend) in FACS buffer [PBS supplemented with 2% FBS and 2 mM EDTA] for 15 min at 37 °C. Subsequently, cells were fixed (eBioscience™), washed, and stained with intracellular markers anti-IFN- $\gamma$ -PE-Cy7 (1:50; #506518; BioLegend), anti-TNF- $\alpha$ -PE/Dazzle™ 594 (1:100; #50296; BioLegend) and IL-2-PerCP-Cy5.5 (1:25; #500322, BioLegend) in PERM buffer (eBioscience™) at RT for 15 min. Samples were stored in FACS buffer at 4 °C and analyzed on the BD Fortessa the following day. A representative gating strategy is shown in Supplementary Fig. 4. Cytokine-secreting memory T cells were identified by excluding CCR7<sup>+</sup>/CD45RO<sup>-</sup> naïve T cells and then gating the individual cytokines on CD4<sup>+</sup> and CD8<sup>+</sup> T cells separately. Results are shown as background (DMSO) subtracted data (Fig. 6). Multifunctional profiles were identified by Boolean gating. Results of the Boolean gates were summed for each sample, based on the number of functions.

#### Statistical analysis

Statistical testing was performed based on R (v4.2.0), using nonparametric tests due to the small sample sizes per cohort. Two-tailed Wilcoxon matched-pairs signed rank test and Mann-Whitney *U* test were used for testing paired and unpaired samples, respectively, as indicated in Supplementary Tables 9–12. The calculated *p*-values were adjusted for multiple comparisons within each figure using the Benjamini & Hochberg correction. Due to the small numbers of study participants per cohort, and the different sample sizes per group, *p*-values have to be interpreted with caution. Correlations were calculated with GraphPad Prism software (v9.5.1) using non-parametric Spearman's correlation. The significance level for all statistical tests was set to 0.05. Analysis of flow cytometry data was done using FlowJo (v.10.8.1). Figures were created using GraphPad Prism (v9.5.1), R (v4.2.0), and BioRender.com. The sample size for each analysis is listed in Supplementary Tables 4–8.

#### Reporting summary

Further information on research design is available in the Nature Research Reporting Summary linked to this article.

#### DATA AVAILABILITY

The datasets used and/or analyzed during the current study are available from the corresponding author upon reasonable request.

#### REFERENCES

- Polack, F. P. et al. Safety and efficacy of the BNT162b2 mRNA Covid-19 Vaccine. *N. Engl. J. Med.* **383**, 2603–2615 (2020).
- Voysey, M. et al. Safety and efficacy of the ChAdOx1 nCoV-19 vaccine (AZD1222) against SARS-CoV-2: an interim analysis of four randomised controlled trials in Brazil, South Africa, and the UK. *Lancet* **397**, 10269 (2020).
- Watson, O. J. et al. Global impact of the first year of COVID-19 vaccination: a mathematical modelling study. *Lancet Infect. Dis.* **22**, 1293–1302 (2022).
- Baden, L. R. et al. Efficacy and safety of the mRNA-1273 SARS-CoV-2 vaccine. *N. Engl. J. Med.* **384.5**, 403–416 (2020).
- van Riel, D. & de Wit, E. Next-generation vaccine platforms for COVID-19. *Nat. Mater.* **19**, 810–812 (2020).
- Jordan, E. et al. Broad antibody and cellular immune response from a phase 2 clinical trial with a novel multivalent poxvirus-based respiratory syncytial virus vaccine. *J. Infect. Dis.* **223**, 1062–1072 (2021).
- Jordan, E. et al. Reduced respiratory syncytial virus load, symptoms, and infections: a human challenge trial of MVA-BN-RSV Vaccine. *J. Infect. Dis.* **108**; <https://doi.org/10.1093/infdis/jiad108> (2023).
- Woolsey, C. & Geisbert, T. W. Current state of Ebola virus vaccines: a snapshot. *PLoS Pathog.* **17**, e1010078 (2021).
- Volz, A. & Sutter, G. Modified vaccinia virus Ankara: history, value in basic research, and current perspectives for vaccine development. *Adv. Virus Res.* **97**, 187–243 (2017).
- Volkman, A. et al. The Brighton Collaboration standardized template for collection of key information for risk/benefit assessment of a Modified Vaccinia Ankara (MVA) vaccine platform. *Vaccine* **39**, 3067–3080 (2021).
- Tscherne, A. et al. Immunogenicity and efficacy of the COVID-19 candidate vector vaccine MVA-SARS-2-S in preclinical vaccination. *Proc. Natl Acad. Sci. USA* **118**, e2026207118 (2021).
- Meyer zu Natrup, C. et al. Stabilized recombinant SARS-CoV-2 spike antigen enhances vaccine immunogenicity and protective capacity. *J. Clin. Investig.* **132**, e159895 (2022).
- Koch, T. et al. Safety and immunogenicity of a modified vaccinia virus Ankara vector vaccine candidate for Middle East respiratory syndrome: an open-label, phase 1 trial. *Lancet Infect. Dis.* **20**, 827–838 (2020).
- Weskamm, L. M. et al. Persistence of MERS-CoV-spike-specific B cells and antibodies after late third immunization with the MVA-MERS-S vaccine. *Cell. Rep. Med.* **3**, 100685 (2022).
- Fathi, A. et al. Increased neutralization and IgG epitope identification after MVA-MERS-S booster vaccination against Middle East respiratory syndrome. *Nat. Commun.* **13**, 4182 (2022).
- Li, F. Structure, function, and evolution of coronavirus spike proteins. *Annu. Rev. Virol.* **3**, 237–261 (2016).
- Song, F. et al. Middle East respiratory syndrome coronavirus spike protein delivered by modified vaccinia virus Ankara efficiently induces virus-neutralizing antibodies. *J. Virol.* **87**, 11950–11954 (2013).
- Du, L. et al. The spike protein of SARS-CoV-a target for vaccine and therapeutic development. *Nat. Rev. Microbiol.* **7**, 226–236 (2009).
- Jackson, L. A. et al. An mRNA vaccine against SARS-CoV-2—preliminary report. *N. Engl. J. Med.* **383**, 1920–1931 (2020).
- Vogel, A. B. et al. BNT162b vaccines protect rhesus macaques from SARS-CoV-2. *Nature* **592**, 283–289 (2021).
- Wrapp, D. et al. Cryo-EM structure of the 2019-nCoV spike in the prefusion conformation. *Science* **367**, 1260–1263 (2020).
- Folegatti, P. M. et al. Safety and immunogenicity of the ChAdOx1 nCoV-19 vaccine against SARS-CoV-2: a preliminary report of a phase 1/2, single-blind, randomised controlled trial. *Lancet* **396**, 467–478 (2020).
- Voysey, M. et al. Single-dose administration and the influence of the timing of the booster dose on immunogenicity and efficacy of ChAdOx1 nCoV-19 (AZD1222) vaccine: a pooled analysis of four randomised trials. *Lancet* **397**, 881–891 (2021).
- Gilbert, P. B. et al. Immune correlates analysis of the mRNA-1273 COVID-19 vaccine efficacy clinical trial. *Science* **375**, 43–50 (2022).
- Khoury, D. S. et al. Neutralizing antibody levels are highly predictive of immune protection from symptomatic SARS-CoV-2 infection. *Nat. Med.* **27**, 1205–1211 (2021).
- Siegrist, C.-A. Vaccine immunology. *Vaccines* (2008).
- Palm, A.-K. E. & Henry, C. Remembrance of things past: long-term b cell memory after infection and vaccination. *Front. Immunol.* **10**, 1787 (2019).
- Akkaya, M., Kwak, K. & Pierce, S. K. B cell memory: building two walls of protection against pathogens. *Nat. Rev. Immunol.* **20**, 229–238 (2020).



29. Bertoletti, A., Le Bert, N., Qui, M. & Tan, A. T. SARS-CoV-2-specific T cells in infection and vaccination. *Cell Mol. Immunol.* **18**, 2307–2312 (2021).
30. Routhu, N. K. et al. A modified vaccinia Ankara vector-based vaccine protects macaques from SARS-CoV-2 infection, immune pathology, and dysfunction in the lungs. *Immunity* **54**, 542–556.e9 (2021).
31. Routhu, N. K. et al. A modified vaccinia Ankara vaccine expressing spike and nucleocapsid protects rhesus macaques against SARS-CoV-2 Delta infection. *Sci. Immunol.* **7**, eabo0226 (2022).
32. Chiappesi, F. et al. Safety and immunogenicity of a synthetic multiantigen modified vaccinia virus Ankara-based COVID-19 vaccine (COH0451): an open-label and randomised, phase 1 trial. *Lancet Microbe* **3**, e252–e264 (2022).
33. Khan, S. et al. Analysis of serologic cross-reactivity between common human coronaviruses and SARS-CoV-2 using coronavirus antigen microarray. Preprint at [<https://www.biorxiv.org/content/10.1101/2020.03.24.006544v1>] (2020).
34. Nguyen-Contant, P. et al. S protein-reactive IgG and memory B cell production after human SARS-CoV-2 infection includes broad reactivity to the S2 subunit. *mBio* **11**, e01991–20 (2020).
35. Loyal, L. et al. Cross-reactive CD4+ T cells enhance SARS-CoV-2 immune responses upon infection and vaccination. *Science* **374**, eabh1823 (2021).
36. Amanat, F. et al. SARS-CoV-2 mRNA vaccination induces functionally diverse antibodies to NTD, RBD, and S2. *Cell* **184**, 3936–3948.e10 (2021).
37. Farkash, I. et al. Anti-SARS-CoV-2 antibodies elicited by COVID-19 mRNA vaccine exhibit a unique glycosylation pattern. *Cell. Rep.* **37**, 110114 (2021).
38. Tejedor Vaquero, S. et al. The mRNA-1273 vaccine induces cross-variant antibody responses to SARS-CoV-2 with distinct profiles in individuals with or without pre-existing immunity. *Front. Immunol.* **12**, 737083 (2021).
39. Barrett, J. R. et al. Phase 1/2 trial of SARS-CoV-2 vaccine ChAdOx1 nCoV-19 with a booster dose induces multifunctional antibody responses. *Nat. Med.* **27**, 279–288 (2021).
40. Irrgang, P. et al. Class switch toward noninflammatory, spike-specific IgG4 antibodies after repeated SARS-CoV-2 mRNA vaccination. *Sci. Immunol.* **8**, eade2798 (2023).
41. Kim, W. et al. Germinal centre-driven maturation of B cell response to mRNA vaccination. *Nature* **604**, 141–145 (2022).
42. Jeannin, P., Lecoanet, S., Delneste, Y., Gauchat, J. F. & Bonnefoy, J. Y. IgE versus IgG4 production can be differentially regulated by IL-10. *J. Immunol.* **160**, 3555–3561 (1998).
43. Sun, X. et al. Neutralization mechanism of a human antibody with pan-coronavirus reactivity including SARS-CoV-2. *Nat. Microbiol.* **7**, 1063–1074 (2022).
44. Ng, K. W. et al. SARS-CoV-2 S2-targeted vaccination elicits broadly neutralizing antibodies. *Sci. Transl. Med.* **14**, eabn3715 (2022).
45. van Doremalen, N. et al. ChAdOx1 nCoV-19 vaccine prevents SARS-CoV-2 pneumonia in rhesus macaques. *Nature* **586**, 578–582 (2020).
46. Hornemann, S. et al. Replication of modified vaccinia virus ankara in primary chicken embryo fibroblasts requires expression of the interferon resistance gene E3L. *J. Virol.* **77**, 8394–407 (2003).
47. Kaynarcalidan, O., Moreno Mascarague, S. & Drexler, I. Vaccinia virus: from crude smallpox vaccines to elaborate viral vector vaccine design. *Biomedicines* **9**, 1780 (2021).
48. Barros-Martins, J. et al. Immune responses against SARS-CoV-2 variants after heterologous and homologous ChAdOx1 nCoV-19/BNT162b2 vaccination. *Nat. Med.* **27**, 1525–1529 (2021).
49. Ewer, K. J. et al. Protective CD8+ T-cell immunity to human malaria induced by chimpanzee adenovirus-MVA immunisation. *Nat. Commun.* **4**, 2836 (2013).
50. Precopio, M. L. et al. Immunization with vaccinia virus induces polyfunctional and phenotypically distinctive CD8+ T cell responses. *J. Exp. Med.* **204**, 1405–1416 (2007).
51. Das, S. et al. Pre-existing antibody levels negatively correlate with antibody titers after a single dose of BBV152 vaccination. *Nat. Commun.* **13**, 3451 (2022).
52. Bošnjak, B. et al. Intranasal delivery of MVA vector vaccine induces effective pulmonary immunity against SARS-CoV-2 in rodents. *Front. Immunol.* **12**, 772240 (2021).
53. Romero-Olmedo, A. J. et al. Induction of robust cellular and humoral immunity against SARS-CoV-2 after a third dose of BNT162b2 vaccine in previously unresponsive older adults. *Nat. Microbiol.* **7**, 195–199 (2022).
54. Heidepriem, J. et al. Longitudinal development of antibody responses in COVID-19 patients of different severity with ELISA, peptide, and glycan arrays: an immunological case series. *Pathogens* **10**, 438 (2021).

## ACKNOWLEDGEMENTS

We thank all volunteers for their engagement in these vaccine studies, specifically under the challenging participating conditions of the COVID-19 pandemic, and their commitment and dedication to research against emerging coronaviruses. We would also like to express our sincere gratitude to all trial center members for their extraordinary work (Clinical Trial Center North GmbH & Co. KG, Hamburg), especially Laura Kaltenberg. We also thank Thomas Brehm for providing additional PBMC and plasma samples, and Jolanda Mezzacapo for her support in generating the VNT data. We dedicate this manuscript to Prof. Gerd Sutter who passed away on Oct 31st, 2023, and thank him for his great contribution. This work was funded by the German Center for Infection Research (DZIF Thematic Translational Unit [TTU] 01.924, TTU 01.921, TTU 01.709, TTU 01.702, TI 07.001\_Mellinghoff, the German Federal Ministry of Education and Research (BMBF), grant number 13XP5050A, and the MPG-FhG cooperation (Glyco3Display). The funder played no role in study design, data collection, analysis and interpretation of data, or the writing of this manuscript.

## AUTHOR CONTRIBUTIONS

Conceptualization, M.M.A., S.Be., G.S., A.F., C.D., S.C.M., A.V., S.Bo.; Methodology, L.M., L.M.W., C.D., J.H., F.F.L., V.K.; Investigation, L.M., L.M.W., M.K., M.L.L., J.H., V.K., A.F., MVA-SARS-2 Study Group; Formal analysis and visualization, L.M., L.M.W.; Writing – original draft, L.M., L.M.W., C.D.; Writing – review and editing, L.M., L.M.W., C.D., M.M.A., A.F., S.C.M., J.H., F.F.L., S.H., G.S., T.H., S.Bo., A.V., V.K.; Supervision, C.D., M.M.A.; Project administration, T.H., S.H., S.Bo.; L.M. and L.M.W. are co-first authors of this manuscript. G.S. passed away on Oct 31st, 2023, after the manuscript was submitted to npj vaccines. He was instrumental in the design, generation and pre-clinical evaluation of the MVA-based viral vector vaccines, as well as the conceptualization of the phase 1 clinical trials presented in this manuscript. He reviewed, edited, and approved the manuscript before submission.

## COMPETING INTERESTS

All authors declare no financial or non-financial competing interests.

## ADDITIONAL INFORMATION

**Supplementary information** The online version contains supplementary material available at <https://doi.org/10.1038/s41541-023-00801-z>.

**Correspondence** and requests for materials should be addressed to Leonie Mayer or Marilyn M. Addo.

**Reprints and permission information** is available at <http://www.nature.com/reprints>

**Publisher's note** Springer Nature remains neutral with regard to jurisdictional claims in published maps and institutional affiliations.



**Open Access** This article is licensed under a Creative Commons Attribution 4.0 International License, which permits use, sharing, adaptation, distribution and reproduction in any medium or format, as long as you give appropriate credit to the original author(s) and the source, provide a link to the Creative Commons license, and indicate if changes were made. The images or other third party material in this article are included in the article's Creative Commons license, unless indicated otherwise in a credit line to the material. If material is not included in the article's Creative Commons license and your intended use is not permitted by statutory regulation or exceeds the permitted use, you will need to obtain permission directly from the copyright holder. To view a copy of this license, visit <http://creativecommons.org/licenses/by/4.0/>.

© The Author(s) 2024

## Supplementary Information

### Supplementary Note 1 | Background and timeline of (pre-)clinical development of rMVA-based vaccines.

Upon the emergence of SARS-CoV-2 at the end of 2019 and its subsequent global spread in 2020, the MVA-SARS-2-S (MVA-S) vaccine candidate was constructed. The safety and efficacy of MVA-S were tested in a pre-clinical model, where BALB/c mice of two dose groups were vaccinated in a prime-boost regimen. Following booster immunization, S-binding serum IgG and neutralizing titers were induced in all animals. Additionally, robust, Th1-skewed, S-specific T cell responses were measured in both, the low and the high dose groups. Upon SARS-CoV-2 challenge, all animals were protected from lung damage in the absence of detectable infectious viruses in the lungs. These data illustrated preclinical safety and efficacy and provided evidence that MVA-S is a promising vaccine candidate for evaluation in humans <sup>1</sup>.

MVA-S then entered phase 1a of clinical evaluation (ClinicalTrials.gov: NCT04569383) in October 2020 to test the safety and immunogenicity of two ascending doses in healthy adults (MVA-S/mRNA cohort described in this manuscript). However, an interim analysis revealed that S-binding antibody titers were lower than expected, and only 33% of individuals reached seroconversion <sup>2</sup>. The clinical study was then amended such that participants received two doses of the (by then licensed) BNT162b2 mRNA vaccine at least six months after completion of the primary vaccination series with MVA-S. Safety and immunogenicity monitoring were continued.

Subsequently, an optimized vaccine candidate expressing the prefusion-stabilized S-protein, namely MVA-SARS-2-ST (MVA-ST) was constructed. MVA-ST was then tested in preclinical models for direct comparison with the MVA-S candidate. MVA-ST induced higher S-binding, RBD-specific, and neutralizing titers than MVA-S in mice. Analysis of antibody responses against the S1 and S2 subunits showed that MVA-S and MVA-ST induced comparable titers of S2-specific IgG. However, MVA-ST induced significantly higher S1-specific titers. Upon challenge, Syrian hamsters vaccinated with MVA-S or MVA-ST both showed no signs of clinical disease, but reduction of viral load was more pronounced in the MVA-ST-vaccinated group <sup>2</sup>.

Thus, MVA-ST entered phase 1b clinical evaluation (ClinicalTrials.gov: NCT04895449) in June 2021 to test the safety and immunogenicity of two ascending doses in healthy adults (MVA-ST cohort described in this manuscript). Due to the progression of the pandemic and the availability of licensed vaccines at that time, an additional group of previously SARS-CoV-2-vaccinated individuals (the mRNA/MVA-ST cohort described in this manuscript) was included in the trial, to test MVA-ST as a booster vaccination.

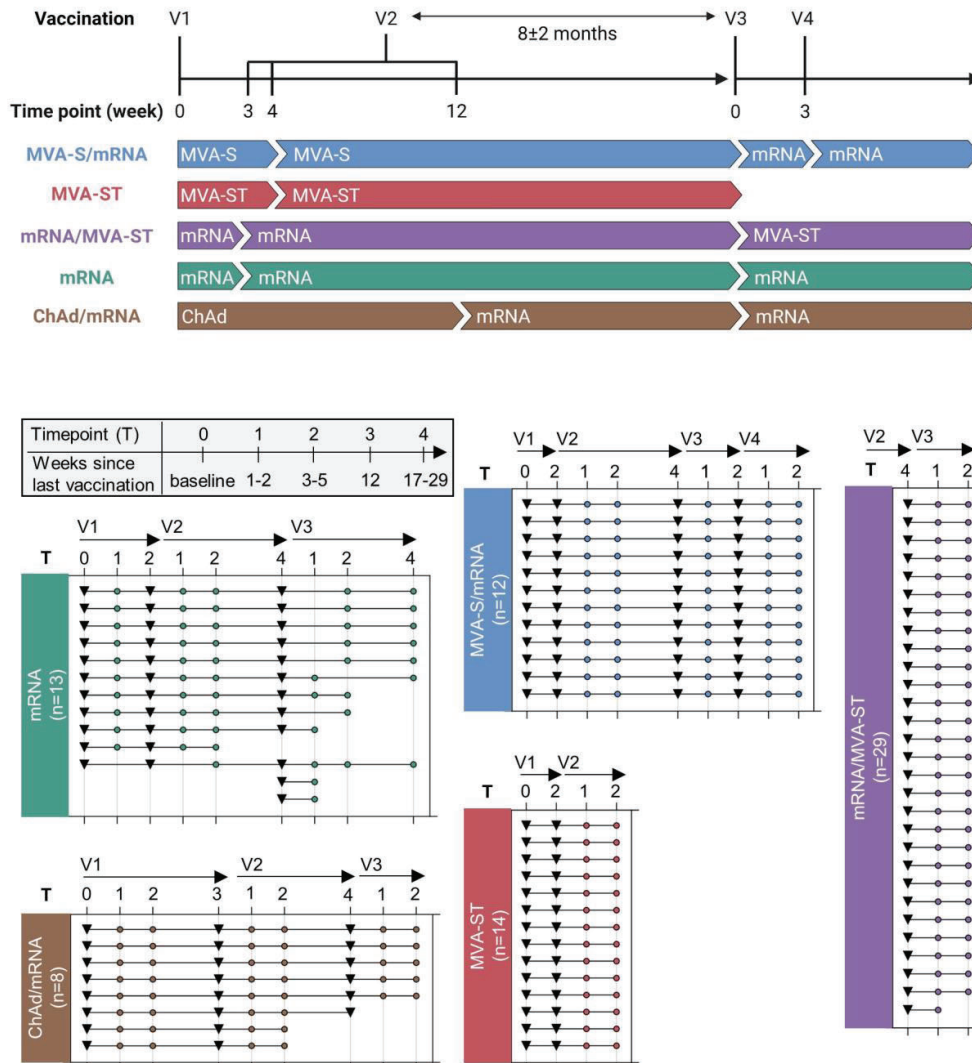
Because of this timeline, clinical studies were performed for both MVA-S and MVA-ST, providing the unique opportunity to directly compare the immunogenicity in humans of two vaccine candidates based on the same viral vector but different S-protein conformations (as described in this manuscript).

1. Tscherne, A. *et al.* Immunogenicity and efficacy of the COVID-19 candidate vector vaccine MVA-SARS-2-S in preclinical vaccination. *Proc. Natl. Acad. Sci. U. S. A.* **118**, e2026207118; doi: 10.1073/pnas.2026207118 (2021).
2. Meyer zu Natrup, C. *et al.* Stabilized recombinant SARS-CoV-2 spike antigen enhances vaccine immunogenicity and protective capacity. *J. Clin. Invest.* **132**, e159895; doi: 10.1172/JCI159895 (2022).

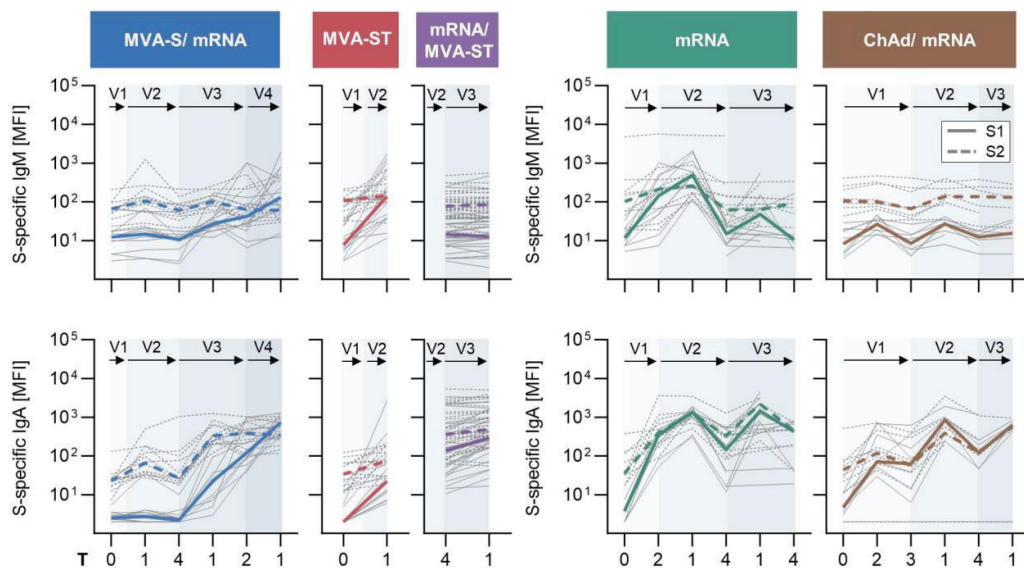
### Supplementary Note 2 | MVA-SARS-2 Study Group

Amelie Alberti, Marie-Louise Dieck, Stefanie Gräfe, Cordula Grüttner, Jana Kochmann, Niclas Renevier, Monika Rottstegge, Maren Sandkuhl, Claudia Schlesner, Yashin Simsek, Paulina Tarnow. All members of the MVA-SARS-2 Study Group are affiliated with the Institute for Infection Research and Vaccine Development (IIRVD) at the University Medical Center Hamburg-Eppendorf, the Department for Clinical Immunology of Infectious Diseases at the Bernhard Nocht Institute for Tropical Medicine (BNITM), and the German Centre for Infection Research (DZIF) partner site Hamburg-Lübeck-Borstel-Riems.

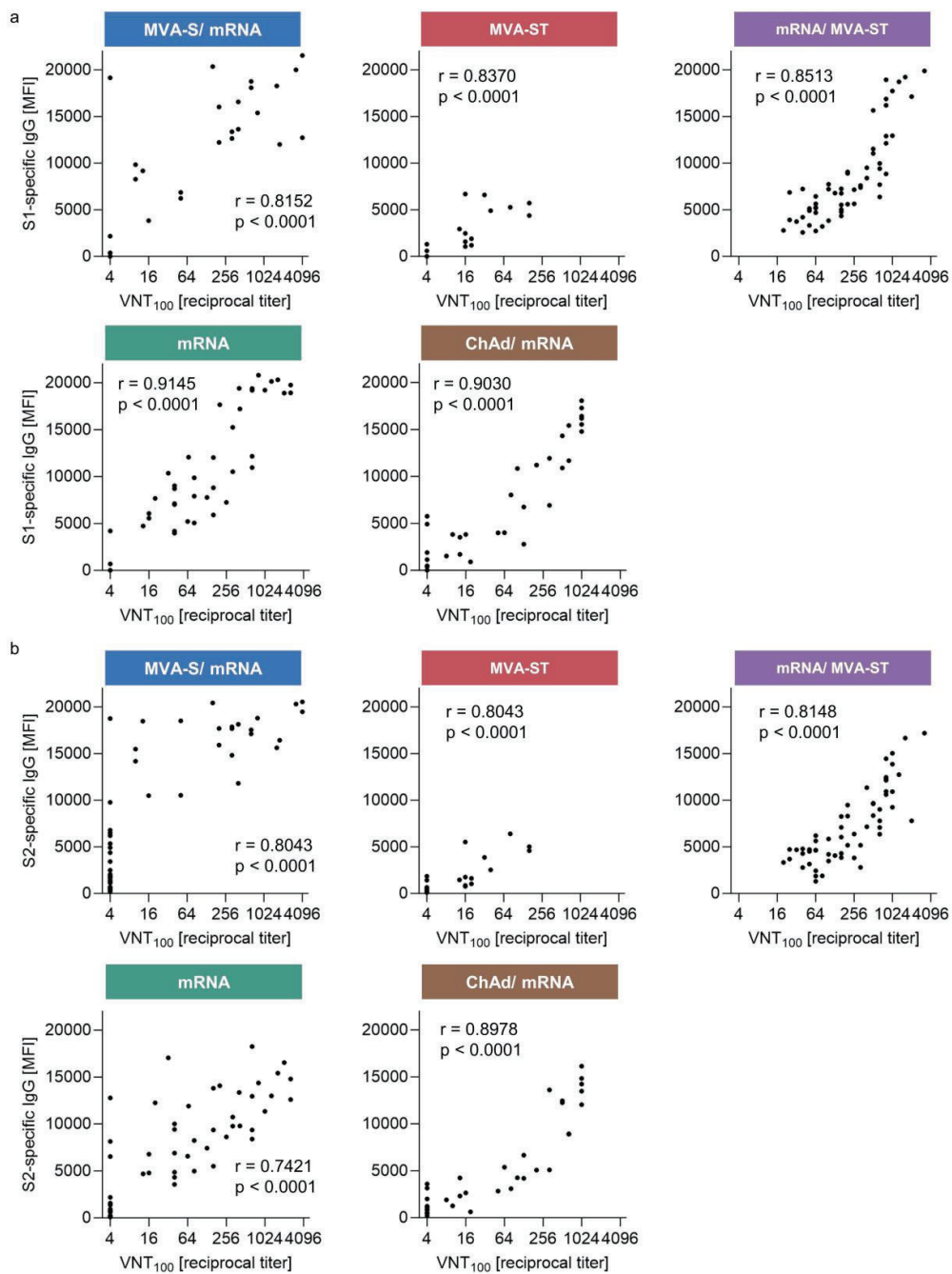
Supplementary Figures



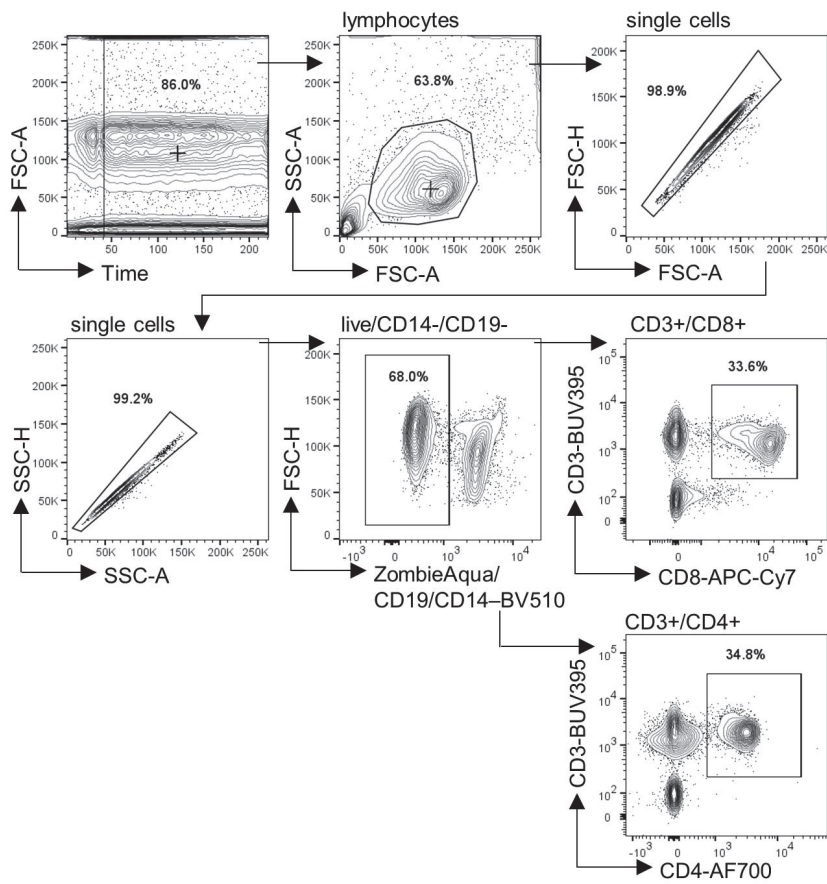
**Supplementary Figure 1 | Longitudinal blood sampling.** Participants of five study cohorts received up to 4 vaccinations (V1 to V4) with different COVID-19 vaccines. Time intervals between vaccinations differed between the cohorts and are indicated in the upper panel. The vaccines administered in this study include the two rMVA-based vaccine candidates MVA-SARS-2-S (MVA-S) and MVA-SARS-2-ST (MVA-ST), as well as the licensed vaccines BNT162b2 and mRNA-1273 (together referred to as mRNA) and ChAdOx1 nCov-19 (ChAd). Blood samples were collected at different time points after vaccination, labeled as T0 (baseline), T1 (1-2 weeks), T2 (3-5 weeks), T3 (12 weeks), and T4 (17-29 weeks), referring to the time since last vaccination (V1-V4). Time points of longitudinal blood sampling are shown in the lower panel for each participant of the different cohorts as colored dots. Vaccinations are shown as black triangles.



**Supplementary Figure 2 | S1/S2-specific IgM and IgA response.** a S1- and S2- specific IgM (top) and IgA (bottom) responses of the different study cohorts measured at baseline and longitudinally after each vaccination. Colored lines depict median MFI (measured by bead-based multiplex immunoassay). Grey lines show dynamics of each study participant.



**Supplementary Figure 3 | Neutralization capacity versus IgG antibody response.** Spearman correlation of serum neutralizing capacity (measured by SARS-CoV-2 virus neutralization test, VNT<sub>100</sub>) with S1- (a) and S2- (b) specific IgG stratified by study cohort.



**Supplementary Figure 4 | T cell gating strategy.** Gating strategy for intracellular cytokine staining T cell assay (related to Fig. 6). Contour plots show representative data from an individual of the ChAd/mRNA cohort at V2:T2.

## Supplementary Tables

Supplementary Table 1 | Baseline characteristics of study participants

	mRNA n=13	ChAd/mRNA n=8	MVA-S/mRNA n=12	MVA-ST n=14	mRNA/MVA-ST n=29
<b>Sex</b>					
Female	8 (62%)	7 (88%)	4 (33%)	9 (64%)	18 (62%)
Male	5 (38%)	1 (12%)	8 (67%)	5 (36%)	11 (38%)
<b>Age</b>					
mean, years	33.2 (8.9)	32.3 (5.9)	37.8 (9.0)	41 (11.1)	32.0 (11.2)
range, years	23-51	24 - 44	21 - 51	22 - 62	19 - 64
<b>BMI</b>					
kg/m <sup>2</sup>	21.4 (2.4)	21.7 (1.3)	24.9 (3.4)	24.0 (3.45)	24.6 (2.9)
Data is shown in mean (SD), unless otherwise indicated. BMI=body-mass index. BMI of n=2 of the mRNA cohort missing.					

Supplementary Table 2 | Time interval between vaccinations

	mRNA n=13	ChAd/mRNA n=8	MVA-S/mRNA n=12	MVA-ST n=14	mRNA/MVA-ST n=29
<b>Vaccination interval</b>					
V1-V2	21 (21-40)	84 (77-84)	28	28	
V2-V3	252 (196-291)	183 (170-211)	203 (185-211)		220.5 (187-364)
V3-V4			22 (21-28)		
Data is shown as median days (range)					

Supplementary Table 3 | Blood collection time since last vaccination

	mRNA n=13	ChAd/mRNA n=8	MVA-S/mRNA n=12	MVA-ST n=14	mRNA/MVA-ST n=29
<b>V1</b>					
T1	7	7 (7-8)	-	-	-
T2	21 (20-23)	28 (28-31)	28 (28-29)	28	-
T3	-	80.5 (56-83)	-	-	-
<b>V2</b>					
T1	7 (7-8)	7 (7-10)	14 (12-16)	14 (14-16)	-
T2	35 (34-38)	36.5 (29-42)	29 (27-33)	28 (28-35)	-
T4	164 (147-169)	169 (168-171)	203 (185-211)	-	220.5 (187-364)
<b>V3</b>					
T1	8.5 (7-15)	7 (7-8)	7	-	7 (7-14)
T2	28 (28-36)	28 (27-32)	21.5 (21-28)		28 (25-34)
T4	124.5 (119-137)	-	-	-	-
<b>V4</b>					
T1	-	-	7 (6-7)	-	-
T2	-	-	28 (28-33)		-
Data is shown as median days (range)					

Supplementary Table 4 | Number of samples – mRNA cohort

Assay	Timepoint	V1:T0	V1:T1	V1:T2	V2:T1	V2:T2	V2:T4	V3:T1	V3:T2	V3:T4
B cell	Antibody isotypes and subclasses	10		10	10		13	6		7
	IgG ELISpot	10	10	10	10		13	5		7
	IgG epitope array	9			9					
T cell	IFN $\gamma$ ELISpot	10	10	10	10	10	13	6	7	7
	Intracellular cytokine staining	10		10		10				

Supplementary Table 5 | Number of samples – ChAd/mRNA cohort

Assay	Timepoint	V1:T0	V1:T1	V1:T2	V1:T3	V2:T1	V2:T2	V2:T4	V3:T1	V3:T2
B cell	Antibody isotypes and subclasses	8		8	8	8		6	5	
	IgG ELISpot	8	8	8	8	8		6	5	
	IgG epitope array	5				5			5	
T cell	IFN $\gamma$ ELISpot	8	8	8	8	8	8	6	5	5
	Intracellular cytokine staining	8		8			8			

Supplementary Table 6 | Number of samples – MVA-S/mRNA cohort

Assay	Timepoint	V1:T0	V1:T2	V2:T1	V2:T2	V2:T4	V3:T1	V3:T2	V4:T1	V4:T2
B cell	Antibody isotypes and subclasses	12		12		12	12	12	12	
	S1-specific IgG ELISpot	12		12		12	S1: 12, S2: 11	S1: 12, S2: 11	12	
	Epitope array	5		5					5	
T cell	IFN $\gamma$ ELISpot	12	10	11	12	12	12	12	12	12
	Intracellular cytokine staining	12						12		12

Supplementary Table 7 | Number of samples – MVA-ST

Assay	Timepoint	V1:T0	V1:T2	V2:T1	V2:T2
B cell	Antibody isotypes and subclasses	14		14	
	IgG ELISpot	S1: 14, S2: 13		14	
	IgG epitope array	7		7	
T cell	IFN $\gamma$ ELISpot	14	14	14	14
	Intracellular cytokine staining				



**Supplementary Table 8 | Number of samples – mRNA/MVA-ST**

Assay	Timepoint	V2:T4	V3:T1	V3:T2
B cell	Antibody isotypes and subclasses	29	29	
	IgG ELISpot	28	29	
	IgG epitope array			
T cell	IFN $\gamma$ ELISpot	29	29	28
	Intracellular cytokine staining			

**Supplementary Table 9 | Statistical analysis of S1/S2-specific IgG responses, related to Figure 2.**

Figure/panel	parameter	cohort	time point	test	adjusted p-value	p-value summary
2a	S1	MVA-S/mRNA	V2T1 vs T0	Wilcoxon	0.0104	*
2a	S1	MVA-S/mRNA	V2T4 vs T0	Wilcoxon	0.5907	ns
2a	S1	MVA-ST	V2T1 vs T0	Wilcoxon	0.0005	***
2a	S1	mRNA	V2T1 vs T0	Wilcoxon	0.0036	**
2a	S1	ChAd/mRNA	V2T1 vs T0	Wilcoxon	0.0119	*
2a	S1	mRNA/MVA-ST	V3T1 vs V2T4	Wilcoxon	0.0007	***
2a	S1	mRNA	V3T1 vs V2T4	Wilcoxon	0.0421	*
2a	S1	ChAd/mRNA	V3T1 vs V2T4	Wilcoxon	0.0754	ns
2a	S2	MVA-S/mRNA	V2T1 vs T0	Wilcoxon	0.0012	**
2a	S2	MVA-S/mRNA	V2T4 vs T0	Wilcoxon	0.0030	**
2a	S2	MVA-ST	V2T1 vs T0	Wilcoxon	0.0005	***
2a	S2	mRNA	V2T1 vs T0	Wilcoxon	0.0036	**
2a	S2	ChAd/mRNA	V2T1 vs T0	Wilcoxon	0.0119	*
2a	S2	mRNA/MVA-ST	V3T1 vs V2T4	Wilcoxon	0.0018	**
2a, 2d	S2	mRNA	V3T1 vs V2T4	Wilcoxon	0.0421	*
2a	S2	ChAd/mRNA	V3T1 vs V2T4	Wilcoxon	0.0754	ns
2b	S1	MVA-S/mRNA vs MVA-ST	V2T1	Mann-Whitney	<0.0001	****
2b	S1	MVA-S/mRNA vs mRNA	V2T1	Mann-Whitney	<0.0001	****
2b	S1	MVA-S/mRNA vs ChAd/mRNA	V2T1	Mann-Whitney	<0.0001	****
2b	S1	MVA-ST vs mRNA	V2T1	Mann-Whitney	<0.0001	****
2b	S1	MVA-ST vs ChAd/mRNA	V2T1	Mann-Whitney	0.0006	***
2b	S1	mRNA vs ChAd/mRNA	V2T1	Mann-Whitney	0.0104	*
2b	S2	MVA-S/mRNA vs MVA-ST	V2T1	Mann-Whitney	0.5952	ns
2b	S2	MVA-S/mRNA vs mRNA	V2T1	Mann-Whitney	<0.0001	****
2b	S2	MVA-S/mRNA vs ChAd/mRNA	V2T1	Mann-Whitney	0.0008	***
2b	S2	MVA-ST vs mRNA	V2T1	Mann-Whitney	<0.0001	****
2b	S2	MVA-ST vs ChAd/mRNA	V2T1	Mann-Whitney	0.0005	***
2b	S2	mRNA vs ChAd/mRNA	V2T1	Mann-Whitney	0.3000	ns
2c	S1	MVA-S/mRNA vs mRNA	V3T2 vs V1T2	Mann-Whitney	0.0807	ns
2c	S2	MVA-S/mRNA vs mRNA	V3T2 vs V1T2	Mann-Whitney	0.0014	**
2d	S1	mRNA/MVA-ST, LD	V3T1 vs V2T4	Wilcoxon	0.0551	ns

2d	S1	mRNA/MVA-ST, MD	V3T1 vs V2T4	Wilcoxon	0.0285	*
2d	S1	mRNA/MVA-ST, HD	V3T1 vs V2T4	Wilcoxon	0.0882	ns
2e	S1	mRNA/MVA-ST, low baseline	V3T1 vs V2T4	Wilcoxon	0.0006	***
2e	S1	mRNA/MVA-ST, high baseline	V3T1 vs V2T4	Wilcoxon	0.3792	ns

Supplementary Table 10 | Statistical analysis of S1/S2-specific B cell responses, related to Figure 4.

Figure/ panel	parameter	cohort	time point	test	adjusted p-value	p-value summary
4a	S1	MVA-S/mRNA	V2T1 vs T0	Wilcoxon	0.0298	*
4a	S1	MVA-ST	V2T1 vs T0	Wilcoxon	0.0156	*
4a	S1	mRNA	V1T2 vs T0	Wilcoxon	0.0201	*
4a	S1	mRNA	V2T1 vs T0	Wilcoxon	0.0066	**
4a	S1	ChAd/mRNA	V1T2 vs T0	Wilcoxon	0.0170	*
4a	S1	ChAd/mRNA	V2T1 vs T0	Wilcoxon	0.0170	*
4a	S1	mRNA/MVA-ST	V3T1 vs V2T4	Wilcoxon	0.8615	ns
4a	S1	mRNA	V3T1 vs V2T4	Wilcoxon	0.0925	ns
4a	S1	ChAd/mRNA	V3T1 vs V2T4	Wilcoxon	0.0925	ns
4a	S2	MVA-S/mRNA	V2T1 vs T0	Wilcoxon	0.0018	**
4a	S2	MVA-ST	V2T1 vs T0	Wilcoxon	0.0078	**
4a	S2	mRNA	V1T2 vs T0	Wilcoxon	0.0419	*
4a	S2	mRNA	V2T1 vs T0	Wilcoxon	0.0156	*
4a	S2	ChAd/mRNA	V1T2 vs T0	Wilcoxon	0.0419	*
4a	S2	ChAd/mRNA	V2T1 vs T0	Wilcoxon	0.0170	*
4a	S2	mRNA/MVA-ST	V3T1 vs V2T4	Wilcoxon	0.3383	ns
4a	S2	mRNA	V3T1 vs V2T4	Wilcoxon	0.2417	ns
4a	S2	ChAd/mRNA	V3T1 vs V2T4	Wilcoxon	0.0925	ns
4b	S1	MVA-S/mRNA vs MVA-ST	V2T1	Mann-Whitney	0.2417	ns
4b	S1	MVA-S/mRNA vs mRNA	V2T1	Mann-Whitney	0.0001	***
4b	S1	MVA-S/mRNA vs ChAd/mRNA	V2T1	Mann-Whitney	0.0003	***
4b	S1	MVA-ST vs mRNA	V2T1	Mann-Whitney	0.0004	***
4b	S1	MVA-ST vs ChAd/mRNA	V2T1	Mann-Whitney	0.0008	***
4b	S1	mRNA vs ChAd/mRNA	V2T1	Mann-Whitney	0.8290	ns
4b	S2	MVA-S/mRNA vs MVA-ST	V2T1	Mann-Whitney	0.0228	*
4b	S2	MVA-S/mRNA vs mRNA	V2T1	Mann-Whitney	0.0017	**
4b	S2	MVA-S/mRNA vs ChAd/mRNA	V2T1	Mann-Whitney	0.0005	***
4b	S2	MVA-ST vs mRNA	V2T1	Mann-Whitney	0.0004	***
4b	S2	MVA-ST vs ChAd/mRNA	V2T1	Mann-Whitney	0.0008	***
4b	S2	mRNA vs ChAd/mRNA	V2T1	Mann-Whitney	0.0973	ns
4c	S1	MVA-S/mRNA vs mRNA	V3T2 vs V1T2	Mann-Whitney	1.0000	ns
4c	S2	MVA-S/mRNA vs mRNA	V3T2 vs V1T2	Mann-Whitney	0.0008	***
4d	S1	mRNA/MVA-ST LD	V3T1 vs V2T4	Wilcoxon	0.8362	ns
4d	S1	mRNA/MVA-ST MD	V3T1 vs V2T4	Wilcoxon	0.3653	ns
4d	S1	mRNA/MVA-ST HD	V3T1 vs V2T4	Wilcoxon	0.1448	ns
4e	S1	mRNA/MVA-ST_low baseline	V3T1 vs V2T4	Wilcoxon	0.3515	ns
4e	S1	mRNA/MVA-ST_high baseline	V3T1 vs V2T4	Wilcoxon	0.3653	ns

**Supplementary Table 11 | Statistical analysis of T cell responses as measured by ELISpot, related to Figure 5.**

Figure/ panel	cohort	time point	test	adjusted p-value	p-value summary
5a	MVA-S/mRNA	V2T1 vs T0	Wilcoxon	0.1782	ns
5a	MVA-ST	V2T1 vs T0	Wilcoxon	0.0249	*
5a	mRNA	V1T2 vs T0	Wilcoxon	0.0714	ns
5a	ChAd/mRNA	V1T2 vs T0	Wilcoxon	0.0165	*
5a	mRNA/MVA-ST	V3T2 vs V2T4	Wilcoxon	0.0012	**
5a, 5g	mRNA	V3T2 vs V2T4	Wilcoxon	0.0990	ns
5a	ChAd/mRNA	V3T2 vs V2T4	Wilcoxon	0.0848	ns
5d	MVA-S/mRNA vs MVA-ST	V2T1	Mann-Whitney	0.0021	**
5d	MVA-S/mRNA vs mRNA	V2T1	Mann-Whitney	0.0012	**
5d	MVA-S/mRNA vs ChAd/mRNA	V2T1	Mann-Whitney	0.0012	**
5d	MVA-ST vs mRNA	V2T1	Mann-Whitney	0.0021	**
5d	MVA-ST vs ChAd/mRNA	V2T1	Mann-Whitney	0.0023	**
5d	mRNA vs ChAd/mRNA	V2T1	Mann-Whitney	0.9654	ns
5f	MVA-S/mRNA vs mRNA	V3T1 vs V1T1	Mann-Whitney	0.0211	*
5g	mRNA/MVA-ST_LD	V3T2 vs V2T4	Wilcoxon	0.4127	ns
5g	mRNA/MVA-ST_MD	V3T2 vs V2T4	Wilcoxon	0.0093	**
5g	mRNA/MVA-ST_HD	V3T2 vs V2T4	Wilcoxon	0.0714	ns
5h	mRNA/MVA-ST_low baseline	V3T2 vs V2T4	Wilcoxon	0.0012	**
5h	mRNA/MVA-ST_high baseline	V3T2 vs V2T4	Wilcoxon	0.4127	ns

**Supplementary Table 12 | Statistical analysis of T cell responses as measured by ICS, related to Figure 6.**

Figure/ panel	parameter	cohort	time point	test	adjusted p-value	p-value summary
6d	CD4_IFNg	MVA-S/mRNA	V4T2 vs V1D0	Wilcoxon	0.0059	**
6d	CD4_IFNg	mRNA	V2T2 vs V1D0	Wilcoxon	0.0275	*
6d	CD4_IL2	MVA-S/mRNA	V4T2 vs V1D0	Wilcoxon	0.0275	*
6d	CD4_IL2	mRNA	V2T2 vs V1D0	Wilcoxon	0.0117	*
6d	CD4_TNFa	MVA-S/mRNA	V4T2 vs V1D0	Wilcoxon	0.0346	*
6d	CD4_TNFa	mRNA	V2T2 vs V1D0	Wilcoxon	0.0418	*
6d	CD8_IFNg	MVA-S/mRNA	V4T2 vs V1D0	Wilcoxon	0.0441	*
6d	CD8_IFNg	mRNA	V2T2 vs V1D0	Wilcoxon	0.0418	*
6d	CD4_IL2	MVA-S/mRNA	V4T2 vs V1D0	Wilcoxon	0.6726	ns
6d	CD4_IL2	mRNA	V2T2 vs V1D0	Wilcoxon	0.1122	ns
6d	CD8_TNFa	MVA-S/mRNA	V4T2 vs V1D0	Wilcoxon	0.2020	ns
6d	CD8_TNFa	mRNA	V2T2 vs V1D0	Wilcoxon	0.0774	ns

**II. Identification of a spike-specific CD8<sup>+</sup> T cell epitope following vaccination against the Middle East respiratory syndrome coronavirus in humans**

Caroline E. Harrer\*, **Leonie Mayer\***, Anahita Fathi, Susan Lassen, My L. Ly, Madeleine E. Zinser, MVAMERS-S Study Group, Timo Wolf, Stephan Becker, Gerd Sutter, Christine Dahlke, Marylyn M. Addo

\*These authors contributed equally.

Advance online publication in *The Journal of Infectious Diseases* (9 January 2024)

doi: [10.1093/infdis/jiad612](https://doi.org/10.1093/infdis/jiad612)

## Identification of a Spike-Specific CD8<sup>+</sup> T-Cell Epitope Following Vaccination Against the Middle East Respiratory Syndrome Coronavirus in Humans

Caroline E. Harrer,<sup>1,2,3,a</sup> Leonie Mayer,<sup>1,2,3,a</sup> Anahita Fathi,<sup>1,2,3,4</sup> Susan Lassen,<sup>1,2,3</sup> My L. Ly,<sup>1,2,3</sup> Madeleine E. Zinser,<sup>1,2,3</sup> Timo Wolf,<sup>5,6</sup> Stephan Becker,<sup>6,7,8</sup> Gerd Sutter,<sup>8,9,b</sup> Christine Dahlke,<sup>1,2,3</sup> and Marylyn M. Addo<sup>1,2,3,4,c</sup>, for the MVA-MERS-S Study Group<sup>d</sup>

<sup>1</sup>Institute for Infection Research and Vaccine Development, University Medical Center Hamburg-Eppendorf; <sup>2</sup>Department for Clinical Immunology of Infectious Diseases, Bernhard Nocht Institute for Tropical Medicine; <sup>3</sup>German Center for Infection Research, partner site Hamburg-Lübeck-Borstel-Riems, Hamburg; <sup>4</sup>First Department of Medicine, Division of Infectious Diseases, University Medical Center Hamburg-Eppendorf, Hamburg; <sup>5</sup>Goethe University Frankfurt, University Hospital, Department of Internal Medicine II, Division of Infectious Diseases, Frankfurt am Main; <sup>6</sup>German Center for Infection Research, partner site Gießen-Marburg-Langen, Marburg; <sup>7</sup>Institute of Virology, Philipps University Marburg, Marburg; <sup>8</sup>German Center for Infection Research, partner site Munich, Munich; and <sup>9</sup>Division of Virology, Institute for Infectious Diseases and Zoonoses, Ludwig Maximilian University of Munich, Munich, Germany

Licensed vaccines against the Middle East respiratory syndrome coronavirus (MERS-CoV), an emerging pathogen of concern, are lacking. The modified vaccinia virus Ankara vector-based vaccine MVA-MERS-S, expressing the MERS-CoV-spike glycoprotein (MERS-S), is one of 3 candidate vaccines in clinical development and elicits robust humoral and cellular immunity. Here, we identified for the first time a MERS-S-specific CD8<sup>+</sup> T-cell epitope in an HLA-A\*03:01/HLA-B\*35:01-positive vaccinee using a screening assay, intracellular cytokine staining, and in silico epitope prediction. As evidence from MERS-CoV infection suggests a protective role of long-lasting CD8<sup>+</sup> T-cell responses, the identification of epitopes will facilitate longitudinal analyses of vaccine-induced T-cell immunity.

**Keywords.** MERS-CoV; epitope; CD8<sup>+</sup> T cells; MVA; viral vector; vaccine.

The Middle East respiratory syndrome coronavirus (MERS-CoV) is an emerging zoonotic pathogen. It belongs to the *Betacoronavirus* genus, which includes the endemic human coronaviruses (HCoV-OC43 and HCoV-HKU1) and the epidemic SARS-CoV and SARS-CoV-2 [1, 2]. Infection with MERS-CoV leads to MERS, a primarily respiratory disease with a case fatality rate of approximately 35% [1, 2]. Since 2012, >2000 cases have been reported, mostly on the Arabian Peninsula [1, 2]. Dromedary camels serve as a natural reservoir for MERS-CoV, harboring a constant risk of spillover to humans and viral evolution [1, 2]. Due to this high epidemic potential, MERS-CoV is listed by the World Health Organization as a priority pathogen of concern for epidemic preparedness measures, such as vaccine development [1, 2].

The current vaccine candidates are predominantly based on the MERS-CoV spike protein (MERS-S), a highly immunogenic surface protein, that facilitates the binding (S1 subunit) and fusion (S2 subunit) of MERS-CoV with its host cells [2]. One of the 3 MERS vaccine candidates in clinical development is the viral vector vaccine MVA-MERS-S, based on the modified vaccinia virus Ankara (MVA) expressing the full-length MERS-S [3]. In a first-in-human phase 1 clinical trial (ClinicalTrials.gov identifier NCT03615911), we previously demonstrated the induction of robust humoral and cellular immunity after 2 MVA-MERS-S vaccinations. MERS-S-specific T-cell responses were detectable in 87% of vaccinees (n = 20/23) upon stimulation with MERS-S-specific overlapping peptide (OLP) pools [4]. Interestingly, in some vaccinees T-cell responses were already measurable after the first dose and persisted for a longer time compared to immunoglobulin G levels [4].

There is still a limited understanding of T-cell immunity elicited by MERS-CoV infection or vaccination, but evidence from MERS survivor studies suggests a protective and long-lasting role [5–7]. In particular, CD8<sup>+</sup> T cells were detectable even in patients with mild or asymptomatic disease, in the absence of relevant antibody titers [5]. MERS-specific CD8<sup>+</sup> T cells may therefore be important for monitoring immunogenicity of MERS vaccines longitudinally. MERS-CoV-specific T-cell epitopes, however, remain mostly unknown, hindering the development of tools, such as tetramers, for the detection, isolation, and characterization of antigen-specific T cells. While several MERS-S-specific CD4<sup>+</sup> T-cell epitopes have been described in MERS survivors [5], MERS-S-specific CD8<sup>+</sup> T-cell epitopes have only been predicted in silico [8] and to date have not been identified in humans.

Received 31 August 2023; editorial decision 27 December 2023

<sup>a</sup>C. E. H. and L. M. contributed equally to this work.

<sup>b</sup>Deceased.

<sup>c</sup>The complete list of MVA-MERS-S Study Group investigators is provided in the Acknowledgments.

Presented in part: European Congress of Clinical Microbiology and Infectious Diseases, Virtual, 9–12 July 2021 [abstract 146]; German Congress for Infectious Diseases and Tropical Medicine, 16–19 June, 2021 [abstract A-367]; and Joint Annual Meeting of the German Society of Infectious Diseases and German Center for Infection Research, Bad Nauheim, Germany, 21–23 November 2019 [abstract A-176].

Correspondence: Caroline Harrer, MD, MSc, The Rockefeller University, 1230 York Ave, New York, NY 10065 (charrer@rockefeller.edu); Marylyn M. Addo, MD, MSc, DTM&H, Institute for Infection Research and Vaccine Development, Division of Infectious Diseases, I. Department of Medicine, University Medical Center Hamburg-Eppendorf, Martinistr. 52, Gebäude 010, Raum-Nr. 02.1.085.1, 20246 Hamburg, Germany (m.addo@uke.de).

The Journal of Infectious Diseases®

© The Author(s) 2024. Published by Oxford University Press on behalf of Infectious Diseases Society of America.

This is an Open Access article distributed under the terms of the Creative Commons Attribution License (<https://creativecommons.org/licenses/by/4.0/>), which permits unrestricted reuse, distribution, and reproduction in any medium, provided the original work is properly cited. <https://doi.org/10.1093/infdis/jiad612>

To address these constraints, the aim of this study was to identify MERS-S-specific CD8<sup>+</sup> T-cell epitopes after vaccination with the viral vector vaccine candidate MVA-MERS-S. We analyzed the T-cell response to single overlapping peptides covering MERS-S in the vaccinee with the highest overall T-cell response in the phase 1 clinical study and identified the first MERS-S-specific CD8<sup>+</sup> T-cell epitope candidate after MERS vaccination.

## METHODS

The vaccinee described here was part of a first-in-human phase 1 clinical trial of the vaccine candidate MVA-MERS-S (NCT03615911, published [4]). The trial consisted of a homologous prime-boost scheme of  $1 \times 10^7$  or  $1 \times 10^8$  plaque-forming units/mL of MVA-MERS-S on days 0 and 28. The study was approved by the competent national authority (Paul Ehrlich Institute) and the Ethics Committee of the Hamburg Medical Association. Informed consent was obtained from all participants. The study was performed in accordance with the Declaration of Helsinki (2013). For immunogenicity analysis, peripheral blood mononuclear cells (PBMCs) were collected on days 7, 14, and 28 after the second vaccination (V2D7, V2D14, and V2D28, respectively). HLA typing was performed using commercially available A and B locus kits (LABType SSO Typing Test, ONE LAMDA) according to the manufacturer's instructions.

MERS-S-specific T-cell responses were assessed using the CTL human interferon-gamma (IFN- $\gamma$ ) single-color 384-well enzyme-linked immunospot (ELISpot) assay (CTL ImmunoSpot). After thawing and overnight resting,  $5 \times 10^4$  PBMCs were stimulated for 16 hours at 37°C and 5% carbon dioxide. For stimulation, OLP pools M1–M5 (15-mers overlapping by 11 amino acids, JPT), spanning the entire MERS-S sequence (GenBank: JX869059), and single peptides (P1–P65) of pool M1 (Supplementary Table 1) were used at a peptide concentration of 1  $\mu$ g/mL. Phytohemagglutinin (Sigma-Aldrich) and a cytomegalovirus–Epstein-Barr–influenza virus pool (JPT) served as positive controls, and dimethyl sulfoxide (DMSO) served as a negative control. Spot-forming cells (SFC) per million PBMCs were counted using an AID ELISpot Reader System (AID GmbH), and the results are reported as the background (DMSO)–subtracted mean count of triplicate wells.

Cytokine secretion was analyzed by intracellular cytokine staining (ICS). PBMCs were stimulated with OLP pools M1–M5 (1  $\mu$ g/mL) at 37°C and 5% carbon dioxide for 7 hours in the presence of Golgi-Stop (BD Biosciences), anti-CD28/CD49 (BD Biosciences), anti-CD107a (BioLegend), and Golgi-Plug (after 2 hours of stimulation; BD Biosciences). DMSO and phorbol-12-myristate-13-acetate (50 ng/mL) plus ionomycin (0.5  $\mu$ g/mL) served as negative and positive controls, respectively. PBMCs were stained with surface

markers anti-CD3-BUV395 (BD Biosciences), anti-CD4-AF700, anti-CD19-BV510, anti-CD14-BV510, anti-CD8-APC-Cy7, anti-CCR7, anti-CD45RO-FITC, and Zombie Aqua Fixable Viability Kit (BioLegend) in FACS buffer (phosphate-buffered saline supplemented with 2% fetal bovine serum and 2 mM ethylenediaminetetraacetic acid). After fixation (eBioscience), PBMCs were stained with intracellular markers anti-IFN- $\gamma$ -PE-Cy7, anti-tumor necrosis factor alpha (TNF- $\alpha$ )–521 PE/Dazzle 594, and anti-interleukin 2 (IL-2)–PerCP-Cy5.5 (BioLegend) in PERM buffer (eBioscience). Samples were measured on a BD Fortessa and analyzed using FlowJo software (v.10.8.1) as shown in Supplementary Figure 1. Memory T cells were identified by excluding CCR7<sup>+</sup>/CD45RO<sup>–</sup> naive T cells. The data were normalized to the negative control. Polyfunctionality was assessed by Boolean gating.

Multiple sequence alignment of the spike protein of human betacoronaviruses was performed using the Clustal Omega web server of the European Bioinformatics Institute. Spike sequences were downloaded from the National Center for Biotechnology Information (NCBI): MERS-CoV (GenBank: JX869059), SARS-CoV-2 Wuhan (GenBank: MN908947.3), SARS-CoV BJ01 (GenBank: AY278488.2), HCoV-OC43 (NCBI reference sequence: NC\_006213.1), and HCoV-HKU1 (GenBank: KF686346.1). Epitope prediction for the HLA-A\*03:01 and HLA-B\*35:01 alleles was performed using the NetMHCpan-4.1 software.

## RESULTS

We analyzed MERS-S-specific T-cell immunity induced by MVA-MERS-S in an HLA-A\*03:01/HLA-B\*35:01 homozygous vaccinee (see detailed description in Supplementary Table 2). We used 5 OLP pools (M1–M5) covering the whole MERS-S sequence, as depicted in Figure 1A, for restimulation and measured the T-cell response by IFN- $\gamma$  ELISpot. The highest IFN- $\gamma$  response was observed after stimulation with the M1 pool (622 SFC/ $1 \times 10^6$  PBMCs) at V2D14 (Figure 1B) [4]. We then used single peptides P1–P65 of the M1 pool to screen for immunogenic epitopes. P19 (GLFPYQGHDHGMVYVY) elicited an IFN- $\gamma$  response of 307 SFC/ $1 \times 10^6$  PBMCs, the highest in magnitude compared with the other M1 peptides (Figure 1C and 1D). P19 mapped to the N-terminal domain of the MERS-S1 subunit outside the receptor-binding domain (RBD) at position 73–87aa (Figure 1A).

To further dissect the cytokine profile and CD4<sup>+</sup>/CD8<sup>+</sup> bias of the T-cell response elicited by P19, we performed an ICS. After restimulation, we observed IFN- $\gamma$ , IL-2, and TNF- $\alpha$  expression in memory CD8<sup>+</sup> T cells (gating shown in Figure 2A), but not in memory CD4<sup>+</sup> T cells (Supplementary Figure 2). Restimulation with individual M1–M5 OLP pools confirmed that the response was dominated by M1-specific T cells

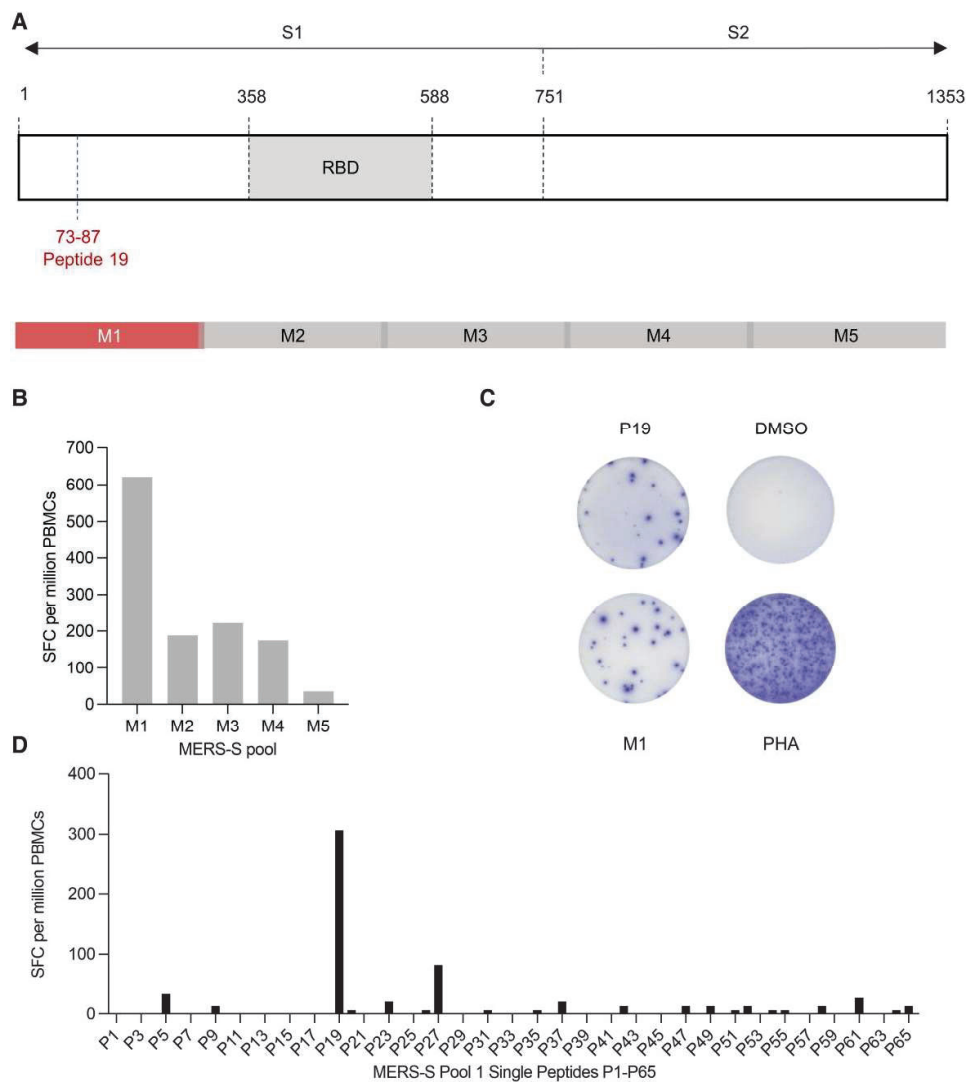


**Figure 1.** T-cell epitope mapping of the Middle East respiratory syndrome coronavirus spike protein (MERS-S) using an interferon gamma (IFN- $\gamma$ ) enzyme-linked immunospot (ELISpot) assay. *A*, Schematic sequence of the 1353aa spanning MERS-S protein (GenBank: JX869059) (top) and location of overlapping peptide pools M1–M5 (bottom) [9]. Peptide 19 mapped to the S1 subunit outside the receptor-binding domain at position 73–87. *B*, Frequencies of IFN- $\gamma$ -producing T cells at V2D14 after restimulation with overlapping peptide pools M1–M5 (shown as SFC per million peripheral blood mononuclear cells [PBMCs] measured by IFN- $\gamma$  ELISpot, mean of technical triplicates). *C*, Representative IFN- $\gamma$  ELISpot assay wells of the unstimulated negative control and after restimulation with the M1 pool, P19 peptide, and positive control. *D*, Frequencies of IFN- $\gamma$ -producing T cells at V2D14 after restimulation with M1 pool single peptides (P1–P65) (shown as spot-forming cells per million PBMCs measured by IFN- $\gamma$  ELISpot, mean of technical triplicates). Abbreviations: DMSO, dimethyl sulfoxide; MERS-S, Middle East respiratory syndrome coronavirus spike protein; PBMCs, peripheral blood mononuclear cells; PHA, phytohemagglutinin P; RBD, receptor-binding domain; SFC, spot-forming cells.

(V2D7 = 0.59%; V2D28 = 0.71%) (Figure 2B, Supplementary Figure 3). The frequency of total cytokine-secreting CD8<sup>+</sup> T cells after restimulation with the single P19 peptide was comparable in magnitude (V2D7 = 0.48%; V2D28 = 0.51%). CD107a expression followed a similar pattern. At V2D28, the highest frequency was observed after M1-5 restimulation (0.49%),

followed by M1 (0.26%) and P19 (0.19%), respectively (Figure 2C). The polyfunctional profile of P19-specific CD8<sup>+</sup> T cells was similar to that of M1-5-specific CD8<sup>+</sup> T cells (Figure 2D). We observed that the majority of P19-specific CD8<sup>+</sup> T cells were memory cells (V2D7 = 80%; V2D28 = 86% of all P19-specific CD8<sup>+</sup> T cells), resembling the findings of

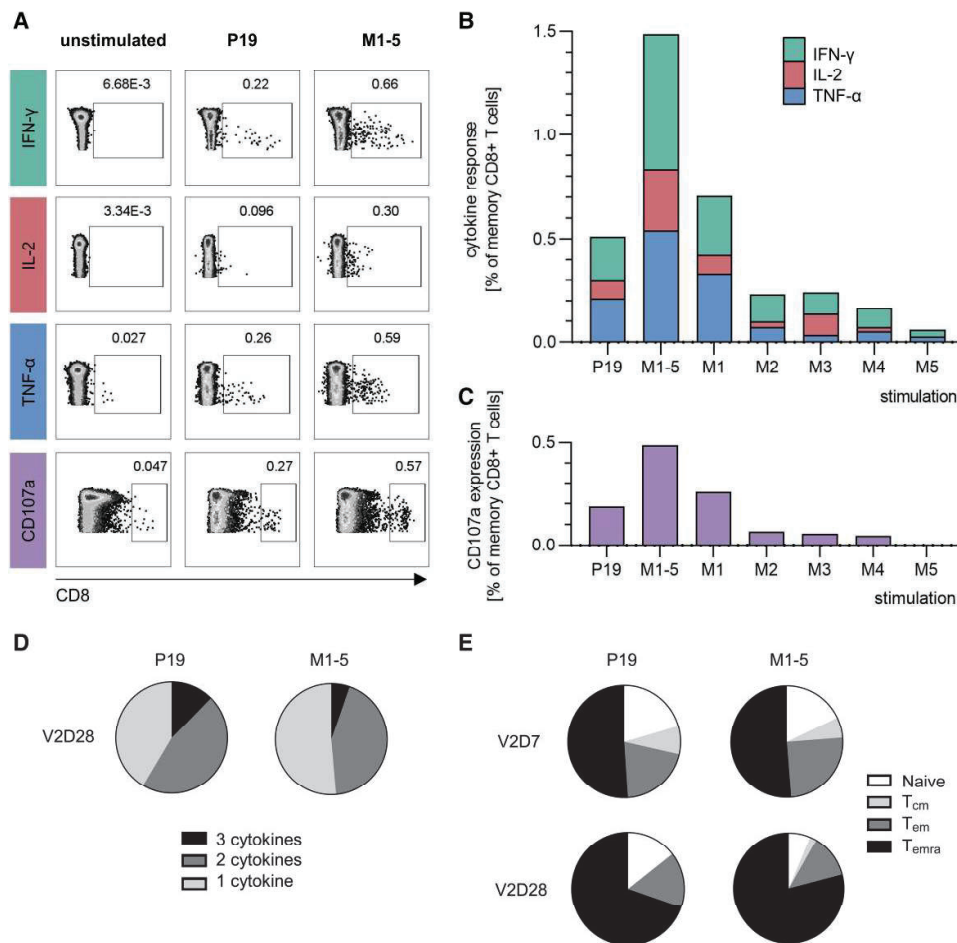


**Figure 2.** Functionality and memory phenotype of P19- compared to full MERS spike protein-specific CD8<sup>+</sup> T cells. Interferon gamma (IFN- $\gamma$ ), interleukin 2 (IL-2), tumor necrosis factor alpha (TNF- $\alpha$ ), and CD107a expression was measured using intracellular cytokine staining, after restimulation with the P19 peptide, M1–M5 pools separately and a combination of all pools (M1-5) covering the whole spike. *A*, Gatings are shown for the unstimulated negative control, after P19 and M1-5 restimulation at V2D28. Cytokine (*B*) and CD107a (*C*) positive cell frequencies are shown as percentages of total memory CD8<sup>+</sup> T cells. *D*, Polyfunctionality of P19- and M1-5-specific CD8<sup>+</sup> memory T cells was assessed using Boolean gating, showing those expressing 1 (IFN- $\gamma$ <sup>+</sup> or IL-2<sup>+</sup> or TNF- $\alpha$ <sup>+</sup>), 2 (IFN- $\gamma$ <sup>+</sup>IL-2<sup>+</sup>TNF- $\alpha$ <sup>+</sup> or IFN- $\gamma$ <sup>+</sup>IL-2<sup>+</sup>TNF- $\alpha$ <sup>+</sup> or IFN- $\gamma$ <sup>+</sup>IL-2<sup>+</sup>TNF- $\alpha$ <sup>+</sup>), or 3 cytokines (IFN- $\gamma$ <sup>+</sup>IL-2<sup>+</sup>TNF- $\alpha$ <sup>+</sup>). *E*, Proportion of memory subsets out of total cytokine-positive cells at V2D7 and V2D28 (naive: CD45RO<sup>+</sup>CCR7<sup>+</sup>; central memory [T<sub>cm</sub>]: CD45RO<sup>+</sup>CCR7<sup>+</sup>; effector memory [T<sub>em</sub>]: CD45RO<sup>+</sup>CCR7<sup>-</sup>; effector memory reexpressing CD45RA [T<sub>emra</sub>]: CD45RO<sup>-</sup>CCR7<sup>-</sup>).

the M1-5-specific response (V2D7 = 82%; V2D28 = 94% of all M1-5-specific CD8<sup>+</sup> T cells). The memory phenotype of P19-specific T cells shifted to a higher frequency of T effector memory cells reexpressing CD45RA (T<sub>emra</sub>) by V2D28 (75% of all P19-specific CD8<sup>+</sup> T cells) compared to V2D7 (50%) (Figure 2E). A similar pattern was observed for M1-5-specific T cells, with a higher frequency of T<sub>emra</sub> at V2D28 (79%) compared to V2D7 (52%).

Multiple sequence alignment revealed that P19 is specific to the MERS-S and not conserved in human betacoronaviruses (Supplementary Table 3). Next, we performed in silico epitope

prediction of the complete MERS-S sequence for HLA-A\*03:01 and HLA-B\*35:01, the HLA-class I alleles for which the vaccinee was homozygous. Notably, an 11-mer (FPYQGDHGDYMY) and a 13-mer epitope (FPYQGDHGDYMYVY) within the P19 peptide were among the top 5 predicted HLA-B\*35:01 MERS-S epitopes with the highest affinity (percentile rank = 0.01; Supplementary Table 4). One 9-mer epitope was identified in the HLA-A\*03:01 prediction analysis, but with a lower affinity (percentile rank = 0.38; Supplementary Table 5).

To investigate if other vaccinees mounted a P19-specific response, we HLA-typed further 20 vaccinees of the study.



By IFN- $\gamma$  ELISpot we could show that the only other HLA-B\*35:01 positive vaccinee of the clinical trial also responded to P19 (Supplementary Figure 4). Notably, P19 was not recognized by the 2 vaccinees who carried the HLA-A\*03:01 but not the HLA-B\*35:01 allele.

## DISCUSSION

The induction of functional and long-lasting immune responses is fundamental for successful vaccine design. The protective and durable nature of CD8<sup>+</sup> T cells in MERS survivor studies makes them interesting targets for monitoring vaccine immunogenicity. Using an epitope-mapping approach, we identified a novel MERS-S-specific CD8<sup>+</sup> T-cell epitope candidate (P19) in an individual vaccinated with MVA-MERS-S and could validate this finding in one further HLA-A\*03:01/HLA-B\*35:01-positive vaccinee. We observed a higher P19-specific T-cell response compared to all other peptides of the M1 pool and the M2–M5 pools, suggesting the potential immunodominance of this peptide within MERS-S.

P19-specific T cells were predominantly polyfunctional CD8<sup>+</sup> T cells, and expressed CD107a, a marker of cytotoxicity. Polyfunctional CD8<sup>+</sup> T cells can exert multiple effector functions and are associated with protection from disease. Interestingly, most P19-specific cells were T<sub>emras</sub>, with an increasing frequency from V2D14 to V2D28. CD8<sup>+</sup> T<sub>emras</sub> have been associated with protection against dengue and symptomatic H1N1 influenza and shown to be long lasting following dengue vaccination [10–11]. While the contribution of MERS-specific T<sub>emras</sub> to protection remains elusive, previous studies have shown that memory T-cell responses, including IFN- $\gamma$ -secreting T<sub>emras</sub>, were detectable up to 6.9 years after infection [5, 7], suggesting that they may drive the maintenance of immune memory.

A beneficial characteristic of P19 for immunogenicity monitoring after MERS vaccination is its location in the N-terminal domain of the S1 subunit, outside the RBD, a region less prone to mutations or cross-reactivity. While the RBD is known to be highly immunogenic, mutations in the RBD have been implicated in the emergence of immune evasion in variants of SARS-CoV-2 [12]. These mutations may not only evade the humoral immune response but may also impact potential T-cell epitopes. Additionally, a report of the ChAdOx1-MERS vaccine clinical trial suggests that the RBD may have a role in T-cell cross-reactivity, given that preexisting T-cell responses detectable in a small number of vaccinees were predominately directed against the RBD [13]. A phylogenetic analysis of 484 MERS-CoV isolates from humans and camels revealed no mutations in the P19 sequence [14]. Furthermore, our sequence alignment showed that P19 is not conserved among HCoV. Taken together, the detected T-cell epitope mapping to a less mutagenic location of the spike with a highly specific

sequence for MERS-CoV seems favorable for the longitudinal assessment of anti-MERS-CoV vaccine responses. This is particularly important given that preexisting immune responses to endemic HCoVs and SARS-CoV-2 are now highly prevalent and may interfere with immune monitoring during upcoming MERS vaccine trials.

In silico prediction revealed that P19 likely encompasses an HLA-B\*35:01-restricted epitope. Notably, the allele frequency for HLA-B\*35:01 ranges from 1.4% to 13.5% worldwide. HLA-B\*35:01 is present in Germany (5.8%) but also in Saudi Arabia (3.0%), where MERS-CoV is endemic [15]. However, further studies are needed to identify the optimal epitope sequence, as MHC-I binding favors amino acid lengths of 9–11. A limitation of this study is that analyses were only performed in a limited number of vaccinees. However, we could show that P19 is recognized by all HLA-B\*35:01-positive vaccinees of our phase 1a clinical trial. In conclusion, the identified CD8<sup>+</sup> T-cell epitope may facilitate the implementation of tetramers to provide novel insights into the role of CD8<sup>+</sup> T cells in anti-MERS-CoV immunity, which may further accelerate MERS-specific immune monitoring and the development of more efficacious vaccine candidates.

## Supplementary Data

Supplementary materials are available at *The Journal of Infectious Diseases* online (<http://jid.oxfordjournals.org/>). Supplementary materials consist of data provided by the author that are published to benefit the reader. The posted materials are not copyedited. The contents of all supplementary data are the sole responsibility of the authors. Questions or messages regarding errors should be addressed to the author.

## Notes

**Acknowledgments.** We thank the MVA-MERS-S study group members for their ongoing support and dedication. The following investigators are part of the MVA-MERS-S study group: Etienne Bartels, Monika Friedrich, Leonie M. Weskamm, Swantje Grundlach, and Joseph H. Poetsch (Institute for Infection Research and Vaccine Development, University Medical Centre Hamburg-Eppendorf, Hamburg, Germany; Department for Clinical Immunology of Infectious Diseases, Bernhard Nocht Institute for Tropical Medicine, Hamburg, Germany; German Center for Infection Research, partner site Hamburg-Lübeck-Borstel-Riems, Hamburg, Germany); Till Koch and Stefan Schmiedel (I. Department of Medicine, University Medical Center Hamburg-Eppendorf, Hamburg, Germany); Bart Haagmanns (Department of Viroscience, Erasmus Medical Centre, Rotterdam, The Netherlands); Thomas Hesterkamp (German Centre for Infection Research, Translational Project Management Office, Brunswick, Germany); Verena Krähling (Institute for Virology, Philipps University Marburg, Marburg, Germany);

German Centre for Infection Research, partner site Gießen-Marburg-Langen, Marburg, Germany); and Asisa Volz (Institute of Virology, University of Veterinary Medicine Hannover, Foundation, Hanover, Germany; German Centre for Infection Research, partner site Hannover-Brunswick, Hanover, Germany). We thank all volunteers for their participation and their commitment and dedication to research against emerging coronaviruses. We thank Dr Vanessa A. Ditt und Melanie Kessler (Institute of Transfusion Medicine, University Medical Center Hamburg-Eppendorf) for the HLA typing of the vaccinees.

**Author contributions.** Conceptualization: M. M. A., C. D., G. S., and S. B. Methodology: C. E. H. and L. M. Investigation: C. E. H., L. M., S. L., M. L. L., and the MVA-MERS-S Study Group. Formal analysis and visualization: C. E. H. and L. M. Writing—original draft: C. E. H. and L. M. Writing—review and editing: C. E. H., L. M., A. F., and M. M. A. Supervision: C. D., M. M. A., M. E. Z., and T. W.

**In memoriam.** We dedicate this manuscript to Prof. Gerd Sutter who passed away on 31 October 2023, and thank him for his great contribution. He was instrumental in the design, generation, and preclinical evaluation of the MVA-based viral vector vaccines, as well as the conceptualization of the phase 1 clinical trials presented in this manuscript.

**Financial support.** This work was funded by the German Center for Infection Research (DZIF Thematic Translational Unit [TTU] 01.908, TTU 01.702, and TTU 01.712). C. E. H. received a DZIF MD stipend (TI 07.003\_Harrer).

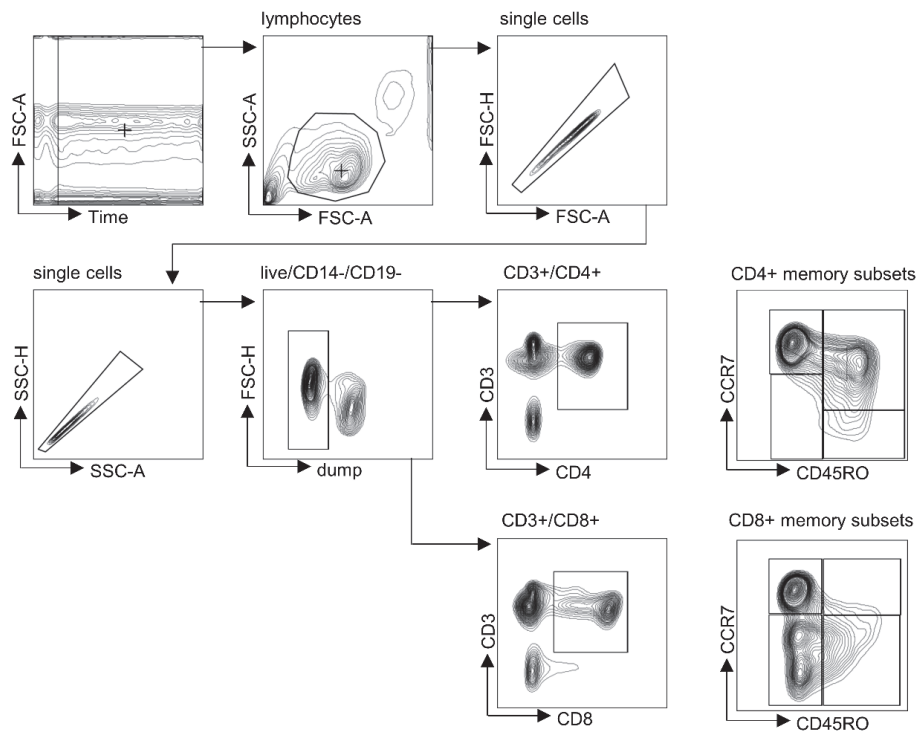
**Potential conflicts of interest.** T. W. received consulting fees and honoraria from Gilead Sciences and Merck Sharp Dome. All other authors: No reported conflicts.

All authors have submitted the ICMJE Form for Disclosure of Potential Conflicts of Interest. Conflicts that the editors consider relevant to the content of the manuscript have been disclosed.

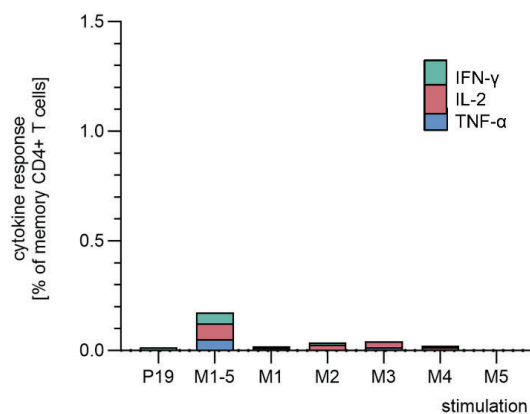
## References

- Memish ZA, Perlman S, Van Kerkhove MD, Zumla A. Middle East respiratory syndrome. *Lancet* **2020**; 395:1063–77.
- Choi J, Kim J-O. Middle East respiratory syndrome coronavirus vaccine development: updating clinical studies using platform technologies. *J Microbiol Seoul Korea* **2022**; 60:238–46.
- Volz A, Kupke A, Song F, et al. Protective efficacy of recombinant modified vaccinia virus Ankara delivering Middle East respiratory syndrome coronavirus spike glycoprotein. *J Virol* **2015**; 89:8651–6.
- Koch T, Dahlke C, Fathi A, et al. Safety and immunogenicity of a modified vaccinia virus Ankara vector vaccine candidate for Middle East respiratory syndrome: an open-label, phase 1 trial. *Lancet Infect Dis* **2020**; 20:827–38.
- Zhao J, Alshukairi AN, Baharoon SA, et al. Recovery from the Middle East respiratory syndrome is associated with antibody and T-cell responses. *Sci Immunol* **2017**; 2:eaa5393.
- Mok CKP, Zhu A, Zhao J, et al. T-cell responses to MERS coronavirus infection in people with occupational exposure to dromedary camels in Nigeria: an observational cohort study. *Lancet Infect Dis* **2021**; 21:385–95.
- Alhabbab RY, Algaissi A, Mahmoud AB, et al. Middle East respiratory syndrome coronavirus infection elicits long-lasting specific antibody, T and B cell immune responses in recovered individuals. *Clin Infect Dis* **2022**; 76:e308–18.
- Mahmud S, Rafi M, Paul GK, et al. Designing a multi-epitope vaccine candidate to combat MERS-CoV by employing an immunoinformatics approach. *Sci Rep* **2021**; 11:15431.
- Mou H, Raj VS, van Kuppeveld FJM, Rottier PJM, Haagmans BL, Bosch BJ. The receptor binding domain of the new Middle East respiratory syndrome coronavirus maps to a 231-residue region in the spike protein that efficiently elicits neutralizing antibodies. *J Virol* **2013**; 87:9379–83. doi:10.1128/JVI.01277-13.
- Sridhar S, Begom S, Bermingham A, et al. Cellular immune correlates of protection against symptomatic pandemic influenza. *Nat Med* **2013**; 19:1305–12.
- Graham N, Eisenhauer P, Diehl SA, et al. Rapid induction and maintenance of virus-specific CD8<sup>+</sup> TEMRA and CD4<sup>+</sup> TEM cells following protective vaccination against dengue virus challenge in humans. *Front Immunol* **2020**; 11:479.
- Liu H, Wei P, Kappler JW, Marrack P, Zhang G. SARS-CoV-2 variants of concern and variants of interest receptor binding domain mutations and virus infectivity. *Front Immunol* **2022**; 13:825256.
- Folegatti PM, Bittaye M, Flaxman A, et al. Safety and immunogenicity of a candidate Middle East respiratory syndrome coronavirus viral-vectored vaccine: a dose-escalation, open-label, non-randomised, uncontrolled, phase 1 trial. *Lancet Infect Dis* **2020**; 20:816–26.
- Mostafa A, Kandeil A, Shehata M, et al. Middle East respiratory syndrome coronavirus (MERS-CoV): state of the science. *Microorganisms* **2020**; 8:991.
- The Allele Frequency Net Database. Allele frequencies in worldwide populations. Available at: [http://www.allele-frequencies.net/hla6006a.asp?hla\\_locus\\_type=Classical&hla\\_locus=B&hla\\_allele1=B\\*35%3A01&hla\\_allele2=B\\*35%3A01&hla\\_selection=&hla\\_pop\\_selection=&hla\\_population=&hla\\_country=&hla\\_dataset=&hla\\_region=&hla\\_ethnic=&hla\\_study=&hla\\_order=order\\_1&hla\\_sample\\_size\\_pattern=bigger\\_than&hla\\_sample\\_size=1000&hla\\_sample\\_year\\_pattern=equal&hla\\_sample\\_year=&hla\\_level\\_pattern=equal&hla\\_level=&standard=a&hla\\_show=](http://www.allele-frequencies.net/hla6006a.asp?hla_locus_type=Classical&hla_locus=B&hla_allele1=B*35%3A01&hla_allele2=B*35%3A01&hla_selection=&hla_pop_selection=&hla_population=&hla_country=&hla_dataset=&hla_region=&hla_ethnic=&hla_study=&hla_order=order_1&hla_sample_size_pattern=bigger_than&hla_sample_size=1000&hla_sample_year_pattern=equal&hla_sample_year=&hla_level_pattern=equal&hla_level=&standard=a&hla_show=). Accessed 14 December 2023.

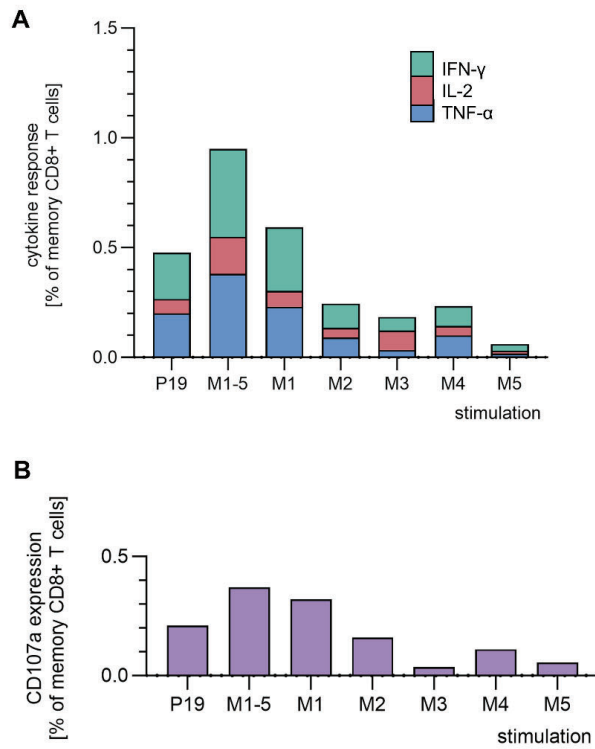
## Supplementary Appendix



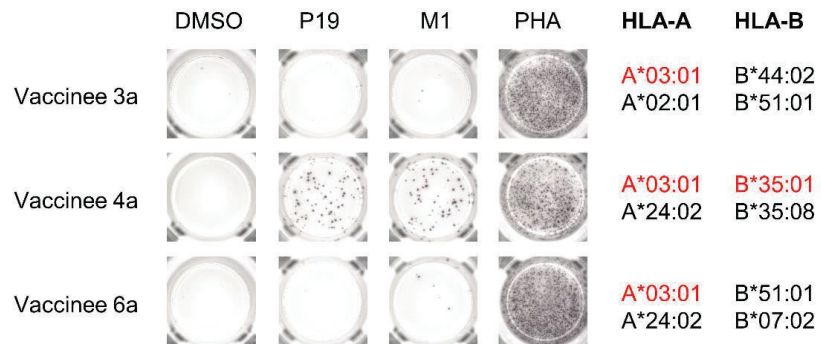
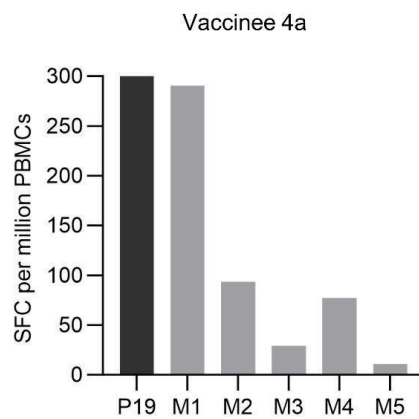
**Supplementary Figure 1: Intracellular staining gating strategy.** Gating strategy for intracellular cytokine staining T cell assay (related to Fig. 2). Memory T cells were identified by exclusion CD45RO-CCR7+ naïve T cells.



**Supplementary Figure 2: Functionality of P19- compared to full MERS-spike-specific CD4+ T cells.** IFN- $\gamma$ , IL-2, TNF- $\alpha$ , and CD107a expression was measured using an intracellular cytokine staining, after re-stimulation with the P19 peptide, M1-M5 pools separately and a combination of all pools (M1-5) covering the whole spike (related to Fig. 2). Cytokine positive cell frequencies are shown as percentages of total memory CD4+ T cells.



**Supplementary Figure 3: Functionality of P19- compared to full MERS-spike-specific CD8+ T cells at V2D7.** IFN- $\gamma$ , IL-2, TNF- $\alpha$ , and CD107a expression was measured using an intracellular cytokine staining, after re-stimulation with the P19 peptide, M1-M5 pools separately and a combination of all pools (M1-5) covering the whole spike. Cytokine **(A)** and CD107a **(B)** positive cell frequencies are shown as percentages of total memory CD8<sup>+</sup> T cells.

**A****B**

**Supplementary Figure 4: IFN- $\gamma$  ELISpot of HLA-B\*35:01 and HLA-A\*03:01 positive MVA-MERS-S phase 1a vaccinees.** Pictures below show representative wells and note the HLA-type of each vaccinee (**A**). The bar graph shows the frequencies of T cells specific for the P19-peptide (black) and peptide pools M1-M5 (grey) covering the complete MERS-CoV spike protein of vaccine 4a who responded to P19 (**B**).

**Supplementary Table 1:** List of customized MERS-S M1 single pool peptides P1-P65 assessed in this study. All MERS-S 15-mer peptides were customized by JPT and had a purity of > 70%.

<b>MERS-S Pool 1 Single Peptide</b>	<b>Sequence</b>
MERS-S Pool 1, Peptide 1	MIHSVFLLMFLLTPT
MERS-S Pool 1, Peptide 2	VFLLMFLLTPTESYV
MERS-S Pool 1, Peptide 3	MFLLTPTESYVDVGP
MERS-S Pool 1, Peptide 4	TPTESYVDVGPDSVK
MERS-S Pool 1, Peptide 5	SYVDVGPDSVKSACI
MERS-S Pool 1, Peptide 6	VGPDSVKSACIEVDI
MERS-S Pool 1, Peptide 7	SVKSACIEVDIQQTF
MERS-S Pool 1, Peptide 8	ACIEVDIQQTFDDKT
MERS-S Pool 1, Peptide 9	VDIQQTFDDKTWPRP
MERS-S Pool 1, Peptide 10	QTFDDKTWPRPIDVS
MERS-S Pool 1, Peptide 11	DKTWPRPIDVSKADG
MERS-S Pool 1, Peptide 12	PRPIDVSKADGIIYP
MERS-S Pool 1, Peptide 13	DVSKADGIIYPQGRT
MERS-S Pool 1, Peptide 14	ADGIIYPQGRYSNI
MERS-S Pool 1, Peptide 15	IYPQGRYSNITITY
MERS-S Pool 1, Peptide 16	GRTYSNITITYQGLF
MERS-S Pool 1, Peptide 17	SNITITYQGLFPYQG
MERS-S Pool 1, Peptide 18	ITYQGLFPYQGDHGD
<b>MERS-S Pool 1, Peptide 19</b>	<b>GLFPYQGDHGDMYVY</b>
MERS-S Pool 1, Peptide 20	YQGDHGDMYVYSAGH
MERS-S Pool 1, Peptide 21	HGDMYVYSAGHATGT
MERS-S Pool 1, Peptide 22	VVYSAGHATGTTTPQK
MERS-S Pool 1, Peptide 23	AGHATGTTTPQKLFVA
MERS-S Pool 1, Peptide 24	TGTTTPQKLFVANYSQ
MERS-S Pool 1, Peptide 25	PQKLFVANYSQDVKQ
MERS-S Pool 1, Peptide 26	FVANYSQDVKQFANG
MERS-S Pool 1, Peptide 27	YSQDVKQFANGFVVR
MERS-S Pool 1, Peptide 28	VKQFANGFVVRIGAA
MERS-S Pool 1, Peptide 29	ANGFVVRIGAAANST
MERS-S Pool 1, Peptide 30	VVRIGAAANSTGTVI
MERS-S Pool 1, Peptide 31	GAAANSTGTVIISPS
MERS-S Pool 1, Peptide 32	NSTGTVIISPSTSAT
MERS-S Pool 1, Peptide 33	TVIISPSTSATIRKI
MERS-S Pool 1, Peptide 34	SPSTSATIRKIYPAF
MERS-S Pool 1, Peptide 35	SATIRKIYPAFMLGS
MERS-S Pool 1, Peptide 36	RKIYPAFMLGSSVGN
MERS-S Pool 1, Peptide 37	PAFMLGSSVGNFSDG
MERS-S Pool 1, Peptide 38	LGSSVGNFSDGKMGR
MERS-S Pool 1, Peptide 39	VGNFSDGKMGRFFNH
MERS-S Pool 1, Peptide 40	SDGKMGRFFNHTLVL
MERS-S Pool 1, Peptide 41	MGRFFNHTLVLLPDG
MERS-S Pool 1, Peptide 42	FNHTLVLLPDGCGTL
MERS-S Pool 1, Peptide 43	LVLLPDGCGTLLRAF
MERS-S Pool 1, Peptide 44	PDGCGTLLRAFYCIL

MERS-S Pool 1, Peptide 45	GTLLRAFYCILEPRS
MERS-S Pool 1, Peptide 46	RAFYCILEPRSGNHC
MERS-S Pool 1, Peptide 47	CILEPRSGNHCPAGN
MERS-S Pool 1, Peptide 48	PRSGNHCPAGNSYTS
MERS-S Pool 1, Peptide 49	NHCPAGNSYTSFATY
MERS-S Pool 1, Peptide 50	AGNSYTSFATYHTPA
MERS-S Pool 1, Peptide 51	YTSFATYHTPATDCS
MERS-S Pool 1, Peptide 52	ATYHTPATDCSDGNY
MERS-S Pool 1, Peptide 53	TPATDCSDGNYNRNA
MERS-S Pool 1, Peptide 54	DCSDGNYNRNASLNS
MERS-S Pool 1, Peptide 55	GNYNRNASLNSFKEY
MERS-S Pool 1, Peptide 56	RNASLNSFKEYFNLR
MERS-S Pool 1, Peptide 57	LNSFKEYFNLRNCTF
MERS-S Pool 1, Peptide 58	KEYFNLRNCTFMYTY
MERS-S Pool 1, Peptide 59	NLRNCTFMYTYNITE
MERS-S Pool 1, Peptide 60	CTFMYTYNITEDEIL
MERS-S Pool 1, Peptide 61	YTYNITEDEILEWFG
MERS-S Pool 1, Peptide 62	ITEDEILEWFGITQT
MERS-S Pool 1, Peptide 63	EILEWFGITQTAQGV
MERS-S Pool 1, Peptide 64	WFGITQTAQGVHLFS
MERS-S Pool 1, Peptide 65	TQTAQGVHLFSSRYV

**Supplementary Table 2:** Characteristics of the 23 analysed participants enrolled in the MVA-MERS-S-study at baseline. The data in the right column depicts the characteristics of the study participant described in this report. Modified from Koch et al. (2020).

Characteristics	Total number	Percentage	Study participant
<b>Age</b>			
Mean (range) [yr]	28.2 (18-47)	-	18
Median (SD) [yr]	28 (7.5)	-	
<b>Sex</b>			
Female	18	78.3%	Female
Male	5	21.7%	
<b>Body Mass Index</b>			
Mean $\pm$ SD [kg/m <sup>2</sup> ]	23.4 $\pm$ 3.0	-	19
<b>Ethnicity</b>			
White	22	95.7%	White
Black or African	0	0%	
<b>American</b>			
Native Hawaiian or	1	4.3%	
<b>Pacific Islander</b>			
Asian	0	0%	



**Supplementary Table 5: Multiple Sequence alignment of human *Betacoronavirus* spike proteins using the Clustal Omega we server. The MERS-S P19 peptide is highlighted in yellow.**

hCoV-OC43	----MFLILLISLPT-AFAVIGDLKCTSDNIN----D--KDTGPPPISTDTVDVTNGLGT	49
hCoV-HKU1	----MLLIIFILPT-TLAVIGDFNCTNFAIN----D--KNTTVPRISEYVVDVSYGLGT	48
MERS-CoV	MIHSVFLLMFLLTPTESYVDVGPDSVKSACIEVDIQQTFFDKTW---PRP-IDVSKADGI	56
SARS-CoV-2	----MFVFLVLLPLV-S-----SQCVN--LTT--RTQLP---PAY--TNSFTRGV	36
SARS-CoV	----MFIFLLFLTLT-S-----GSDL-D--RCTTFDDVQA---PNYTQHTSSMRGV	40
	: : : : : . : . : : : : : : : : *	
hCoV-OC43	YYVLDRVYLNNTTFLNGYYPTSGSTYRNM-----ALKGSVLLSR--LWFKPPFLSDFIN	101
hCoV-HKU1	YYILDRVYLNNTTILFTGYFPKSGANFRDL-----SLKGTTYLST--LWYQKPFLSDFNN	100
MERS-CoV	IYPQGRYTSNITITYQGLR-PYQGDHGDMMYVY SAGHATGTTTPQKLFVANYSQD-VKQFAN	114
SARS-CoV-2	YYPDKVFRSSVLHSTQDLFLPFFSNVT---WFHAIHVS GTNGTKR----FDNP-VLPFND	88
SARS-CoV	YYPDEIFRSDTLYLTQDLFLPFFSNVT---GFHTIN-----HT----FDNP-VIPFKD	85
	* . . . : . . . : . : : : : * : :	
hCoV-OC43	GIFAKVKNTKVIKDRVM-----YSEFPAITIGSTFVNTSY-----SVVVQPR	143
hCoV-HKU1	GIFSRVKNTKLYVNKTL-----YSEFSTIVIGSVFINNSY-----TIVVQPH	142
MERS-CoV	GFVVRIGAAANSTGTVIISPSTSATIRKIYPAFMLGSSVGNFSDGKMGRRFNHTLVLLPD	174
SARS-CoV-2	GVYFASTE-----KSNIIIRGWI FGTTLDSKTQ-----SLLIVNN	122
SARS-CoV	GIYFAATE-----KSNVVRGWVFGSTMNKSQ-----SVIIINN	119
	* . . . : : * : : : : : : : : :	
hCoV-OC43	TINSTQDGDNKLQGLLEVSVQCYNMCEYPQTICHPNLGNHRKELWHLDTGVVSC-----	197
hCoV-HKU1	-----NGVLEITACQYTMCEYPHTICKS-KGSSRNESWHFDKSEPLC-----	183
MERS-CoV	-----G-----CGTLLRAF--YCILEPRSGNHCPAGNSYTSFATYHTPATDCSDGNYN	220
SARS-CoV-2	-----A-----TNVVIKVCFEQFCNDPFLGVYHKNN-----	149
SARS-CoV	-----S-----TNVVIRACNFELCDNPFFAVSKEMGT-----	146
	: . . * . . .	
hCoV-OC43	-----LYKRNFTYDVN--AD-----YLY-----FHFYQEGGTFYAYFTDT-	230
hCoV-HKU1	-----LFKKNFTYNVS--TD-----FLY-----FHFYQERGTFYAYADS-	216
MERS-CoV	RNASLNSFKEYFNLRNCTFMITYNITEDEILEWFGITQTAQG-VHLFSSRYVDLYGGR--	277
SARS-CoV-2	KSWMESEFRVYSSANCTFEYVVSQPFMLDLEGGKQGNFKNLREFVFKNIDGYFKIYKSHTP	209
SARS-CoV	----QHTMIFDNFNCTFEYISDAFSLDVSEKSGNFKHLREFVFKNKDGFYLVYKGYQP	202
	: . * * . . . . *	
hCoV-OC43	-----GVV-TKFLFNVYLGMAISHYVVMPLTCNS-----KLTLEYWVTP	268
hCoV-HKU1	-----GMP-TTFLFSLYLGLTLLSHYVYVPLTCNA-----ISSNTDNETLQYWVTP	260
MERS-CoV	-----MFQFATLPVYDTIKYYSIIPHRSIRS---IQSDRKAW---AAFYVYK	317
SARS-CoV-2	INLVRDLPSGFSALEPLVDLPIGINITRFPQTLALHRSYLTLPDSSSGWTAGAAAYVGY	269
SARS-CoV	IDVVRDLPSGFNTLKP I FKLPLGINITNFRAILTAF-----SPAQDTWGTSAAYFVGY	256
	: : : : : : : : : : : *	
hCoV-OC43	LTSRQYLLAFNQDGIIFNAVDCMSDFMSEIKCKTQSIAPPTGVYELNGYTVQPIADVYRR	328
hCoV-HKU1	LSKRQYLLKFDNRGVITNAVDCSSFFSEIQCKTKSLLPNTGVYDLSGFTVKPVATVHRR	320
MERS-CoV	LQPLTFLLDVSVVGYIRRAIDCGFNDSLQHCYSIESFDVESGVYSVSSFEAKPSGVSVEQ	377
SARS-CoV-2	LQPRTFLLKYNENGTITDAVDCALDPLSETKCTLKSFTVEKGIYQTSNFRVQPTESIVRF	329
SARS-CoV	LKPTTFMLKYDENGITITDAVDCSQNPLAELKCSVKSFEIDKGIYQTSNFRVVPDGVVRF	316
	* : * : . * * * : * * . : : : * : * : * : * . . . . *	
hCoV-OC43	KPNLPNCNIEAWLNDKSVPSPLNWERKTFSNCFNMSSLMSFIQADSFTCNNIDAANKIYG	388
hCoV-HKU1	IPDLPCDIDKWLNNFNVPSPLNWERKIFSNCFNLSLTLRLVHTDSFSCNNFDESKIYG	380
MERS-CoV	AEG-VECDFSPLLSG-TPPQVYNFKRLVFTNCNINLTKLLSLFVNDFTCSQISPAAIAS	435
SARS-CoV-2	PNITNLCPFGVEFNATRFASVYAWNRKRISNCVADYSVLYNSASFSTFKCYGVSPTKLND	389
SARS-CoV	ENITNLCPFGVEFNATKFPVSVYAWERKKISNCVADYSVLYNSTFFSTFKCYGVSATKLND	376
	* : : . . . : * : * * : : * . * * . . : : .	
hCoV-OC43	MCFSITIDKFAIPNGRKVDLQLGNLGYLQSFNYRIDTTATSCQLYYNLPAAVSVSRFN	448
hCoV-HKU1	SCFKSIVLDKFAIPNSRRSDLQLGSSGFLQSSNYKIDTSSSCQLYYSLPAINVTINNYN	440
MERS-CoV	NCYSSLILDYFSYPLSMKSDLSVSSAGPISQFNKYQSFNSPTCLL IATVPHNLTITKPK-	494
SARS-CoV-2	LCFTNVYADSFVIRGDEVQRQIAPGQGTGKIADYNYKLPDDFTGCVIAWNSNNLDSKVGGN-	448
SARS-CoV	LCSNVYADSFVVKGDVDRQIAPGQGTGVIADYNYKLPDDFMGCVLAWNRNIDATSTGN-	435
	* : . . . * * . : : . . * : . * * : * : . . .	
hCoV-OC43	PSTWNKRFGFIEDSVFKPRPAGVLTNHDVVYAQHCFKAPKNFCPCCKLNGSCVSGSPGKNN	508
hCoV-HKU1	PSSWNRRYGFNNE-----NLSHSSVYYSRYCFSVNNTFCPCAKPSFAS-SCKSHKP	490

MERS-CoV	-----LKYSYINKCSR-----LLSDDRTEVPQLVNNAN--QYSPCVSI-----V-	530
SARS-CoV-2	-----YNYLYRLFRKS-----NLKPFERDISTEIYQA--GSTPCNGV-----E-	484
SARS-CoV	-----YNYKYRYLRHG-----KLRPFERDISNVPFSP--DGKPCPT-----P-	470
	: : * **	
hCoV-OC43	GIGTCPAGTNYLTCD-----NLCTPDPITFTGTYKCPQTKSLVGI GEHC SGLA	556
hCoV-HKU1	PSASCPIGTNYRSCESTTVLDHTDWCRCSCLPDPI TAYDPRSCS QKSLVGVGEHCAGFG	550
MERS-CoV	-PST-----VWEDGDYRKL--SPLEGGWLVA-----SGST	560
SARS-CoV-2	-GFNC-----YF-----PLQSYGFQPT-----NGVG	504
SARS-CoV	-ALNC-----YW-----PLNDYGFYTT-----TGIG	490
	. * : *	
hCoV-OC43	VKSDYCGG-----NSCTCRPQAF LGSADSC LQGDKCNI FANFILH D VNSGLT CST--D	608
hCoV-HKU1	VDEKCGVLDGSYNVSCLCSTDAFLGWSYDTCVSNRNCNIFSNFILNGINS GTTCSN--D	608
MERS-CoV	VAMT-----EQLQMGF-----GITVQYGTDTNSVC PKLEF	590
SARS-CoV-2	YQPY-----RVVLSF-----ELL---HAPATVCGP---	527
SARS-CoV	YQPY-----RVVLSF-----ELL---NAPATVCGP---	513
	: : . *	
hCoV-OC43	LQKANTDII LGVCVNYDLYGILGQGI FVEVNATYYNSWQNL LYDSNGNLY--GFRDYITNR	667
hCoV-HKU1	LLQNTTEVYTDVCDVYDLYGITGQGI FKEVSVAVYYNSWQNL LYDSNGNII--GFKDFVTNK	667
MERS-CoV	ANDTKIASQLGNCVEYSLYGVSGRQVFNCTAVGV--RQRFFVYDAYQNLVGYYS D--DGN	647
SARS-CoV-2	--KKSTNLVKNKCVNFNFNGLTGTGVLTESNKKFL--PFQFGRDIADTT--DAVRDPQ TLE	583
SARS-CoV	--KLSTDLIKNCVNFNFNGLTGTGVLTPSSKRFQ--PFQFGRDVSDF T--DSVRDPKTSE	569
	. . * * : : * * * * : . * : *	
hCoV-OC43	TFMIRSCYSGRVSAAFH--ANSSE PALLFRN I K C N Y V F N N S L T R Q L Q P I -----N	715
hCoV-HKU1	TYNIFPCYAGRVSAAFH--QNASSLAL LYRN LKCSYV LNNIS---LATQ-----P	712
MERS-CoV	YYCLRACVSVPVSVIYD--KETKTHATLFGSVACEHISSTMSQYSRSTRSMLKRRDSTYG	705
SARS-CoV-2	ILDITPCSFGGVSITPGTNTSNQVAVLYQDVNCTEVPVAIHADQLT--PTWRVYSTGSN	641
SARS-CoV	ILDISPCSFSGGVSITPGTNASSEVAVLYQDVNCTDVS TAIHADQLT--PAWRIYSTGNN	627
	: * ** . : . * * : : * :	
hCoV-OC43	YFDSYLGCVVNAYNSTAISVQTCDLTVGSGYCVDYS----KNRRSRGAI TGYRFTNFE	770
hCoV-HKU1	YFDSYLGCVFNADNLTDYSVSSCALRMGSGFCVDYNSPFS SRRKRRS ISAS YRFVTFE	772
MERS-CoV	PLQTPVGCVLGLVNSS--LFVEDCKLPLGQSLCALPDT PSTLT PRSVRSVPGE--MRLAS I-	762
SARS-CoV-2	VFQTRAGCLIGA EHVN--NSYECDIPIGAGICASYQTQT--NSPRRARSVASQ--SI---I-	693
SARS-CoV	VFQTAQAGCLIGA EHV D--TSYECDIPIGAGICASYHTVS--L---LRSTS QK--SI---V-	675
	: : * * : : * : * : * . * : *	
hCoV-OC43	PFTVNS--VNDSLEPVGGLYEIQIPSEFTIGNMVEFIQTSSPKVTIDCAAFVCGDYAACKS	829
hCoV-HKU1	PFNVSF--VNDSIESVGLYEIKIPTNFTIVGQEEFIQTNSPKVTIDCSLFVCSNYAACHD	831
MERS-CoV	AFNHPIQV--DQL--NSSYFKLSIPTNFSFGVTQEYIQTITQKVTVDCKQYV CNGFQKCEQ	819
SARS-CoV-2	AYTMSLGAENSV--AYSNN SIAIPTNFTISVTEILPVMSTKTSVDCTMYICGDS TECSN	751
SARS-CoV	AYTMSLGAENSV--AYSNN SIAIPTNFTISVTEILPVMSTKTSVDCTMYICGDS TECSN	733
	: . . : : . : * * : : * : * : * : * : *	
hCoV-OC43	QLVEYGSFCDNINAILTEVNE LLDTTQLQVANSLMNGVTLSTK LKDG VNFVDDINFSPV	889
hCoV-HKU1	LLSEYGTFCDNINSILDEVNGLLDTTQLHVADTLMQGVTLSSNLNLTNLHFDVDNINFKSL	891
MERS-CoV	LLREYGFQCSKINQALHGANLRQDDSVRNLFASVKSSQSSPIIPGFG-----GDFNL TLL	874
SARS-CoV-2	LLLQYGSFCTQLNRALTGIAVEQDKNTQEVFAQVQVIYKTPPIKDFG-----GF-NFSQI	805
SARS-CoV	LLLQYGSFCTQLNRALS G IAAEQDRNTREVFQAQVKMYKPTPLKYFG-----GF-NFSQI	787
	* : * * * : * * * : * : . : . : . : * : *	
hCoV-OC43	LGCLGSECSKASSRS AIEDLLFDKVKLS DVG FVEAYNNCT--GGAEIRD LICVQSYKGIK	947
hCoV-HKU1	VGCLGPHCGS--SSRSFFEDLLFDKVKLS DVG FVEAYNNCT--GGSEIRD LLCVQSFNGIK	948
MERS-CoV	EP--VSI STGSR SRS AIEDLLFDKVTIADPGYMQGYD DCMQGGPASARD LICAYVAGYK	933
SARS-CoV-2	LP-DP---SKPSKR SFIEDLLFNKVT LADAGFIKQYGDCL--GDIAARD LICAQKFNGLT	859
SARS-CoV	LP-DP---LKPTKRS FIEDLLFNKVT LADAGFMKQYGECL--GDINARD LICAQKFNGLT	841
	. : * * : * * * * : * * : : * : * * * * : * *	
hCoV-OC43	VLPPLLSENQISGYTLAATSASLFPWP TAA---AGVPFYLNVQYR INGLGVTMDVLSQN	1003
hCoV-HKU1	VLPPILSESQISGYTTAATVAAMFP PWSAA---AGIPFSLNVQYR INGLGVTMDV LNKN	1004
MERS-CoV	VLPP LMDVNMEAA YTSLLGSIAGVGWTAGLSSFAAI PFAQSI FYRLNGVITQQVLS EN	993
SARS-CoV-2	VLPP L L T D E M I A Q Y T S A L L A G T I T S G W T F G A G A A L Q I P F A M Q M A Y R F N G I G V T Q N V L Y E N	919
SARS-CoV	VLPP L L T D D M I A A Y T A A L V S G T A T A G W T F G A G A A L Q I P F A M Q M A Y R F N G I G V T Q N V L Y E N	901
	* * * * : : . : * * : . * : . : * * : : * * * * : * * * : *	
hCoV-OC43	QKLIANAFNNALYAIQEGFDATNSALVKIQAVVNANA EALNNLQQLS NRFGAISASLQE	1063
hCoV-HKU1	QKLIATAFNALLSIQNGFSATNSALAKIQSVVNNAQALNSLLQQLFNKFGAISSSLQE	1064
MERS-CoV	QKLIANKFNQALGAMQTGF TTTNEAFQKQVQD VNNNAQALSKLASELSNTFGAISASIGD	1053



**Supplementary Table 3:** MERS-S epitopes predicted to be strong HLA-B\*35:01 binders (% rank < 0.5) using the NetMHCpan - 4.1 software. Epitopes overlapping with P19 are highlighted in grey.

allele	start	end	length	peptide	score	percentile rank
HLA-B*35:01	284	292	9	LPVYDTIKY	0.992963	0.01
HLA-B*35:01	75	85	11	FPYQGDHGDYMY	0.988827	0.01
HLA-B*35:01	970	978	9	IPFAQSIFY	0.988076	0.01
HLA-B*35:01	786	794	9	FSFGVTQEY	0.978991	0.01
HLA-B*35:01	75	87	13	FPYQGDHGDYMYVY	0.975461	0.01
HLA-B*35:01	633	641	9	DAYQNLVGY	0.936625	0.03
HLA-B*35:01	1036	1044	9	LASELSNTF	0.9327	0.03
HLA-B*35:01	1142	1153	12	YPSNHIEVVSAY	0.931641	0.03
HLA-B*35:01	766	777	12	HPIQVDQLNSSY	0.911709	0.04
HLA-B*35:01	569	577	9	MGFGITVQY	0.876102	0.05
HLA-B*35:01	284	293	10	LPVYDTIKYY	0.872338	0.05
HLA-B*35:01	555	563	9	VASGSTVAM	0.851512	0.06
HLA-B*35:01	75	84	10	FPYQGDHGDYMY	0.828621	0.07
HLA-B*35:01	1195	1204	10	EPITSLNTKY	0.77512	0.09
HLA-B*35:01	655	663	9	VSPVSVIY	0.748666	0.1
HLA-B*35:01	1142	1150	9	YPSNHIEVV	0.740425	0.1
HLA-B*35:01	10	18	9	FLLTPTESY	0.729393	0.11
HLA-B*35:01	199	207	9	NSYTSFATY	0.729038	0.11
HLA-B*35:01	782	794	13	IPNFSGVTQEY	0.715325	0.12
HLA-B*35:01	58	71	14	YPQGRYTSNITITY	0.695981	0.13
HLA-B*35:01	283	292	10	TLPVYDTIKY	0.67593	0.13
HLA-B*35:01	429	438	10	SPAAIASNCY	0.673934	0.13
HLA-B*35:01	56	64	9	IYYPQGRTY	0.669525	0.13
HLA-B*35:01	1204	1211	8	YVAPQVTY	0.654079	0.13
HLA-B*35:01	681	689	9	HISSTMSQY	0.637099	0.15
HLA-B*35:01	769	777	9	QVDQLNSSY	0.629193	0.15
HLA-B*35:01	533	541	9	TVWEDGDYY	0.625745	0.15
HLA-B*35:01	514	523	10	VPQLVNANQY	0.618331	0.15
HLA-B*35:01	281	292	12	FATLPVYDTIKY	0.614785	0.16
HLA-B*35:01	780	788	9	LSIPTNFSF	0.613408	0.16
HLA-B*35:01	967	978	12	FAAIPFAQSIFY	0.59598	0.17
HLA-B*35:01	195	204	10	CPAGNSYTSF	0.5834	0.17
HLA-B*35:01	561	569	9	VAMTEQLQM	0.565008	0.19
HLA-B*35:01	1256	1264	9	NTLLDLTY	0.561576	0.19
HLA-B*35:01	96	105	10	TPQKLFVANY	0.540863	0.21
HLA-B*35:01	1184	1192	9	WSYTGSSFY	0.535099	0.22
HLA-B*35:01	279	287	9	FQFATLPVY	0.531689	0.22
HLA-B*35:01	64	71	8	YSNITITY	0.51915	0.22

HLA-B*35:01	386	397	12	SPLLSGTTPPVY	0.509222	0.23
HLA-B*35:01	969	978	10	AIPFAQSIFY	0.502182	0.23
HLA-B*35:01	1192	1200	9	YAPEPITSL	0.499505	0.23
HLA-B*35:01	308	316	9	KAWAAFVYVY	0.497469	0.23
HLA-B*35:01	319	327	9	QPLTFLLDF	0.496951	0.23
HLA-B*35:01	448	456	9	YPLSMKSDL	0.456832	0.26
HLA-B*35:01	46	58	13	RPIDVSKADGIY	0.456191	0.26
HLA-B*35:01	1272	1280	9	VVKALNESY	0.453888	0.27
HLA-B*35:01	968	978	11	AAIPFAQSIFY	0.44856	0.27
HLA-B*35:01	1145	1153	9	NHIEVVSAY	0.440703	0.28
HLA-B*35:01	343	351	9	DLSQLHCSY	0.432436	0.29
HLA-B*35:01	766	773	8	HPIQVDQL	0.423642	0.3
HLA-B*35:01	900	909	10	IADPGYMQGY	0.410211	0.31
HLA-B*35:01	530	541	12	VPSTVWEDGDYY	0.409431	0.31
HLA-B*35:01	785	794	10	NFSFGVTQEY	0.404677	0.31
HLA-B*35:01	633	642	10	DAYQNLVGY	0.403071	0.32
HLA-B*35:01	352	361	10	ESFDVESGVY	0.400968	0.32
HLA-B*35:01	172	180	9	LPDGC GTLL	0.400751	0.32
HLA-B*35:01	970	977	8	IPFAQSIF	0.389297	0.33
HLA-B*35:01	69	77	9	ITYQGLFPY	0.378013	0.34
HLA-B*35:01	1163	1171	9	NCIAPVNGY	0.372321	0.35
HLA-B*35:01	632	641	10	YDAYQNLVGY	0.369111	0.35
HLA-B*35:01	459	467	9	SSAGPISQF	0.358234	0.36
HLA-B*35:01	63	71	9	TYSNITITY	0.351844	0.37
HLA-B*35:01	489	497	9	TTITKPLKY	0.335614	0.39
HLA-B*35:01	766	778	13	HPIQVDQLNSSYF	0.331209	0.39
HLA-B*35:01	738	745	8	LPDTPSTL	0.319647	0.4
HLA-B*35:01	729	738	10	LPLGQSLCAL	0.308649	0.41
HLA-B*35:01	389	397	9	LSGTPPVY	0.307979	0.41
HLA-B*35:01	282	292	11	ATLPVYDTIKY	0.30616	0.41
HLA-B*35:01	935	943	9	LPPLMDVNM	0.30267	0.41
HLA-B*35:01	222	231	10	NASLNSFKEY	0.299597	0.42
HLA-B*35:01	74	85	12	LFPYQGDHGDY	0.297851	0.42
HLA-B*35:01	258	266	9	QTAQGVHLF	0.297206	0.42
HLA-B*35:01	491	499	9	ITKPLKYSY	0.291933	0.43
HLA-B*35:01	1193	1204	12	APEPITSLNTKY	0.291805	0.43
HLA-B*35:01	75	86	12	FQYQGDHGDYV	0.269157	0.46
HLA-B*35:01	709	717	9	TPVGCVLGL	0.265006	0.48

**Supplementary Table 4:** MERS-S epitopes predicted to be strong HLA-A\*03:01 binders (% rank < 0.5) using the NetMHCpan - 4.1 software. Epitopes overlapping with P19 are highlighted in grey.

allele	start	end	length	peptide	score	Percentile rank
HLA-A*03:01	42	52	11	KTWPRPIDVSK	0.919727	0.02
HLA-A*03:01	62	71	10	RTYSNITITY	0.838926	0.05
HLA-A*03:01	359	369	11	GVYSVSSFEAK	0.827648	0.06
HLA-A*03:01	1275	1284	10	ALNESYIDLK	0.804656	0.08
HLA-A*03:01	758	766	9	RLASIAFNH	0.72362	0.14
HLA-A*03:01	1025	1035	11	AVNNNAQALSK	0.715454	0.15
HLA-A*03:01	1102	1112	11	KVNECVKAQSK	0.691151	0.17
HLA-A*03:01	482	493	12	ATVPHNLTITK	0.68517	0.17
HLA-A*03:01	56	64	9	IYYPQGRTY	0.674618	0.18
HLA-A*03:01	282	291	10	ATLPVYDTIK	0.640538	0.21
HLA-A*03:01	459	470	12	SSAGPISQFNYK	0.622	0.23
HLA-A*03:01	1092	1100	9	AALSAQLAK	0.621145	0.23
HLA-A*03:01	493	502	10	KPLKYSYINK	0.538059	0.29
HLA-A*03:01	299	308	10	SIRSIQSDRK	0.515772	0.32
HLA-A*03:01	687	698	12	SQYSRSTRSMLK	0.504269	0.33
HLA-A*03:01	1093	1102	10	ALSAQLAKDK	0.489793	0.35
HLA-A*03:01	1266	1274	9	MLSLQQVVK	0.481924	0.37
HLA-A*03:01	69	77	9	ITYQGLFPY	0.471845	0.38
HLA-A*03:01	489	497	9	TTITKPLKY	0.456958	0.4
HLA-A*03:01	845	854	10	SVRNLFASVK	0.45648	0.4
HLA-A*03:01	807	816	10	KQYVCNGFQK	0.453291	0.4
HLA-A*03:01	308	317	10	KAWAAFVYVK	0.407662	0.47
HLA-A*03:01	130	142	13	VIISPSTSATIRK	0.406598	0.47

**III. SARS-CoV-2-specific cellular response following third COVID-19 vaccination in patients with chronic lymphocytic leukemia**

Sibylle C. Mellinshoff\*, **Leonie Mayer\***, Sandra Robrecht, Leonie M. Weskamm, Christine Dahlke, Henning Gruell, Maïke Schlotz, Kanika Vanshylla, Hans A. Schloser, Martin Thelen, Anna-Maria Fink, Kirsten Fischer, Florian Klein, Marylyn M. Addo, Barbara Eichhorst, Michael Hallek, Petra Langerbeins

\*These authors contributed equally.

Published in *Haematologica* **107**, 2480–2484 (2022)

doi: [10.3324/haematol.2022.280982](https://doi.org/10.3324/haematol.2022.280982)

## LETTER TO THE EDITOR

## SARS-CoV-2-specific cellular response following third COVID-19 vaccination in patients with chronic lymphocytic leukemia

With great interest we read the study published by Blixt *et al.* showing that compared to healthy controls (HC), half as many of chronic lymphocytic leukemia (CLL) patients developed a T-cell response after two COVID-19 vaccine doses.<sup>1</sup> Effects of a third vaccine dose on T cells in CLL patients is yet unknown, while approximately 20% fail achieving a humoral immune response.<sup>2</sup> In this prospective cohort study we investigated the interplay of humoral and cellular response and report follow-up data of CLL patients 31 days (range, 19-94 days) after third vaccination (V3).<sup>3</sup>

Blood samples of CLL registry (clinicaltrials.gov. Identifier: NCT02863692) patients were evaluated after three COVID-19 vaccinations. Six of the initially 21 patients<sup>3</sup> were included in the analyses, three with homologous and three with heterologous vaccination schedule (mean interval between vaccination 2 [V2] and V3 163 days; minimum 117 days and maximum 189 apart). Four vaccinated health care workers served as HC (mean interval between V2 and V3 266 days; range, 254-291 days). Both studies were approved by the local ethics committee. Patient and disease characteristics as well as vaccination schedules are summarized in Table 1.

SARS-CoV-2 spike receptor binding domain (RBD)-specific immunoglobulin G (IgG) antibodies, determined using the Alinity ci SARS-CoV-2 IgG II Quant assay (Abbott), were detectable in four of six (66.7%) CLL patients after compared to two of six (33.3%) before booster vaccination (Figure 1A), cut-off  $\geq 7.1$  BAU/mL. In the one individual with detectable RBD-specific IgG after V2, V3 resulted in increased levels. In another individual, the V3 raised the IgG titer to similar levels as seen shortly after V2 (Figure 1B and C). Detectable neutralizing serum activity, determined by a lentivirus-based pseudovirus neutralization assay against the Wu01 strain of SARS-CoV-2 was limited to the two individuals with the highest levels of RBD-binding IgG (Figure 1D).

Peripheral blood mononuclear cells (PBMC) were used for SARS-CoV-2 spike-specific T-cell analyses (Human IFN $\gamma$  ELISpot<sup>PLUS</sup> [ALP] kit [Mabtech]). Results are reported as spot-forming cells (SFC) per million PBMC. A SARS-CoV-2 peptide pool (15-mers overlapping by 11 amino acids which stimulate responses mediated by both CD4 + and CD8 + T cells) spanning the entire spike protein was used for measuring T-cell responses. The median number of SARS-CoV-2 spike-specific T cells in the CLL cohort after V2

BNT162b was 31 SFC (interquartile range [IQR], 4.0-96.0) (Figure 2A). The response after V2 in the here described subgroup was significantly lower (1.7 SFC; IQR, 0.0-3.8 but increased to 8 SFC; IQR, 5.7-21.3) after booster vaccination. Overall, four of six (66.7%) showed a detectable increase of T-cell activity and two a decrease (Figure 2B). In comparison, T-cell responses in HC remained above the cut-off in 100% (4/4), but did not increase further.

Of the included patients, all received either B-cell-depleting (anti-CD20 monoclonal antibodies) or -directed (bruton tyrosine kinase inhibitors) treatment within 6 months prior to V3. Despite B-cell-affecting treatment, the majority (4/6) showed an increase of serum IgG (Figure 1C). Patients under B-cell-depleting treatment (2/6) mounted low levels of IgG antibodies after boost that did not result in detectable neutralizing serum activity (Table 1). Patients without detectable T cells prior to boost that received a heterologous booster immunization showed an increase in T-cell response. In contrast, homologous booster led to an increase in only one of three patients and did not show an effect on the remaining two patients (Figure 2B). A discordant immune response with T cell, but lacking humoral response was seen in two of six patients, indicating that cellular protection may be generated, probably in patients with lesser extent of CLL-associated T-cell exhaustion, whereas treatment-associated B-cell impairment may not be overcome.

In conclusion, we report an increase of vaccine-induced cellular and humoral immune responses in CLL patients by a V3 COVID-19 vaccination.

Recent data showed a significant increased humoral response after COVID-19 vaccination, but less pronounced enhancement of the cellular response in healthy individuals, likely to be dependent on the specific booster vaccine.<sup>4-6</sup> Our data from the HC cohort – all vaccinated with a homologous BNT162b2 dose – confirm these findings and show a stable, but not relevantly increased T-cell response. As already shown for rheumatologic and solid organ transplant patients, this may not generally be the case for immunocompromised patients.<sup>7,8</sup>

We here report an increase of the humoral response in CLL patients after COVID-19 V3 despite B-cell-depleting treatment, as reported elsewhere,<sup>9</sup> and in addition, an increase of the cellular response in four of six patients.

Our data show that V3 enhances IgG response in CLL patients, also in those that lacked detectable IgG after V2.



LETTER TO THE EDITOR

**Table 1.** Patient characteristics and outcomes versus healthy controls.

Patient	Sex	Age in years	Vaccine (Prime)	Vaccine (Boost)	Days of sampling after booster	After V2			After V3			B-cell-depleting therapy	B-cell-directed therapy	State of disease
						IgG**	Serum ID <sub>50</sub> ***	T cells*	IgG**	Serum ID <sub>50</sub> ***	T cells*			
1	M	78	BNT/BNT	BNT	13	33	<10	4	42,9	44	25	No	Yes	PR
2	M	78	BNT/BNT	AZD	31	neg.	<10	0	neg.	<10	9	No	Yes	PR
3	M	76	BNT/BNT	BNT	28	2.225	1.206	3	10.999	19.214	0	No	Yes	PR
4	M	71	BNT/BNT	AD	63	neg.	<10	0	8,3	<10	7	Yes	Yes	CR
5	F	73	BNT/BNT	AD	36	neg.	<10	0	11,8	<10	81	Yes	No	CR
6	M	71	BNT/BNT	BNT	31	neg.	<10	23	neg.	<10	5	No	Yes	PD

Healthy control	Sex	Age in years	Vaccine (Prime)	Vaccine (Boost)	Days of sampling after booster	After V2		After V3	
						T cells*	IgG**	T cells*	IgG**
1	F	25	BNT/BNT	BNT	28	165.3	202.7	404	428
2	M	30	BNT/BNT	BNT	28	381.3	428	428	77.3
3	F	38	BNT/BNT	BNT	37	692	116	116	116
4	F	49	BNT/BNT	BNT	27	116	116	116	116

\*S-specific T cells (spot-forming cells/10<sup>6</sup> peripheral blood mononuclear cells); \*\*RBD-specific IgG (BAU/mL); \*\*\*neutralization activity (serum ID50 Wu01 Pseudovirus). V2: second vaccination; V3: third vaccination; IgG: immunoglobulin G; F: female; M: male; ID<sub>50</sub>: infective dose; AD: Ad26.COVID, AZ: AZD1222, BNT: BNT162b2; CR: complete remission; PD: progressive disease; PR: partial remission; neg: negative.

## LETTER TO THE EDITOR

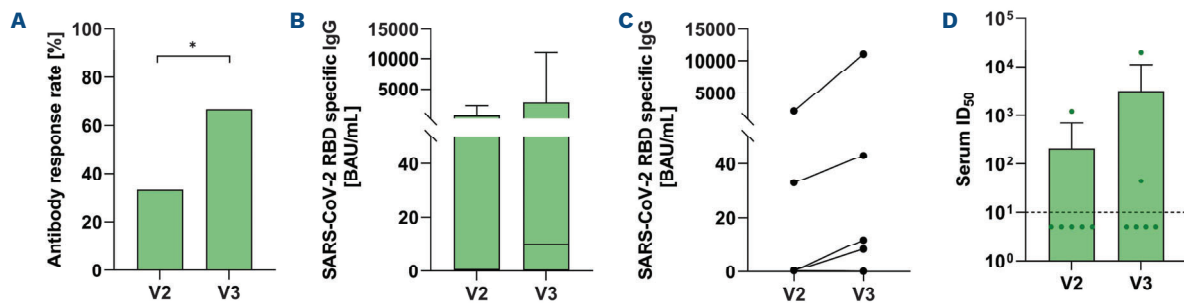


**Figure 1. Humoral immune responses after COVID-19 vaccination** (A) Antibody response rate in chronic lymphocytic leukemia (CLL) patients after second (V2) and after third (V3) vaccination. (B) SARS-CoV-2 spike receptor binding domain (RBD)-specific immunoglobulin G (IgG) in CLL patients after V2 and V3 (median 10.05 BAU/ml, range 0.1-10,998.6) measured by chemiluminescent microparticle immunoassay. (C) Individual course of IgG anti-bodies in CLL patients after V2 and V3. (D) Serum neutralizing activity (50% inhibitory serum dilution) determined in a pseudovirus neutralizing assay against the Wu-01 pseudovirus strain. Bars indicating geometric mean ID<sub>50</sub> with 95% confidence intervals. Dashed line indicates limit of detection (LOD, 10). Samples with no detectable neutralization (ID<sub>50</sub> <10) were plotted with an ID<sub>50</sub> of 5 (1/2 LOD) for graphical representation.

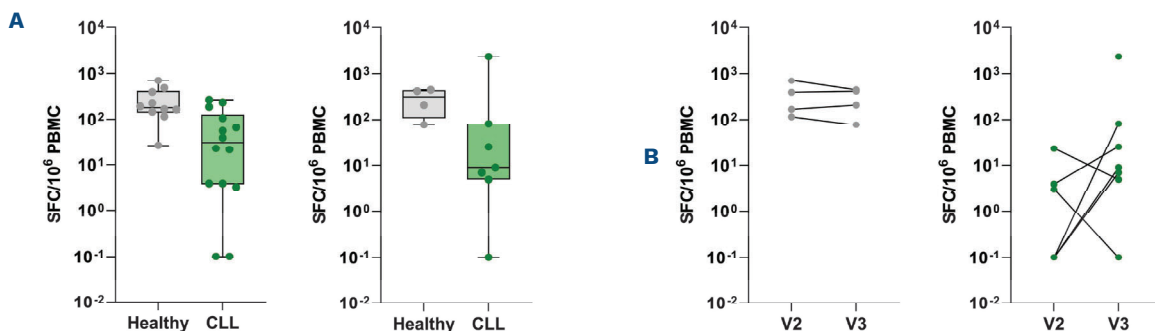


**Figure 2. T-cell immune responses after COVID-19 vaccination.** (A) Interferon- $\gamma$  T-cell ELISpot response in chronic lymphocytic leukemia (CLL) patients and healthy controls (HC). Shown values are mean spots of duplicate wells, where background in negative control wells is subtracted from peptide-stimulated wells. The line displays the median response after second (V2) (left) and third (V3) vaccination (right). The limit of detection is 8 spot-forming cells/10<sup>6</sup> peripheral blood mononuclear cells. Samples were acquired 28 days after V3 in HC and at a median of 47 and 31 days (V2 and V3, respectively) in CLL patients. (B) Individual course of Interferon- $\gamma$  T cell ELISpot response in HC (left) and CLL patients (right) after V2 and V3.

We found that anti-SARS CoV-2 antibodies were higher in patients who received three doses of BNT162b2 compared to two doses of BNT162b2 and a vector vaccine as booster, but that the latter vaccine combination was able to mount a serologic response in two of three previously negative patients. Yet, neutralizing serum activity was only partly detectable. In order to elicit a neutralizing serum response, a fourth dose might be beneficial by further increasing IgG levels.<sup>10,11</sup>

We can confirm previous data from immunocompromised patients with rheumatological disease,<sup>7</sup> solid organ transplantation<sup>8</sup> and solid malignancies<sup>12</sup> within our CLL cohort revealing that T-cell responses are enhanced following V3. Further indepth analyses may provide insights into their (poly-)functionality, proliferation capacity, or epigenetic profile change after (booster) vaccination despite the low

response-altitude and whether the response is biased towards CD4+ or CD8+ T cells.

Interestingly, all patients who received a heterologous boost (vector vaccine) showed an increased T cell response compared to our previous analysis, while only one of three after homologous boost. This supports recently published data from randomized controlled as well as observational studies suggesting a benefit of a heterologous boost for eliciting stronger T-cell responses compared to homologous immunization.<sup>4,13</sup> If this offers additional protection for patients with low or absent neutralizing antibodies is yet unclear, particularly considering the low response levels with respect to quantity. Considering recent data on SARS-CoV-2-specific T cells from patients with agammaglobulinaemia<sup>14,15</sup> showing protection from severe disease and even in patients infected with variants

## LETTER TO THE EDITOR

of concern,<sup>16</sup> we hypothesize a potential benefit of increased T-cell immunity. The impact of a fourth vaccine dose on altitude and functionality of T cells should be subject of forthcoming studies.

A limitation of this study is the small sample size. In addition, our small cohort consists of mostly male and comparably old patients. Male sex and advanced age known as relevant factors for an impaired immune response which likely affect our results, but also reflect the CLL patient population well.

In conclusion, we demonstrate an inferior T-cell response to COVID-19 vaccines in CLL patients as compared to HC, but possibly higher capacity in those patients to boost such response by V3 COVID-19. While the ideal primeboost regime is yet to determine, our data encourage to evaluate heterologous immunization by clinical trials in CLL patients.

## Authors

Sibylle C. Mellingshoff,<sup>1,2,3\*</sup> Leonie Mayer,<sup>3,4,5\*</sup> Sandra Robrecht,<sup>1</sup> Leonie M. Weskamm,<sup>3,4,5</sup> Christine Dahlke,<sup>3,4,5</sup> Henning Gruell,<sup>5</sup> Maïke Schlotz,<sup>6</sup> Kanika Vanshylla,<sup>6</sup> Hans A. Schlöber,<sup>7</sup> Martin Thelen,<sup>7</sup> AnnaMaria Fink,<sup>1</sup> Kirsten Fischer,<sup>1</sup> Florian Klein,<sup>2,6,7</sup> Marylyn M. Addo,<sup>3,4,5</sup> Barbara Eichhorst,<sup>1</sup> Michael Hallek<sup>1</sup> and Petra Langerbeins<sup>1</sup>

<sup>1</sup>Faculty of Medicine and University Hospital of Cologne, Department I of Internal Medicine, Center for Integrated Oncology Aachen Bonn Cologne Düsseldorf (CIO ABCD), University of Cologne, Cologne; <sup>2</sup>German Center for Infection Research (DZIF), partner site Bonn-Cologne, Cologne; <sup>3</sup>Department of Clinical Immunology of Infectious Diseases, Bernhard Nocht Institute for Tropical Medicine, Hamburg; <sup>4</sup>Division of Infectious Diseases, First Department of Medicine, University Medical Center Hamburg-Eppendorf, Hamburg; <sup>5</sup>German Center for Infection Research (DZIF), Partner Site Hamburg-Lübeck-Borstel-Riems, Hamburg; <sup>6</sup>Institute of Virology, Faculty of Medicine and University Hospital Cologne, University of Cologne, Cologne and <sup>7</sup>Center for Molecular Medicine Cologne, University of Cologne, Faculty of Medicine and University Hospital Cologne, Cologne, Germany

\*SCM and LM contributed equally as co-first authors.

Correspondence:  
S.C. MELLINGHOFF - sibylle.mellingshoff@uk-koeln.de

## References

1. Blixt L, Wullimann D, Aleman S, et al. T cell immune responses following vaccination with mRNA BNT162b2 against SARS-CoV-2 in patients with chronic lymphocytic leukemia: results from a prospective open-label clinical trial. *Haematologica*. 2022;107(4):1000-1003.
2. Herishanu Y, Rahav G, Levi S, et al. Efficacy of a third BNT162b2 mRNA COVID-19 vaccine dose in patients with CLL who failed standard 2-dose vaccination. *Blood*. 2022;139(5):678-685.

<https://doi.org/10.3324/haematol.2022.280982>

Received: March 14, 2022.

Accepted: June 14, 2022.

Prepublished: June 23, 2022.

©2022 Ferrata Storti Foundation

Published under a CC BY-NC license 

### Disclosures

SCM reports grants from DZIF (Clinical Leave Stipend). AMF reports research funding from Celgene/Bristol Myers Squibb (Inst), AstraZeneca (Inst), and travel expenses from AbbVie. KF reports other support from Roche and AbbVie. BE reports grants and personal fees from Janssen-Cilag, AbbVie, Roche and Gilead, personal fees from Novartis, Celgene, ArQule, AstraZeneca and Oxford Biomedica (UK), as well as grants from BeiGene, outside the submitted work. MH reports other support from AbbVie, F. Hoffman-LaRoche, Gilead, Janssen-Cilag and Mundipharma, during the conduct of the study. PL reports grants and personal fees from Janssen-Cilag, personal fees from AbbVie and AstraZeneca, and other support from F. Hoffman-LaRoche. SR reports honoraria from AstraZeneca. All other authors have no conflicts of interest to disclose.

### Contributions

SCM and PL implemented the research and design of the study. They were responsible for data assessment, coordination and conduct of the study and authored the manuscript. LM performed the T-cell vaccine response laboratory analyses and co-authored the manuscript. HG and KV performed the humoral vaccine response laboratory analyses and co-authored the manuscript. HAS, MS and MT performed blood sample processing and co-authored the manuscript. LMW, SR, CD, MMA, FK, AMF, KF, BE and MH supervised the conduct of the study, gave advice for study design and laboratory analyses and co-authored the manuscript.

### Acknowledgments

We thank the working groups of PD Dr. Hans-Anton Schlöber, Prof. Dr. Florian Klein and Prof. Dr. Marylyn M. Addo for all logistical and technical support. Especially, we thank Larisa Idrizovic, and Tatjana Lammertz for their continuous support.

### Data-sharing statement

Data may be available upon request to the corresponding author.

## LETTER TO THE EDITOR

3. Mellinghoff SC, Robrecht S, Mayer L, et al. SARS-CoV-2 specific cellular response following COVID-19 vaccination in patients with chronic lymphocytic leukemia. *Leukemia*. 2022;36(2):562-565.
4. Munro APS, Janani L, Cornelius V, et al. Safety and immunogenicity of seven COVID-19 vaccines as a third dose (booster) following two doses of ChAdOx1 nCov-19 or BNT162b2 in the UK (COV-BOOST): a blinded, multicentre, randomised, controlled, phase 2 trial. *Lancet*. 2021;398(10318):2258-2276.
5. Liu X, Shaw RH, Stuart ASV, et al. Safety and immunogenicity of heterologous versus homologous prime-boost schedules with an adenoviral vectored and mRNA COVID-19 vaccine (Com-COV): a single-blind, randomised, non-inferiority trial. *Lancet*. 2021;398(10303):856-869.
6. Flaxman A, Marchevsky NG, Jenkin D, et al. Reactogenicity and immunogenicity after a late second dose or a third dose of ChAdOx1 nCov-19 in the UK: a substudy of two randomised controlled trials (COV001 and COV002). *Lancet*. 2021;398(10304):981-990.
7. Bonelli M, Mrak D, Tobudic S, et al. Additional heterologous versus homologous booster vaccination in immunosuppressed patients without SARS-CoV-2 antibody seroconversion after primary mRNA vaccination: a randomised controlled trial. *Ann Rheum Dis*. 2022;81(5):687-694.
8. Schrezenmeier E, Rincon-Arevalo H, Stefanski A-L, et al. B and T cell responses after a third dose of SARS-CoV-2 vaccine in kidney transplant recipients. *J Am Soc Nephrol*. 2021;32(12):3027-3033.
9. Marlet J, Gatault P, Maakaroun Z, et al. Antibody responses after a third dose of COVID-19 vaccine in kidney transplant recipients and patients treated for chronic lymphocytic leukemia. *Vaccines (Basel)*. 2021;9(10):1055.
10. Krammer F. A correlate of protection for SARS-CoV-2 vaccines is urgently needed. *Nat Med*. 2021;27(7):1147-1148.
11. Earle KA, Ambrosino DM, Fiore-Gartland A, et al. Evidence for antibody as a protective correlate for COVID-19 vaccines. *Vaccine*. 2021;39(32):4423-4428.
12. Fendler A, Au L, Shepherd STC, et al. Functional antibody and T cell immunity following SARS-CoV-2 infection, including by variants of concern, in patients with cancer: the CAPTURE study. *Nat Cancer*. 2021;2(12):1321-1337.
13. Pozzetto B, Legros V, Djebali S, et al. Immunogenicity and efficacy of heterologous Cha-dOx1/BNT162b2 vaccination. *Nature*. 2021;600(7890):701-706.
14. Soresina A, Moratto D, Chiarini M, et al. Two X-linked agammaglobulinemia patients develop pneumonia as COVID-19 manifestation but recover. *Pediatr Allergy Immunol*. 2020;31(5):565-569.
15. Breathnach AS, Duncan CJA, Bouzidi KE, et al. Prior COVID-19 protects against reinfection, even in the absence of detectable antibodies. *J Infect*. 2021;83(2):237-279.
16. Keeton R, Tincho MB, Ngomti A, et al. T cell responses to SARS-CoV-2 spike cross-recognize Omicron. *Nature*. 2022;603(7901):488-492.

**IV. SARS-CoV-2 specific cellular response following COVID-19 vaccination in patients with chronic lymphocytic leukemia**

Sibylle C. Mellinghoff, Sandra Robrecht, **Leonie Mayer**, Leonie M. Weskamm, Christine Dahlke, Henning Gruell, Kanika Vanshylla, Hans A. Schlösser, Martin Thelen, Anna-Maria Fink, Kirsten Fischer, Florian Klein, Marylyn M. Addo, Barbara Eichhorst, Michael Hallek, Petra Langerbeins

Published in *Leukemia* **36**, 562–565 (2022)

doi: [10.1038/s41375-021-01500-1](https://doi.org/10.1038/s41375-021-01500-1)

## LETTER OPEN



## CHRONIC LYMPHOCYTIC LEUKEMIA

## SARS-CoV-2 specific cellular response following COVID-19 vaccination in patients with chronic lymphocytic leukemia

Sibylle C. Mellingshoff<sup>1,2,3</sup>✉, Sandra Robrecht<sup>1</sup>, Leonie Mayer<sup>1,3,4,5</sup>, Leonie M. Weskamm<sup>1,3,4,5</sup>, Christine Dahlke<sup>1,3,4,5</sup>, Henning Gruell<sup>6</sup>, Kanika Vanshylla<sup>6</sup>, Hans A. Schlösser<sup>7</sup>, Martin Thelen<sup>7</sup>, Anna-Maria Fink<sup>1</sup>, Kirsten Fischer<sup>1</sup>, Florian Klein<sup>6</sup>, Marylyn M. Addo<sup>1,3,4,5</sup>, Barbara Eichhorst<sup>1</sup>, Michael Hallek<sup>1</sup> and Petra Langerbeins<sup>1</sup>

© The Author(s) 2021

*Leukemia* (2022) 36:562–565; <https://doi.org/10.1038/s41375-021-01500-1>

Chatzikonstantinou et al. [1] conducted a large follow-up analysis of COVID-19 in patients with chronic lymphocytic leukemia (CLL) and confirmed a high mortality rate, especially in patients with older age, comorbidity and previous CLL-treatment. The results emphasize the importance of prevention and mitigation of COVID-19 by vaccination, especially in patients with hematological malignancies. The COVID-19 vaccine-induced immunity is mediated by the interaction of both, humoral and cellular components [2, 3]. While several studies have confirmed low humoral immunogenicity in CLL patients [4–7], very few describe cellular responses to determine immunogenicity and report reduced T cell response [8]. In this prospective cohort study, we hence investigated cellular immunogenicity and the interplay with humoral immunogenicity following COVID-19 vaccination in SLL/CLL patients as compared with healthy controls (HC).

Blood samples of CLL registry (NCT02863692) patients were centrally evaluated after full COVID-19 vaccination. In total, 21/23 patients were included in the analyses (samples missing in 2/23). Vaccinated healthcare workers served as HC cohort ( $n = 12$ ). Both studies were approved by the local ethics committee.

Patient and disease characteristics and vaccination schedules are summarized in Table 1 and Supplemental Table 1. Patient blood samples were collected at a median of 47 (range 19–94 days) and HC at a median of 35 (range 32–38) days after the second vaccination.

SARS-CoV-2 receptor-binding domain (RBD) specific IgG antibodies, determined using Alinity ci SARS-CoV-2 IgG II Quant assay (Abbott), were detectable in 8/21 (38.1%) patients with SLL/CLL and 100% of HC ( $p = 0.001$ ; Fig. 1A, B). Neutralizing activity, determined by using heat-inactivated serum in a lentiviral-based pseudovirus neutralization assay against Wu-01 strain of SARS-CoV-2, was observed in serum samples from all HC (GeoMean  $ID_{50}$  409) (Fig. 1C). No neutralizing activity ( $ID_{50} < 10$ ) was detectable in the majority of CLL patients (14/21, 67%, 0), including all seronegative individuals.

However, CLL patients with detectable activity (7/21, 30%) had a response that was comparable to HC ( $ID_{50}$  523,  $p = 0.9$ ).

Peripheral blood mononuclear cells (PBMCs) were used for SARS-CoV-2 spike-specific T cells (Human IFN $\gamma$  ELISpot<sup>PLUS</sup> [ALP] kit [Mabtech]) and B cells (IgG ELISpot) analyses. Results are reported as spot-forming cells (SFC) per million PBMCs. T cell responses to SARS-CoV-2 peptide pool ([15-mers overlapping by 11 amino acids] spanning the entire spike protein) were considered positive if higher than twice the median response of pre-pandemic HC (48 SFC/10<sup>6</sup>). The median number of SARS-CoV-2 specific T cells was 21.3 SFC (interquartile range [IQR] 0.0–145.0) for CLL patients as compared with 177.3 SFC [IQR 138.0–403.3] in HC ( $p = 0.008$ ; Fig. 1D). While 8/21 (38.1%) CLL patients had a SARS-CoV-2 spike-specific T cell response measurable above cut-off, 90% of HC mounted a response ( $p = 0.009$ ).

SARS-CoV-2 S1/2-specific antibody-secreting cells (ASC) were analyzed in 14/21 (66.7%) SLL/CLL patients. The cut-off value for positive responses were defined as the mean plus two standard deviations of the responses observed in pre-pandemic HC (62 SFC/10<sup>6</sup>). Overall, 1/14 SLL/CLL patients (7.1%) had detectable S-specific ASC (138 SFC) as compared with 100% in HC (median 193 SFC, range 89–464 SFC). The SARS-CoV-2 specific IgG titer of the ASC responding patient was with 11 360 BAU/ml the highest within the group of CLL patients. Looking at total IgG-secreting B cells, 13 patients without S-specific ASC did neither show any IgG-secreting B cells. Spots were too faint to be counted or detected at numbers below the cut-off.

In a descriptive analysis (Table 1 and Supplemental Table 2 and 3), potential variables to be associated with humoral and T cell responses were investigated. While 3/21 (14.3%) of patients had both a humoral and a T cellular response, eight patients (38.1%) were double negative and a discordant response, defined by detection of either T cellular or humoral immune response to vaccination was found in most patients (10/21, 47.6%).

<sup>1</sup>Faculty of Medicine and University Hospital of Cologne, Department I of Internal Medicine, Centre for Integrated Oncology Aachen Bonn Cologne Düsseldorf (CIO ABCD), German CLL Group (GCLLSG), University of Cologne, Cologne, Germany. <sup>2</sup>German Centre for Infection Research (DZIF), partner site Bonn-Cologne, Cologne, Germany. <sup>3</sup>Department of Clinical Immunology of Infectious Diseases, Bernhard Nocht Institute for Tropical Medicine, Hamburg, Germany. <sup>4</sup>Division of Infectious Diseases, First Department of Medicine, University Medical Centre Hamburg-Eppendorf, Hamburg, Germany. <sup>5</sup>German Centre for Infection Research (DZIF), Partner Site Hamburg-Lübeck-Borstel-Riems, Hamburg, Germany. <sup>6</sup>Institute of Virology, Faculty of Medicine and University Hospital Cologne, University of Cologne, Cologne, Germany. <sup>7</sup>Centre for Molecular Medicine Cologne, University of Cologne, Faculty of Medicine and University Hospital Cologne, Cologne, Germany. ✉email: sibylle.mellingshoff@uk-koeln.de

Received: 8 November 2021 Revised: 2 December 2021 Accepted: 10 December 2021  
Published online: 22 December 2021

**Table 1.** Patients baseline characteristics and disease characteristics in the overall cohort and by subgroups.

Parameters N (%)	Patients with CLL (N = 23)				
	Overall cohort	Humoral response negative T cell response negative	Humoral response negative, T cell response positive	Humoral response positive, T cell response negative	Humoral response positive, T cell response positive
<b>Overall COVID-19 vaccine immune response</b>		8 (38.1) <sup>a</sup>	5 (23.8) <sup>a</sup>	5 (23.8) <sup>a</sup>	3 (14.3) <sup>a</sup>
<b>Age, median (range) (years)</b>	70 (46–79)	70.5 (48–79)	71.0 (53–79)	74.0 (62–77)	59.0 (49–62)
<b>Age group (years)</b>					
>65	13 (56.5)	6 (75.0)	3 (60.0)	4 (80.0)	0 (0.0)
>70	11 (47.8)	4 (50.0)	3 (60.0)	4 (80.0)	0 (0.0)
<b>Male sex</b>	20 (87)	6 (75.0)	4 (80.0)	5 (100.0)	3 (100.0)
<b>Disease / treatment status</b>					
Treatment-naïve	1 (4.3)	0 (0.0)	0 (0.0)	1 (20.0)	0 (0.0)
Previously treated	22 (95.7)	8 (100.0)	5 (100.0)	4 (80.0)	3 (100.0)
<b>Treatment prior vaccination</b>	22 (95.7)				
Line of treatment, median (range)	2 (1–8)	2 (1–8)	3 (2–5)	2 (1–5)	2 (1–2)
1 <sup>st</sup> line	6 (27.3)	2 (25.0)	0 (0.0)	2 (50.0)	1 (33.3)
>1 <sup>st</sup> line	16 (72.7)	6 (75.0)	5 (100.0)	2 (40.0)	2 (66.7)
Treatment < 12 months prior vaccination	9 (40.9)	3 (37.5)	4 (80.0)	1 (25.0)	0 (0.0)
without anti CD20 <sup>b</sup>	2 (9.1)	0 (0.0)	1 (20.0)	1 (20.0)	0 (0.0)
with anti CD20 <sup>c</sup>	7 (31.8)	3 (37.5)	3 (60.0)	0 (0.0)	0 (0.0)
<b>Type according to hierarchical model<sup>d</sup></b>	21 (91.3)				
del(17p)	4 (19.0)	3 (37.5)	1 (20.0)	0 (0.0)	0 (0.0)
del(11q)	5 (23.8)	1 (12.5)	1 (20.0)	1 (33.3)	2 (66.7)
Trisomy 12	4 (19.0)	1 (12.5)	0 (0.0)	0 (0.0)	1 (33.3)
No abnormalities	1 (4.8)	0 (0.0)	0 (0.0)	1 (33.3)	0 (0.0)
del(13q) [single]	7 (33.3)	3 (37.5)	3 (60.0)	1 (33.3)	0 (0.0)
<b>IGHV mutational status</b>	18 (78.3)				
Unmutated	13 (72.2)	6 (75.0)	2 (66.7)	2 (66.7)	2 (100.0)
Mutated	5 (27.8)	2 (25.0)	1 (33.3)	1 (33.3)	0 (0.0)
<b>TP53 mutational status</b>	19 (82.6)				
Mutated	2 (10.5)	5 (71.4)	4 (100.0)	3 (100.0)	3 (100.0)
Unmutated	17 (89.5)	2 (28.6)	0 (0.0)	0 (0.0)	0 (0.0)

<sup>a</sup>Humoral and T cell response measured in 21/23 patients.<sup>b</sup>Acalabrutinib, Ibrutinib.<sup>c</sup>Obinutuzumab, Obinutuzumab/Venetoclax, Acalabrutinib/Obinutuzumab, Acalabrutinib/Obinutuzumab/Venetoclax.<sup>d</sup>Cytogenetic subgroups were determined according to the hierarchical model of Döhner et al. [11].

In conclusion, humoral and cellular immunogenicity following COVID-19 vaccination was significantly impaired in patients with SLL/CLL as described previously. SARS-CoV-2 specific antibodies and T cells were detectable in 38.1% each. In the majority of seroconverted patients, SARS-CoV-2 neutralizing serum activity of diverse magnitude was detectable indicating functionality of antibodies if at all mounted. While less than 15% of patients had both a humoral and cellular response, most patients showed a discordant response with only either detectable humoral or cellular response. Clinical features of the two subgroups differed with regard to previous treatment lines, which seem to affect the humoral more than the T cell axis. CLL-targeted treatments as well the underlying diseases itself affect B cells and self-evidently impact the humoral response. Our findings encourage immunization of

patients even at advanced disease stages or heavily pre-treated as a subgroup that may respond with the T cellular axis.

Two patients showed a particular strong T cell response: One had been vaccinated thrice and the other had received a heterologous boosting (Fig. 1D). Data from more patients will need to prove if a booster vaccination is more likely to induce T cell response. Our data emphasize the importance of assessing the T cell response in patients with a limited serologic response. The best vaccination regime to promote those key players remains to be investigated. While heterologous immunization appears to elicit stronger T cell responses than homologous immunization [9], the chronological order for immunocompromised patients is unclear and needs further study.

A limitation of this study is the small sample size and the younger age of the control group (as compared with the SLL/CLL

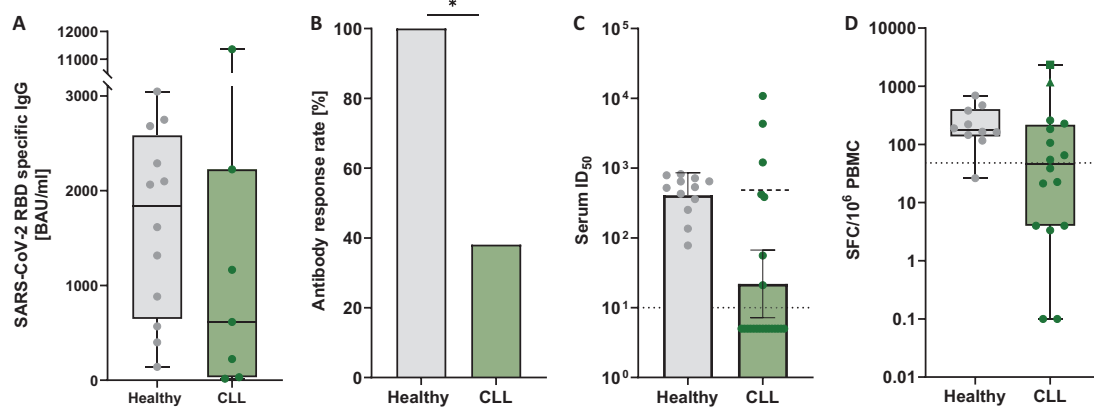


**Fig. 1 Humoral and T cell immune responses after COVID-19 vaccination.** **A** SARS-CoV-2 RBD specific IgG in CLL patients (median 889.9 BAU/ml, IQR 80.2-2127.4, for responders) and healthy controls (median 1839.8 BAU/ml, IQR 647.0-2583.4) measured by ELISA. **B** Antibody response rate in CLL patients and healthy volunteers. \* $p = 0.001$ . **C** Serum neutralizing activity (50% inhibitory serum dilution) determined in a pseudovirus neutralizing assay against the Wu-01 pseudovirus strain. Bars indicating geometric mean ID<sub>50</sub> with 95% confidence intervals. A dashed line indicates limit of detection [10]. Samples with no detectable neutralization (ID<sub>50</sub> < 10) were plotted with an arbitrary ID<sub>50</sub> of 5 for graphical representation. Dashed line in the CLL group shows geometric mean ID<sub>50</sub> for individuals with a detectable neutralizing response. **D** Interferon- $\gamma$  T cell ELISpot response in CLL patients and HC. Shown values are mean spots in peptide-stimulated wells minus background in negative control wells. Error bars represent median  $\pm$  interquartile range. The dotted line indicates the positive threshold of 48 SFC/10<sup>6</sup> PBMC. Samples were acquired 35 days after the second vaccination in HC and at a median of 47 days after second vaccination in CLL patients. Two patients had much higher correlated of T cell immunity after vaccination: One was vaccinated thrice and one was the only patient of the entire cohort that had received heterologous prime-boost immunization with BNT162b and ChAdOx1. BNT BNT162b, ChAd ChAdOx1, HC Healthy Control.

patients), as older individuals respond with lower antibody levels to vaccination. However, in the rather small fraction of SLL/CLL patients who responded to vaccination, similar titers of neutralizing antibodies were detectable in HC. Further, we only included one treatment-naïve patient and therefore cannot fully conclude the impact of CLL-directed treatment as compared with untreated CLL on cellular immunity. Previous trials reported inferior serologic immunogenicity in treatment-naïve patients as compared with patients previously treated [4, 5, 10]. Future studies should provide more data comparing those two subgroups of CLL patients and further focus on cellular immunity.

In conclusion, we demonstrate inferior T cell response to COVID-19 vaccines in SLL/CLL patients as compared with HC, supporting the importance of a third vaccine dose for those. The prime-boost regime, in particular the choice of best vaccine combination, is yet to determine. Our observation of discordant immune responses in the majority of patients indicates that the humoral response may not be reliable as the sole surrogate marker of protection in the patients with CLL and further B cell depleting malignancies, at least if negative.

## REFERENCES

- Chatzikonstantinou T, Kapetanakis A, Scarfò L, Karakatsoulis G, Allsup D, Cabrero AA, et al. COVID-19 severity and mortality in patients with CLL: An update of the international ERIC and Campus CLL study. *Leukemia*. 2021;35:3444–54.
- Koch T, Mellinghoff SC, Shamsrizi P, Addo MM, Dahlke C. Correlates of vaccine-induced protection against SARS-CoV-2. *Vaccines*. 2021;9:238.
- Braun J, Loyal L, Frensch M, Wendisch D, Georg P, Kurth F, et al. SARS-CoV-2-reactive T cells in healthy donors and patients with COVID-19. *Nature*. 2020;587:270–4.
- Benjamini O, Rokach L, Itchaki G, Braester A, Shvidel L, Goldschmidt N, et al. Safety and efficacy of BNT162b mRNA Covid19 Vaccine in patients with chronic lymphocytic leukemia. *Haematologica*. 2021. <https://doi.org/10.3324/haematol.2021.279196>. Epub ahead of print.
- Herishanu Y, Avivi I, Aharon A, Shefer G, Levi S, Bronstein Y, et al. Efficacy of the BNT162b2 mRNA COVID-19 vaccine in patients with chronic lymphocytic leukemia. *Blood*. 2021;137:3165–73.
- Tadmor T, Benjamini O, Braester A, Rahav G, Rokach L. Antibody persistence 100 days following the second dose of BNT162b mRNA Covid19 vaccine in patients with chronic lymphocytic leukemia. *Leukemia*. 2021;35:2727–30.

- Parry H, McIlroy G, Bruton R, Ali M, Stephens C, Damery S, et al. Antibody responses after first and second Covid-19 vaccination in patients with chronic lymphocytic leukaemia. *Blood. Cancer J*. 2021;11:136.
- Ehmsen S, Asmussen A, Jeppesen SS, Nilsson AC, Østerlev S, Vestergaard H, et al. Antibody and T cell immune responses following mRNA COVID-19 vaccination in patients with cancer. *Cancer Cell*. 2021;39:1034–6.
- Pozzetto B, Legros V, Djebali S, Barateau V, Guibert N, Villard M, et al. Immunogenicity and efficacy of heterologous ChAdOx1-BNT162b2 vaccination. *Nature*. 2021. <https://doi.org/10.1038/s41586-021-04120-y>. Epub ahead of print.
- da Cunha-Bang C, Kirkby NS, Friis-Hansen L, Niemann CU. Serological response following vaccination with BNT162b2 mRNA in patients with chronic lymphocytic leukemia. *Leuk Lymphoma*. 2021;1–3. <https://doi.org/10.1080/10428194.2021.1973673>. Epub ahead of print.
- Döhner H, Stilgenbauer S, Benner A, Leupolt E, Kröber A, Bullinger L, et al. Genomic aberrations and survival in chronic lymphocytic leukemia. *N Engl J Med*. 2000;343:1910–6.

## ACKNOWLEDGEMENTS

We thank the working groups of PD Hans-Anton Schlößer, Florian Klein, and Marylyn M. Addo for all logistical and technical support. Especially, we thank Larisa Idrizovic and Tatjana Lammertz for their continuous support.

## AUTHOR CONTRIBUTIONS

SCM and PL implemented the research and design of the study. They were responsible for data assessment, coordination, and conduction of the study and authored the paper. SR performed the statistical analyses and co-authored the paper. LMW and LM performed the T and B cell vaccine response laboratory analyses and co-authored the paper. HG and KV the humoral vaccine response laboratory analyses and co-authored the manuscript. HAS and MT performed blood sample processing and co-authored the paper. CD, MMA, FK, AMF, KF, BE, and MH supervised the conduct of the study, gave advice for study design and laboratory analyses, and co-authored the paper.

## FUNDING

Open Access funding enabled and organized by Projekt DEAL.



### COMPETING INTERESTS

SCM reports grants from DZIF (Clinical Leave Stipend). AMF reports research funding from Celgene/Bristol Myers Squibb (Inst), AstraZeneca (Inst), and travel Expenses by AbbVie. KF reports other from Roche, other from AbbVie. BE reports grants and personal fees from Janssen-Cilag, grants and personal fees from Roche, personal fees from Novartis, grants and personal fees from AbbVie, personal fees from Celgene, personal fees from ArQule, personal fees from AstraZeneca, personal fees from Oxford Biomedica (UK), grants and personal fees from Gilead, grants from BeiGene, outside the submitted work. MH reports other from AbbVie, other from F. Hoffman-LaRoche, other from Gilead, other from Janssen-Cilag, other from Mundipharma, during the conduct of the study. PL reports grants and personal fees from Janssen-Cilag, personal fees from Abbvie, other from F. Hoffman-LaRoche, personal fees from AstraZeneca. The remaining authors declare no competing financial interests for this study.

### ADDITIONAL INFORMATION

**Supplementary information** The online version contains supplementary material available at <https://doi.org/10.1038/s41375-021-01500-1>.

**Correspondence** and requests for materials should be addressed to Sibylle C. Mellinghoff.

**Reprints and permission information** is available at <http://www.nature.com/reprints>

**Publisher's note** Springer Nature remains neutral with regard to jurisdictional claims in published maps and institutional affiliations.



**Open Access** This article is licensed under a Creative Commons Attribution 4.0 International License, which permits use, sharing, adaptation, distribution and reproduction in any medium or format, as long as you give appropriate credit to the original author(s) and the source, provide a link to the Creative Commons license, and indicate if changes were made. The images or other third party material in this article are included in the article's Creative Commons license, unless indicated otherwise in a credit line to the material. If material is not included in the article's Creative Commons license and your intended use is not permitted by statutory regulation or exceeds the permitted use, you will need to obtain permission directly from the copyright holder. To view a copy of this license, visit <http://creativecommons.org/licenses/by/4.0/>.

© The Author(s) 2021

**Supplemental Table 1.** Vaccination schemes in CLL patients and healthy volunteers.

Type of vaccination	Patients with CLL	Healthy control population
<b>Analysis population, N</b>	23	12
<b>Sequence of vaccination, N (%)</b>		
AZD   AZD	2 (8.7)	1 (8.3)
AZD   BNT	2 (8.7)	1 (8.3)
BNT   BNT	18 (78.3)	10 (83.3)
BNT   BNT   BNT	1 (4.3)	0 (0.0)

**Supplemental Table 2.** Humoral Responses by subgroups

Parameters N (%)	Patients with CLL (N=21)	
	Humoral response negative	Humoral response positive
<b>Humoral response</b> with detection of anti-SARS-CoV-2 spike-RBD IgG $\geq$ 7.1 BAU/ml, N (%)	13 (61.9)	8 (38.1)
<b>Age, median (range)</b> (years)	71.0 (48-79)	67.5 (49-77)
<b>Age group</b> (years)		
>65	9 (69.2)	4 (50.0)
>70	7 (53.8)	4 (50.0)
<b>Male sex</b>	10 (76.9)	8 (100.0)
<b>Disease / treatment status</b>		
Treatment-naïve	0 (0.0)	1 (14.3)
Previously treated	13 (100.0)	7 (87.5)
<b>Treatment prior vaccination</b>		
Line of treatment, median (range)	2 (1-8)	2 (1-5)
1 <sup>st</sup> line	2 (15.4)	3 (42.9)
>1 <sup>st</sup> line	11 (84.6)	4 (50.0)
Treatment < 12 months prior vaccination	8 (61.5)	1 (12.5)
without anti CD20 <sup>1</sup>	3 (37.5)	0 (0.0)

with anti CD20 <sup>2</sup>	5 (62.6)	1 (100.0)
<b>Type according to hierarchical model†</b>		
del(17p)	4 (30.8)	0 (0.0)
del(11q)	2 (15.4)	3 (50.0)
Trisomy 12	1 (7.7)	1 (16.7)
No abnormalities	0 (0.0)	1 (16.7)
del(13q) [single]	6 (46.2)	1 (16.7)
<b>IGHV mutational status</b>		
Unmutated	8 (72.7)	4 (80.0)
Mutated	3 (27.3)	1 (20.0)
<b>TP53 mutational status</b>		
Mutated	9 (81.8)	6 (100.0)
Unmutated	2 (18.2)	0 (0.0)

† Cytogenetic subgroups were determined according to the hierarchical model of Döhner et al.<sup>1</sup>

<sup>1</sup> Obinutuzumab, Obinutuzumab/Venetoclax; <sup>2</sup> Acalabrutinib, Acalabrutinib/Obinutuzumab, Acalabrutinib/Obinutuzumab/Venetoclax, Ibrutinib

**Supplemental Table 3.** T Cell Responses by subgroups

Parameters N (%)	Patients with CLL (N=21)	
	Cellular response negative	Cellular response positive
<b>Cellular response</b> with detection of SARS-CoV-2 specific T cells > 48 SFC/10 <sup>6</sup> PBMC, N (%)	13 (61.9)	8 (38.1)
<b>Age, median (range)</b> (years)	72 (48-79)	63 (49-79)
<b>Age group</b> (years)		
>65	10 (76.9)	3 (37.5)
>70	8 (61.5)	3 (37.5)
<b>Male sex</b>	11 (84.6)	7 (87.5)
<b>Disease / treatment status</b>		
Treatment-naïve	1 (7.7)	0 (0.0)
Previously treated	12 (92.3)	8 (100.0)
<b>Treatment prior vaccination</b>		
Line of treatment, median (range)	2 (1-8)	2 (1-5)

1 <sup>st</sup> line	4 (33.3)	1 (12.5)
>1 <sup>st</sup> line	8 (61.5)	7 (87.5)
Treatment < 12 months prior vaccination	4 (33.3)	4 (50.0)
without anti CD20 <sup>1</sup>	3 (75.0)	0 (0.0)
with anti CD20 <sup>2</sup>	1 (25.0)	4 (100.0)
<b>Type according to hierarchical model†</b>		
del(17p)	3 (27.3)	1 (12.5)
del(11q)	2 (18.2)	3 (37.5)
Trisomy 12	1 (9.1)	1 (12.5)
No abnormalities	1 (9.1)	0 (0.0)
del(13q) [single]	4 (36.4)	3 (37.5)
<b>IGHV mutational status</b>		
Unmutated	8 (72.7)	4 (80.0)
Mutated	3 (27.3)	1 (20.0)
<b>TP53 mutational status</b>		
Mutated	8 (80.0)	7 (100.0)
Unmutated	2 (20.0)	0 (0.0)

† Cytogenetic subgroups were determined according to the hierarchical model of Döhner et al.<sup>1</sup>

<sup>1</sup> Obinutuzumab, Obinutuzumab/Venetoclax; <sup>2</sup> Acalabrutinib, Acalabrutinib/Obinutuzumab, Acalabrutinib/Obinutuzumab/Venetoclax, Ibrutinib

## References

1. Döhner H, Stilgenbauer S, Benner A, et al. Genomic aberrations and survival in chronic lymphocytic leukemia. *N Engl J Med*. 2000;343(26):1910-1916.

**V. SARS-CoV-2-specific Humoral and T cell Immune Response After Second Vaccination in Liver Cirrhosis and Transplant Patients**

Darius F. Ruether, Golda M. Schaub, Paul M. Duengelhof, Friedrich Haag, Thomas T. Brehm, Anahita Fathi, Malte Wehmeyer, Jacqueline Jahnke-Triankowski, **Leonie Mayer**, Armin Hoffmann, Lutz Fischer, Marylyn M. Addo, Marc Lütgehetmann, Ansgar W. Lohse, Julian Schulze Zur Wiesch, Martina Sterneck

Published in *Clinical Gastroenterology and Hepatology* **20**, 162-172 (2022)

doi: [10.1016/j.cgh.2021.09.003](https://doi.org/10.1016/j.cgh.2021.09.003)

## SARS-CoV2-specific Humoral and T-cell Immune Response After Second Vaccination in Liver Cirrhosis and Transplant Patients



Darius F. Ruether,<sup>\*,a</sup> Golda M. Schaub,<sup>\*,§,a</sup> Paul M. Duengelhoefer,<sup>‡</sup> Friedrich Haag,<sup>‡</sup> Thomas T. Brehm,<sup>\*,§</sup> Anahita Fathi,<sup>\*,§,||</sup> Malte Wehmeyer,<sup>\*</sup> Jacqueline Jahnke-Triankowski,<sup>#</sup> Leonie Mayer,<sup>§,||</sup> Armin Hoffmann,<sup>||</sup> Lutz Fischer,<sup>#</sup> Marylyn M. Addo,<sup>\*,§,||</sup> Marc Lütgehetmann,<sup>§,||</sup> Ansgar W. Lohse,<sup>\*,§</sup> Julian Schulze zur Wiesch,<sup>\*,||,b</sup> and Martina Sterneck<sup>\*,b</sup>

<sup>\*I. Department of Internal Medicine, University Medical Center Hamburg-Eppendorf, Hamburg, Germany; <sup>‡</sup>Institute of Immunology, University Medical Center Hamburg-Eppendorf, Hamburg, Germany; <sup>§</sup>German Center for Infection Research (DZIF), Partner Site Hamburg-Lübeck-Borstel-Riems, Germany; <sup>||</sup>Bernhard-Nocht-Institute for Tropical Medicine, Department for Clinical Immunology of Infectious Diseases, Hamburg, Germany; <sup>||</sup>Institute of Medical Microbiology, Virology and Hygiene, University Medical Center Hamburg-Eppendorf, Hamburg, Germany; <sup>#</sup>Department of Visceral Transplantation, University Medical Center Hamburg-Eppendorf, Hamburg, Germany</sup>

**BACKGROUND & AIMS:** Detailed information on the immune response after second vaccination of cirrhotic patients and liver transplant (LT) recipients against severe acute respiratory syndrome coronavirus type 2 (SARS-CoV-2) is largely missing. We aimed at comparing the vaccine-induced humoral and T-cell responses of these vulnerable patient groups.

**METHODS:** In this prospective cohort study, anti-SARS-CoV-2 spike-protein titers were determined using the DiaSorin LIAISON (anti-S trimer) and Roche Elecsys (anti-S RBD) immunoassays in 194 patients (141 LT, 53 cirrhosis Child-Pugh A-C) and 56 healthy controls before and 10 to 84 days after second vaccination. The spike-specific T-cell response was assessed using an interferon-gamma release assay (EUROIMMUN). A logistic regression analysis was performed to identify predictors of low response.

**RESULTS:** After the second vaccination, seroconversion was achieved in 63% of LT recipients and 100% of cirrhotic patients and controls using the anti-S trimer assay. Median anti-SARS-CoV-2 titers of responding LT recipients were lower compared with cirrhotic patients and controls ( $P < .001$ ). Spike-specific T-cell response rates were 36.6%, 65.4%, and 100% in LT, cirrhosis, and controls, respectively. Altogether, 28% of LT recipients did neither develop a humoral nor a T-cell response after second vaccination. In LT recipients, significant predictors of absent or low humoral response were age >65 years (odds ratio [OR], 4.57; 95% confidence interval [CI], 1.48-14.05) and arterial hypertension (OR, 2.50; 95% CI, 1.10-5.68), whereas vaccination failure was less likely with calcineurin inhibitor monotherapy than with other immunosuppressive regimens (OR, 0.36; 95% CI, 0.13-0.99).

**CONCLUSION:** Routine serological testing of the vaccination response and a third vaccination in patients with low or absent response seem advisable. These vulnerable cohorts need further research on the effects of heterologous vaccination and intermittent reduction of immunosuppression before booster vaccinations.

**Keywords:** Immunosuppression; Liver Cirrhosis; Liver Transplant Recipients; SARS-CoV-2 Vaccination.

<sup>a</sup>Authors share co-first authorship. <sup>b</sup>Authors share co-senior authorship.

**Abbreviations used in this paper:** Anti-S RBD, anti-SARS-CoV-2 antibodies in Roche Elecsys immunoassay; anti-S trimer, anti-SARS-CoV-2 antibodies in DiaSorin LIAISON immunoassay; BAU, binding antibody units; CI, confidence interval; CNi, calcineurin inhibitor; COVID-19, Coronavirus disease 2019; eGFR, estimated glomerular filtration rate; IGRA, interferon gamma release assay; IFN- $\gamma$ , interferon-gamma; IQR, interquartile range; LC, liver cirrhosis; LT, liver transplant; MMF, mycophenolate mofetil; mTORi, mammalian target of rapamycin inhibitors; OR, odds ratio; RBD,

receptor binding domain; SARS-CoV-2, severe acute respiratory syndrome coronavirus type 2; SD, standard deviation; SOT, solid-organ transplantation; TIPS, transjugular intrahepatic portosystemic shunt.

Most current article

© 2022 by the AGA Institute  
1542-3565/\$36.00

<https://doi.org/10.1016/j.cgh.2021.09.003>

In the initial clinical trials investigating the efficacy and safety of severe acute respiratory syndrome coronavirus type 2 (SARS-CoV-2) vaccines, various immunocompromised or immunosuppressed patient populations (ie, patients with liver cirrhosis [LC] or liver transplant [LT] recipients) were not included.<sup>1,2</sup> However, a markedly increased mortality due to Coronavirus disease 2019 (COVID-19) has been described for both patient groups compared with the healthy population, indicating the need for SARS-CoV-2 vaccination.<sup>3,4</sup>

Preliminary data showed that LT recipients might be less likely to reach seroconversion after SARS-CoV-2 vaccination,<sup>5,6</sup> but up to now, few detailed data are available on patients with cirrhosis. Also, individual risk factors for an inadequate vaccination response have not been studied comprehensively in these populations so far. An ongoing trial found an overall seroconversion rate of 89% in immunocompromised patients and the highest risk of non-seroconversion in patients with vasculitis and B-cell depletion.<sup>7</sup>

This prospective observational study explores the humoral and T-cell response to SARS-CoV-2 vaccination in a large cohort of patients with compensated and decompensated LC and LT recipients. Also, predictors of low response to vaccination were identified in this highly vulnerable patient population.

## Methods

### *Study population and data collection*

Non-pregnant patients  $\geq 18$  years with LC presenting for LT or patients post LT were enrolled in this prospective observational cohort study at the University Medical Center Hamburg-Eppendorf in case of SARS-CoV-2 vaccination with a 2-dose regimen, consisting of an mRNA (BNT162b2; BioNTech SE/Pfizer or mRNA-1273; Moderna Biotech) or vector-based vaccine (AZD1222; AstraZeneca). LT recipients receiving a combined transplantation and cirrhotic patients under immunosuppression were excluded. Clinical data were obtained from the patients' electronic medical records. In addition, control subjects matched for age and vaccination regimen were included. In all participants, the immune response was determined 10 to 84 days after the second vaccination, and in a subgroup also directly before the first and second vaccination. The study was approved by the local Ethics Committee of Hamburg, Germany (Reg. number PV7103) and the Paul Ehrlich Institute, the German Federal Institute for Vaccines and Biomedicines (Reg. number NIS508). All participants signed written informed consent, and all authors had access to the study data and reviewed and approved the final manuscript.

## What You Need to Know

### Background

After vaccination against severe acute respiratory syndrome coronavirus type 2, the immune response is reduced in organ transplant recipients as compared with the healthy population.

### Findings

Older age, arterial hypertension, and immunosuppression other than calcineurin inhibitor monotherapy predict vaccination failure in liver transplant recipients. In decompensated liver cirrhosis patients, the humoral immune response is comparable to healthy controls.

### Implications for patient care

Identification of predictors of no or low immune response after initial vaccinations will help to decide on further booster strategies. Patients with liver cirrhosis should be vaccinated pre transplantation.

### *Investigation of the vaccine-specific humoral and T-cell response*

The vaccine-specific humoral immune response was quantitatively determined by 2 different anti-SARS-CoV-2 spike immunoassays in parallel: The DiaSorin LIAISON XL anti-SARS-CoV-2 TrimericS IgG ChemiLuminescent ImmunoAssay (sensitivity, 99.4%; specificity, 99.8%; cutoff, 33.8 binding antibody units [BAU]/mL<sup>8</sup>), with spike S1 glycoproteins assembled as trimers allowing to detect a broad range of antibodies including responses to the N terminal regions of the spike protein (anti-S trimer) and the Roche Elecsys anti-SARS-CoV-2 S Ig ElectroChemiLuminescent ImmunoAssay (sensitivity, 93.9%; specificity, 99.6%; cutoff, 0.8 U/mL<sup>9</sup>) with a receptor-binding domain protein (RBD) sandwich assay design (anti-S RBD). For both assays, a low positive response was defined from 33.8 to 100 BAU/mL and from 0.8 to 100 U/mL, respectively, based on thresholds of validating studies and on cutoffs used in randomized trials.<sup>10,11</sup>

The SARS-CoV-2 spike protein-specific T-cell response was determined by a commercial, standardized interferon-gamma (IFN- $\gamma$ ) release assay (IGRA) using the EUROIMMUN SARS-CoV-2 IGRA stimulation tube set (product No. ET 2606-3003) and EUROIMMUN IFN- $\gamma$  enzyme-linked immunosorbent assay (product No. EQ 6841-960). The specific T-cell response was quantified according to the manufacturer's instructions and values  $>100$  mIU/mL were interpreted as low positive, values  $>200$  mIU/mL as positive.<sup>12</sup>

### Statistical analysis

Epidemiologic data and test results are displayed as mean and standard deviation (SD) for normally distributed, or as median and interquartile range (IQR) for non-normally distributed continuous variables and as number of patients and percentage for categorical variables, respectively. The Pearson  $\chi^2$  test was used to test the difference in dichotomous variables between 2 or more groups. If test assumptions were not fulfilled, the Fisher exact test was used instead. Normally and abnormally distributed continuous variables were compared by the *t* test and Mann-Whitney *U* test when comparing 2 groups or the Kruskal-Wallis test when comparing more than 2 groups, respectively. Differences of dependent variables were evaluated by the McNemar (categorical) and Wilcoxon (continuous) tests. The correlation of humoral and T-cell immune response was calculated using the Spearman rank test. A binary logistic regression model was constructed based on rational assumptions to predict a positive immune response. Significance was expected for *P*-values smaller than .05. SPSS Statistics Version 26 for Mac (IBM Corp, Armonk, NY) and GraphPad Prism version 8.0.0 for Mac (GraphPad Software, San Diego, CA) were used for statistical analyses and to create figures, respectively.

## Results

### Patient characteristics

Altogether, 194 patients (53 cirrhotic patients with Child-Pugh class A to C and 141 LT recipients) and 56 controls were enrolled in this study (Figure 1). Nine convalescents recovered from COVID-19 (2 LC, 3 LT) were analyzed separately.

The clinical characteristics of the patients and controls included in the main analysis are shown in Table 1. All patients with liver cirrhosis were presenting for evaluation of liver transplantation or check-up investigations on the waiting list. Of those, 32 patients (66.7%) had a decompensated Child B or C cirrhosis, and 9 (18.8%) had undergone implantation of a transjugular intrahepatic portosystemic stent-shunt (TIPS). Most LT recipients were long-term recipients (median time since LT, 7 years), whereas 17 (12.3%) were vaccinated within 1 year post LT. Altogether, fewer patients with cirrhosis than LT recipients had arterial hypertension (37.5% vs 61.6%) or suffered from chronic kidney disease (16.7% vs. 37.3%).

Calcineurin inhibitor (CNI) therapy was used in almost all patients (92.8%), with 23.9% receiving a CNI monotherapy, and additional mycophenolate mofetil (MMF), mammalian target of rapamycin inhibitors (mTORis), or prednisone in the remaining cases. Laboratory values are shown in Table 1.

The vaccination regimen used (Table 1) as well as vaccination side effects (Supplementary Figures 1 and 2) did not differ between the groups.

### The humoral immune response after the second vaccination

After the second vaccination (median, 29 days), significantly fewer LT recipients tested positive for anti-SARS-CoV-2 Ig compared with cirrhotic patients and controls using the anti-S RBD (73.9% vs 100% vs 100%, respectively) or the anti-S trimer assay (63.0% vs 97.9% vs 100%, respectively). A negative or weak anti-SARS-CoV-2 response was seen in 2% (anti-S RBD) and 6% (anti-S trimer) of the cirrhotic patients and 46% (anti-S RBD) and 48% (anti-S trimer) of the LT recipients,

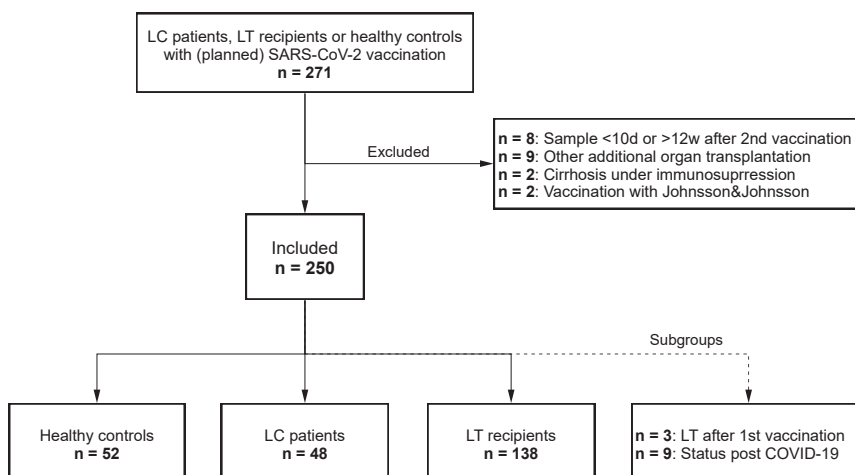


Figure 1. Flowchart of study cohort.



**Table 1.** Baseline Characteristics and Laboratory Values Before the First SARS-CoV-2 Vaccination

	LC patients (n = 48)	LT recipients (n = 138)	Controls (n = 52)	P
Age, y	53.8 (9.5)	55.0 (13.19)	50.9 (11.6)	.095
Females	19 (39.6)	59 (42.8)	33 (63.5)	<b>.021</b>
Vaccine regimen				.068
mRNA/mRNA	44 (91.6)	121 (87.7)	39 (75.0)	
BNT162b2	38 (79.2)	110 (79.7)	36 (69.2)	
mRNA-1273	6 (12.4)	11 (8.0)	3 (5.8)	
AZD1222/AZD1222	1 (2.1)	6 (4.3)	2 (3.8)	
AZD1222/mRNA	3 (6.3)	11 (8.0)	11 (21.2)	
Days 1st to 2nd vaccine	42 (41–43)	42 (40–42)	36 (22–63)	.054
Days 2nd vaccine to follow-up	28 (21–41)	29 (25–39)	49 (28–74)	<b>&lt; .001</b>
BMI, kg/m <sup>2</sup>	26.3 (23.4–29.8)	24.8 (22.4–28.5)		.069
Diabetes	12 (25.0)	29 (21.0)		.566
Arterial hypertension	18 (37.5)	85 (61.6)		<b>.004</b>
CKD with eGFR 30–59 mL/min	6 (16.7)	38 (37.3)		<b>.026</b>
eGFR <30 mL/min	1 (2.8)	8 (7.8)		.446
Etiology of liver disease				<b>.006</b>
ALD	23 (47.9)	28 (20.3)		
Viral	3 (6.3)	17 (12.3)		
AILD	11 (22.9)	40 (29.0)		
NASH	4 (8.3)	7 (5.1)		
Pediatric	–	5 (3.6)		
Cryptogenic	5 (10.4)	13 (9.4)		
ALF	1 (2.1)	5 (3.6)		
Other	1 (2.1)	23 (16.7)		
HCC	5 (10.4)	25 (18.1)		.212
Child-Pugh class				
A	16 (33.3)			
B	18 (37.5)			
C	14 (29.2)			
TIPS	9 (18.9)			
Time from 1st LT, y		7 (2–17)		
Vaccination < 1 y post LT		17 (12.3)		
Prednisone		43 (31.2)		
CNI		128 (92.8)		
Tacrolimus		95 (68.8)		
Cyclosporin		33 (23.9)		
CNI monotherapy		33 (23.9)		
CNI + prednisone		19 (13.8)		
CNI + mTORi		17 (12.3)		
CNI + MMF		48 (34.8)		
CNI + azathioprine		9 (6.5)		
Biologicals		8 (5.8)		
≥3 Immunosuppressants		18 (13.0)		
	LC <sup>a</sup>	LT <sup>b</sup>		P
HbA1c, % (ref. 4.8-5.6)	4.4 (4.1–5.9)	5.7 (5.1–6.0)		.080
Creatinine, mg/dL (ref. 0.55-1.02)	0.9 (0.8–1.1)	1.1 (0.9–1.5)		<b>&lt; .001</b>
eGFR, mL/min	80.5 (66.0–102.8)	64.0 (43.5–82.3)		<b>.001</b>

Table 1. Continued

	LC <sup>a</sup>	LT <sup>b</sup>	<i>P</i>
MELD	14 (10–19)	–	
IgG, g/L (ref. 6.5–16.0)	14.7 (11.9–19.1)	10.6 (8.4–12.0)	< .001
IgA, g/L (ref. 0.4–3.5)	4.2 (3.6–5.6)	1.7 (1.3–2.6)	< .001
IgM, g/L (ref. 0.5–3.0)	1.8 (1.0–2.7)	1.1 (0.7–1.7)	.053
Lymphocytes, / $\mu$ l (ref. 1000–3600)	994 (757–1422)	950 (667–1404)	.786
T-lymphocytes, / $\mu$ l (ref. 900–2900)	626 (406–933)	746 (391–1044)	.488
B-lymphocytes, / $\mu$ l (ref. 80–500)	128 (84–252)	92 (56–130)	.100
CD4-helper cells, / $\mu$ l (ref. 500–1350)	504 (264–682)	413 (225–572)	.447
CD8-cytotoxic cells, / $\mu$ l (ref. 290–930)	112 (86–240)	242 (158–440)	.004
NK-cells, / $\mu$ l (ref. 35–350)	174 (67–326)	122 (63–207)	.263
CD4/CD8 ratio (ref. 0.6–3.6)	3.3 (2.1–5.1)	1.5 (1.1–2.2)	< .001

Note: Data are presented as number (%), mean (standard deviation), or median (interquartile range).

Note: Boldface *P* values indicate statistical significance.

AILD, Autoimmune liver disease; ALD, alcoholic liver disease; ALF, acute liver failure; BMI, body mass index; CKD, chronic kidney disease; CNI, calcineurin inhibitor; eGFR, estimated glomerular filtration rate; HC, healthy control; HCC, hepatocellular carcinoma; IQR, interquartile range; LC, liver cirrhosis; LT, liver transplant; MELD, Model for End-Stage Liver Disease; MMF, mycophenolate mofetil; mTORi, mammalian target of rapamycin inhibitors; NASH, nonalcoholic steatohepatitis; SARS-CoV-2, severe acute respiratory syndrome coronavirus type 2; SD, standard deviation; TIPS, transjugular intrahepatic portosystemic shunt.

<sup>a</sup>n ranges from 17 to 36.

<sup>b</sup>n ranges from 42 to 102.

respectively (Figure 2D-F). Furthermore, the median titers of anti-SARS-CoV-2 Ig were significantly lower in patients post LT as compared with patients with liver cirrhosis (Figure 2A-C). Thus, in contrast to LT recipients, cirrhotic patients were not found to have an impaired humoral immune response compared with controls based on concerning seroconversion rate and median antibody titers of responding patients (Supplementary Table 1).

Of note, there was a high concordance between both immunoassays (Supplementary Figure 3). Therefore, for all subsequent analyses the results of the trimer assay are shown. Additionally, the results of the RBD assay are provided as numerical values in the corresponding tables and as additional figures in the supplementary.

#### *Development of anti-SARS-CoV-2 Ig titers after the first and second vaccination*

The anti-SARS-CoV-2 Ig titers after the first and second vaccination (19 LC, 88 LT) are shown in Supplementary Figures 4A and B. The seroconversion rate markedly increased in cirrhotic patients (from 77.8% to 100%) and LT recipients (from 15.4% to 55.4%). In patients who did not develop a detectable humoral response after the first vaccination, the probability of seroconversion after the second vaccination was 100% for cirrhotic patients and 43.6% for LT recipients. Also, there was a significant 28- and 19-fold increase of the median anti-SARS-CoV-2 Ig titers in cirrhotic patients and LT recipients, respectively, at last follow-up 5  $\pm$  3 weeks after vaccination.

#### *The T-cell response after the second vaccination*

The cellular immune response assessed by semi-quantitative analysis of IFN- $\gamma$  release after spike-specific stimulation of T-cells was determined in a subgroup of 26 cirrhotic patients, 82 LT recipients, and 19 controls. Overall, after the second vaccination, a T-cell response (cutoff >100 mIU/mL) was less frequently detectable in LT recipients (37%) and cirrhotic patients (65%) compared with controls (100%) (Figure 2F). Only 32% of LT recipients and 46% of cirrhotic patients showed a strong response (cutoff >200 mIU/mL) as compared with 100% of controls. Also, the median concentration of IFN- $\gamma$  release was significantly lower in patients with cirrhosis and LT recipients compared with controls (Figure 2C, Supplementary Table 1).

#### *Correlation between the vaccine-induced humoral and T-cell response*

Although in controls positive and negative test results correlated in 100% of cases between the trimer immunoassay and the IGRA, there was a high discordance in cirrhotic and LT patients (Supplementary Figure 5). Nine of 32 LT patients (27%) without detectable antibody response had a positive T-cell response. On the other hand, 29 of 50 LT patients (58%) with a negative IGRA result tested positive for anti-S trimer antibodies. Altogether, 23 of 82 LT recipients (28%) did show neither a

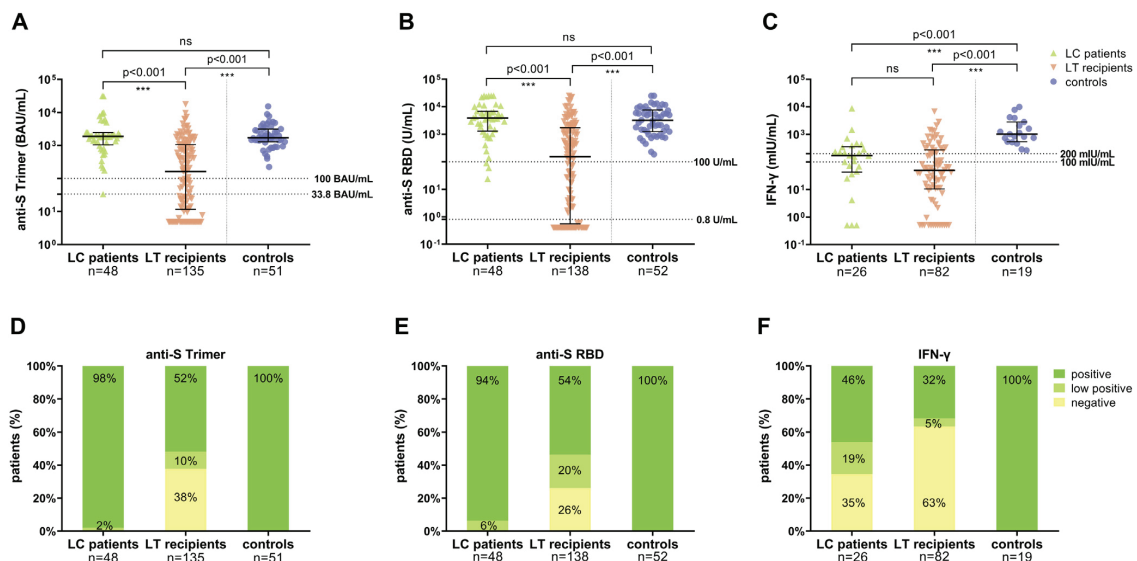


**Figure 2.** Serological and T-cell response after second SARS-CoV-2 vaccination in cirrhotic patients, LT recipients, and healthy controls. **(A)** Anti-S Trimer; **(B)** anti-S RBD; **(C)** IFN- $\gamma$  release. Statistical analysis was performed by Mann-Whitney test. *Solid horizontal lines* indicate medians and interquartile range; *dotted horizontal lines* indicate cutoff values for no response, low positive, and positive response. The respective proportions are provided as bar graphs. **(D)** Anti-S Trimer; **(E)** anti-S RBD; **(F)** IFN- $\gamma$  release.

detectable spike-specific humoral nor a T-cell response, and even 40% showed no or a low humoral and T-cell response. Also, 35% of patients with cirrhosis with a positive antibody response tested negative for a T-cell response.

#### *Risk factors for no or a low humoral immune response in LT recipients*

Parameters investigated by univariate and multivariate binary logistic regression analysis as potential predictors for a low immune response after the second SARS-CoV-2 vaccination in LT recipients are given in [Table 2](#) and [Supplementary Table 2](#). Independent prognostic factors for no or only a weak antibody response were age >65 years (odds ratio [OR], 4.57; 95% confidence interval [CI], 1.48-14.05) and arterial hypertension (OR, 2.50; 95% CI, 1.10-5.68), whereas calcineurin inhibitor monotherapy was a positive prognostic factor for a response as compared with other immunosuppressive regimens (OR, 0.36; 95% CI, 0.13-0.99) ([Figure 3](#)). In the LT cohort, only 19.2% of patients were >65 years, but 59.6% of patients <65 years attained anti-S trimer titers above 100 BAU/mL ([Supplementary Table 3](#)). Of note, laboratory values were not considered for multivariate analysis because of limited baseline values (n = 42). However, the seroconversion rate (31.6% vs 60.6%;  $P = .044$ ) and median antibody titers ( $P = .039$ ) significantly

differed between LT recipients with B-lymphocytes below and above the reference value (80/ $\mu$ L) ([Figure 3F](#)). For easy clinical use, we added a table to estimate the relative risk of no or low immune response in case of multiple risk factors ([Supplementary Table 4](#)).

#### *Special patient groups*

##### *LT recipients who obtained heterologous vaccination.*

A significantly better immune response was found in LT recipients with mixed (AZD1222/mRNA, n = 11) as compared with homologous mRNA vaccination (n = 121) in terms of the level of antibody titers and IFN- $\gamma$  titers ([Supplementary Figure 6](#), [Supplementary Table 5](#)). Similarly, significantly higher anti-SARS-CoV-2 antibody responses were detectable in cirrhotic patients and controls after heterologous vaccination.

*Immune response according to Child-Pugh class.* There were no differences between patients with varying Child-Pugh classes with regard to the humoral and cellular immune response based on the seroconversion rate ([Supplementary Table 6](#)) and the level of antibody titers or IFN- $\gamma$  production ([Figure 4A](#) and [B](#)), and vaccination side effects ([Supplementary Figure 1C](#) and [D](#)), respectively. Compared with LT recipients, higher antibody titers were found in both patients with compensated (Child-Pugh class A) and decompensated liver cirrhosis (Child-Pugh class B and C). Also, no differences in the antibody titers were found in the subgroup of cirrhotic patients after TIPS

implantation (n = 9; 18.9%) compared with patients without TIPS (Supplementary Table 6).

*Convalescents with a booster vaccination.* All nine convalescents (2 LC, 3 LT, 4 controls) received an mRNA-based vaccine. All subjects developed very high anti-SARS-CoV-2 titers with a 29- to 76-fold increase (Supplementary Figure 7) and additionally showed high titers of IFN- $\gamma$  in the IGRA (1 LC, 1 LT, and 3 controls) of 2127 and 9738 mIU/mL.

## Discussion

This prospective study analyzed the humoral and cellular immune response in patients with different stages of LC and LT recipients. Cirrhotic patients, including patients with decompensated Child-Pugh class B or C or after TIPS implantation, had an overall serological response comparable to healthy controls. In contrast, almost one-half of LT recipients showed no or

**Table 2.** Risk of LT Recipients of No or Only a Low Humoral Immune Response After Second SARS-CoV-2 Vaccination Based on the Trimer Immunoassay

	Univariate OR (95% CI)	P	Multivariate OR (95% CI)	P
Age >65 y	<b>6.21 (2.18–17.69)</b>	<b>.001</b>	<b>4.57 (1.48–14.05)</b>	<b>.008</b>
Sex (male)	2.10 (1.04–4.22)	.038		
Vaccination regimen	1.47 (0.71–3.04)	.300		
LT <1 y before vaccination	2.94 (0.98–8.88)	.055		
Obesity (BMI $\geq$ 30 kg/m <sup>2</sup> )	0.74 (0.28–2.01)	.557		
eGFR <45 mL/min	<b>11.10 (3.07–40.15)</b>	<b>&lt; .001</b>	N/A	
Arterial hypertension	<b>2.82 (1.37–5.83)</b>	<b>.005</b>	<b>2.50 (1.10–5.68)</b>	<b>.028</b>
Diabetes	<b>2.48 (1.05–5.84)</b>	<b>.038</b>	1.78 (0.67–4.77)	.251
CNI monotherapy	<b>0.26 (0.11–0.63)</b>	<b>.003</b>	<b>0.36 (0.13–0.99)</b>	<b>.049</b>
CNI + MMF	<b>3.08 (1.47–6.45)</b>	<b>.003</b>	1.78 (0.74–4.30)	.198
CNI + mTORi	1.94 (0.66–5.68)	.227		
CNI + azathioprine	0.29 (0.06–1.43)	.127		
CNI + prednisone	0.49 (0.17–1.40)	.183		
No CNI	4.77 (0.97–23.38)	.054		
Prednisone >5 mg	1.32 (0.38–4.56)	.659		
Triple immunosuppression	2.42 (0.85–6.87)	.098		
Biological	3.46 (0.67–17.79)	.138		
Re-cirrhosis	0.38 (0.10–1.48)	.161		
IgG <13.8 g/L	N/A			
IgA <3.9 g/L	N/A			
IgM <1.8 g/L	3.71 (0.35–38.93)	.275		
Lymphocytes <1000/ $\mu$ l	1.36 (0.46–4.07)	.578		
B-lymphocytes <80/ $\mu$ l	<b>3.33 (1.01–10.99)</b>	<b>.048</b>	N/A	
T-lymphocytes <900/ $\mu$ l	1.07 (0.35–3.28)	.910		
NK-cells <35/ $\mu$ l	0.46 (0.04–5.42)	.537		
CD4+ cells <400/ $\mu$ l	0.80 (0.27–2.42)	.695		
CD8+ cells <290/ $\mu$ l	1.09 (0.37–3.24)	.875		
CD4/CD8 ratio <0.6	N/A			

Note: For laboratory values, the lower levels of normal were set as thresholds.

Note: Bold values indicate statistical significance.

BMI, Body mass index; CI, confidence interval; CNI, calcineurin inhibitor; eGFR, estimated glomerular filtration rate; LT, liver transplantation; MMF, mycophenolate mofetil; mTORi, mTOR inhibitor; N/A, not applicable: laboratory values that were not considered for univariate or multivariate analysis because of insufficient baseline values; OR, odds ratio; SARS-CoV-2, severe acute respiratory syndrome coronavirus type 2.

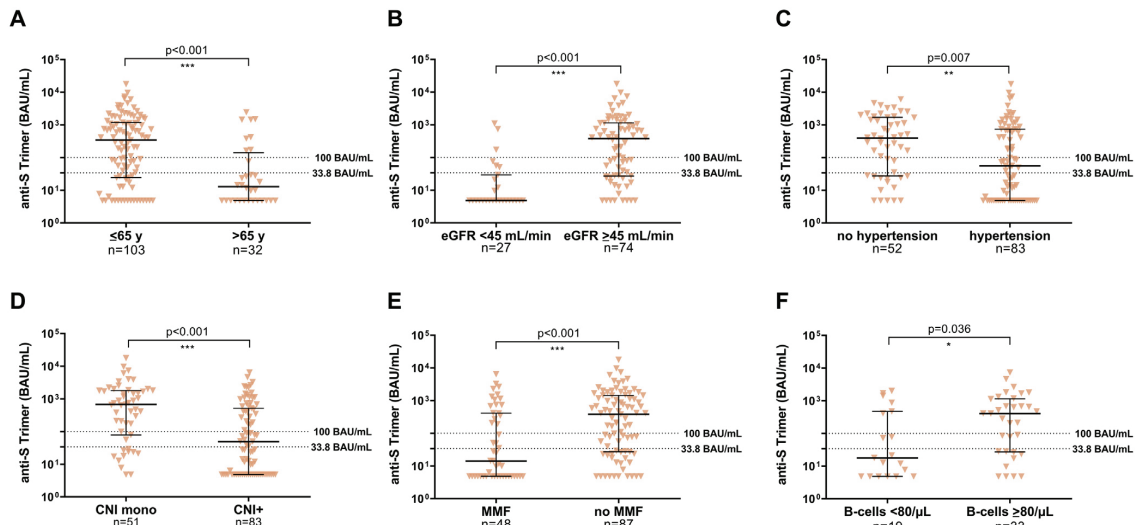


**Figure 3.** All values were measured with anti-S trimer (BAU/mL). **(A)** Age groups  $\leq 65$  years and  $>65$  years. **(B)** Normal blood pressure vs arterial hypertension. **(C)** eGFR  $<45$  mL/min vs  $\geq 45$  mL/min. **(D)** CNI mono vs CNI plus additional immunosuppressive drugs. **(E)** MMF vs no MMF as an additional drug to CNI. **(F)** Baseline B-lymphocytes  $<80$  and  $\geq 80$  per  $\mu\text{L}$ . Statistical analysis was performed by Mann-Whitney test. Solid horizontal lines indicate medians and interquartile range; dotted horizontal lines indicate cutoff values.

only a low spike-specific antibody response after the second vaccination. Moreover, there was no evidence of a spike-specific T-cell response in the majority of LT recipients without any detectable antibody response. More than one-quarter of the LT recipients were left potentially immunologically unprotected against SARS-CoV-2 infection, and an additional 20% of patients were considered to have only a suboptimal immune response.

In this study, we used 2 different immunoassays to determine the humoral immune response: the more commonly used anti-S RBD assay (Roche Elecsys) and the anti-S trimer assay (DiaSorin LIAISON). The latter assay was previously shown to correlate highly with the current gold standard for detection of neutralizing

antibodies.<sup>8</sup> Here, both assays showed a very high correlation in patients and controls ( $r = 0.94$ ).

In addition, we also evaluated the T-cell immune response by assessing the ex vivo IFN- $\gamma$  release after spike-specific stimulation of T-cells in a commercial, standardized IGRA assay. It has been suggested that the vaccine-induced T-cell response may have a protective effect even in the absence of a detectable vaccine-induced B-cell response by limiting the extent of viral replication and by supporting long-term immunological memory.<sup>13</sup> Therefore, solid organ transplant (SOT) recipients with a strong T-cell response may be protected against a severe course of SARS-CoV-2 infection even in the absence of a seroconversion.<sup>14</sup> Our results

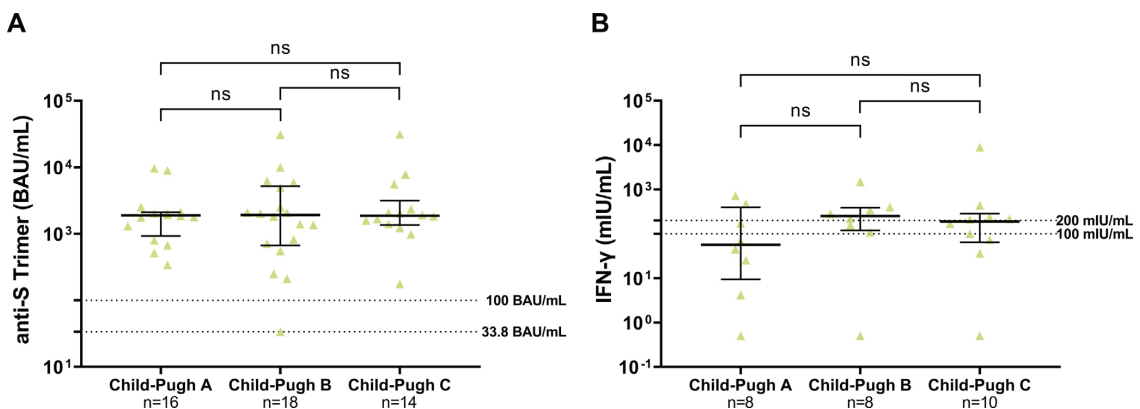


**Figure 4.** Comparison of humoral and cellular immune responses in cirrhotic patients. **(A)** Anti-S Trimer (BAU/mL). **(B)** IFN- $\gamma$  release (mIU/mL). Statistical analysis was performed by Mann-Whitney test. Solid horizontal lines indicate medians and interquartile ranges; dotted horizontal lines indicate cutoff values.

demonstrate a spike-specific T-cell response only in around one-fifth (22%) of LT recipients without seroconversion, being in line with previously reported results in cardiothoracic (20%), and kidney transplant recipients (29.8%).<sup>15,16</sup> Furthermore, in 54% of the patients with liver cirrhosis who attained seroconversion, the IFN- $\gamma$  release in the IGRA was below the cutoff. Whether this correlates with a lower protection against COVID-19 disease has to be further investigated in larger prospective studies.

Previously, Rabinowich et al identified age, low estimated glomerular filtration rate (eGFR), high-dose prednisone, triple immunosuppression, and MMF use as predictors of a missing immune response after vaccination in a cohort of 80 LT recipients.<sup>6</sup> In patients with autoimmune rheumatic diseases receiving immunosuppression lymphopenia and B-cell depletion, among other factors, were associated with lack of seroconversion after the second vaccination.<sup>17</sup> In our cohort, we confirmed older age and low eGFR as predictors for a low or negative humoral immune response. Additionally, a pre-vaccination B-lymphocyte count below the reference value of 80  $\mu$ l was a negative predictive factor, whereas CNI monotherapy was a predictor for a positive humoral response. In principle, our results are in line with those of Rabinowich et al, revealing that higher immunosuppression reduces the response to vaccination<sup>6</sup> and adds to the knowledge that LT recipients with low B-lymphocytes and arterial hypertension are at increased risk of failure to SARS-CoV-2 vaccination.

In our small group of LT recipients who received prime AZD1222 and second mRNA vaccination (n = 11), a seroconversion rate of 81.8% and high titers were found. This extends the recently published data describing significantly higher titers of neutralizing antibodies after heterologous vaccination of this highly vulnerable population.<sup>16</sup> New approaches to improve the immune response of LT recipients are urgently needed because breakthrough infections have been reported to occur more frequently in SOT recipients than in the healthy population.<sup>18</sup> Although recently a randomized trial found significantly higher antibody titers in this population after a third homologous vaccination, the seroconversion rate remained low with only 50% of previously nonresponsive SOT recipients attaining anti-S RBD titer  $\geq$ 100 U/mL.<sup>11</sup> Therefore, before the third vaccination, temporary discontinuation of the anti-proliferative immunosuppressive medication and the preference of a heterologous vaccination scheme should be considered in older, long-term LT recipients with a stable graft function and no history of a recent rejection episode but with risk factors for vaccination failure.

Our data also indicate a high probability of vaccine response even in patients with decompensated Child-Pugh class C liver cirrhosis without an increase of side effects. This is of great importance due to the markedly increased mortality of cirrhotic patients infected with COVID-19, in particular in case of decompensated

patients.<sup>19,20</sup> Our data are in line with another retrospective study, which showed that for fully immunized patients with cirrhosis, the risk of COVID-19 disease and hospitalization is reduced by 78.6% and 100%, respectively.<sup>21</sup> These results underline the relevance of immunizing cirrhotic patients as proposed by interim recommendations.<sup>22</sup>

In comparison to previous studies,<sup>5,6</sup> this study included different vaccination regimens, measured immune response in more detail, and also investigated pre-transplant patients with decompensated cirrhosis.

Nonetheless, the study is not without limitations. First, due to the study design, the time interval between the second vaccination and blood sample varied between 10 and 84 days in patients and was longer in the controls. However, the data presented here and those of previous studies of our group<sup>23</sup> did not show a significant increase or decrease of antibody titers over the defined inclusion period (Supplementary Figure 8). Second, different time intervals between the 2 vaccinations may impact the immune response. Third, sample sizes were too small to detect potential inherent effects of TIPS placement on the vaccination response. Finally, it should be kept in mind that the level of circulating SARS-CoV-2 antibodies that renders sterile protection against infection has not been established yet. So, the chosen cutoffs, in particular those for suboptimal titers, should only be regarded as estimates based on the current data in the healthy population and based on correlation with neutralizing antibody assays. According to the literature, titers above the cutoff should provide protection against severe COVID-19 disease for most individuals, but not against asymptomatic SARS-CoV-2 infection.<sup>14,24,25</sup> Case reports also demonstrated that even high antibody titers did not render protection in individual constellations. Therefore, it can be assumed that protective titers may vary between patient populations and different SARS-CoV-2 variants.<sup>24</sup>

This study has important clinical implications. Due to the preserved vaccine-induced humoral immune response of cirrhotic patients,<sup>14</sup> this group of patients, including those with decompensated cirrhosis, should be vaccinated before transplantation. However, the clinical significance of the low cellular vaccine response in approximately one-third of the cirrhotic patients is currently unknown and should be carefully monitored concerning the extent and duration of vaccination protection.

On the other hand, a considerable proportion of LT recipients, and the majority of older or lymphopenic patients, showed an absent or reduced humoral and T-cell immune response to SARS-CoV-2 vaccination, which correlated with the intensity of immunosuppression.

Therefore, we suggest a third or even a fourth booster vaccination in all LT recipients and cirrhotic patients with low or missing antibody titers. Further prospective studies are needed to establish an effective vaccination strategy for non-responders. This may include intermittent reduction of the immunosuppression to a CNI monotherapy, or in older patients heterologous vaccination schemes.

## Supplementary Material

Note: To access the supplementary material accompanying this article, visit the online version of *Clinical Gastroenterology and Hepatology* at [www.cghjournal.org](http://www.cghjournal.org), and at <http://doi.org/10.1016/j.cgh.2021.09.003>.

### References

1. Baden LR, El Sahly HM, Essink B, et al. COVE Study Group. Efficacy and safety of the mRNA-1273 SARS-CoV-2 vaccine. *N Engl J Med* 2021;384:403–416.
2. Polack FP, Thomas SJ, Kitchin N, et al. C4591001 Clinical Trial Group. Safety and efficacy of the BNT162b2 mRNA Covid-19 vaccine. *N Engl J Med* 2020;383:2603–2615.
3. Marjot T, Moon AM, Cook JA, et al. Outcomes following SARS-CoV-2 infection in patients with chronic liver disease: an international registry study. *J Hepatol* 2021;74:567–577.
4. Webb GJ, Marjot T, Cook JA, et al. Outcomes following SARS-CoV-2 infection in liver transplant recipients: an international registry study. *Lancet Gastroenterol Hepatol* 2020;5:1008–1016.
5. Boyarsky BJ, Werbel WA, Avery RK, et al. Antibody response to 2-dose SARS-CoV-2 mRNA vaccine series in solid organ transplant recipients. *JAMA* 2021;325:2204–2206.
6. Rabinowich L, Grupper A, Baruch R, et al. Low immunogenicity to SARS-CoV-2 vaccination among liver transplant recipients. *J Hepatol* 2021;75:435–438.
7. Kearns P, Siebert S, Willicombe M, et al. Examining the immunological effects of COVID-19 vaccination in patients with conditions potentially leading to diminished immune response capacity – the OCTAVE trial, 2021. Available at: <https://ssrn.com/abstract=3910058>. Accessed August 24, 2021.
8. Bonelli F, Blocki FA, Bunnell T, et al. Evaluation of the automated LIAISON(R) SARS-CoV-2 TrimericS IgG assay for the detection of circulating antibodies. *Clin Chem Lab Med* 2021; 59:1463–1467.
9. Patel EU, Bloch EM, Clarke W, et al. Comparative performance of five commercially available serologic assays to detect antibodies to SARS-CoV-2 and identify individuals with high neutralizing titers. *J Clin Microbiol* 2021;59: e02257–20.
10. Resman Rus K, Korva M, Knap N, et al. Performance of the rapid high-throughput automated electrochemiluminescence immunoassay targeting total antibodies to the SARS-CoV-2 spike protein receptor binding domain in comparison to the neutralization assay. *J Clin Virol* 2021;139:104820.
11. Hall VG, Ferreira VH, Ku T, et al. Randomized trial of a third dose of mRNA-1273 vaccine in transplant recipients. *N Engl J Med* 2021;385:1244–1246.
12. Huzly D, Panning M, Smely F, et al. Validation and performance evaluation of a novel interferon- $\gamma$  release assay for the detection of SARS-CoV-2 specific T-cell response. *medRxiv* 2021:2021.07.17.21260316.
13. Le Bert N, Tan AT, Kunasegaran K, et al. SARS-CoV-2-specific T cell immunity in cases of COVID-19 and SARS, and uninfected controls. *Nature* 2020;584:457–462.
14. Khoury DS, Cromer D, Reynaldi A, et al. Neutralizing antibody levels are highly predictive of immune protection from symptomatic SARS-CoV-2 infection. *Nat Med* 2021;27:1205–1211.
15. Schramm R, Costard-Jackle A, Rivinius R, et al. Poor humoral and T-cell response to two-dose SARS-CoV-2 messenger RNA vaccine BNT162b2 in cardiothoracic transplant recipients. *Clin Res Cardiol* 2021;110:1142–1149.
16. Schmidt T, Klemis V, Schub D, et al. Immunogenicity and reactogenicity of heterologous ChAdOx1 nCoV-19/mRNA vaccination. *Nat Med* 2021;27:1530–1535.
17. Prendecki M, Clarke C, Edwards H, et al. Humoral and T-cell responses to SARS-CoV-2 vaccination in patients receiving immunosuppression. *Ann Rheum Dis* 2021;80:1322–1329.
18. Qin CX, Moore LW, Anjan S, et al. Risk of breakthrough SARS-CoV-2 infections in adult transplant recipients. *Transplantation* 2021:Online ahead of print.
19. Kim D, Bonham CA, Konyn P, et al. Mortality trends in chronic liver disease and cirrhosis in the united states, before and during COVID-19 pandemic. *Clin Gastroenterol Hepatol* 2021. Online ahead of print.
20. Kim D, Adeniji N, Latt N, et al. Predictors of outcomes of COVID-19 in patients with chronic liver disease: US multi-center study. *Clin Gastroenterol Hepatol* 2021;19:1469–1479.e19.
21. John BV, Deng Y, Scheinberg A, et al. Association of BNT162b2 mRNA and mRNA-1273 vaccines with COVID-19 infection and hospitalization among patients with cirrhosis. *JAMA Intern Med* 2021;181:1306–1314.
22. Rolak S, Hayney MS, Farraye FA, et al. What gastroenterologists should know about COVID-19 vaccines. *Clin Gastroenterol Hepatol* 2021;19:657–661.
23. Brehm TT, Thompson M, Ullrich F, et al. Low SARS-CoV-2 infection rate and high vaccine-induced immunity among German healthcare workers at the end of the third wave of the COVID-19 pandemic. *medRxiv* 2021:2021.08.02.21260667.
24. Feng S, Phillips DJ, White T, et al. Correlates of protection against symptomatic and asymptomatic SARS-CoV-2 infection. *medRxiv* 2021:2021.06.21.21258528.
25. Gilbert PB, Montefiori DC, McDermott A, et al. Immune correlates analysis of the mRNA-1273 COVID-19 vaccine efficacy trial. *medRxiv* 2021:2021.08.09.21261290.

### Reprint requests

Address requests for reprints to: Prof Dr Med Julian Schulze zur Wiesch, I. Department of Internal Medicine, University Medical Center Hamburg-Eppendorf, Martinstraße 52, 20249 Hamburg, Germany. e-mail: [j.schulze-zur-wiesch@uke.de](mailto:j.schulze-zur-wiesch@uke.de).

### Acknowledgment

The authors wish to thank all study participants and contributing departments of the University Medical Center Hamburg-Eppendorf for their active participation in the study. The authors would like to thank Elaine Hussey for her critical review of the manuscript.

### CRedit Authorship Contributions

Dr Darius Ferenc Ruether (Data curation: Equal; Formal analysis: Lead; Visualization: Equal; Writing – original draft: Lead; Writing – review & editing: Equal)

Golda Meline Schaub (Data curation: Equal; Formal analysis: Supporting; Investigation: Equal; Methodology: Supporting; Visualization: Lead; Writing – original draft: Supporting; Writing – review & editing: Supporting)

Paul-Maria Duengelhoefer (Data curation: Equal; Investigation: Supporting; Validation: Supporting; Visualization: Supporting)

Prof Dr Friedrich Haag (Supervision: Supporting; Writing – review & editing: Supporting)

Dr Thomas Theo Brehm (Investigation: Supporting; Resources: Supporting; Writing – review & editing: Supporting)

Dr Anahita Fathi (Conceptualization: Supporting; Funding acquisition: Equal; Writing – review & editing: Supporting)

Dr Malte Wehmeyer (Resources: Supporting; Writing – review & editing: Supporting)

Jacqueline Jahnke-Triankowski (Data curation: Supporting; Investigation: Supporting; Project administration: Supporting)

Leonie Mayer (Methodology: Supporting)

Armin Hoffmann (Investigation: Supporting)

**172 Ruether et al****Clinical Gastroenterology and Hepatology Vol. 20, No. 1**

Prof Dr Lutz Fischer (Resources: Supporting; Writing – review & editing: Supporting)

Prof Dr Marylyn Martina Addo (Conceptualization: Equal; Funding acquisition: Equal; Project administration: Supporting; Resources: Supporting; Writing – review & editing: Supporting)

Dr Marc Luetgehetmann (Investigation: Equal; Resources: Equal; Supervision: Supporting; Writing – review & editing: Supporting)

Prof Dr Ansgar Wilhelm Lohse (Conceptualization: Supporting; Funding acquisition: Supporting; Resources: Supporting; Supervision: Supporting; Writing – review & editing: Equal)

Prof Dr Julian Schulze zur Wiesch, MD (Conceptualization: Supporting; Funding acquisition: Supporting; Resources: Supporting; Supervision: Equal; Visualization: Supporting; Writing – original draft: Equal; Writing – review & editing: Equal)

Prof Dr Martina Sterneck (Conceptualization: Lead; Funding acquisition: Lead; Project administration: Lead; Resources: Supporting; Supervision: Lead; Writing – original draft: Equal; Writing – review & editing: Lead)

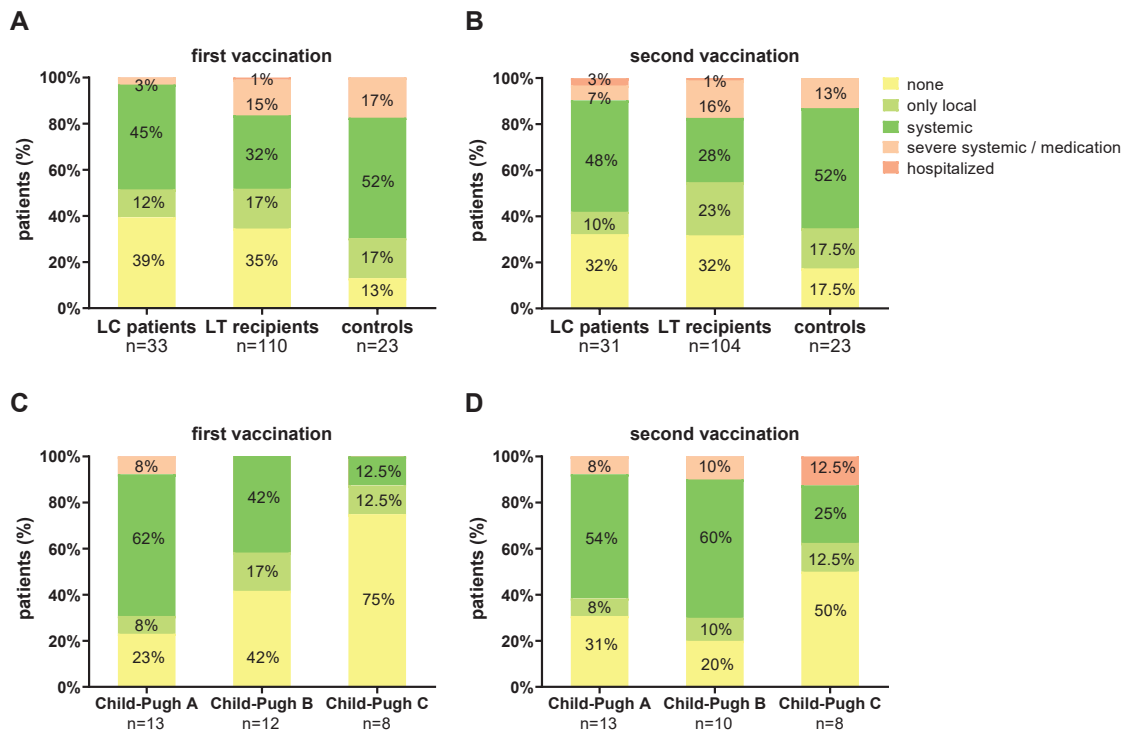
**Conflicts of interest**

The authors disclose no conflicts.

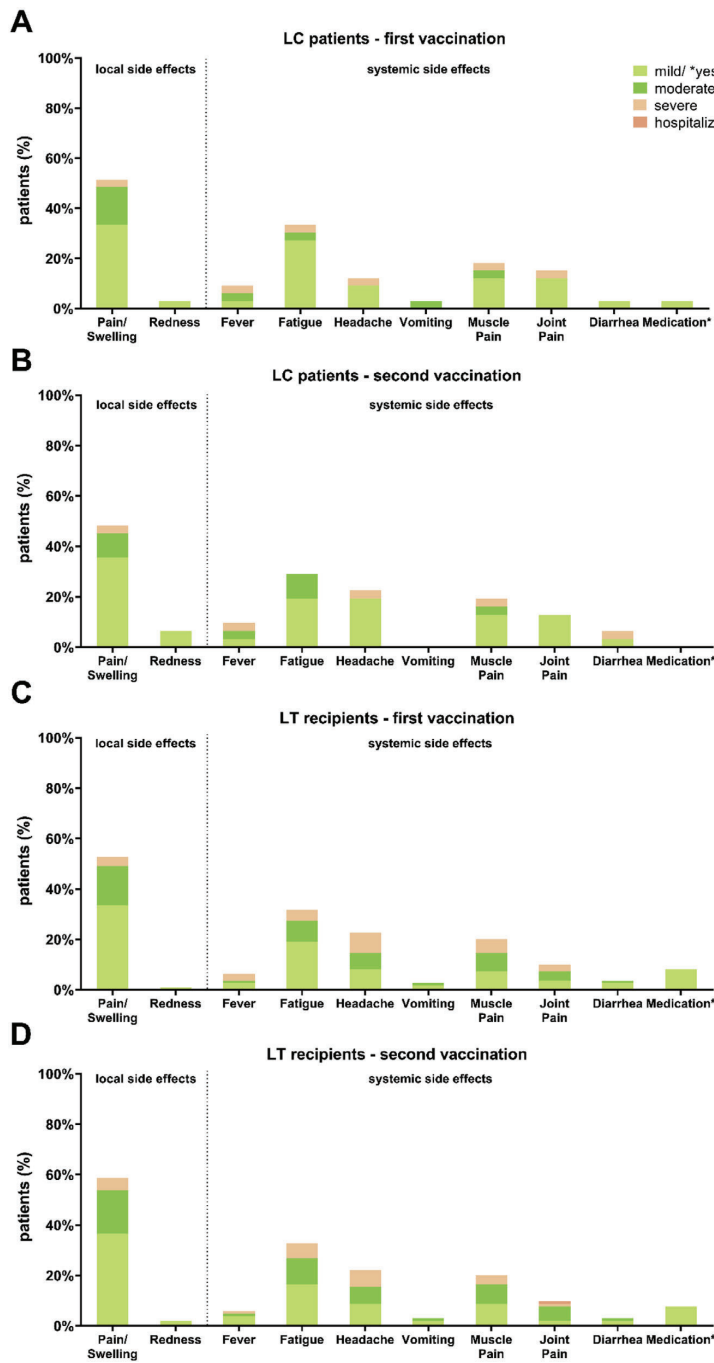
**Funding**

Friedrich Haag and Julian Schulze zur Wiesch report research funding from SFB1328, project A12; Golda Meline Schaub was supported by a DZIF MD Stipend through the DZIF academy. Anahita Fahti, Marylyn Martina Addo, and Leonie Mayer report funding from the DZIF TTU 01709. No further funding was used for the research reported.





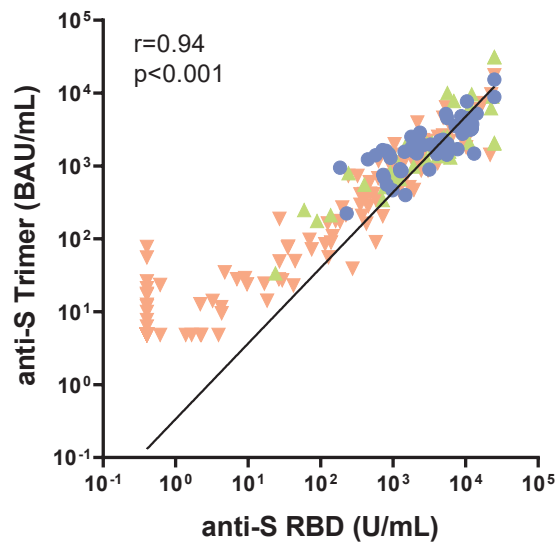
**Supplementary Figure 1.** Comparison of side effects after first and second SARS-CoV-2 vaccination in all patients and in cirrhotic patients with different Child-Pugh classes. Side effects were classified into 5 groups: none, only local, systemic, severe systemic/medication, and hospitalized. (A) Side effects after first vaccination in LC patients, LT recipients, and controls. (B) Side effects after second vaccination in the 3 groups. (C) Side effects after first vaccination in LC patients with different Child-Pugh classes. (D) Side effects after second vaccination in LC patients with different Child-Pugh classes. Statistical analysis was performed by Wilcoxon matched pairs rank test. All *P*-values were > .05.



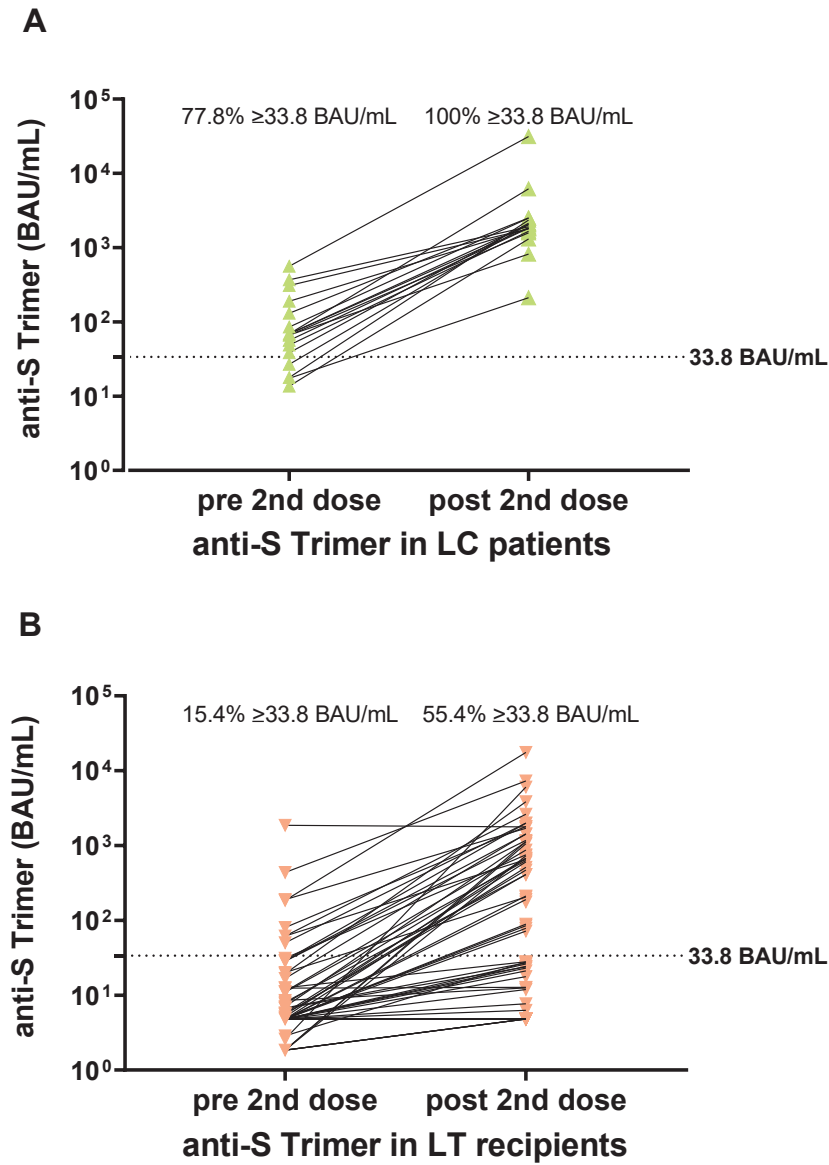
**Supplementary Figure 2.** Comparison of local and systemic side effects after first and second vaccination in cirrhotic patients and LT recipients. Detailed comparison of local and systemic side effects in LC patients and LT recipients. Side effects were classified into mild, moderate, severe, and hospitalized. Medications have been classified only into yes (light green) or no. (A) Side effects after first vaccination in LC patients. (B) Side effects after second vaccination in LC patients. (C) Side effects after first vaccination in LT recipients. (D) Side effects after second vaccination in LT recipients.

January 2022

Immune Response to SARS-CoV2 Vaccination 172.e3



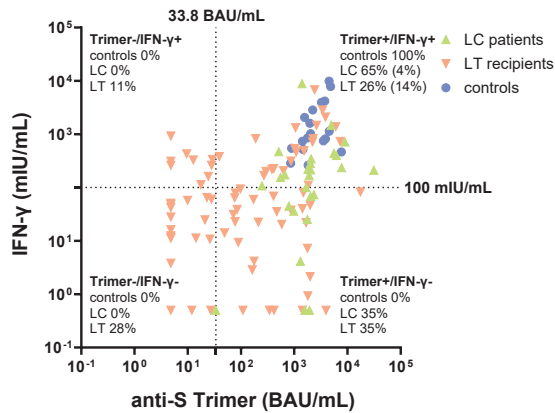
**Supplementary Figure 3.** Correlation of anti-SARS-CoV-2 spike RBD and spike trimer. Correlation between anti-S RBD (U/mL) and anti-S trimer (BAU/mL) for cirrhotic patients (*green ascending triangles*), LT recipients (*orange descending triangles*), and controls (*blue dots*). Statistical analysis was performed by Spearman  $r$  with a 95% CI.



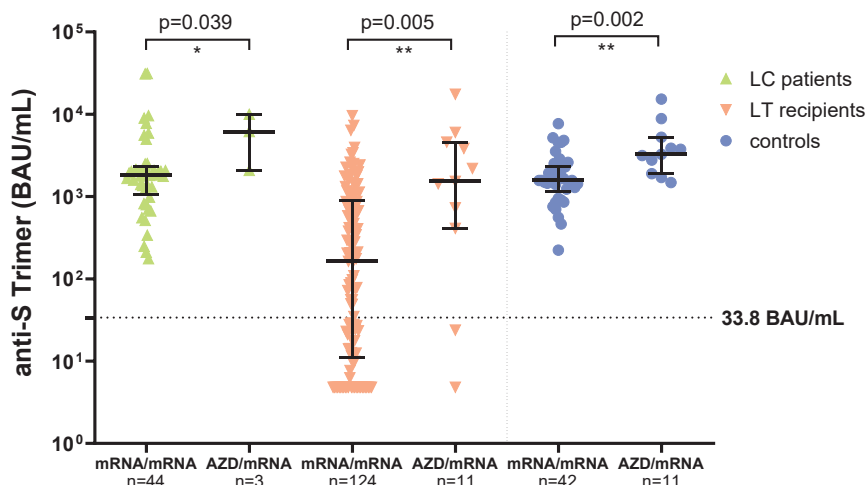
**Supplementary Figure 4.** Comparison of antibody titers after first and second SARS-CoV-2 vaccination. Comparison of anti-S trimer (BAU/mL) titers after first and second SARS-CoV-2 vaccination in cirrhotic patients (*green*) and LT recipients (*orange*). (A) Anti-S trimer in cirrhotic patients. (B) Anti-S Trimer in LT recipients. Statistical analysis was performed by Wilcoxon matched pairs rank test. Percentages indicate the seroconversion rate; *dotted horizontal lines* indicate cutoff values.

January 2022

Immune Response to SARS-CoV2 Vaccination 172.e5



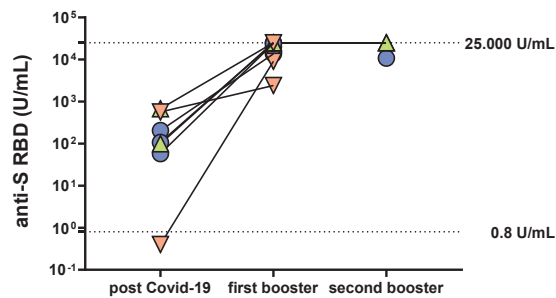
**Supplementary Figure 5.** Correlation between humoral and T-cell immune response. Correlation between humoral and T-cell immune response for cirrhotic patients (*green ascending triangles*), LT recipients (*red descending triangles*), and controls (*blue dots*). Humoral response measured with anti-S trimer (BAU/mL); T-cell response measured with IFN- $\gamma$  release (mIU/mL). *Dotted lines* indicate cutoff values. Percentages indicate proportions of values for every patient group. In addition, low positive responses (cutoff values 100 BAU/mL and 200 mIU/mL) are shown in brackets.



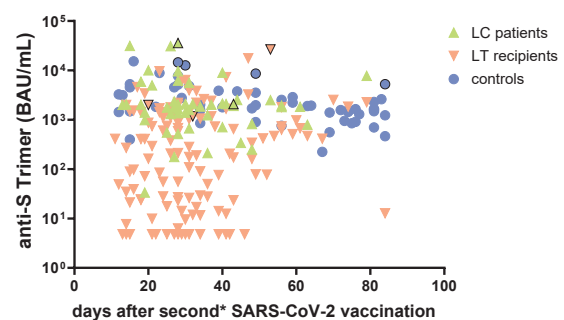
**Supplementary Figure 6.** Humoral immune response for homologous vs heterologous vaccination regimens. Comparison of homologous (mRNA/mRNA) and heterologous (mRNA/AZD1222) vaccination regimens by detection of anti-S trimer (BAU/mL) in cirrhotic patients (*green ascending triangles*), LT recipients (*orange descending triangles*), and controls (*blue dots*). Statistical analysis was performed by Mann-Whitney test. *Solid horizontal lines* indicate medians and interquartile ranges; *dotted horizontal lines* indicate cutoff values.

172.e6 Ruether et al

Clinical Gastroenterology and Hepatology Vol. 20, No. 1



**Supplementary Figure 7.** Humoral immune response in convalescents after 1 or 2 booster vaccinations. Humoral immune response in patients with previous SARS-CoV-2 infection and 1 or 2 booster mRNA vaccinations by detection of anti-S RBD (U/mL). Cirrhotic patients (green), LT recipients (orange), and controls (blue). Lower dotted horizontal line indicates cutoff value; upper dotted horizontal line indicates maximum value.



**Supplementary Figure 8.** Humoral immune response over time after second vaccination. Comparison of humoral immune response according to the time point after second SARS-CoV-2 vaccination in cirrhotic patients (green ascending triangles), LT recipients (orange descending triangles), and controls (blue dots). Convalescents were indicated with a black border line and have received 1<sup>st</sup> mRNA booster vaccination. Detection by anti-S trimer titers (BAU/mL).

**Supplementary Table 1.** Humoral and T-cell Immune Response of All and Only Responding Patients 10 to 84 Days After Second SARS-CoV-2 Vaccination

	LC median (IQR)	LT median (IQR)	<i>P</i>
Anti-S trimer titer, BAU/mL	1880 (1044–2455)	163 (12–1060)	<b>&lt; .001</b>
Only responders ( $\geq 33.8$ BAU/mL)	1910 (1230–2490)	678 (197–1735)	<b>&lt; .001</b>
Anti-S RBD titer, U/mL	3883 (1295–6791)	154 (1–1723)	<b>&lt; .001</b>
Only responders ( $\geq 0.8$ U/mL)	–	555 (64–2477)	<b>&lt; .001</b>
IFN- $\gamma$ release titer, mIU/mL	170 (43–359)	49 (10–274)	.086
Only responders ( $\geq 100$ mIU/mL)	236 (170–454)	404 (226–853)	.111

Note: Boldface *P* values indicate statistical significance.

Anti-S RBD, anti-SARS-CoV-2 antibodies in Roche Elecsys immunoassay; anti-S trimer, anti-SARS-CoV-2 antibodies in DiaSorin LIAISON immunoassay; BAU, binding antibody units; IFN- $\gamma$ , interferon gamma; IQR, interquartile range; LC, liver cirrhosis patients; LT, liver transplant recipients; RBD, receptor binding domain; SARS-CoV-2, severe acute respiratory syndrome coronavirus type 2.

January 2022

Immune Response to SARS-CoV2 Vaccination 172.e7

**Supplementary Table 2.** Risk of LT Recipients for No or Only a Low Humoral Immune Response After Second SARS-CoV-2 Vaccination Based on the RBD Immunoassay

	Univariate OR (95% CI)	<i>P</i>	Multivariate OR (95% CI)	<i>P</i>
Age >65 y	<b>7.23 (2.55–20.53)</b>	< .001	<b>5.79 (1.90–17.70)</b>	<b>.002</b>
Sex (male)	1.91 (0.96–3.80)	.066		
Vaccination regimen	0.92 (0.45–1.86)	.811		
LT <1 y before vaccination	2.35 (0.82–6.78)	.113		
Obesity (BMI ≥30 kg/m <sup>2</sup> )	0.82 (0.30–2.22)	.699		
eGFR <45 mL/min	<b>9.12 (2.86–29.07)</b>	< .001	N/A	
Arterial hypertension	<b>2.62 (1.28–5.37)</b>	<b>.009</b>	<b>2.53 (1.13–5.65)</b>	<b>.024</b>
Diabetes	2.24 (0.97–5.20)	.060		
CNI monotherapy	<b>0.23 (0.09–0.58)</b>	<b>.002</b>	0.37 (0.13–1.05)	.063
CNI + MMF	<b>3.63 (1.73–7.59)</b>	<b>.001</b>	2.19 (0.92–5.19)	.077
CNI + mTORi	1.35 (0.49–3.73)	.563		
CNI + azathioprine	0.13 (0.02–1.08)	.059		
CNI + prednisone	0.64 (0.23–1.72)	.372		
No CNI	<b>5.14 (1.05–25.18)</b>	<b>.043</b>		
Prednisone >5 mg	0.96 (0.28–3.31)	.949		
Triple immunosuppression	1.53 (0.56–4.14)	.405		
Biological	3.72 (0.72–19.15)	.115		
Re-cirrhosis	0.41 (0.10–1.60)	.197		
IgG <13.8 g/L	N/A			
IgA <3.9 g/L	N/A			
IgM <1.8 g/L	4.13 (0.39–43.38)	.238		
Lymphocytes <1000/μl	1.40 (0.47–4.20)	.548		
B-lymphocytes <80/μl	<b>4.33 (1.30–14.51)</b>	<b>.017</b>	N/A	
T-lymphocytes <900/μl	0.82 (0.27–2.54)	.735		
NK-cells <35/μl	0.54 (0.05–6.40)	.628		
CD4+ cells <400/μl	0.86 (0.28–2.58)	.782		
CD8+ cells <290/μl	0.83 (0.28–2.48)	.745		
CD4/CD8 ratio <0.6	N/A	N/A		

Note: For laboratory values, the lower levels of normal were set as thresholds.

Note: Bold values indicate statistical significance.

BMI, Body mass index; CI, confidence interval; CNI, calcineurin inhibitor; eGFR, estimated glomerular filtration rate; LT, liver transplantation; MMF, mycophenolate mofetil; mTORi, mTOR inhibitor; N/A, not applicable; laboratory values that were not considered for univariate or multivariate analysis because of insufficient baseline values; OR, odds ratio; RBD, receptor binding domain; SARS-CoV-2, severe acute respiratory syndrome coronavirus type 2.

**Supplementary Table 3.** Predictors for No or Only a Low Humoral Immune Response in LT Recipients After Second SARS-CoV-2 Vaccination Based on the Trimer Immunoassay (Cutoff 33.8 BAU/mL)

	Anti-S trimer, BAU/mL n, % within group		P	Median anti-S trimer (IQR), BAU/mL
	< 33.8	≥ 33.8		
Age >65 y	21 (80.8)	5 (19.2)	<b>&lt; .001</b>	10 (5–41)
Age ≤65 y	44 (40.4)	65 (59.6)		294 (24–1245)
Arterial hypertension	48 (57.8)	35 (42.2)	<b>.004</b>	56 (5–732)
No arterial hypertension	17 (32.7)	48 (57.8)		394 (27–1693)
CNI mono	8 (24.2)	25 (75.8)	<b>.002</b>	753 (137–2020)
CNI + other IS	56 (55.4)	45 (44.6)		72 (5–664)
B-lymphocytes <80/μl	13 (68.4)	6 (31.6)	<b>.044</b>	18 (5–471)
B-lymphocytes ≥80/μl	13 (39.4)	20 (60.6)		407 (27–1145)

Note: Boldface P values indicate statistical significance.

Anti-S trimer, Anti-SARS-CoV-2 antibodies in DiaSorin LIAISON immunoassay; BAU, binding antibody units; CNI, calcineurin inhibitor; IQR, interquartile range; IS, immunosuppression; LT, liver transplant; SARS-CoV-2, severe acute respiratory syndrome coronavirus type 2.

**Supplementary Table 4.** Risk of Vaccination Failure in LT Recipients With More Than One Negative Prognostic Predictor

			Proportion of patients with anti-S trimer <100 BAU/mL, % (n/N)	Ratio of relative risk
CNI and other	Age >65 y	eGFR <45 mL/min	100 (7/7)	6.25
		eGFR ≥45 mL/min	100 (6/6)	6.25
	Age ≤65 y	eGFR <45 mL/min	87 (13/15)	5.44
		eGFR ≥45 mL/min	45 (22/49)	2.81
CNI mono	Age ≤65 y	eGFR ≥45 mL/min	16 (3/19)	1
		eGFR <45 mL/min	75 (3/4)	4.69
	Age >65 y	eGFR ≥45 mL/min	1/1	
		eGFR <45 mL/min	0	

Anti-S trimer, Anti-SARS-CoV-2 antibodies in DiaSorin LIAISON immunoassay; BAU, binding antibody units; CNI, calcineurin inhibitor; eGFR, estimated glomerular filtration rate; LT, liver transplant.

The table illustrates the risk of vaccination failure, defined by anti-S trimer <100 BAU/mL, in LT recipients with a combination of several risk factors. The percentage of patients with vaccination failure in the respective patient group is indicated. Also, the relative risk compared with LT patients with optimal prognostic parameters (ie, CNI monotherapy plus ≤65 years plus eGFR ≥45 mL/min) is given.

Colors visualize the relative risk: green 1.0, yellow >1 and ≤4, orange >4 and ≤6, red >6, grey: not available due to low number of subjects)



January 2022

Immune Response to SARS-CoV2 Vaccination 172.e9

**Supplementary Table 5.** Humoral and T-cell immune response after second SARS-CoV-2 vaccination with mRNA/mRNA vs. AZD1222/mRNA

	mRNA/mRNA, median (IQR)	AZD1222/mRNA, median (IQR)	<i>P</i>
LC (n = 44 vs 3)			
Anti-S trimer titer, BAU/mL	1840 (1044–2295)	6180 (2080–x)	<b>.043</b>
Anti-S RBD titer, U/mL	3798 (1295–6456)	22422 (5595–x)	<b>.043</b>
IFN- $\gamma$ release titer, mIU/mL	N/A	N/A	N/A
LT (n = 121 vs 11)			
Anti-S trimer titer, BAU/mL	163 (11–895)	1530 (411–4590)	<b>.006</b>
Only responders ( $\geq 33.8$ BAU/mL)	641 (186–1535)	2200 (1081–5310)	<b>.004</b>
Anti-S RBD titer, U/mL	128 (1–1411)	4892 (323–15,503)	<b>.004</b>
Only responders ( $\geq 0.8$ U/mL)	474 (43–2179)	5448 (482–17,072)	<b>.007</b>
IFN- $\gamma$ release titer, mIU/mL	44 (10–223)	926 (288–1738)	<b>.004</b>
Only responders ( $\geq 100$ mIU/mL)	328 (214–778)	1151 (602–1919)	<b>.043</b>
Controls (n = 39 vs 11)			
Anti-S trimer titer, BAU/mL	1610 (1230–2520)	3260 (1900–5240)	<b>.004</b>
Anti-S RBD titer, U/mL	2079 (888–5503)	12194 (8840–14,245)	<b>&lt; .001</b>
IFN- $\gamma$ release titer, mIU/mL	N/A	N/A	

Note: Boldface *P* values indicate statistical significance.

Anti-S RBD, anti-SARS-CoV-2 antibodies in Roche Elecsys immunoassay; anti-S trimer, anti-SARS-CoV-2 antibodies in DiaSorin LIAISON immunoassay; BAU, binding antibody units; IFN- $\gamma$ , interferon gamma; LT, liver transplant; N/A, not available; RBD, receptor binding domain; SARS-CoV-2, severe acute respiratory syndrome coronavirus type 2.

**Supplementary Table 6.** Comparison of Response Between Different C-P Classes in Cirrhotic Patients and Between Decompensated Patients With I and LT Recipients After Second SARS-CoV-2 Vaccination

	C-P class			<i>P</i>
	A (n = 16), median (IQR)	B (n = 18), median (IQR)	C (n = 14), median (IQR)	
Anti-S trimer titer, BAU/mL	1890 (925–2105)	1915 (668–5205)	1870 (1358–3155)	.923
Anti-S RBD titer, U/mL	4124 (1542–6456)	2951 (786–10307)	4134 (2645–7849)	.576
IFN- $\gamma$ release titer, mIU/mL	56 (9–396)	252 (119–386)	189 (64–286)	.423

	Patients with decompensated LC vs LT recipients				
	CP B+C (n = 34), median (IQR)	TIPS (n = 9), median (IQR)	LT (n = 82), median (IQR)	CP B+C vs LT	TIPS vs LT
Anti-S trimer titer, BAU/mL	1870 (1044–4350)	1910 (1053–3990)	163 (12–1060)	<b>&lt; .001</b>	<b>.001</b>
Anti-S RBD titer, U/mL	3812 (1128–9230)	3693 (2186–4966)	154 (1–1723)	<b>&lt; .001</b>	<b>.002</b>
IFN- $\gamma$ release titer, mIU/mL	212 (93–359)	168 (66–4532)	49 (10–275)	<b>.040</b>	.176

Note: Boldface *P* values indicate statistical significance.

Anti-S RBD, anti-SARS-CoV-2 antibodies in Roche Elecsys immunoassay; anti-S trimer, anti-SARS-CoV-2 antibodies in DiaSorin LIAISON immunoassay; BAU, binding antibody units; CP, Child-Pugh class; IFN- $\gamma$ , interferon gamma; IQR, interquartile range; LC, liver cirrhosis patients; LT, liver transplant recipients; RBD, receptor binding domain; SARS-CoV-2, severe acute respiratory syndrome coronavirus type 2; TIPS, transjugular intrahepatic portosystemic stent-shunt.

**VI. Stabilized recombinant SARS-CoV-2 spike antigen enhances vaccine immunogenicity and protective capacity**

Christian Meyer Zu Natrup, Alina Tscherne, Christine Dahlke, Malgorzata Ciurkiewicz, Dai-Lun Shin, Anahita Fathi, Cornelius Rohde, Georgia Kalodimou, Sandro Halwe, Leonard Limpinsel, Jan H. Schwarz, Martha Klug, Meral Esen, Nicole Schneiderhan-Marra, Alex Dulovic, Alexandra Kupke, Katrin Brosinski, Sabrina Clever, Lisa-Marie Schünemann, Georg Beythien, Federico Armando, **Leonie Mayer**, Marie L. Weskamm, Sylvia Jany, Astrid Freudenstein, Tamara Tuchel, Wolfgang Baumgärtner, Peter Kremsner, Rolf Fendel, Marylyn M. Addo, Stephan Becker, Gerd Sutter, Asisa Volz

Published in *The Journal of Clinical Investigation* **132(24)**, e159895 (2022)

doi: [10.1172/JCI159895](https://doi.org/10.1172/JCI159895)

# JCI The Journal of Clinical Investigation

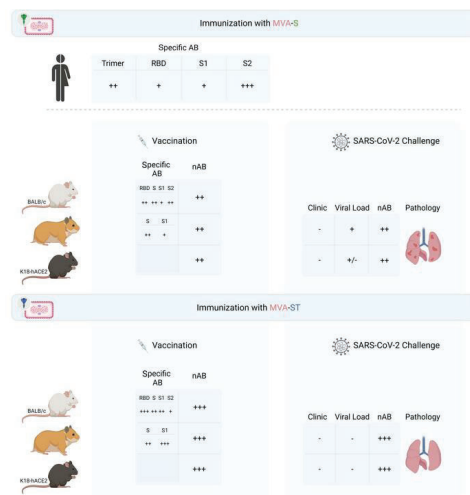
## Stabilized recombinant SARS-CoV-2 spike antigen enhances vaccine immunogenicity and protective capacity

Christian Meyer zu Natrup, ... , Gerd Sutter, Asisa Volz

*J Clin Invest.* 2022;132(24):e159895. <https://doi.org/10.1172/JCI159895>.

Research Article Infectious disease Vaccines

### Graphical abstract



Find the latest version:

<https://jci.me/159895/pdf>



# Stabilized recombinant SARS-CoV-2 spike antigen enhances vaccine immunogenicity and protective capacity

Christian Meyer zu Natrup,<sup>1</sup> Alina Tscherne,<sup>2,3</sup> Christine Dahlke,<sup>4,5</sup> Malgorzata Ciurkiewicz,<sup>6</sup> Dai-Lun Shin,<sup>1</sup> Anahita Fathi,<sup>4,5,7</sup> Cornelius Rohde,<sup>8,9</sup> Georgia Kalodimou,<sup>2,3</sup> Sandro Halwe,<sup>9</sup> Leonard Limpinsel,<sup>2</sup> Jan H. Schwarz,<sup>2</sup> Martha Klug,<sup>10,11</sup> Meral Esen,<sup>10,11</sup> Nicole Schneiderhan-Marra,<sup>12</sup> Alex Dulovic,<sup>12</sup> Alexandra Kupke,<sup>8,9</sup> Katrin Brosinski,<sup>2</sup> Sabrina Clever,<sup>1</sup> Lisa-Marie Schünemann,<sup>1</sup> Georg Beythien,<sup>6</sup> Federico Armando,<sup>6</sup> Leonie Mayer,<sup>4,5,7</sup> Marie L. Weskamm,<sup>4,5,7</sup> Sylvia Jany,<sup>2</sup> Astrid Freudenstein,<sup>2</sup> Tamara Tuchel,<sup>1</sup> Wolfgang Baumgärtner,<sup>6</sup> Peter Kremsner,<sup>10,11,13</sup> Rolf Fendel,<sup>10,11</sup> Marylyn M. Addo,<sup>5,10</sup> Stephan Becker,<sup>8,9</sup> Gerd Sutter,<sup>2,3</sup> and Asisa Volz<sup>1,14</sup>

<sup>1</sup>Institute of Virology, University of Veterinary Medicine Hannover, Foundation, Hannover, Germany. <sup>2</sup>Division of Virology, Department of Veterinary Sciences, LMU Munich, Munich, Germany. <sup>3</sup>German Center for Infection Research, partner site Munich, and <sup>4</sup>partner site Hamburg-Lübeck-Borstel-Riems. <sup>5</sup>University Medical Center Hamburg-Eppendorf, Institute for Infection Research and Vaccine Development (IIRVD), Hamburg, Germany. <sup>6</sup>Department of Pathology, University of Veterinary Medicine Hannover, Foundation, Hannover, Germany. <sup>7</sup>University Medical Center Hamburg-Eppendorf, Division of Infectious Diseases, Hamburg, Germany. <sup>8</sup>German Center for Infection Research, partner site Gießen-Marburg-Langen. <sup>9</sup>Institute of Virology, Philipps University Marburg, Marburg, Germany. <sup>10</sup>German Center for Infection Research, partner site Tübingen. <sup>11</sup>Institute of Tropical Medicine, University of Tübingen, Tübingen, Germany. <sup>12</sup>NMI Natural and Medical Sciences Institute at the University of Tübingen, Reutlingen, Germany. <sup>13</sup>Centre de Recherches Médicales de Lambarene, Gabon. <sup>14</sup>German Center for Infection Research, partner site Hanover-Braunschweig.

The SARS-CoV-2 spike (S) glycoprotein is synthesized as a large precursor protein and must be activated by proteolytic cleavage into S1 and S2. A recombinant modified vaccinia virus Ankara (MVA) expressing native, full-length S protein (MVA-SARS-2-S) is currently under investigation as a candidate vaccine in phase I clinical studies. Initial results from immunogenicity monitoring revealed induction of S-specific antibodies binding to S2, but low-level antibody responses to the S1 domain. Follow-up investigations of native S antigen synthesis in MVA-SARS-2-S-infected cells revealed limited levels of S1 protein on the cell surface. In contrast, we found superior S1 cell surface presentation upon infection with a recombinant MVA expressing a stabilized version of SARS-CoV-2 S protein with an inactivated S1/S2 cleavage site and K986P and V987P mutations (MVA-SARS-2-ST). When comparing immunogenicity of MVA vector vaccines, mice vaccinated with MVA-SARS-2-ST mounted substantial levels of broadly reactive anti-S antibodies that effectively neutralized different SARS-CoV-2 variants. Importantly, intramuscular MVA-SARS-2-ST immunization of hamsters and mice resulted in potent immune responses upon challenge infection and protected from disease and severe lung pathology. Our results suggest that MVA-SARS-2-ST represents an improved clinical candidate vaccine and that the presence of plasma membrane-bound S1 is highly beneficial to induce protective antibody levels.

## Introduction

All COVID-19 vaccines licensed to date include the complete SARS-CoV-2 spike (S) protein as key antigen to elicit protective immune responses. Trimers of this large viral surface protein form the distinctive spikes of the coronavirus (1). Monomeric S is a glycosylated transmembrane protein consisting of a large N-terminal ectodomain and a short C-terminal endodomain. The full-length SARS-CoV-2 S protein is cleaved by a furin-like protease into 2 almost equally sized polypeptides called S1 (N-terminus of S) and S2 (membrane-anchored C-terminus of S). S1 harbors the receptor

binding domain (RBD), which interacts with the cellular receptor molecule angiotensin-converting enzyme 2 (ACE2) and serves, together with other parts of S1, as an important target for antibodies that can interfere with host cell receptor binding capable of neutralizing SARS-CoV-2 infection. S2 mediates fusion between the virus and cell membrane, and is also an important target for antibodies that can interfere with virus entry.

S-specific virus-neutralizing antibodies are a major component of the vaccine-induced immune response protecting against SARS-CoV-2 infection (2). COVID-19 vaccines with reported efficacy deliver as an antigen either native S polypeptides (3–5) or modified versions of the full-length S protein (6–9). The modified S antigens contain 2 proline amino acid substitutions in the S2 protein between the fusion peptide and the first hinge region sequence to arrest the S protein in the prefusion conformation (1). Two S vaccine antigens harbor additional mutations to prevent S1/S2 cleavage by furin-like proteases (6, 8). While all of the different candidate vaccines based on S antigens elicit protective

**Authorship note:** CMZN and AT contributed equally to this work

**Conflict of interest:** The authors have declared that no conflict of interest exists.

**Copyright:** © 2022, Meyer zu Natrup et al. This is an open access article published under the terms of the Creative Commons Attribution 4.0 International License.

**Submitted:** March 3, 2022; **Accepted:** October 21, 2022; **Published:** December 15, 2022.

**Reference information:** *J Clin Invest.* 2022;132(24):e159895.

<https://doi.org/10.1172/JCI159895>.

immunity in humans, they seem to induce distinct levels of vaccine efficacy and S-specific antibody responses (10). Structural features of the various S antigens might account for these differences in vaccine immunogenicity and/or vaccine efficacy and warrant further investigation. Moreover, recent studies demonstrated that the persistence of immune responses induced by approved COVID-19 vaccines and/or infection is limited. While all approved vaccine candidates provide a high level of protection against severe disease and death, protection against SARS-CoV-2 infection and/or transmission declines due to the waning of S-specific antibodies and the emergence of variants. To address this limitation, improved vaccination strategies that could be used as booster vaccines are urgently needed.

Modified vaccinia virus Ankara (MVA), a replication-deficient orthopoxvirus vaccine strain, has long served as an advanced vaccine technology platform for developing viral vector vaccines against emerging infectious disease (10–14).

Recent work addressed the preclinical development of MVA vector vaccines against COVID-19, including our candidate vaccine MVA-SARS-2-S (MVA-S) (15). Immunizations with MVA-S in animal models demonstrated the safety, immunogenicity, and protective efficacy of this vector vaccine delivering the native full-length SARS-CoV-2 S antigen. Further, MVA-S entered phase Ia clinical evaluation to assess the clinical safety and tolerability of 2 administrations and 2 ascending dose levels in healthy adults (ClinicalTrials.gov NCT04569383).

One objective of this study was to more closely examine the S-specific antibody responses following MVA-S immunization. Preliminary data from this immunogenicity monitoring suggested that most of the vaccine-induced native S-antigen-specific antibodies bound to the S2 but not the S1 antigen domain. This interesting observation prompted us to construct a vaccine vector delivering a modified stabilized version of the SARS-CoV-2 S antigen, with an inactivated S1/S2 cleavage site, called MVA-SARS-2-ST (for stabilized S antigen, MVA-ST) to compare with the original MVA-S in preclinical studies.

Here, we show that MVA-ST produces a full-length SARS-CoV-2 S protein that is not processed into S1 and S2 protein subunits, but anchored to the membrane of MVA-ST-infected cells. We found enhanced levels of cell-surface S1 antigen upon infection with MVA-ST compared with MVA-S. Moreover, when comparatively tested as a vaccine in animal models, MVA-ST not only elicited substantially higher levels of S1-binding and SARS-CoV-2-neutralizing antibodies, but also robustly protected vaccinated mice and hamsters against SARS-CoV-2 respiratory infection and lung pathology. Currently, MVA-ST is being investigated in a phase Ib clinical trial as an optimized MVA vector candidate vaccine against COVID-19.

## Results

*Antibody response against different S protein domains in human volunteers vaccinated with MVA-S.* The MVA-based candidate vaccine MVA-S, encoding an unmodified, full-length SARS-CoV-2 S protein, is being tested in a phase Ia clinical study. This involved a prime-boost intramuscular vaccination schedule comparing low dose ( $1 \times 10^7$  infectious units [IU]) versus high dose ( $1 \times 10^8$  IU). The full prime-boost vaccination regimen was administered to

30 participants at an interval of 28 days. We collected blood from these individuals at several time points, including before vaccination (day 0), after the first vaccination (day 28), and at 2 time points after the second vaccination (days 42 and 84).

To characterize the antigen binding capacities of the SARS-CoV-2-specific antibodies, we performed a high-throughput, automated bead-based multiplex assay called Multi-CoV-Ab (16, 17), where 4 different SARS-CoV-2-specific antigens (trimeric full-length S protein [S trimer], receptor-binding domain [RBD], and S1 and S2) are expressed and immobilized on LUMINEX MAGPLEX beads. Seroconversion was estimated by a comparison relative to a calibrator sample. To examine MVA-S-induced seroconversion, we used the trimer antigen assay (Figure 1A). All individuals vaccinated with the low dose mounted low levels of trimer-binding antibodies that peaked on day 42, with a mean titer expressed as a median fluorescence intensity (MFI) of 787.7. Thirty-three percent ( $n = 5/15$ ) of the individuals reached antibody titers relevant for seroconversion. In the high-dose vaccination group, we detected marginally increased trimer-specific antibody responses with a mean titer of 1274 MFI peaking 2 weeks after the second vaccine dose, and 33.3% ( $n = 5/15$ ) of the individuals seroconverted (Figure 1A).

When evaluating serum reactivity against the RBD of the SARS-CoV-2 S protein we found markedly lower quantities of antigen-binding antibodies (Figure 1B). Only 26.7% ( $n = 4/15$ ) of the vaccinees receiving the high-dose immunization produced an anti-RBD response (with a peak mean titer of 232.9 MFI on day 42), and of these, only 2 individuals reached elevated RBD-specific antibody levels compared with the calibrator. In the sera from low-dose vaccinees, we did not detect any RBD-specific antibodies.

Analyzing the IgG response directed against the S1 and S2 subdomains of the SARS-CoV-2 spike protein (Figure 1, C and D) revealed marginal levels of S1-specific antibodies in a few individuals only, irrespective of the dosage used for vaccination (Figure 1C). In contrast, we measured substantial quantities of S2-binding antibodies in sera from all vaccinees, irrespective of the dosage used for vaccination (Figure 1D). Again, seroconversion was estimated by comparison relative to a calibrator sample. To avoid any false positive results due to extensive background fluorescence associated with the S2 subdomain, we defined the cutoff values as  $2 \times$  (day 0 MFI). The S2-specific antibody response peaked on day 84 in the low-dose group, with a mean titer of 4206.5 MFI. In the high-dose group, half of the vaccinees exhibited a peak on day 42 (mean titer of 3271.2 MFI), whereas the rest developed steadily increasing levels of SARS-CoV-2 S2-binding antibodies until day 84 (mean titer of 2928.9 MFI). Altogether, these results indicated that vaccination with the candidate vaccine MVA-S expressing a full-length unmodified S protein predominantly induces an S2-specific antibody response in humans.

*Generation and characterization of the modified candidate vaccine MVA-ST.* To investigate the possible impact of fusogenic activity and proteolytic cleavage of the native full-length S protein delivered by MVA-S, we generated a matching MVA vector vaccine producing a modified version of the SARS-CoV-2 S antigen, MVA-ST. To obtain an S antigen stabilized in a prefusion conformation we introduced 5 amino acid (aa) exchanges within the 1273-aa S polypeptide, inactivating the S1/S2 furin cleavage site and creating 2 new proline residues (K986P, V987P) between the first heptad repeat (HR1)

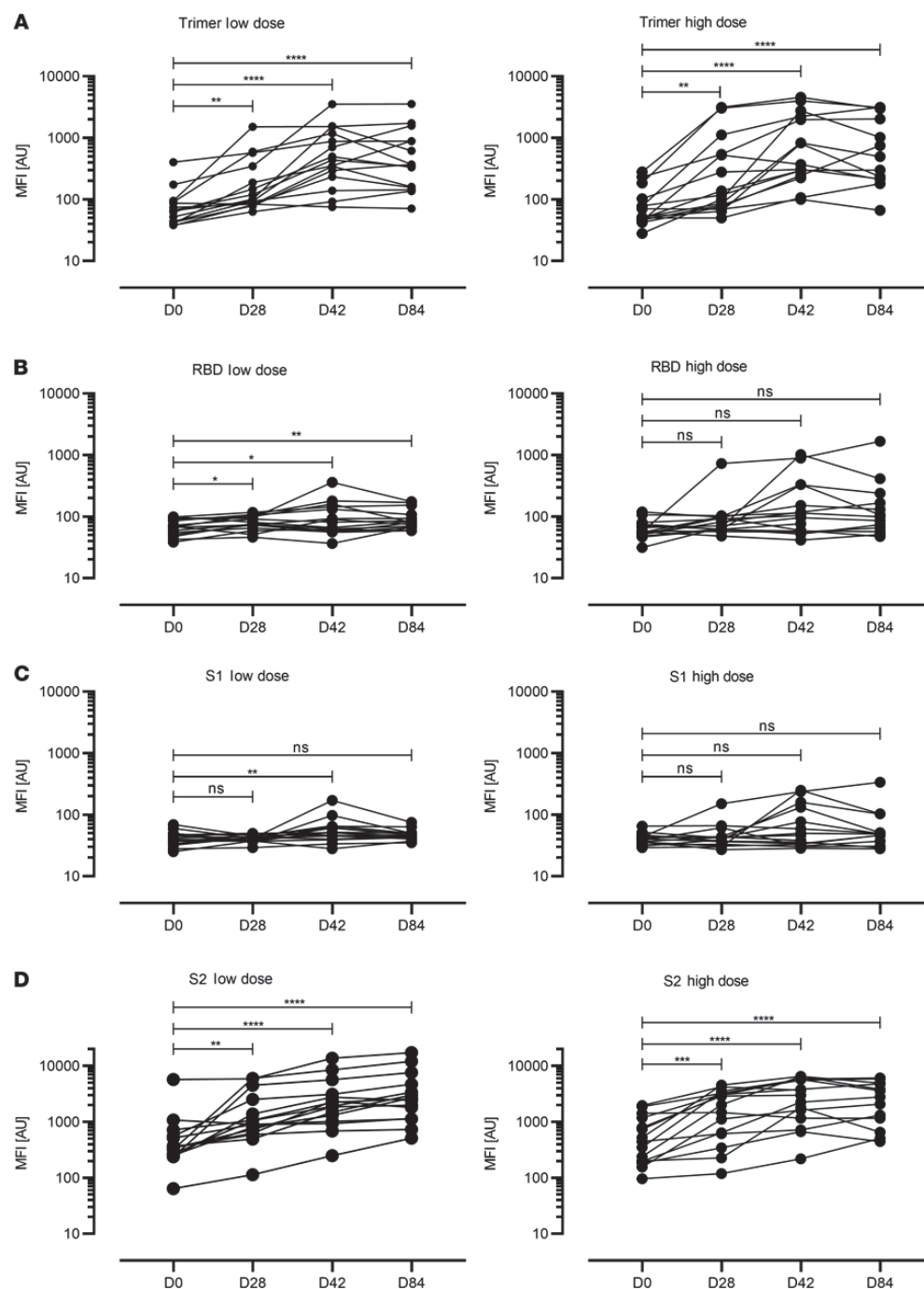


**Figure 1. SARS-CoV-2-specific antibody responses in human volunteers vaccinated with MVA-S.** Scatterplots represent data from individual participants. Humoral immunity against the SARS-CoV-2 spike protein domains were characterized using a multiplex bead array. Antibody reactivity was measured against (A) the full spike protein expressed as a trimeric antigen (S), (B) the receptor binding domain of the spike protein (RBD), (C) the S1 domain (S1), and (D) the S2 domain (S2). Antibody levels were quantified at baseline (BL), before vaccine boost (D28), 2 weeks after vaccine boost (D42), and 8 weeks after vaccine boost (D84) in the low- (left panels) and high-dose (right panels) groups. Seroconversion was estimated by comparison to a calibrator sample. Cutoff values: trimer = 1085 MFI, RBD = 640 MFI, S2 = 2 × BL MFI. \* $P < 0.05$ , \*\* $P < 0.01$ , \*\*\* $P < 0.001$ , \*\*\*\* $P < 0.0001$  by 1-way ANOVA with Dunnett's multiple comparisons test of log-transformed data.

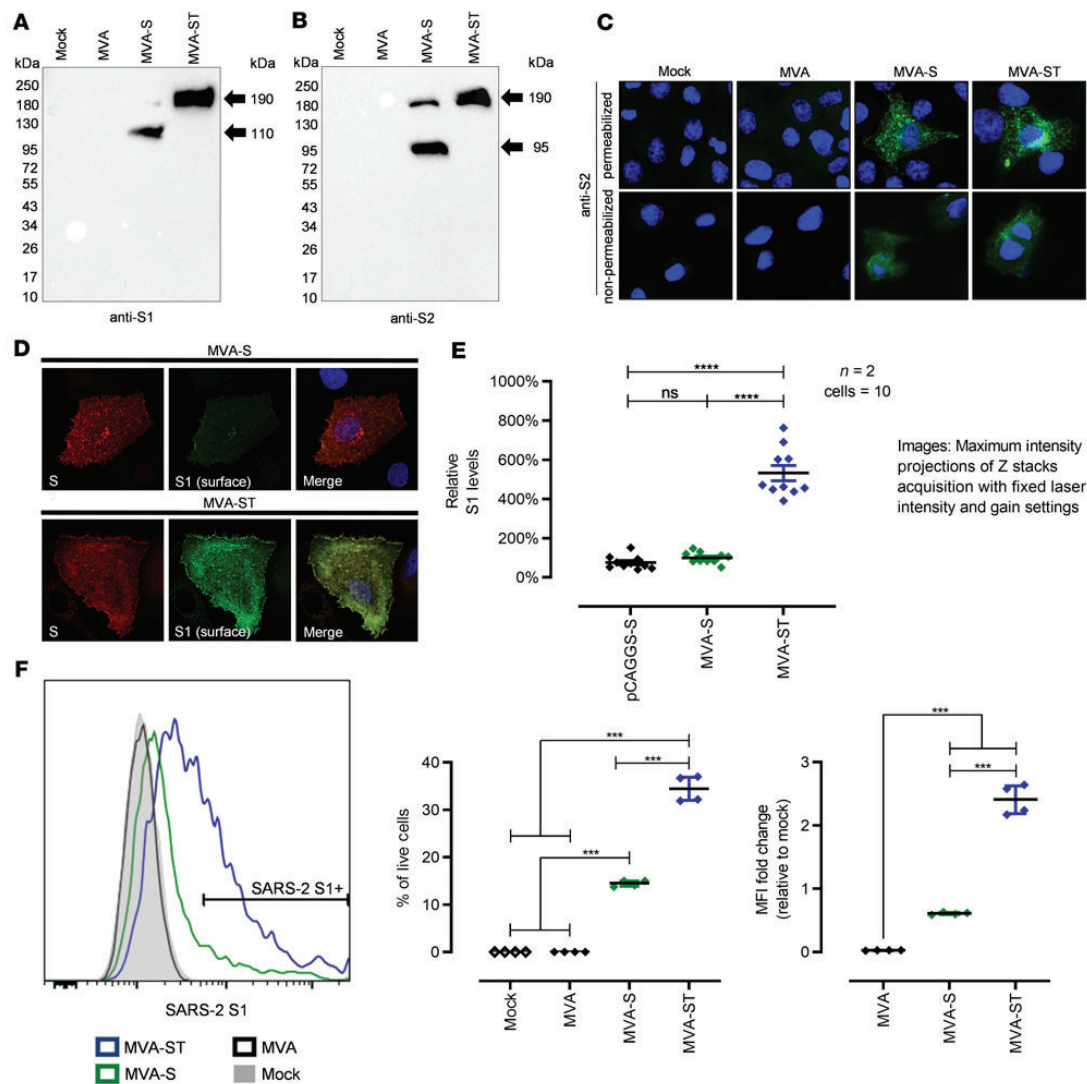


**Figure 2. Synthesis and processing of spike glycoprotein (S) in MVA-S- and MVA-ST-infected cells.** (A and B) Western blot analysis of S in lysates of MVA-S- and MVA-ST-infected cells. Noninfected (mock) or MVA-infected cells served as controls. DF-1 and Vero cells were infected with an MOI of 10 and collected 24 hours after infection. Polypeptides were resolved by SDS-PAGE and analyzed with a monoclonal antibody against (A) SARS-CoV-2 S1 or (B) SARS-CoV-2 S2. (C) Immunofluorescent staining of S in MVA-, MVA-S-, and MVA-ST-infected Vero cells (MOI = 0.5). Cells were permeabilized or non-permeabilized and probed with mouse monoclonal antibodies against SARS-CoV-2 S protein (S2 domain, green). Cell nuclei were counterstained with DAPI (blue). (D and E) Immunofluorescent single-cell staining of surface S levels. Huh-7 cells were infected with MVA-S, MVA-ST, or transfected with plasmids encoding unmodified S (pCAGGS-S). (D) At 18 hours after infection, cell-surface S was labeled with anti-S1 monoclonal antibody and total S was labeled with anti-S2 antibody after fixation and permeabilization. Nuclei were counterstained with DAPI. Original magnification,  $\times 100$  (C) and  $\times 630$  (D). (E) For quantification, fluorescence intensity of surface S was measured and set in relation to that of total S. In total, 10 cells from 2 independent experiments were analyzed for each setup. (F) Flow cytometric analysis of surface S1 expression by MVA-S- or MVA-ST-infected A549 cells. Graphs show the percentage of S1<sup>+</sup> cells ( $n = 4$ ) and the fold change in S1 median fluorescence intensity (MFI) relative to the mock control ( $n = 4$ ). \*\*\* $P < 0.001$ , \*\*\*\* $P < 0.0001$  by 1-way ANOVA with Tukey's multiple comparisons test.

and the central helix of the S2 protein (Supplemental Figure 1, A-C; supplemental material available online with this article; <https://doi.org/10.1172/JCI159895DS1>). The recombinant MVA-ST was clonally isolated in plaque purifications in DF-1 cell cultures and

PCR analyses of the viral genome confirmed the genetic integrity and genetic stability of the vector virus (Supplemental Figure 1, D-G). The suitability of MVA-ST for production at industrial scale under conditions of biosafety level 1 was indicated by data from

growth testing in DF-1 producer cells and in cell lines of human origin (Supplemental Figure 2).

Synthesis of the stabilized ST antigen in MVA-ST-infected cell cultures was demonstrated by Western blot analysis, which confirmed the absence of proteolytic cleavage. A single protein band with a molecular mass of approximately 190 kDa was detected in cells infected with MVA-ST using either S1- or S2-specific monoclonal antibodies (Figure 2, A and B). In contrast, lysates from cells infected with the original recombinant MVA-S contained additional protein bands that migrated at molecular masses corresponding to the sizes of the S1 and S2 cleavage products.

Next, we used immunofluorescent staining with S2-specific primary antibodies to assess cell surface expression and trafficking of the different S proteins in Vero cells infected with MVA-ST compared to cells infected with MVA-S (Figure 2C). Similar to our findings with MVA-S, we observed a reticular pattern with juxtanuclear accumulation of the stabilized S protein in permeabilized and MVA-ST-infected cells. Immunostaining without cell permeabilization specifically revealed abundant S2 protein on the cell surface of either MVA-S- or MVA-ST-infected cells.

To comparatively analyze and quantify predicted cellular localization of the S1 and S2 subunits by confocal microscopy, we infected Huh-7 cells with either MVA-S or MVA-ST (Figure 2, D and E). Infected cells were fixed 18 hours after infection and S located at the cell surface was labeled prior to fixation using an anti-S1 human-derived monoclonal antibody (18). Subsequently, cells were fixed, permeabilized, and total S was labeled using an anti-S2 antibody from mouse and secondary Alexa Fluor 488- and 594-conjugated antibodies (18). As anticipated, we saw a similar staining pattern for both recombinant viruses using S2-specific antibodies, indicating comparable amounts of S2 protein on the cell surface of both MVA-S- and MVA-ST-infected cells.

In MVA-ST-infected cells, the S1-specific immunostaining also revealed ample amounts of S1 protein on the cell surface. Surprisingly, and in contrast, we observed significantly lower levels of S1-specific cell surface staining in MVA-S-infected cells (Figure 2, D and E). Likewise, analyzing infected cells for S1 cell surface expression using immunostaining and FACS analysis detected significantly lower levels of S1 cell surface expression in cells infected with MVA-S (14.4%), in contrast to S1-specific staining in 34.5% of viable human A549 cells infected with MVA-ST. This was also confirmed when analyzing the fold change in S1 MFI relative to mock infection in the live cell compartment (0.61-fold change for MVA-S, 2.40-fold change for MVA-ST; Figure 2F).

*MVA-ST-induced S-specific immune responses in BALB/c mice.* To comparatively assess vaccine safety and immunogenicity, we vaccinated BALB/c mice intramuscularly with  $1 \times 10^8$  PFU of MVA-S or MVA-ST using a 21-day interval prime-boost schedule (Supplemental Figure 3).

The induction of S-binding antibodies was analyzed by ELISA using different SARS-CoV-2 S polypeptides as target antigens (full-length S, RBD, S1, or S2) (Figure 3, A-D). Initially, we confirmed seroconversion by ELISA using wells coated with purified trimeric S protein. Seroconversion was detected in 100% of vaccinated mice after prime-boost vaccination, with a mean titer of 1:1125 for MVA-S and 1:1200 for MVA-ST (Figure 3A). All MVA-ST-immunized mice already mounted antibodies binding to RBD on day 18, with a mean

titer of 1:1500 (Figure 3B). Only 16.7% ( $n = 1/6$ ) of MVA-S-vaccinated animals produced measurable amounts of RBD-specific antibodies, with a titer of 1:300. Boost vaccination on day 21 resulted in lower levels of RBD-specific antibodies following MVA-S vaccination (mean titer of 1:1850) than the significantly increased levels induced by MVA-ST vaccination (mean titer of 1:30,375).

In S1 ELISAs, no or only low-level responses were detected in sera of vaccinated mice after prime immunization (Figure 3C). We found that 37.5% ( $n = 3/8$ ) of mice vaccinated with MVA-ST mounted S1-binding antibodies with a mean titer of 1:100. However, substantial levels of S1-binding antibodies developed after the boost vaccination with MVA-ST, with a mean titer of 1:6075; in contrast, mice that received MVA-S developed a significantly lower titer of 1:337. Marginal levels of antibodies binding to S2 protein were measured after a single vaccination with MVA-S or MVA-ST (Figure 3D). Boost vaccination significantly increased the amounts of S2-binding antibodies for both candidate vaccines, with a mean titer of 1:728 for MVA-ST-vaccinated and 1:1350 for MVA-S-vaccinated animals.

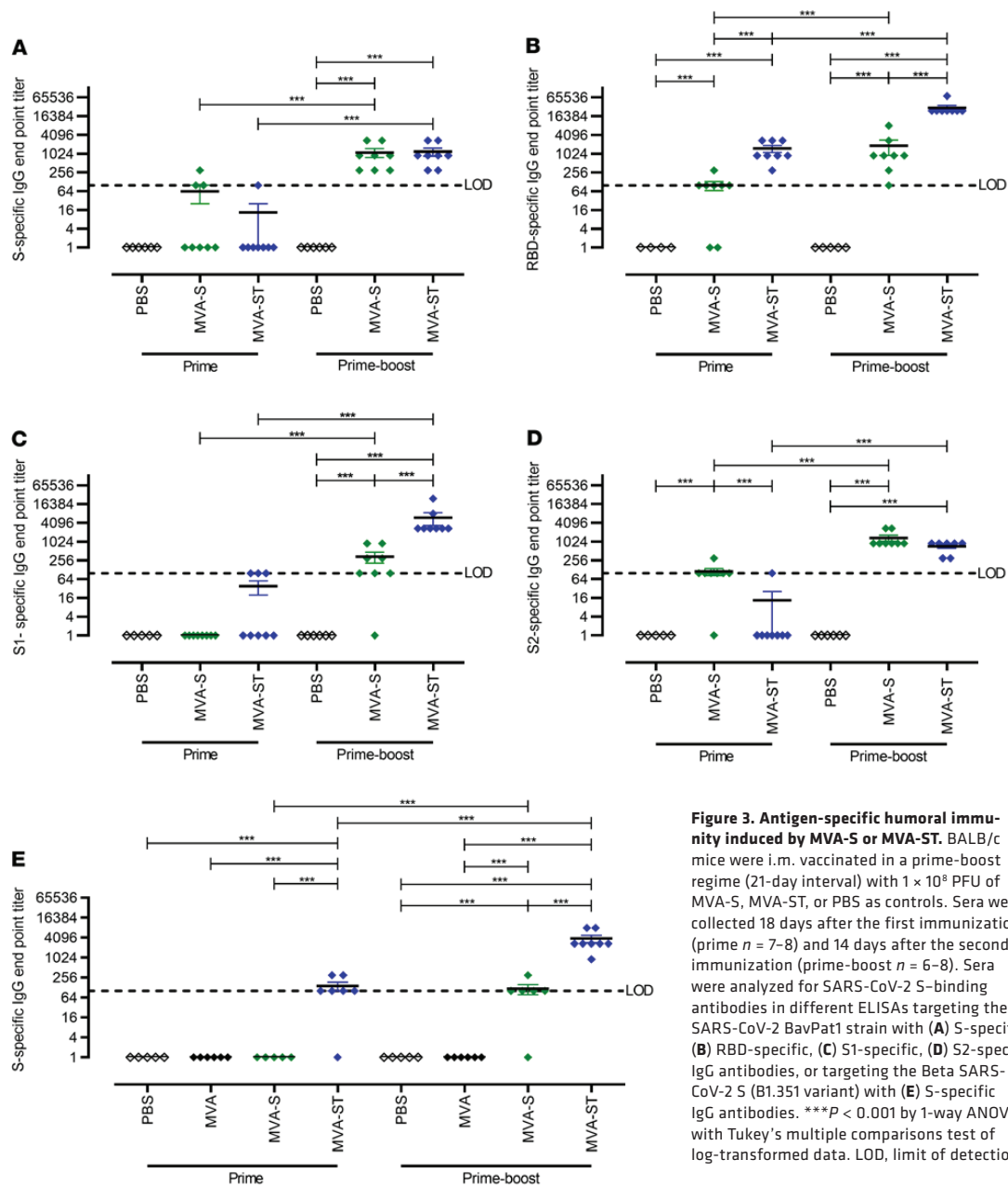
In addition, we analyzed antibody binding capacity against the Beta variant of SARS-CoV-2 using ELISA plates coated with synthetic Beta SARS-CoV-2 S protein (Figure 3E). A single MVA-S vaccination did not result in obvious levels of binding antibodies, whereas mice vaccinated with MVA-ST mounted detectable levels of binding antibodies, with a mean titer of 1:143. After boost vaccination, MVA-S-vaccinated mice did show activation of antibodies specific for the Beta variant S protein, with a mean titer of 1:116. However, MVA-ST booster immunization significantly increased these antibody levels, with a mean titer of 1:3825.

To evaluate neutralizing antibodies, we performed the 50% plaque reduction neutralization test (PRNT<sub>50</sub>) as well as the virus neutralization titer (VNT<sub>100</sub>) assay (Figure 4). Immunization with MVA-S induced low levels of neutralizing antibodies against the SARS-CoV-2 isolate Germany/BavPat1/2020 (henceforth called SARS-CoV-2 BavPat1), reaching a mean titer of 1:3437 in the more sensitive PRNT<sub>50</sub> and a mean titer of 1:81 in the more demanding VNT<sub>100</sub> assay (Figure 4, A and B). In comparison, MVA-ST prime-boost vaccination resulted in significantly better SARS-CoV-2 BavPat1 neutralization, with mean titers of 1:6400 in PRNT<sub>50</sub> and 1:848 in the VNT<sub>100</sub> assay (Figure 4, A and B).

Our candidate vaccines are based on the S protein sequence of the SARS-CoV-2 isolate Wuhan HU-1 from 2020 (15). Thus, we used the mouse sera generated above to evaluate the capacity of the antibody responses to neutralize infections with SARS-CoV-2 variants Alpha (B.1.1.7), Beta (B.1.351), and Zeta (P.2) using the VNT<sub>100</sub> assay (Figure 4C). Similar to previous findings using this assay, MVA-S vaccination resulted in low levels of detectable neutralizing antibodies against the original SARS-CoV-2 BavPat1 (geometric mean titer 31). In accordance with these results, only a few mice mounted neutralizing responses against the SARS-CoV-2 variants Alpha (2/6, mean titer of 1:46), Beta (1/6, mean titer of 1:8), and Zeta (1/6, mean titer 1:31). In sharp contrast, MVA-ST vaccination elicited robust levels of circulating antibodies that neutralized the original SARS-CoV-2 BavPat1 (6/6, mean titer of 1:1874) and the variant viruses Alpha (6/6, mean titer of 1:1761), Beta (6/6, mean titer of 1:1002), and Zeta (6/6, mean titer of 1:824).

To characterize the neutralizing capacities against the more recent SARS-CoV-2 variants Delta (B.1.617.2) and the highly





contagious Omicron (B.1.1.529), we again performed prime-boost vaccination in BALB/c mice as above (Figure 4, D and E). Control mice that had been either mock or nonrecombinant MVA vaccinated did not mount any neutralizing antibodies against Delta or Omicron. MVA-S-vaccinated mice mounted low levels of Delta-neutralizing antibodies, with a mean titer of 1:90. In contrast, MVA-ST vaccination resulted in robust activation of Delta-neutralizing antibodies, with a mean titer of 1:275. When analyzing neutralization against Omicron, MVA-S-vaccinated

mice showed low titers resulting in a mean titer of 1:8, compared with MVA-ST-vaccinated mice, with a mean of 1:184. To ensure comparability with the BALB/c vaccination experiments above, PRNT<sub>50</sub> against the BavPat1 isolate was performed (Supplemental Figure 4). Altogether, these results indicate that immunization with MVA-ST induces a superior anti-SARS-CoV-2-S humoral response resulting in the generation of cross-neutralizing anti-SARS-CoV-2 S antibodies against all the variants tested so far: Alpha, Beta, Zeta, Delta, and Omicron.

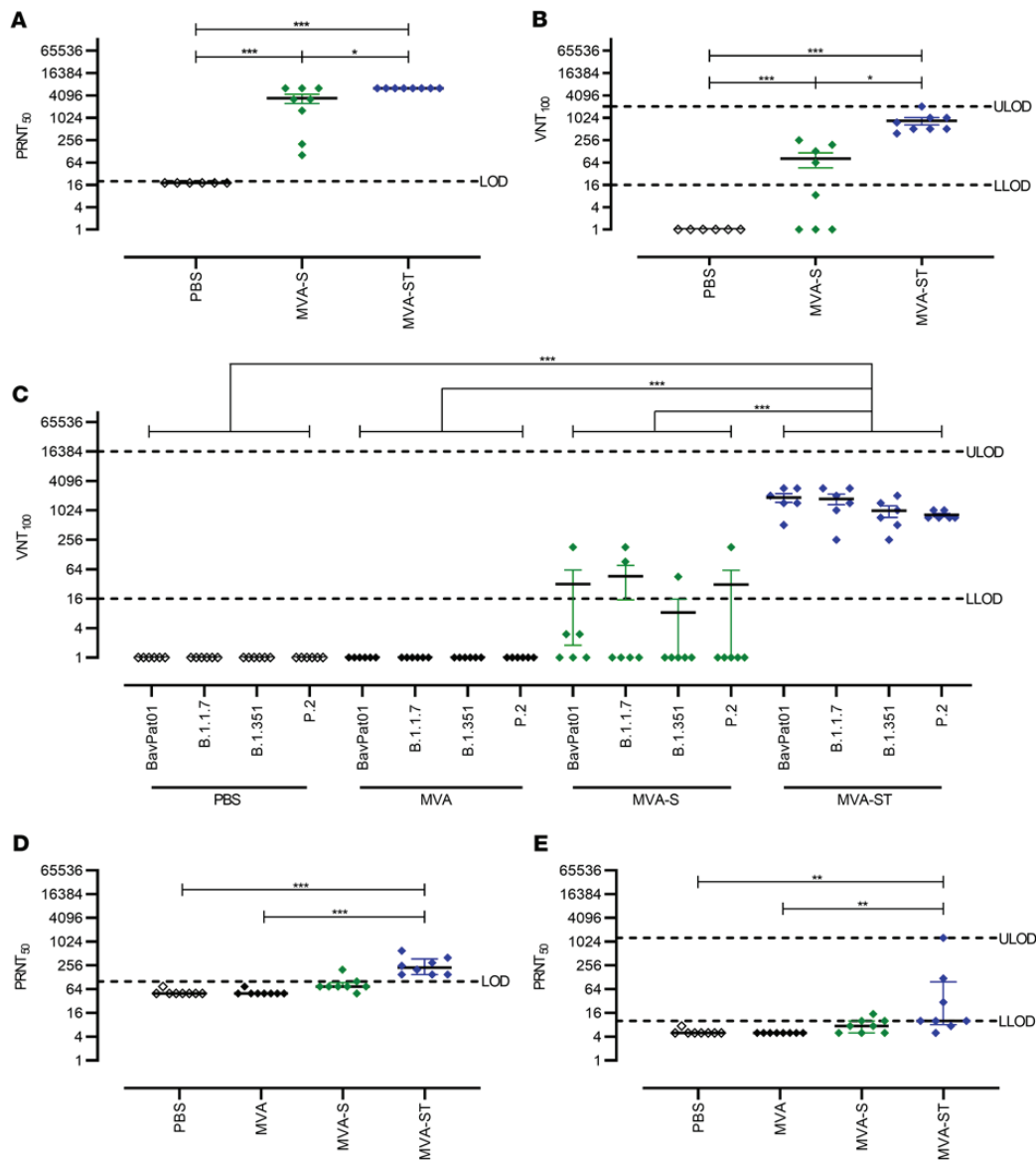


**Figure 4. Virus-neutralizing antibody responses to SARS-CoV-2 BavPat1, Alpha, Beta, Zeta, Delta, and Omicron variants in vaccinated BALB/c mice.** SARS-CoV-2 neutralization titers measured by the plaque reduction assay ( $PRNT_{50}$ ) and virus neutralization test ( $VNT_{100}$ ) from BALB/c mice vaccinated with PBS, MVA, MVA-S, or MVA-ST. (A)  $PRNT_{50}$  and (B)  $VNT_{100}$  assays using SARS-CoV-2 BavPat1. (C)  $VNT_{100}$  against SARS-CoV-2 BavPat1, Alpha, Beta, and Zeta variants.  $PRNT_{50}$  assay using SARS-CoV-2 (D) Delta and (E) Omicron variants. \* $P < 0.05$ , \*\* $P < 0.01$ , \*\*\* $P < 0.001$  by 1-way ANOVA with Tukey's multiple comparisons test of log-transformed data (A–C) and Kruskal-Wallis test with Dunn's multiple comparisons test (D and E). LOD, limit of detection; ULOD and LLOD, upper and lower LOD.

To characterize the activation of SARS-CoV-2-specific cellular immunity following prime-boost vaccination in BALB/c mice, we monitored S1 epitope-specific  $CD8^+$  T cells using IFN- $\gamma$  ELISPOT assays and FACS analysis (Figure 5). Boost vaccinations with MVA-S activated substantial numbers of  $S_{268-276}$  epitope-specific  $CD8^+$  T cells, with a mean number of 1571 IFN- $\gamma^+$  spot-forming cells (SFC) in

$1 \times 10^6$  splenocytes (Figure 5A). Comparable results were obtained for boost vaccinations with MVA-ST (mean of 1349 IFN- $\gamma^+$  SFC; Figure 5A). In agreement with these data, FACS analysis of T cells stimulated in vitro with peptide  $S_{268-276}$  and stained for intracellular IFN- $\gamma$  showed robust frequencies of IFN- $\gamma^+$   $CD8^+$  T cells in splenocytes from mice immunized with MVA-S (mean of 1.51%) or MVA-ST (mean

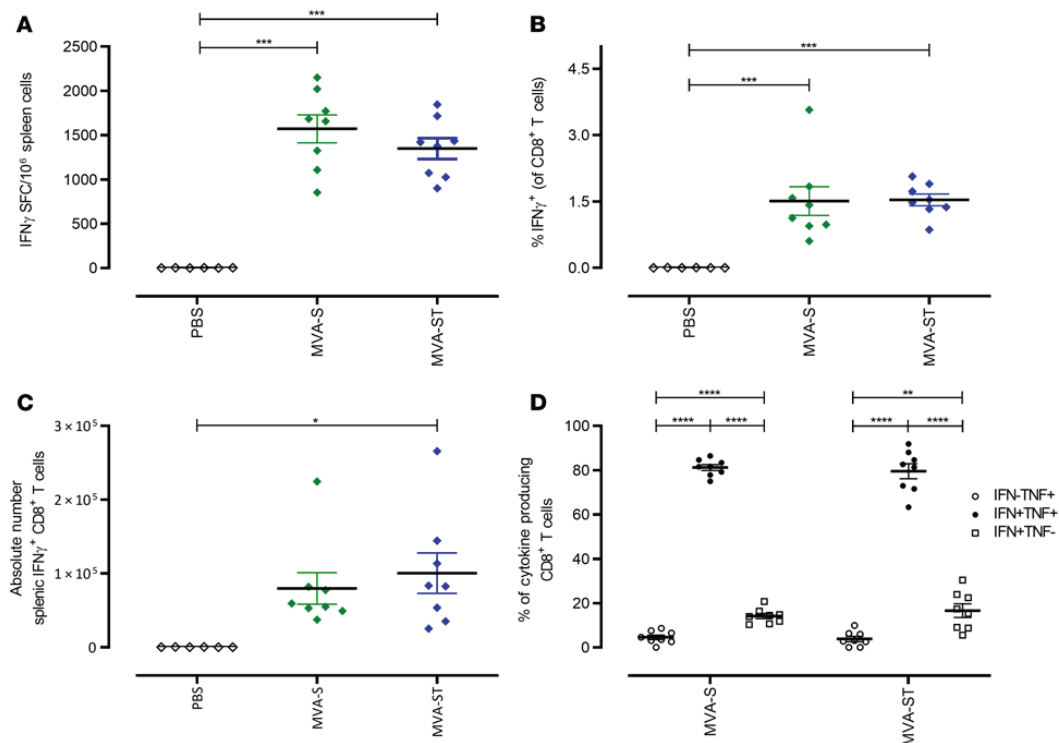


**Figure 5. Activation of S-specific CD8<sup>+</sup> T cells after prime-boost immunization with MVA-S or MVA-ST.** Groups of BALB/c mice ( $n = 4-8$ ) were immunized i.m. twice with  $1 \times 10^8$  PFU MVA-S, MVA-ST, or PBS as negative controls. (A–D) Splenocytes were collected and prepared on day 14 after boost immunization and stimulated with the H2-Kd-restricted peptide S<sub>268-276</sub> (S1; GYLQPRFL) and tested using ELISPOT assays and ICS FACS analyses. (A) IFN- $\gamma$ <sup>+</sup> SFC measured by ELISPOT assays. (B and C) IFN- $\gamma$ -producing CD8<sup>+</sup> T cells measured by FACS analysis. (D) IFN- $\gamma$ - and TNF- $\alpha$ -producing CD8<sup>+</sup> T cells measured by FACS analysis. \* $P < 0.05$ , \*\* $P < 0.01$ , \*\*\* $P < 0.001$ , \*\*\*\* $P < 0.0001$  by 1-way ANOVA with Tukey's multiple comparisons test.

of 1.53%) compared with mock-vaccinated control mice (mean of 0.01%) (Figure 5, B and C). Substantial numbers of the activated IFN- $\gamma$ <sup>+</sup>CD8<sup>+</sup> T cells also coexpressed TNF- $\alpha$  (81% for MVA-S and 79% for MVA-ST; Figure 5D). Of note, mice immunized with MVA-S or MVA-ST mounted similar levels of SARS-CoV-2-S-specific CD8<sup>+</sup> T cells and MVA-specific CD8<sup>+</sup> T cells (Supplemental Figure 5).

**Protective capacity of MVA-S and MVA-ST upon SARS-CoV-2 respiratory challenge in Syrian hamsters.** To further investigate the impact of prime-boost immunization against SARS-CoV-2-induced disease, we used Syrian hamsters as a well-established preclinical model for efficacy testing (Figures 6 and 7). Two cohorts of hamsters were vaccinated within a 21-day interval twice intramuscularly with  $1 \times 10^8$  PFU candidate vaccine in each case, comparing MVA and MVA-S and then MVA and MVA-ST. Safety and immunogenicity were analyzed as established before (Supplemental Figure 6). SARS-CoV-2-binding antibodies were analyzed by different ELISAs specific for trimeric S protein or S1 subunit antigen. Immunizations with nonrecombinant vector elicited no detectable S-specific antibodies in control hamsters (MVA; Figure 6A). However, antibodies specific for trimeric S proteins could be detected in all hamsters vaccinated with MVA-S (mean titer 1:700) or MVA-ST (mean titer 1:728) already after single vaccination. Boost vacci-

nations further increased the levels, resulting in comparable titers of 1:2250 for MVA-S and 1:1157 for MVA-ST vaccination.

Underlining the mouse model results, we observed a different pattern for vaccine-induced S1-binding antibodies. Only 37.5% ( $n = 3/8$ ) of MVA-S-vaccinated hamsters mounted S1-binding antibodies after the first immunization (mean titer of 1:38), while boost vaccinations elicited low-level seroconversion in 87.5% ( $n = 7/8$ ) of MVA-S-vaccinated animals (mean titer of 1:112). In sharp contrast, prime MVA-ST vaccination induced high levels of S1-binding antibodies (100% seroconversion, mean titer of 1:2442), and boost vaccination on day 21 further increased these levels to a mean titer of 1:4242 (Figure 6B).

Similarly, after prime immunization we measured low levels of SARS-CoV-2 BavPat1-neutralizing antibodies in sera from 87.5% ( $n = 7/8$ ) of MVA-S-vaccinated hamsters (mean titer of 1:65; Figure 6C), whereas all hamsters immunized with MVA-ST mounted readily detectable neutralizing antibodies (100% seroconversion), with an average titer of 1:321 PRNT<sub>50</sub> at 3 weeks after priming (Figure 6C).

Compared with SARS-CoV-2 BavPat1, reduced neutralizing activity against Delta and Omicron were measured. MVA-S vaccination resulted in marginal antibody titers neutralizing Delta (mean titer of 1:71; Figure 6D). No detectable titers against Omicron were

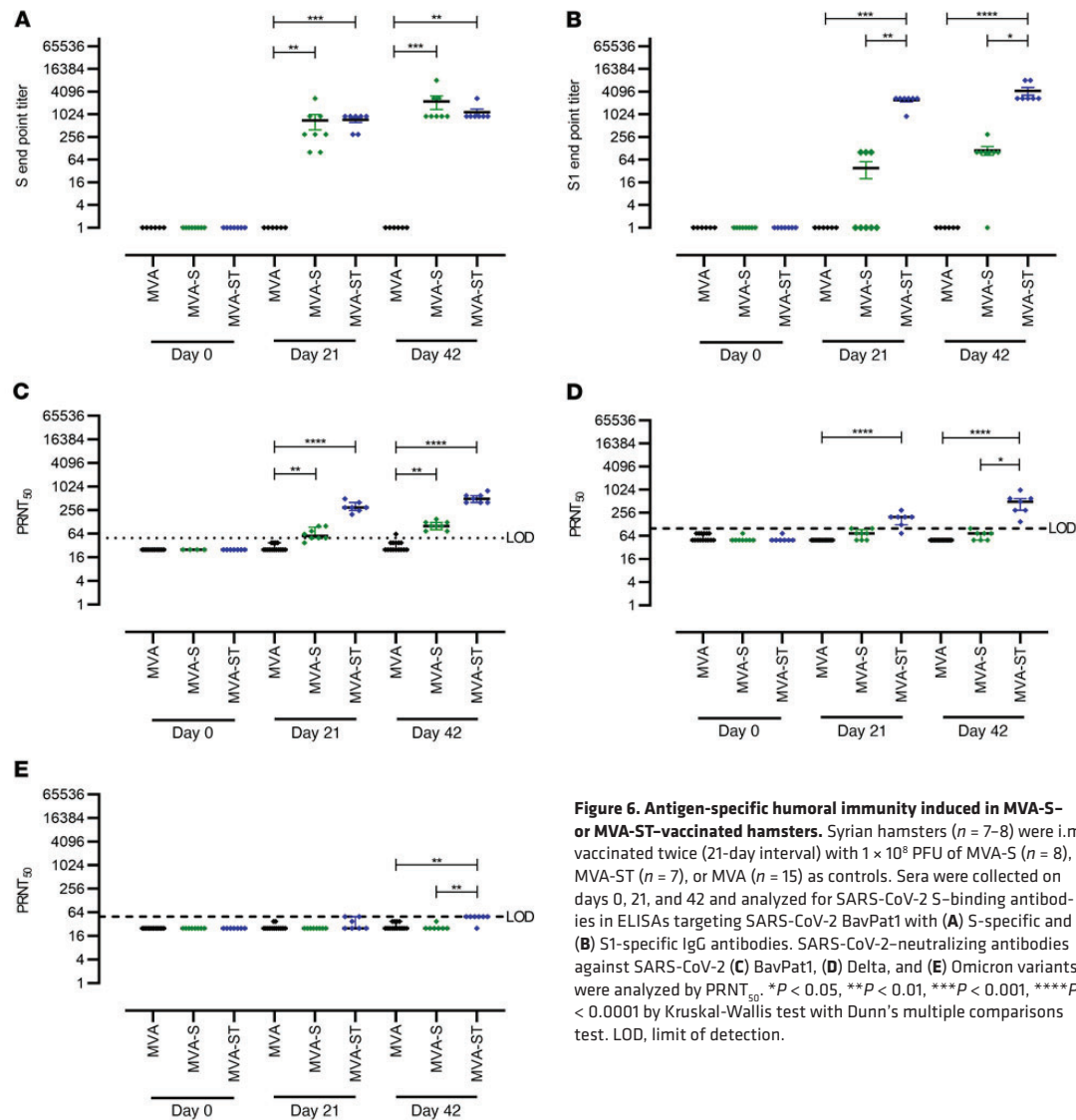


**Figure 6. Antigen-specific humoral immunity induced in MVA-S- or MVA-ST-vaccinated hamsters.** Syrian hamsters ( $n = 7-8$ ) were i.m. vaccinated twice (21-day interval) with  $1 \times 10^8$  PFU of MVA-S ( $n = 8$ ), MVA-ST ( $n = 7$ ), or MVA ( $n = 15$ ) as controls. Sera were collected on days 0, 21, and 42 and analyzed for SARS-CoV-2 S-binding antibodies in ELISAs targeting SARS-CoV-2 BavPat1 with (A) S-specific and (B) S1-specific IgG antibodies. SARS-CoV-2-neutralizing antibodies against SARS-CoV-2 (C) BavPat1, (D) Delta, and (E) Omicron variants were analyzed by PRNT<sub>50</sub>. \* $P < 0.05$ , \*\* $P < 0.01$ , \*\*\* $P < 0.001$ , \*\*\*\* $P < 0.0001$  by Kruskal-Wallis test with Dunn's multiple comparisons test. LOD, limit of detection.

measured after prime MVA-S vaccination (Figure 6E). Hamsters that had been vaccinated with MVA-ST mounted a mean titer of 1:185.7 against Delta (Figure 6D) and a titer below the detection limit against Omicron (mean titer of 1:33.9; Figure 6E). After the boost vaccination, sera from all MVA-S-vaccinated hamsters (100% seroconversion) revealed low neutralizing activity, with minor titers of approximately 1:100 PRNT<sub>50</sub> against SARS-CoV-2 BavPat1 (Figure 6C). One out of 7 animals had confirmed seroconversion against Delta, exhibiting a mean titer of 1:67 after boost vaccination (Figure 6D). In MVA-S-vaccinated animals, no seroconversion was detected against Omicron (Figure 6E). In contrast, in all sera from hamsters vaccinated with MVA-ST we detected increased amounts of SARS-CoV-2-neutralizing antibodies against SARS-CoV-2 BavPat1 after the boost immunization, with a mean titer of 1:529 PRNT<sub>50</sub>

(Figure 6C). For Delta, a mean titer of 1:500 was measured in these vaccinated animals (100% seroconversion; Figure 6D), whereas no obvious titers of Omicron-neutralizing antibodies were detected in MVA-ST-vaccinated animals (mean titer of 1:46; Figure 6E).

Four weeks after the boost immunization, the animals were intranasally infected with  $1 \times 10^4$  50% tissue culture infectious dose (TCID<sub>50</sub>) SARS-CoV-2 BavPat1 (Figure 7). Starting on day 3, MVA-vaccinated control hamsters demonstrated reduced body weights, and at 6 days after infection all animals had lost approximately 10% of their initial body weight. No body weight loss could be detected for hamsters immunized with MVA-S or MVA-ST (Figure 7A). Control animals also showed characteristic clinical symptoms associated with SARS-CoV-2 respiratory tract infection, including labored breathing, reduced activity, and scruffy fur.

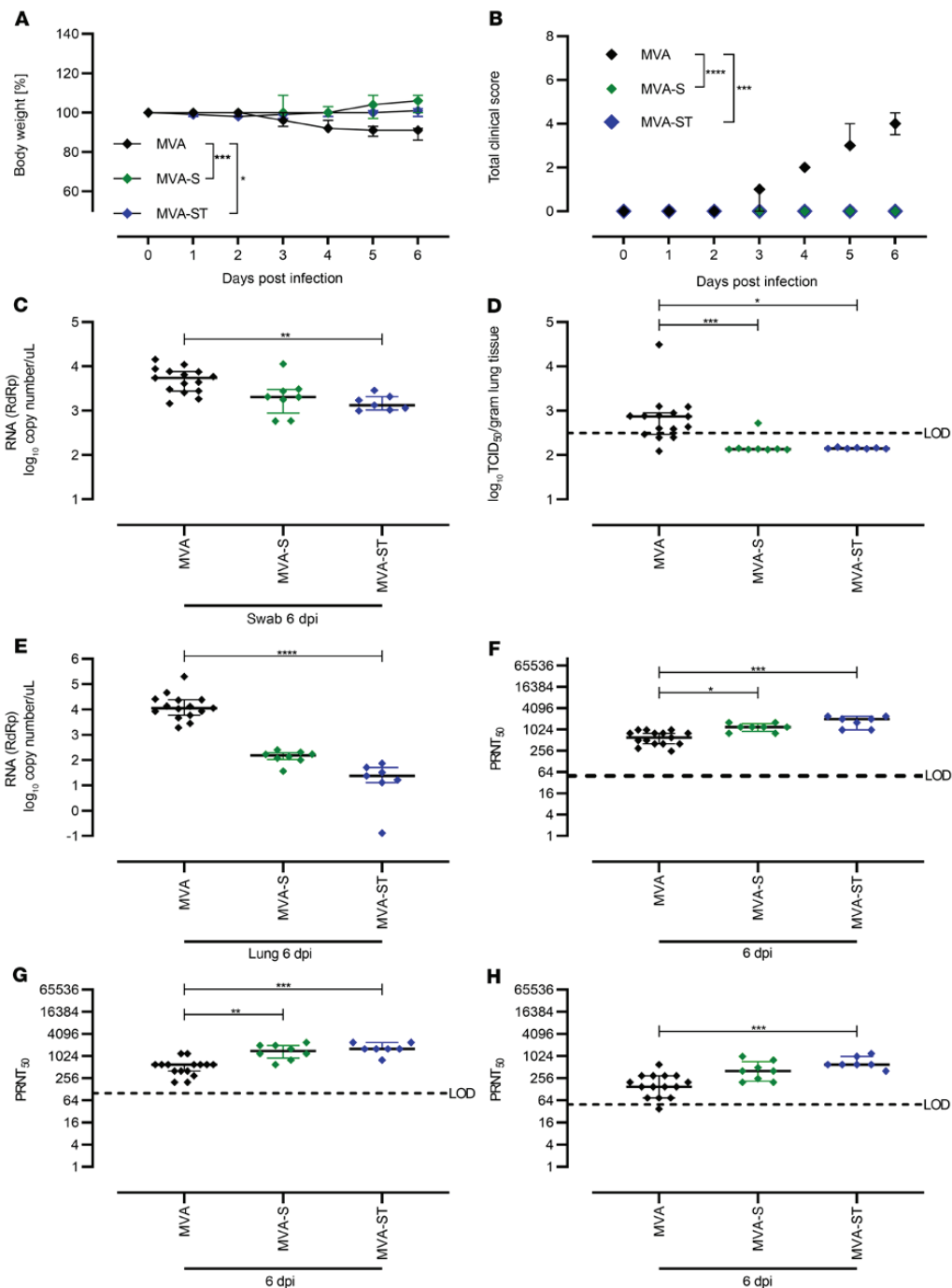


**Figure 7. Protective capacity of MVA-S or MVA-ST immunization against SARS-CoV-2 BavPat1 infection in Syrian hamsters.** Syrian hamsters vaccinated with MVA ( $n = 15$ ) control, MVA-S ( $n = 8$ ), or MVA-ST ( $n = 7$ ) were i.n. challenged with  $1 \times 10^4$  TCID<sub>50</sub> SARS-CoV-2 BavPat1. (A) Body weight was monitored daily and (B) spontaneous behavior and general condition were evaluated by clinical scores. (C) Oropharyngeal swabs on day 6 after challenge infection were analyzed for SARS-CoV-2 gRNA copies. (D and E) Lungs were harvested and analyzed for (D) infectious SARS-CoV-2 by TCID<sub>50</sub>/gram lung tissue, and (E) SARS-CoV-2 gRNA copies. Sera were prepared on day 6 after challenge and analyzed for SARS-CoV-2 (F) BavPat1, (G) Delta, and (H) Omicron variant-neutralizing antibodies by PRNT<sub>50</sub>. \* $P < 0.05$ , \*\* $P < 0.01$ , \*\*\* $P < 0.001$ , \*\*\*\* $P < 0.0001$  by Kruskal-Wallis test with Dunn's multiple comparisons test (C-H) of AUC (A and B). LOD, limit of detection.

No MVA-S- or MVA-ST-vaccinated animals showed any signs of clinical disease (Figure 7B).

To evaluate viral loads and pathological changes in lung tissues, we euthanized all animals at 6 days after infection. Blood and swab samples were taken at necropsy, and lungs were harvested for further analysis. Substantial amounts of viral RNA were detected in oropharyngeal swabs of control animals (mean of  $7.7 \times 10^3$  RNA copy numbers/ $\mu$ L; Figure 7C). Swab samples from hamsters vaccinated with MVA-S contained marginally reduced levels of viral RNA (on average  $3 \times 10^3$  RNA copy numbers/ $\mu$ L), whereas swabs from animals vaccinated with MVA-ST contained significantly reduced levels of SARS-CoV-2 RNA (mean of  $1.6 \times 10^3$  RNA copy numbers/ $\mu$ L; Figure 7C).

Correspondingly, lung tissues from control hamsters harbored infectious SARS-CoV-2 (mean of  $2.9 \times 10^3$  TCID<sub>50</sub>/gram lung tissue; Figure 7D), whereas no infectious SARS-CoV-2 was detected in the lungs of vaccinated hamsters (with the exception of tissue from 1 MVA-S-vaccinated animal containing  $5.6 \times 10^2$  TCID<sub>50</sub>/gram lung tissue). These data were confirmed by real-time RT-PCR analysis of viral RNA loads. In lung tissues from both MVA-S- and MVA-ST-immunized animals, we found lower levels of SARS-CoV-2 RNA compared with control hamsters ( $<3 \times 10^1$  genome equivalents/ng total RNA; Figure 7E).

Only after SARS-CoV-2 BavPat1 infection did we detect SARS-CoV-2-binding antibodies in control (MVA) hamsters, with a mean titer of 1:16,883 for S-specific antibodies and 1:5600 for S1-binding antibodies (Supplemental Figure 7, A and B). Thus, although all the control hamsters became moribund, we observed detectable titers of SARS-CoV-2 BavPat1-neutralizing antibodies that averaged to 1:632 PRNT<sub>50</sub> after challenge infection (Figure 7F). Against Delta, an average mean titer of 1:1013 was measured in control MVA-vaccinated hamsters (Figure 7G). Lower titers reaching a mean of 1:204 were present against Omicron detected by PRNT<sub>50</sub> (Figure 7H). In line with data from viral load and clinical disease outcome, we detected markedly higher levels of SARS-CoV-2 S-specific antibodies in sera from immunized hamsters. After challenge, we measured substantial levels of S-binding antibodies, with a mean titer of 1:38,185 or 1:50,194 after MVA-S or MVA-ST immunization (Supplemental Figure 7B). S1-binding antibodies in MVA-S-vaccinated hamsters reached a mean titer of 1:23,528; MVA-ST-vaccinated hamsters had a higher mean titer of 1:72,900 (Supplemental Figure 7A). MVA-S vaccination resulted in SARS-CoV-2 BavPat1-neutralizing activities with an average PRNT<sub>50</sub> titer of 1:1200, compared with the MVA-ST mean titer of 1:1771 (Figure 7F). In MVA-S-vaccinated hamsters, a mean titer of 1:1475 against Delta and 1:468 against Omicron were detected (Figure 7, G and H). After MVA-ST vaccination, hamsters mounted mean titers of 1:1714 against Delta and 1:714 against Omicron (Figure 7, G and H).

To evaluate lung pathology in vaccinated and infected animals, we performed histological analysis of hematoxylin and eosin-stained lung sections (Figure 8). Control hamsters (MVA) had large areas of lung consolidation. Alveolar lesions were characterized by the accumulation of neutrophils and mononuclear cells that expanded alveolar septae and filled alveolar lumina (Figure 8, A and E). Inflammation was associated with necrosis of alveolar epithelia, fibrin exudation, and a prominent pneumocyte type II hyperplasia. A mixed inflammatory infiltrate, epithelial degeneration, and hyperplasia were found in bronchi and bronchioli. In addition, animals showed

marked vascular lesions, characterized by endothelial hypertrophy, endothelialitis, mural and perivascular infiltrates, loss of vascular wall integrity, and perivascular edema.

MVA-S-vaccinated hamsters also revealed areas of inflammation and consolidation, although the overall extent of alveolar, bronchial/bronchiolar, and vascular lesions was less than in control animals (Figure 8C). Lungs of MVA-ST-vaccinated hamsters showed negligible or markedly reduced lung pathology (Figure 8G). Almost all the animals in this group demonstrated only mild to moderate inflammatory lesions confined to the airways and some vessels, while alveolar lesions were absent or minimal, affecting less than 1% of the lung lobes. Only 1 animal showed higher lesion scores in the alveolar and vascular compartment, affecting below 25% of the entire lobe.

Semiquantitative scoring of alveolar, airway, and vascular lesions showed a significant reduction in all parameters in animals vaccinated with recombinant MVA vaccines compared with the control group (Figure 8I). Importantly, MVA-ST-vaccinated hamsters showed substantially lower inflammation scores than MVA-S-vaccinated animals. Using immunohistochemistry, SARS-CoV-2 nucleoprotein was detected in the lungs of all control hamsters, but in none of the MVA-S- or MVA-ST-immunized animals (Figure 8, J and K).

*MVA-S or MVA-ST vaccination provides protection from lethal SARS-CoV-2 disease outcomes in K18-hACE2 mice.* To evaluate immunogenicity and protective efficacy in a lethal animal model, we used K18-hACE2 mice. K18-hACE2 mice are highly susceptible to intranasal SARS-CoV-2 infection characterized by high viral loads in the lungs, severe interstitial pneumonia, and death by day 6 or 8 after inoculation. Mice were vaccinated with MVA, MVA-S, or MVA-ST using an intramuscular prime-boost schedule as above.

As expected, we did not detect SARS-CoV-2 BavPat1-neutralizing antibodies in control mice vaccinated with MVA. Single vaccination with MVA-S or MVA-ST resulted in obvious titers of neutralizing antibodies against SARS-CoV-2 BavPat1, with a mean titer of 1:880 for MVA-S and 1:2880 for MVA-ST. Boost vaccination on day 21 further increased SARS-CoV-2 BavPat1-neutralizing antibodies to a mean titer of 1:660 or 1:3840 in MVA-S- or MVA-ST-vaccinated mice (Figure 9A). However, neutralizing activities against SARS-CoV-2 Delta and Omicron were lower compared with SARS-CoV-2 BavPat1 following MVA-S and MVA-ST vaccination (Figure 9, B and C).

Mice immunized with MVA-S mounted sufficient levels of Delta-neutralizing antibodies after prime or boost application (Figure 9B; mean of 1:208 or 1:575). MVA-ST vaccination resulted in a mean titer of 1:675 after prime and 1:1400 after boost (Figure 9B). For Omicron, no detectable titers of neutralizing antibodies were present in mice after single vaccination with either candidate vaccine. MVA-S boost vaccination again did not result in obvious titers of Omicron-neutralizing antibodies (Figure 9C). Marginal titers of Omicron-neutralizing antibodies were present in sera of mice after boost vaccination with MVA-ST (Figure 9C; mean titer of 1:75).

At 4 weeks after boost vaccinations, mice were intranasally challenged with a lethal dose of  $3.6 \times 10^4$  TCID<sub>50</sub> SARS-CoV-2 BavPat1. Control mice significantly lost weight and showed clinical signs of disease starting on day 3, and all succumbed to infection by day 6, whereas MVA-S- and MVA-ST-vaccinated mice showed no weight loss or clinical disease (Figure 9, D-F). At 4 days after infection, substantial levels of viral RNA shedding were observed from the upper respiratory tract of control vaccinated mice (mean

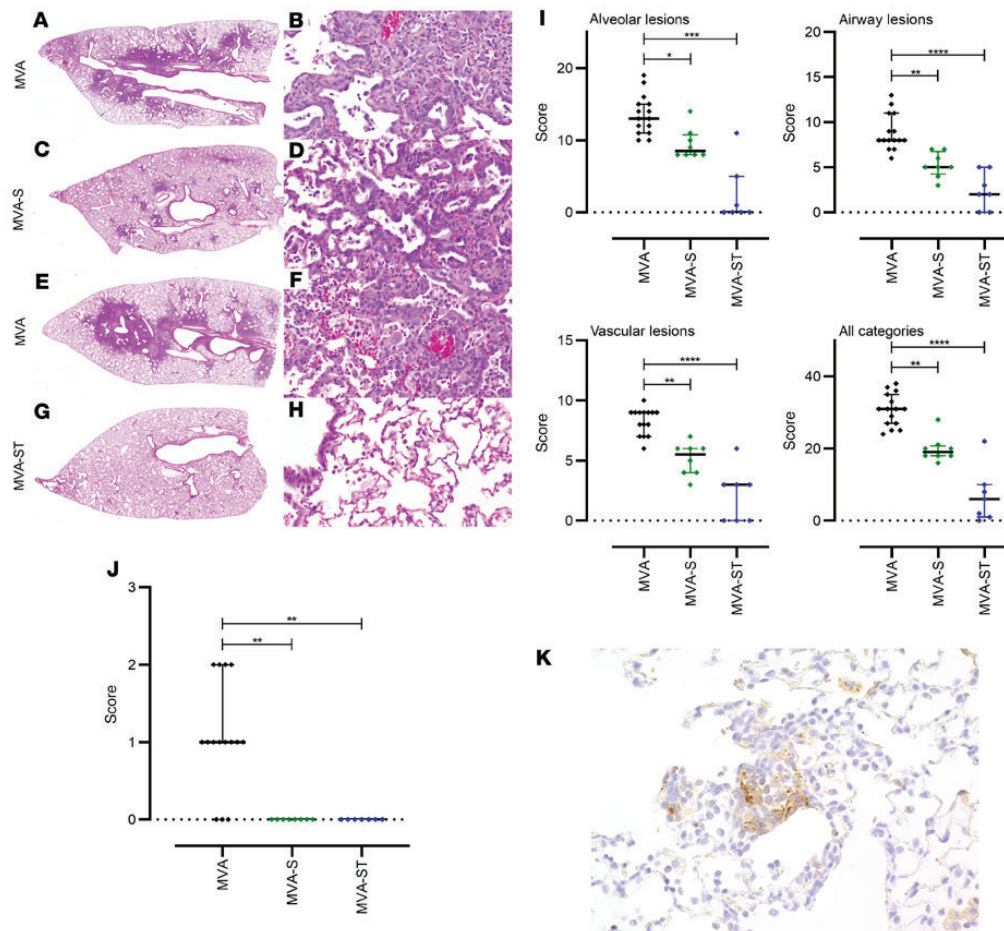


**Figure 8. Histopathological lesions in the lungs of SARS-CoV-2 BavPat1-challenged hamsters vaccinated with MVA, MVA-S, or MVA-ST.** (A, C, E, and G) Representative overview images of hematoxylin and eosin-stained lung sections and (B, D, F, and H) associated  $\times 100$  magnifications. (A and E) Images from MVA control-vaccinated animals show extensive areas of alveolar consolidation (arrowheads). Higher magnification (B and F) reveals markedly thickened alveolar septae, inflammatory infiltrates, and prominent pneumocyte type II hyperplasia with many atypical, large cells (arrowheads) and mitotic figures (arrow). (C and D) MVA-S-vaccinated animals show less lung pathology with multifocal, small foci of alveolar consolidation, which are qualitatively similar to the lesions in controls. (E) Quantification of histopathological lesions. Vaccination with recombinant MVAs significantly reduces lung lesions compared with control groups. (J and K) Immunohistochemistry for SARS-CoV-2 nucleoprotein in the lungs of hamsters vaccinated with MVA (control), MVA-S, or MVA-ST, challenged with SARS-CoV-2 BavPat1. (J) Semiquantitative scoring of viral antigen amount. No viral antigen was detected in MVA-S- or MVA-ST-vaccinated animals. (K) SARS-CoV-2 antigen (brown signal) is predominantly found in pneumocytes lining alveoli ( $\times 100$  magnification). Dotted lines mark the zero value. \* $P < 0.05$ , \*\* $P < 0.01$ , \*\*\* $P < 0.001$ , \*\*\*\* $P < 0.0001$  by Kruskal-Wallis test with Dunn's multiple comparisons test.

of  $6.6 \times 10^3$  genome equivalents/ $\mu\text{L}$ ). In MVA-S-vaccinated mice, we found low but detectable levels of SARS-CoV-2 RNA shedding in oropharyngeal swabs (mean of 27 genome equivalents/ $\mu\text{L}$ ). MVA-ST-vaccinated mice did not produce detectable viral RNA levels in oropharyngeal swabs (Figure 9G).

When monitoring viral loads in the lung and brain homogenates of mice at time of death (day 6 after infection [MVA-vaccinated mice] or 8 days after challenge [MVA-S/MVA-ST-vaccinated animals]), we failed to detect SARS-CoV-2 BavPat1 in the lungs and brains of MVA-S- or MVA-ST-vaccinated mice, but found large amounts of

infectious virus in the organs from control MVA-vaccinated mice (Figure 9H). These data were confirmed by real-time RT-PCR analysis of viral RNA loads. In the control MVA-vaccinated mice, we detected substantial levels of viral RNA, with a mean of  $1.19 \times 10^7$  or  $1.14 \times 10^8$  genome equivalents/ng total RNA in lungs or brains. Both MVA-S- and MVA-ST-immunized animals exhibited lower levels of SARS-CoV-2 RNA than control mice in the lungs (a mean of  $3.7 \times 10^2$  genome equivalents/ng total RNA for MVA-S and 1.31 for MVA-ST; Figure 7I) and in the brains (a mean of 9.73 genome equivalents/ng total RNA for MVA-S and 1.58 for MVA-ST).

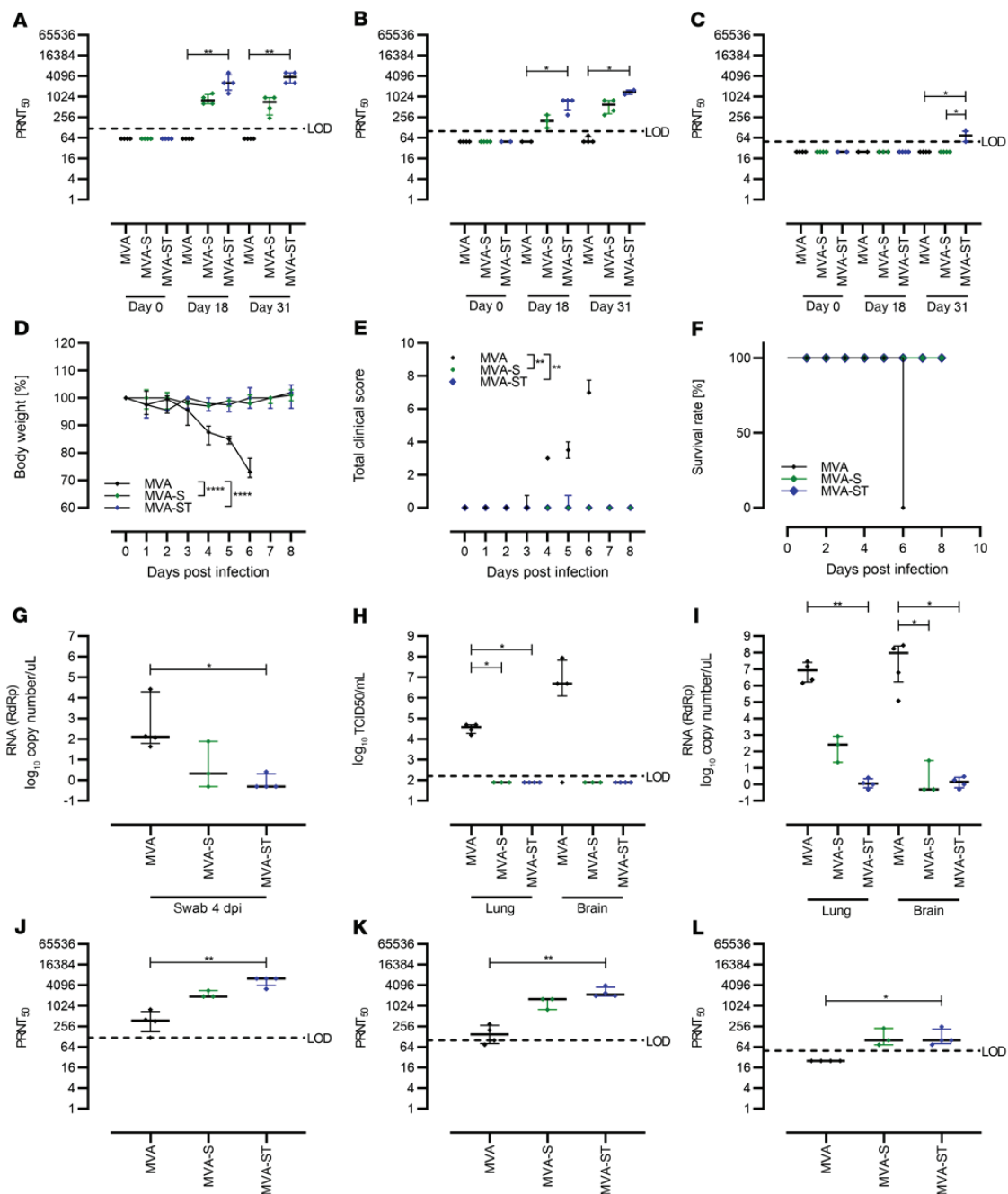


**Figure 9. Protective capacity of MVA-S or MVA-ST immunization against SARS-CoV-2 in K18-hACE2 mice.** K18-hACE2 mice were i.m. immunized twice with  $1 \times 10^8$  PFU MVA-S ( $n = 4$ ), MVA-ST ( $n = 4$ ), or MVA ( $n = 4$ ) as a control in a 21-day interval. Sera were collected on days 0, 18, and 31 and analyzed for SARS-CoV-2-neutralizing antibodies against (A) BavPat1, (B) Delta, and (C) Omicron variants by PRNT<sub>50</sub>. After SARS-CoV-2 BavPat1 challenge infection, (D) body weight was monitored daily, (E) spontaneous behavior and general condition were evaluated in clinical scores, and (F) survival rate was determined retrospectively. (G) Oropharyngeal swabs from 4 days after infection were analyzed for SARS-CoV-2 gRNA copies. RdRp, RNA-dependent RNA polymerase. At the end of the experiment (day 6 for MVA-, day 8 for MVA-S/MVA-ST-vaccinated mice), lungs and brains were harvested and analyzed for (H) amounts of infectious SARS-CoV-2 by TCID<sub>50</sub>/mL and (I) viral RNA by qRT-PCR. Sera were analyzed for (J) BavPat1, (K) Delta, and (L) Omicron variant-neutralizing antibodies by PRNT<sub>50</sub>. \* $P < 0.05$ , \*\* $P < 0.01$ , \*\*\*\* $P < 0.0001$  by Kruskal-Wallis test with Dunn's multiple comparisons test (A-C and G-L) of AUC (E) and 1-way ANOVA with Tukey's multiple comparisons test of AUC (D). LOD, limit of detection.



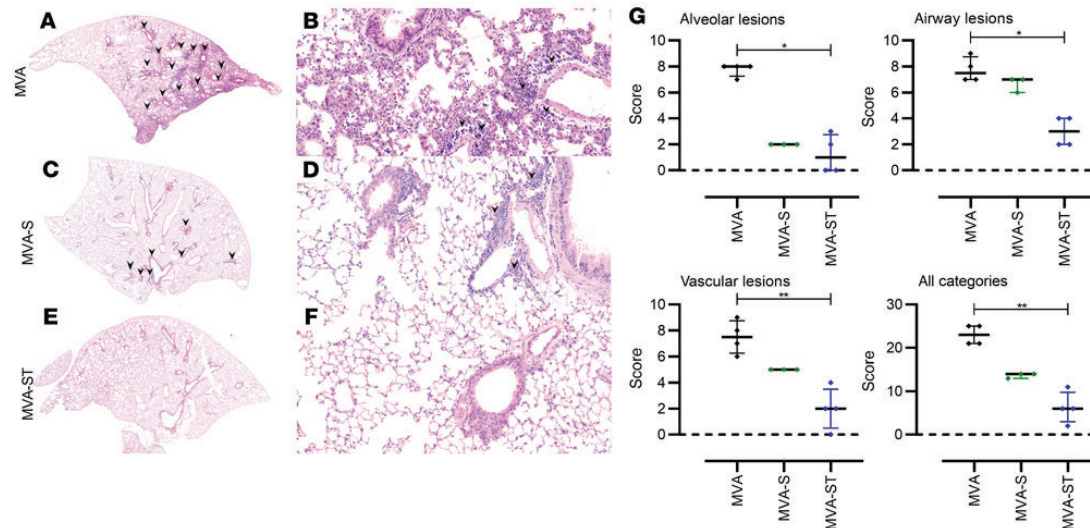


**Figure 10. Histopathological lesions in the lungs of K18-hACE2 mice vaccinated with MVA, MVA-S, or MVA-ST, challenged with SARS-CoV-2 BavPat1.** (A, C, and E) Representative overview images of hematoxylin and eosin–stained lung sections and (B, D, and F) associated  $\times 100$  magnifications. (A) MVA control–vaccinated animals show multifocal areas of immune cell infiltration (arrowheads). (B) Higher magnification reveals markedly thickened alveolar septae, inflammatory infiltrates, and a prominent perivascular immune cell infiltration (arrowheads) as well as multifocal perivascular edema. (C and D) MVA-S–vaccinated animals show less lung pathology with multifocal, small foci of thickened alveolar septae and mild to moderate perivascular infiltrates. (E and F) Most MVA-ST–vaccinated animals show no alveolar and fewer vascular lesions. (G) Quantification of histopathological lesions. Vaccination with recombinant MVAs reduces lung lesions compared with the control MVA group. Dotted lines mark the zero value.  $*P < 0.05$ ,  $**P < 0.01$  by Kruskal–Wallis test with Dunn’s multiple comparisons test.

Neutralizing antibodies against ancestral SARS-CoV-2 BavPat1, SARS-CoV-2 Delta, and Omicron were analyzed at the end of the experiment. Marginal titers of BavPat1- and Delta-neutralizing antibodies were present in sera of control MVA-vaccinated mice after SARS-CoV-2 BavPat1 challenge infection (mean of 1:420 for BavPat1, mean of 1:168.75 for Delta; Figure 9, J and K). No titers of Omicron-neutralizing antibodies were found in MVA-vaccinated animals (Figure 9L). However, robust titers of neutralizing antibodies were present in sera of MVA-S- and MVA-ST-vaccinated mice after SARS-CoV-2 BavPat1 challenge infection (Figure 9, J–L). Against BavPat1, MVA-S vaccination resulted in a mean titer of 1:2240; MVA-ST vaccination resulted in an even higher mean titer of 1:5600.

Against Delta, MVA-S vaccination resulted in a mean titer of 1:1333. Confirming previous results, antibody levels in MVA-ST-vaccinated mice were markedly higher, with a mean titer of 1:2400. However, against Omicron, a lower mean titer of 1:133 was measured for both candidate vaccines (Figure 9L).

Consistent with data from viral load in the lungs, control MVA-vaccinated animals showed pronounced lung pathology, which was associated with moderate to severe perivascular edema and inflammation with lymphocytes, macrophages, and small numbers of neutrophils surrounding small and intermediate vessels. Considerable inflammatory changes were also found in the alveolar and peribronchiolar compartments, characterized by moderate to marked interstitial and luminal immune cell infiltrates, with multifocal areas of completely obscured alveolar architecture. In animals vaccinated with MVA-S, despite the absence of severe and widespread inflammation in the alveolar compartment, substantial

perivascular and peribronchiolar inflammation was also present in the lungs. Interestingly, MVA-ST-vaccinated mice showed only very mild signs of pulmonary lesions after SARS-CoV-2 BavPat1 challenge infection (Figure 10). Our data so far showed that robust protective vaccination by a prime-boost application of  $1 \times 10^8$  PFU MVA candidate vaccines is associated with substantial titers of neutralizing antibodies in K18-hACE2 mice.

## Discussion

Here, we report that vaccination with a prefusion, stabilized SARS-CoV-2 S protein (ST) expressed by recombinant MVA (MVA-ST) elicits a better humoral immune response and provides protection upon SARS-CoV-2 BavPat1 challenge infection compared with the original recombinant MVA vaccine delivering the nonmodified SARS-CoV-2 S antigen (MVA-S).

Although several approved vaccines against SARS-CoV-2 are currently available, COVID-19 vaccine development still remains an important goal due to unsolved questions such as longevity and duration of immunity, virus transmission after asymptomatic infection, and arising virus variants of concern (VOCs). Thus, the development of innovative vaccination modalities that also confer robust and more broadly effective protection are urgently required. In general, there are several strategies to further improve vaccine candidates. A promising approach includes the presentation of a selected antigen. This may be of importance when processable fusion proteins are used as immunogens in vaccine development, since their metastability or processing also affects the kinetics of immune responses.

Based on our positive experience using a nonmodified S protein for generating an MVA-based candidate vaccine against MERS-CoV (11), we initially decided to use the same strategy to develop a COVID-19 candidate vaccine. Our MVA-S candidate vaccine expressing the authentic 2019 Wuhan Hu-1 S protein was confirmed to be immunogenic and protective in preclinical evaluation when tested in a mouse model for COVID-19 (15). Comparable results have been reported from the Oxford-AstraZeneca ChAdOx1 nCoV-19 vaccine, which also expresses a nonstabilized S protein and was confirmed to be immunogenic and protective in different preclinical animal models (19–21). Of note, the Oxford-AstraZeneca ChAdOx1 nCoV-19 was approved as a COVID-19 vaccine for application in humans and more than 2 billion doses of the vaccine have already been administered (22, 23).

In this current study, we report on the evaluation of the COVID-19 candidate vector vaccine MVA-S in a phase Ia clinical trial in humans. Here, we again confirmed advantageous safety and tolerability (data not shown). However, preliminary results revealed a pattern of antibody responses in individuals vaccinated with high or low doses of MVA-S, indicating a low S1-specific antibody response irrespective of vaccine dosage, while these individuals mounted substantial titers of S2-binding antibodies. Overall, levels of S-specific antibodies were shown to be below the levels of a comparable study evaluating an MVA-based candidate vaccine against MERS-CoV (11).

A recent study indicated that the efficiency of furin-mediated cleavage in the S1/S2 polybasic cleavage site in SARS-CoV-2 is enhanced compared with MERS-CoV (24). From these preliminary *in vitro* results, we hypothesize that a lower furin-mediated cleavage in MERS-CoV S protein expressed by MVA results in S protein that is still maintained in a prefusion state, still allowing S1-specific immune response activation. Since our recent data suggested proper folding and authentic presentation of the trimeric S protein expressed by the MVA vector (15), we hypothesized that processing involving furin-mediated cleavage of the S protein into its membrane-associated S2 subunit and the distal S1 subunit also occurs. Proteolytic cleavage can be followed by shedding of S1, leaving the S2 subunit anchored within the membrane (25). Our results again confirmed the authentic processing of the nonmodified S protein, with prominent S2 expression on the cell surface and obvious S1 shedding.

In previous studies, betacoronavirus S1 shedding had already been observed to inadvertently influence the activation of S-specific antibodies (6, 26, 27). This has also been confirmed for the activation of SARS-CoV-2-neutralizing antibodies after vaccination with the Oxford-AstraZeneca ChAdOx1 nCoV-19 vaccine. The authors discuss that the shedding of cleaved S1 may contribute to a higher proportion of non-neutralizing relative to neutralizing antibodies (28). This is in line with data from a recent study where Barros-Martins and colleagues evaluated the impact of heterologous versus homologous ChAdOx1nCoV-19/BNT162b2 vaccination in humans. Here, individuals who received a homologous BNT162b2 vaccination in a prime-boost schedule showed stronger antibody responses than those receiving homologous ChAdOx1nCoV-19 immunizations (29). Since BNT162b2 is based on a stabilized S protein, we hypothesized that S protein presentation influences immunogenicity, and that S1 dissociation from S2 influences the quantity and quality of MVA-S-activated immune responses. In another study, Dangi and colleagues confirmed that humans vaccinated

with a modified S protein exhibited a cross-protective immune response against heterologous coronaviruses (30).

Several approaches have been used to stabilize various class I fusion proteins in their precleaved conformation through structure-based design. For betacoronaviruses it has been suggested that presentation of the S protein in pre- or postfusion conformation has a substantial impact on the ratio of immune responses. In previous studies, 2 proline substitutions at the apex of the central helix and HR1 have been identified that could effectively stabilize MERS-CoV, SARS-CoV, and human coronavirus HKU1 S proteins in the precleaved conformation (27, 31, 32). Such stabilized S proteins were confirmed to be more immunogenic than wild-type S proteins (33, 34).

To evaluate the impact of structural processing of the labile S protein using our vector platform technology, we generated an MVA candidate vaccine expressing precleavage-stabilized S (MVA-ST). Modifications of full-length SARS-CoV-2 S protein expressed by MVA have already been used in other studies (26, 30, 35). As expected, when tested *in vivo* in mice and hamsters, we observed an improved antibody response after MVA-ST vaccination compared with the original MVA-S candidate vaccine. In line with previous results (36), the general activation of neutralizing antibodies against the Omicron variant was markedly reduced compared with ancestral BavPat1 and Delta variant. Of note, MVA-ST vaccination still induced marginally improved levels of Omicron-neutralizing antibodies compared with MVA-S.

The pattern of antibody responses in MVA-ST-immunized mice clearly exhibited advantageous activation of RBD-, S1-, and S2-binding antibodies. RBD is located in the S1 subunit known as the S protein ectodomain, and both are involved in binding to the specific cellular receptor. Thus both RBD-binding antibodies and those binding S1 elsewhere contribute to efficiently blocking SARS-CoV-2 receptor binding. Moreover, since the fusion peptide region is located within the S2 subunit, S2-binding antibodies are important for inhibiting fusion of the viral and host membranes, which enables release of the viral genome into host cells.

Since coronaviruses can readily generate antibody-escape mutations in the RBD and S1 subunit, activation of antibodies covering the entire S protein is considered desirable to ameliorate vaccine-induced immunity in such events. Indeed, the effectiveness of broadly reactive antibodies has already been confirmed for COVID-19 where REGN-COV2, an antibody cocktail mixture containing 2 neutralizing antibodies targeting the RBD of the SARS-CoV-2 S protein, efficiently reduced viral load in COVID-19 patients (37). Thus, the activation of antibodies targeting different epitopes within the S protein could also be effective against different SARS-CoV-2 VOCs. This was confirmed by our findings that, compared with MVA-S vaccination, superior activation of neutralizing antibodies specific for the S protein of Alpha, Beta, and Gamma variants and against the more recent SARS-CoV-2 variants Delta and Omicron, was achieved in mice and hamsters vaccinated with MVA-ST. The Omicron-characteristic immune evasion is based on a high number of amino acid substitutions present in the RBD. Yet, there is a fraction of broadly reactive antibodies that bind to sites inside and outside the RBD and potentially neutralize Omicron (38).

Based on previous studies from other betacoronaviruses, and also from influenza viruses, we hypothesize that this broadly neutralizing capacity may be explained by abundant presentation of

## RESEARCH ARTICLE

## The Journal of Clinical Investigation

the prefusion S2 conformation. S2 has been confirmed to be more highly conserved than S1, and represents a promising antigen to contribute to the induction of broadly protective immunity against current and newly arising coronaviruses (27, 39, 40). In our study, we confirmed more prominent presentation of S2 as a precleavage-stabilized cell-surface protein. This S2 prefusion conformation, in contrast to the postfusion S2 structure, might also contribute to more effectively activating host immune responses (41, 42) and against VOCs harboring high numbers of mutations in S1. We also confirmed the characteristic pattern of S-specific humoral immunity when we comprehensively tested our COVID-19 candidate vaccines in K18-hACE2 mice and the Syrian hamster model. Interestingly, despite these obvious differences in activation of humoral immune responses, the activation of an S1-specific cellular immune response appeared to be comparable following MVA-S and MVA-ST vaccination in mice. In our case, the S1 subunit including the presumed immunodominant SARS-CoV-2 S H2-Kd epitope S<sub>269-278</sub> is required to induce S1 epitope-specific CD8<sup>+</sup> T cells (15).

However, since both of the S proteins are initially processed via the *trans*-Golgi network, direct MHC-I presentation should also be efficient in activating CD8<sup>+</sup> T cell responses specific for S1 epitopes. This is further confirmed by results from Western blot analysis, which detected sufficient and comparable production of S1 antigen in the cell lysates of both MVA-S candidate vaccines. From these data we hypothesize that S1 is properly processed by direct antigen presentation, resulting in sufficient activation of S1-specific CD8<sup>+</sup> T cells. Here it will be of interest to further characterize levels of S1- and S2-epitope-specific T cells in more detail, especially concerning their role in protective efficacy. A robust activation of S1-epitope-specific T cells should also contribute to a protective immune response against SARS-CoV-2 variants including Omicron that has been confirmed to efficiently evade recognition by many RBD-specific antibodies. Indeed, Omicron-specific CD8<sup>+</sup> and CD4<sup>+</sup> T cell responses are well conserved, suggesting negligible immune escape at the level of cellular immunity (43).

Thus, we hypothesize that robust MVA-ST-mediated protection against SARS-CoV-2 variants, including Omicron, will rely on the activation of broadly reactive antibodies targeting conserved antigenic sites within the S protein and the induction of cellular immunity.

Intriguingly, when we evaluated protective efficacy against intranasal SARS-CoV-2 BavPat1 infection, the clinical outcome of both MVA-S- and MVA-ST-vaccinated animals appeared similar, since neither group showed any weight loss or morbidity. Since the primary goal of current SARS-CoV-2 vaccine development and approved vaccines is to prevent symptomatic COVID-19 (2), our results from the infection models indicate that both MVA COVID candidate vaccines are suitable for achieving this. Reduced morbidity is matched by reduced viral loads in the upper and lower respiratory tract of vaccinated animals, although MVA-ST appeared to increase the rate of reduction. One can surmise that significantly reducing SARS-CoV-2 viral load in the lungs results in moderating the severity of the disease. Of note, compared with the MVA-S-vaccinated hamsters, those vaccinated with MVA-ST also showed significantly reduced viral shedding on day 6. This might also be the result of the broader reactive antibody response combined with a robust activation of neutralizing antibodies, leading to rapid virus control in the upper and lower respiratory tract.

Of particular interest, when we characterized the vaccination effect in the hamsters in more detail, postmortem at 6 days after infection, we found that MVA-ST-vaccinated animals seemed more robustly protected from lung pathology, particularly in the alveolar compartment. Diffuse alveolar damage resulting from SARS-CoV-2 BavPat1 infection represents a clinically relevant pathomorphological lesion associated with impaired gas exchange, potentially resulting in acute respiratory distress syndrome. Here, in most of the MVA-ST-vaccinated animals alveolar lesions were completely absent or minimal. In the MVA-S-vaccinated group, the extent of alveolar inflammation and damage was also reduced compared with controls, correlating with the lack of clinical symptoms. However, mild to moderate lesions involving up to 25% to 50% of the lung lobe were still present in all these animals, suggesting incomplete protection of these tissues.

The absence of substantial alveolar pathology and inflammation without any SARS-CoV-2 N antigen expression in the lungs of MVA-ST-vaccinated hamsters favors the idea that the risk of developing long COVID is also reduced. However, this needs to be confirmed in future studies. Since the K18-hACE2 mouse model recapitulates the outcome of severe COVID-19 in humans, efficacy testing of SARS-CoV-2 candidate vaccines in the K18hACE2 SARS-CoV-2 infection model is of substantial value (32, 42). We confirmed the severe and lethal disease outcome in this model for mice that had been vaccinated with nonrecombinant MVA. Despite the absence of death, disease, and even viral load in the lungs of MVA-S-vaccinated mice, substantial pulmonary pathology, including vasculitis and bronchitis, were observed. Of note, vasculitis has been also described as one of the complications of COVID-19 in humans (43).

In contrast, such pathological outcomes were not detected at all in mice vaccinated with MVA-ST. However, since the severity of disease in this model is also mediated by neurological involvement, both the candidate vaccines appeared to readily protect against the lethal outcome of disease presumably through rapidly inhibiting initial replication in the respiratory tract (44). Despite this robust protection achieved in these mice, the observed differences in the outcome of pathology in this model further support the advantage of the modified S protein.

Vice versa, our data also indicate that authentic S processing during viral infection plays an important role in terms of SARS-CoV-2 pathogenesis as an immune evasion strategy. This hypothesis is supported by our results that MVA-S immunogenicity is markedly lower than that of the MVA-ST candidate vaccine. Importantly, we confirmed that a precleavage-stabilized S protein activates a beneficial antibody response. These data suggest that a deeper understanding of the SARS-CoV-2 replication cycle and its potential immune evasion strategies is not only important for better understanding the viral pathogenesis, but also for developing new vaccination strategies.

Taken together, the results show that the availability of a vaccine that not only prevents the obvious development of clinical disease after SARS-CoV-2 infection, but also avoids excessive alveolar damage, inflammation, and subsequent remodeling is highly desirable.

Here, we confirmed the improved efficacy of MVA-ST in pre-clinical models. These findings merit clinical studies using the MVA-ST candidate vaccine to further characterize the immune responses in humans, not only in homologous immunization cohorts but also

in heterologous schedules using mRNA or adenoviral vectors as primary vaccinations. It will also be of particular interest to evaluate how long protective immune responses are maintained and whether broader protection can be achieved. These studies are important due to the still ongoing pandemic and the fact that we still lack data on the impact of vaccine-induced immune-response durability on protection against SARS-CoV-2 infection.

## Methods

### Study design and participants

A phase I clinical trial was conducted to address safety and immunogenicity of the vaccine candidate MVA-S in healthy adults (ClinicalTrials.gov NCT04569383). The study was conducted in Hamburg (Germany) at the University Medical Center Hamburg-Eppendorf (UKE). Study participants were divided into 2 dose groups that received either  $1 \times 10^7$  IU (low dose) or  $1 \times 10^8$  IU (high dose) on days 0 and 28 (11).

### Bead-based serological multiplex assay

Serum samples were obtained by venipuncture from vaccinated individuals. Bead-based serological multiplex assay was performed using the MultiCoV-Ab assay validated previously (16, 17). MagPlex Microspheres (Luminex) conjugated to different parts of the S protein based on SARS-CoV-2 Wuhan-Hu-1 reference strain (GenBank accession no. MN908947.3) were used: purified trimeric S protein, S1 domain, RBD (all produced in-house), and S2 domain (Sino Biological). Serum samples were incubated at a dilution of 1:400 for 2 hours at room temperature. Subsequently, the beads were washed using 100  $\mu$ L of washing buffer (PBS supplemented with 0.05% [v/v] Tween 20) per well with the aid of a LifeSep magnetic separator unit (Dexter Magnetic Technologies). After 3 washing steps, bound antibodies were detected using PE-coupled secondary anti-human IgG antibodies (Dianova, 109-116-098, lot 148837; 3  $\mu$ g/mL), incubated for 45 minutes at room temperature. Samples were measured using the Bio-Plex 200 System (Bio-Rad Laboratories), controlled by BioPlex manager software, version 5.0.0.531. Cutoff samples with a known MFI value were generated as previously established (44) and included on each plate as quality control.

### Immunofluorescent staining and confocal microscopy

To quantify the cellular localization of S1 and S2, Huh-7 cells were infected with MVA-S or -ST (MOI 0.5) or transfected with plasmids encoding non-stabilized S protein. Eighteen hours after transfection/infection, S located at the cell surface was labeled at 4°C prior to fixation using a human-derived anti-S1 monoclonal antibody (generated and provided by F. Klein, Institute of Virology, University Hospital of Cologne, Germany; ref. 18). Subsequently, cells were fixed with 4% paraformaldehyde, permeabilized with 0.1% Triton X-100, and total S was labeled using anti-S2 antibody from mouse (GeneTex, GTX632604, clone 1A9; 1:100). Polyclonal goat anti-mouse-Alexa Fluor 594 (catalog A-11005) and goat anti-human-Alexa Fluor 488 (catalog A-48276) secondary antibodies (Thermo Fisher Scientific; 1:200) were used to visualize S-specific staining by fluorescence. Nuclei were stained with 1  $\mu$ g/mL DAPI (Sigma-Aldrich, D9542) and cells were analyzed using the Leica SP2 confocal microscope (Leica) with  $\times 63$  objective. All quantification of immunofluorescence-related data was performed with ImageJ/Fiji v.1.51 (45). To quantify surface S, optical sections of Huh-7 cells (500 nm/slice) were acquired in order to project the entire cell. Pixel intensities were measured in S1 (surface

and in S2 (total S) channels. The ratio between S1 and S2 values was calculated to yield the relative surface expression. Prior to each analysis, cell borders were determined using standard selection tools.

### SARS-CoV-2 S1 surface staining for flow cytometry

A549 cells were infected with 1 MOI MVA-S/-ST and MVA and incubated for 16 hours at 37°C, and cells were harvested and plated onto 96-well U-bottom plates at  $2 \times 10^5$  cells/well. Cells were incubated with purified anti-mouse CD16/CD32 (Fc block; BioLegend, clone 93; 1:500) for 15 minutes on ice. Cells were incubated with anti-S1 human monoclonal antibody (see above) for 30 minutes on ice and then with goat anti-human IgG (H+L)-Alexa Fluor 488 (Thermo Fisher Scientific, A-48276; 1:3000) for 30 minutes on ice. Cells were then stained with fixable dead cell viability dye Zombie Aqua (BioLegend, 423101; 1:1000). After staining, cells were fixed using Fixation Buffer (BioLegend) according to the manufacturer's protocol. Data were acquired using the MACSQuant VYB Flow Analyzer (Miltenyi Biotec) and analyzed using FlowJo (FlowJo LLC, BD Life Sciences).

### PRNT<sub>50</sub>

Serum samples were used to analyze neutralization capacity against SARS-CoV-2 (isolate Germany/BavPat1/2020; isolate hCoV-19/USA/PHC658/2021, lineage B.1.617.2 Delta variant; isolate hCoV-19/USA/MD-HP20874/2021, lineage B.1.1.529, Omicron variant) received from BEI Resources, NIAID, NIH, as previously described with some modifications (46). Heat-inactivated serum samples were serially diluted 2-fold in duplicate in 50  $\mu$ L DMEM. Then, 50  $\mu$ L of virus suspension (600 TCID<sub>50</sub>) was added to each well and incubated at 37°C for 1 hour before placing the mixtures on Vero E6 cells (ATCC, CRL-1586), seeded in 96-well plates. After incubation for 45 minutes, 100  $\mu$ L of a 1:1 mixture of prewarmed DMEM and Avicel RC-591 (Dupont, Nutrition & Biosciences) was added and plates were incubated for 24 hours. After incubation, cells were fixed with 4% formaldehyde/PBS and stained with a polyclonal rabbit antibody against SARS-CoV-2 nucleoprotein (Sino Biological, 40588-T62; 1:2000) and a secondary HRP-labeled goat anti-rabbit IgG (Agilent Dako, PO44801-2; 1:1000). The signal was developed using a precipitate-forming TMB substrate (True Blue, KPL SeraCare, 5510-0030) and the number of infected cells per well was counted by using an ImmunoSpot reader (CTL Europe GmbH). The reciprocal of the highest serum dilution allowing reduction of greater than 50% plaque formation was calculated as the serum neutralization titer (PRNT<sub>50</sub>) using the BioSpot Software Suite (CTL Europe GmbH).

### SARS-CoV-2 VNT<sub>100</sub>

The neutralizing activity of mouse serum antibodies was investigated based on a previously published protocol (47). Briefly, samples were serially diluted in 96-well plates starting from a 1:16 serum dilution. Samples were incubated for 1 hour at 37°C together with 100 PFU of SARS-CoV-2. Cytopathic effects on Vero cells were analyzed 4 days (BavPat1, Alpha, Gamma) or 6 days (Zeta) after infection. Neutralization was defined as absence of the cytopathic effects compared with virus controls. For each test, a positive control (human monoclonal antibody; refs. 18, 48) was used in quadruplicate as an interassay neutralization standard.

### Challenge-infection experiments in Syrian hamsters and K18-hACE2 mice

For SARS-CoV-2 challenge infection, animals were kept in individually ventilated cages (IVCs, Tecniplast) in approved BSL-3 facilities.

## RESEARCH ARTICLE

## The Journal of Clinical Investigation

All animal and laboratory work with infectious SARS-CoV-2 was performed in a BSL-3e laboratory and facilities at the Research Center for Emerging Infections and Zoonoses (RIZ), University of Veterinary Medicine, Hanover, Germany.

All animals were infected under anesthesia via the intranasal route with  $1 \times 10^4$  (hamsters) or  $3.6 \times 10^4$  (mice) TCID<sub>50</sub> of SARS-CoV-2 (isolate Germany/BavPat1/2020, NR-52370) received from BEI Resources, NIAID, NIH. After challenge infection, hamsters and mice were monitored at least twice daily for well being, health constitution, and clinical signs using a clinical score sheet (Supplemental Table 2). Body weights were checked daily.

**Viruses**

SARS-CoV-2 (isolate Germany/BavPat1/2020, NR-52370; isolate hCoV-19/USA/PHC658/2021, lineage B.1.617.2 Delta variant, NR-55611; isolate hCoV-19/USA/MD-HP20874/2021, lineage B.1.1.529, Omicron variant, NR-56461) received from BEI Resources, NIAID, NIH, were propagated in Vero cells in DMEM (Sigma-Aldrich) supplemented with 2% FBS, 1% penicillin-streptomycin, and 1% L-glutamine at 37°C. All infection experiments with SARS-CoV-2 were performed in BSL-3 laboratories at the RIZ, University of Veterinary Medicine Hannover, Germany or the Institute of Virology, Philipps University Marburg, Germany.

**Measurement of viral burden**

Lung tissue samples of immunized and challenged hamsters or mice excised from the right lung lobes, and brain tissue excised from the right brain of mice were homogenized in 1 mL DMEM containing antibiotics (penicillin and streptomycin, Gibco). Tissue was homogenized using the TissueLyser-II (Qiagen), and aliquots were stored at -80°C. Viral titers were determined on Vero cells as median TCID<sub>50</sub> units. Briefly, Vero cells were seeded in 96-well plates and serial 10-fold dilutions of homogenized lung samples in DMEM containing 5% FBS. After incubation for 96 hours at 37°C, cytopathic effects in Vero cells were evaluated and calculated as TCID<sub>50</sub> unit per gram or mL using the Reed-Muench method. For samples without cytopathic effect, data points were set to half of the detection limit for statistical analysis purposes.

**Statistics**

Data were prepared using GraphPad Prism 9.0.0 and R 4.2.1 (<https://cran.r-project.org/>) and expressed as mean  $\pm$  standard error of the mean (SEM) or median  $\pm$  interquartile range. Data were analyzed by 1-way ANOVA and Kruskal-Wallis test to compare 3 or more groups. A *P* value of less than 0.05 was used as the threshold for statistical significance.

**Study approval**

**Human specimens.** The study design was reviewed and approved by the Competent National Authority (Paul-Ehrlich-Institut [PEI], Langen, Germany) and the Ethics Committee of the Hamburg Medical Association. The study was performed in accordance with the Declaration of

Helsinki in its version of Fortaleza 2013 and ICH-GCP. All participants voluntarily enrolled in the study by signing an informed consent form after receiving detailed information about the clinical study.

**Hamster and mouse studies.** All animal experiments including SARS-CoV-2 infection under BSL-3 conditions were handled in compliance with the European and national regulations for animal experimentation (European Directive 2010/63/EU; Animal Welfare Acts in Germany) and Animal Welfare Act, approved by the Regierung von Oberbayern (Munich, Germany) and the Niedersächsisches Landesamt für Verbraucherschutz und Lebensmittelsicherheit (LAVES, Lower Saxony, Germany).

**Author contributions**

AV and GS conceptualized the study and revised the manuscript. AT constructed and characterized the vaccines, and performed experiments for safety and immunogenicity in BALB/c mice together with JHS, LL, GK, KB, SJ, and A Freudenstein. CMZN established in vivo SARS-CoV-2 infection models, performed in vitro and in vivo experiments to characterize safety, immunogenicity, and efficacy together with DLS, TT, SC, LMS, and AV. CR, SH, AK, and SB characterized S protein expression and VNT<sub>100</sub>-CD, A Fathi, MLW, LM, and MMA provided human sera from the phase I trial. RF, MK, ME, NSM, AD, and PK analyzed human sera. MC, FA, GB, and WB provided pathological investigations. CMZN and AT performed experiments, acquired data, interpreted data, and revised the manuscript. CMZN, AT, AV, and GS wrote the manuscript together with all coauthors.

**Acknowledgments**

We thank Monika Berg, Saskia Oppermann, Darren Markillie, Matthias Herberg, Bernd Vollbrecht, and Sandra Pfeifer for expert help in animal studies. We thank Patrizia Bonert, Ursula Klostermeier, Johannes Döring, and Axel Groß for expert help in mouse studies. We thank the phase I clinical study participants for their dedication and willingness to contribute to this research study in the middle of a pandemic. We thank the Hamburg clinical trial and laboratory teams for conducting the first-in-human clinical study and specimen processing. This work was supported by the German Center for Infection Research (DZIF: projects TTU 01.921 to GS, MMA, and SB; TTU 01.712 to GS), the Federal Ministry of Education and Research (BMBF 01KI20702 to GS, MMA, and SB; ZOO-VAC 01KI1718 to AV; RAPID 01KI1723G to AV and WB), Ministry of Science and Culture of Lower Saxony, Germany (14 - 76103-184 CORONA-15/20 to AV and WB), and the DFG (German Research Foundation 398066876/GRK 2485/1 to AV, GS, and WB).

Address correspondence to: Asisa Volz, Institute of Virology, University of Veterinary Medicine Hannover, Buenteweg 17, 30559 Hanover, Germany. Phone: 49.511.953.8857; Email: [Asisa.Volz@tiho-hannover.de](mailto:Asisa.Volz@tiho-hannover.de).

1. Wrapp D, et al. Cryo-EM structure of the 2019-nCoV spike in the prefusion conformation. *Science*. 2020;367(6483):1260-1263.

2. Corbett KS, et al. Immune correlates of protection by mRNA-1273 vaccine against SARS-CoV-2 in nonhuman primates. *Science*. 2021;373(6561):eabj0299.

3. Folegatti PM, et al. Safety and immunogenicity of the ChAdOx1 nCoV-19 vaccine against SARS-CoV-2: a preliminary report of a phase 1/2, single-blind, randomised controlled trial. *Lancet*. 2020;396(10249):467-478.

4. Logunov DY, et al. Safety and immunogenicity of an rAd26 and rAd5 vector-based heterologous

prime-boost COVID-19 vaccine in two formulations: two open, non-randomised phase 1/2 studies from Russia. *Lancet*. 2020;396(10255):887-897.

5. Zhu FC, et al. Safety, tolerability, and immunogenicity of a recombinant adenovirus type-5 vectored COVID-19 vaccine: a dose-escalation, open-label, non-randomised, first-in-human

- trial. *Lancet*. 2020;395(10240):1845–1854.
6. Bos R, et al. Ad26 vector-based COVID-19 vaccine encoding a prefusion-stabilized SARS-CoV-2 spike immunogen induces potent humoral and cellular immune responses. *NPJ Vaccines*. 2020;5(1):91.
  7. Jackson LA, et al. An mRNA vaccine against SARS-CoV-2 - preliminary report. *N Engl J Med*. 2020;383(20):1920–1931.
  8. Keech C, et al. Phase 1-2 trial of a SARS-CoV-2 recombinant spike protein nanoparticle vaccine. *N Engl J Med*. 2021;384(16):1576–1577.
  9. Skowronski DM, De Serres G. Safety and efficacy of the BNT162b2 mRNA Covid-19 vaccine. *N Engl J Med*. 2021;384(16):1576–1577.
  10. Sadarangani M, et al. Immunological mechanisms of vaccine-induced protection against COVID-19 in humans. *Nat Rev Immunol*. 2021;21(8):475–484.
  11. Koch T, et al. Safety and immunogenicity of a modified vaccinia virus Ankara vector vaccine candidate for Middle East respiratory syndrome: an open-label, phase 1 trial. *Lancet Infect Dis*. 2020;20(7):827–838.
  12. Krejtz JHCM, et al. Safety and immunogenicity of a modified-vaccinia-virus-Ankara-based influenza A H5N1 vaccine: a randomised, double-blind phase 1/2a clinical trial. *Lancet Infect Dis*. 2014;14(12):1196–1207.
  13. Volz A, et al. Protective efficacy of recombinant modified vaccinia virus ankara delivering Middle East respiratory syndrome coronavirus spike glycoprotein. *J Virol*. 2015;89(16):8651–8656.
  14. Volz A, Sutter G. Modified vaccinia virus ankara: history, value in basic research, and current perspectives for vaccine development. *Adv Virus Res*. 2017;97:187–243.
  15. Tschernie A, et al. Immunogenicity and efficacy of the COVID-19 candidate vector vaccine MVA-SARS-2-S in preclinical vaccination. *Proc Natl Acad Sci U S A*. 2021;118(28):e2026207118.
  16. Becker M, et al. Immune response to SARS-CoV-2 variants of concern in vaccinated individuals. *Nat Commun*. 2021;12(1):3109.
  17. Becker M, et al. Exploring beyond clinical routine SARS-CoV-2 serology using MultiCoV-Ab to evaluate endemic coronavirus cross-reactivity. *Nat Commun*. 2021;12(1):1152.
  18. Kreer C, et al. Longitudinal isolation of potent near-germline SARS-CoV-2-neutralizing antibodies from COVID-19 patients. *Cell*. 2020;182(4):843–854.
  19. van Doremalen N, et al. Intranasal ChAdOx1 nCoV-19/AZD1222 vaccination reduces viral shedding after SARS-CoV-2 D614G challenge in preclinical models. *Sci Transl Med*. 2021;13(607):eab0755.
  20. Fischer RJ, et al. ChAdOx1 nCoV-19 (AZD1222) protects Syrian hamsters against SARS-CoV-2 B.1.351 and B.1.1.7. *Nat Commun*. 2021;12(1):5868.
  21. van Doremalen N, et al. ChAdOx1 nCoV-19 vaccine prevents SARS-CoV-2 pneumonia in rhesus macaques. *Nature*. 2020;586(7830):578–582.
  22. European commission. Public Health - Union Register of medicinal products. <https://ec.europa.eu/health/documents/community-register/html/h1529.htm>. Updated October 7, 2022. Accessed October 10, 2022.
  23. AstraZeneca. Zwei Milliarden Dosen des AstraZeneca-Impfstoffs gegen COVID-19 in weniger als zwölf Monaten weltweit zur Verfügung gestellt. <https://www.astrazeneca.de/medien/press-releases/2021/zwei-milliarden-dosen-des-astrazeneca-impfstoffs-gegen-covid-19-zur-verfuegung-gestellt.html>. Updated November 23, 2021. Accessed February 7, 2022.
  24. Örd M, et al. The sequence at Spike S1/S2 site enables cleavage by furin and phospho-regulation in SARS-CoV2 but not in SARS-CoV1 or MERS-CoV. *Sci Rep*. 2020;10(1):16944.
  25. Brun J, et al. Assessing antigen structural integrity through glycosylation analysis of the SARS-CoV-2 viral spike. *ACS Cent Sci*. 2021;7(4):586–593.
  26. Liu R, et al. One or two injections of MVA-vectored vaccine shields hACE2 transgenic mice from SARS-CoV-2 upper and lower respiratory tract infection. *Proc Natl Acad Sci U S A*. 2021;118(12):e2026785118.
  27. Pallesen J, et al. Immunogenicity and structures of a rationally designed prefusion MERS-CoV spike antigen. *Proc Natl Acad Sci U S A*. 2017;114(35):E7348–E7357.
  28. Watanabe Y, et al. Native-like SARS-CoV-2 spike glycoprotein expressed by ChAdOx1 nCoV-19/AZD1222 vaccine. *ACS Cent Sci*. 2021;7(4):594–602.
  29. Barros-Martins J, et al. Immune responses against SARS-CoV-2 variants after heterologous and homologous ChAdOx1 nCoV-19/BNT162b2 vaccination. *Nat Med*. 2021;27(9):1525–1529.
  30. Dangi T, et al. Cross-protective immunity following coronavirus vaccination and coronavirus infection. *J Clin Invest*. 2021;131(24):e151969.
  31. Kirchdoerfer RN, et al. Pre-fusion structure of a human coronavirus spike protein. *Nature*. 2016;531(7592):118–121.
  32. Walls AC, et al. Cryo-electron microscopy structure of a coronavirus spike glycoprotein trimer. *Nature*. 2016;531(7592):114–117.
  33. Graham BS, Corbett KS. Prototype pathogen approach for pandemic preparedness: world on fire. *J Clin Invest*. 2020;130(7):3348–3349.
  34. Graham BS, Sullivan NJ. Emerging viral diseases from a vaccinology perspective: preparing for the next pandemic. *Nat Immunol*. 2018;19(1):20–28.
  35. Routhu NK, et al. A modified vaccinia Ankara vector-based vaccine protects macaques from SARS-CoV-2 infection, immune pathology, and dysfunction in the lungs. *Immunity*. 2021;54(3):542–556.
  36. Cheng SMS, et al. Neutralizing antibodies against the SARS-CoV-2 Omicron variant BA.1 following homologous and heterologous CoronaVac or BNT162b2 vaccination. *Nat Med*. 2022;28(3):486–489.
  37. Weinreich DM, et al. REGN-COV2, a neutralizing antibody cocktail, in outpatients with Covid-19. *N Engl J Med*. 2020;384(3):238–251.
  38. Cameroni E, et al. Broadly neutralizing antibodies overcome SARS-CoV-2 Omicron antigenic shift. *Nature*. 2022;602(7898):664–670.
  39. Ekiert DC, et al. Antibody recognition of a highly conserved influenza virus epitope. *Science*. 2009;324(5924):246–251.
  40. Yassine HM, et al. Hemagglutinin-stem nanoparticles generate heterosubtypic influenza protection. *Nat Med*. 2015;21(9):1065–1070.
  41. Cai Y, et al. Distinct conformational states of SARS-CoV-2 spike protein. *Science*. 2020;369(6511):1586–1592.
  42. McLellan JS, et al. Structure-based design of a fusion glycoprotein vaccine for respiratory syncytial virus. *Science*. 2013;342(6158):592–598.
  43. GeurtsvanKessel CH, et al. Divergent SARS-CoV-2 Omicron-reactive T and B cell responses in COVID-19 vaccine recipients. *Sci Immunol*. 2022;7(69):eabo2202.
  44. Planatscher H, et al. Systematic reference sample generation for multiplexed serological assays. *Sci Rep*. 2013;3(1):3259.
  45. Schindelin J, et al. Fiji: an open-source platform for biological-image analysis. *Nat Methods*. 2012;9(7):676–682.
  46. Okba NMA, et al. Severe acute respiratory syndrome coronavirus 2-specific antibody responses in Coronavirus disease patients. *Emerg Infect Dis*. 2020;26(7):1478–1488.
  47. Halwe S, et al. Intranasal administration of a monoclonal neutralizing antibody protects mice against SARS-CoV-2 infection. *Viruses*. 2021;13(8):1498.
  48. Vanshylla K, et al. Kinetics and correlates of the neutralizing antibody response to SARS-CoV-2 infection in humans. *Cell Host Microbe*. 2021;29(6):917–929.

Ich versichere, dass dieses gebundene Exemplar der Dissertation und das in elektronischer Form eingereichte Dissertationsexemplar (über den Docata-Upload) und das bei der Fakultät (Studienbüro Biologie) zur Archivierung eingereichte gedruckte gebundene Exemplar der Dissertationsschrift identisch sind.

I, the undersigned, declare that this bound copy of the dissertation and the dissertation submitted in electronic form (via the Docata upload) and the printed bound copy of the dissertation submitted to the faculty (Academic Office Biology) for archiving are identical.



Leonie Mayer

Hamburg, 18.01.2024